

Can data fusion techniques predict adverse physiological events during haemodialysis?

Dr Clare R MacEwen

St Cross College
University of Oxford

Thesis submitted for the Degree of Doctor of Philosophy

University of Oxford

·Hilary Term 2016·

Abstract

Intra-dialytic haemodynamic instability is a common and disabling problem which may lead to morbidity and mortality though repeated organ ischaemia, but it has proven difficult to link any particular blood pressure threshold with hard patient outcomes. The relationship between blood pressure and downstream organ ischaemia during haemodialysis has not been well characterised. Previous attempts to predict and prevent intra-dialytic hypotension have had mixed results, partly due to patient and event heterogeneity.

Using the brain as the indicator organ, we aimed to model the dynamic relationship between blood pressure, real-time symptoms, downstream organ ischaemia during haemodialysis, in order to identify the most physiologically grounded, prognostic definition of intra-dialytic decompensation. Following on from this, we aimed to predict the onset of intra-dialytic decompensation using personalised, probabilistic models of multivariate, continuous physiological data, ultimately working towards an early warning system for intra-dialytic adverse events.

This was a prospective study of 60 prevalent haemodialysis patients who underwent extensive, continuous physiological monitoring of haemodynamic, cardiorespiratory, tissue oxygenation and dialysis machine parameters for 3-4 weeks. In addition, longitudinal cognitive function testing was performed at baseline and at 12 months.

Despite their use in clinical practice, we found that blood pressure thresholds alone have a poor trade off between sensitivity and specificity for predicting downstream tissue ischaemia during haemodialysis. However, the performance of blood pressure thresholds could be improved by stratification for the presence or absence of cerebral autoregulation, and personalising thresholds according to the individual lower limit of autoregulation. For patients without autoregulation, the optimal blood pressure target was a mean arterial pressure (MAP) of 70mmHg. A key finding was that cumulative intra-dialytic exposure to

cerebral ischaemia, but not to hypotension per se, corresponded to change in executive cognitive function over 12 months. Therefore we chose cerebral ischaemia as the definition of intra-dialytic decompensation for predictive modelling.

We were able to demonstrate that the development of cerebral desaturation could be anticipated from earlier deviations of univariate physiological data from the expected trajectory for a given patient, but sensitivity was limited by the heterogeneity of events even within one individual. The most useful physiological data streams included peripheral saturation variance, cerebral saturation variance, heart rate and mean arterial pressure. Multivariate data fusion techniques using these variables created promising personalised models capable of giving an early warning of decompensation. Future work will involve the refinement and prospective testing of these models. In addition, we envisage a prospective study assessing the benefit of autoregulation-guided blood pressure targets on short term outcomes such as patient symptoms and wellbeing, as well as longer term outcomes such as cognitive function.

Dedicated to Sebastian Rupert

With icy roar, the tide crashed through the wall
And erstwhile shadows from the surf broke free
My clouded, shrouded eyes again could see
For miles, pain whipped away on coastal squall:
And there you stood, forever, proud and tall
The salty dampness of the Hebrides
Fresh on my ravaged cheeks, kissed by the sea
My heart swells, scrambling rocks to heed your call -
But cruel mirage! Awaits no beating chest!
Cruel trick of id, duplicitous caress!
The lights turn on, the colour ebbs away
Despair resurges with harsh glare of day
Cruel trick of time and tide, to bring so near
Then sweep yet further still what we hold dear

Contents

Abstract **2**

Acknowledgments **10**

Abbreviations **11**

1 Introduction and Background **13**

1.1 Objectives . . . 13

1.2 Background . . . 14

1.3 Tissue Perfusion . . . 16

1.3.1 Cardiac Perfusion . . . 17

1.3.2 Cerebral Perfusion . . . 18

1.3.3 Splanchnic perfusion . . . 21

1.3.4 Other . . . 22

1.3.5 Section Summary . . . 23

1.4 Preventing adverse events on haemodialysis . . . 23

1.5 Summary . . . 25

2 Generic Methods and Data collection **27**

2.1 Trial Structure . . . 27

2.1.1 Dialysis procedures . . . 29

2.2 Measurement techniques . . . 30

2.2.1 Finometer . . . 30

2.2.2 Transonic monitor . . . 31

2.2.3 Near-infrared Spectroscopy . . . 32

2.2.4 Visi Black Shadow . . . 33
2.2.5 Cognitive function tests . . . 33
2.3 Signal Quality Indexes (SQI) . . . 34
2.3.1 Finometer SQI . . . 34
2.3.2 Belt SQI . . . 34
2.3.3 PPG SQI . . . 35
2.3.4 ECG SQI . . . 35
2.4 Demographics . . . 36
2.5 Statistics and Modelling Overview . . . 36

3 Association of blood pressure with cerebral ischaemia and symptoms during haemodialysis 39

3.1 Introduction . . . 39
3.2 Methods . . . 40
3.2.1 Analysis 1: Overview of association between MAP thresholds and adverse events . 41
3.2.2 Analysis 2: Sensitivity, specificity and predictive value of MAP changes for cerebral ischaemia . . . 41
3.2.3 Analysis 3: Modelling total ischaemia AUC during a haemodialysis session . . . 42
3.2.4 Analysis 4: Predicting symptoms during a haemodialysis session . . . 43
3.3 Results . . . 44
3.3.1 Analysis 1: Overview of association of between MAP and adverse events . . . 44
3.3.2 Analysis 2: Sensitivity, specificity and predictive value of MAP changes for cerebral ischaemia . . . 50
3.3.3 Analysis 3: Modelling total ischaemia AUC during a haemodialysis session . . . 54
3.3.4 Analysis 4: Predicting symptoms during a haemodialysis session . . . 57
3.4 Discussion . . . 58
3.5 Conclusions . . . 60

4 Cerebral autoregulation and vulnerability to ischaemic insults 62

4.1 Introduction . . . 62
4.2 Methods . . . 63
4.2.1 Analysis 1: Cerebral autoregulation limits . . . 64

4.2.2 Analysis 2: Predicting presence of autoregulation and its lower limit 67
4.2.3 Analysis 3: Sensitivity, specificity and predictive value of autoregulation lower limit for cerebral ischaemia 67
4.3 Results 68
4.3.1 Analysis 1: Cerebral autoregulation limits 68
4.3.2 Analysis 2: Predicting presence of autoregulation and its lower limit 75
4.3.3 Analysis 3: Sensitivity, specificity and predictive values of autoregulation lower limit for cerebral ischaemia 78
4.4 Discussion 85
4.5 Conclusion 88

5 Comparison of oscillometric and finger volume-clamp blood pressure measurements in the haemodialysis population 89

5.1 Introduction 89
5.2 Methods 91
5.3 Results 92
5.3.1 Population-level agreement between methods 93
5.3.2 Patient-level agreement between methods 99
5.4 Discussion 104
5.5 Conclusion 106

6 Cardiac Output Measurement 107

6.1 Introduction 107
6.2 Methods 108
6.3 Results 109
6.3.1 Baseline values 109
6.3.2 Trend over haemodialysis 114
6.4 Discussion 118
6.5 Conclusion 119

7 Surrogate measures of continuous blood pressure 120

7.1 Introduction 120
7.2 Methods 122

7.2.1 Pulse transit time processing and analysis . . . 122
7.2.2 Access pressure processing and analysis . . . 124
7.3 Results . . . 127
7.3.1 Pulse transit time . . . 127
7.3.2 Access pressures . . . 141
7.4 Discussion . . . 155
7.5 Conclusions . . . 159

8 Relationship between deterioration in cognitive function testing and intra-dialytic physiology 160

8.1 Introduction . . . 160
8.2 Methods . . . 161
8.3 Results . . . 163
8.3.1 Baseline cognitive function tests . . . 163
8.3.2 Deterioration in cognitive function over 12 months . . . 166
8.4 Discussion . . . 169
8.5 Conclusions . . . 172

9 Prediction of cerebral desaturation on haemodialysis using univariate variables at the population level 173

9.1 Introduction . . . 173
9.2 Methods . . . 174
9.2.1 Data pre-processing . . . 175
9.2.2 Determination of distance between normal and abnormal sessions . . . 177
9.3 Results . . . 179
9.3.1 Visual comparison of univariate physiological variables . . . 179
9.3.2 Haemodynamic variables . . . 179
9.3.3 Indicators of volume status . . . 180
9.3.4 Respiratory and oxygenation variables . . . 181
9.3.5 Statistical analysis . . . 197
9.4 Discussion . . . 207
9.5 Conclusions . . . 208

10 Prediction of cerebral desaturation on haemodialysis using univariate variables at the personal level **209**

10.1 Introduction . . . 209

10.2 Methods . . . 209

10.2.1 Visualisation and Statistical Analysis . . . 210

10.3 Results . . . 212

10.4 Discussion (see in addition discussion of chapters 9 and 11) . . . 225

10.5 Conclusions . . . 226

11 Prediction of cerebral desaturation on haemodialysis using multivariate variables at the personal level **227**

11.1 Introduction . . . 227

11.2 Methods . . . 227

11.3 Results . . . 233

11.3.1 First set of input variables: rSO2 Variance, Pulse, MAP, Peripheral Saturation Variability . . . 233

11.3.2 Second set of input variables: Respiratory Rate, Pulse, MAP, Peripheral Saturation Variability . . . 240

11.4 Discussion . . . 246

11.5 Conclusion . . . 248

12 Conclusions and Future Work **249**

12.1 Primary Objectives . . . 249

12.2 Secondary Objectives . . . 251

Acknowledgments

This project was generously funded by a doctoral research fellowship provided by the NIHR, as well as a fellowship grant provided by the Oxford Health Sciences Research Council. I would like to thank the following people for their time, support, and assistance: Sheera Sutherland, David Meredith, Joanna Carter, Allie Thornley, Andy Mosson, Jon Daly, David Clifton, Mauro Villaroel, Joao Jorge, Alessandro Guazzi, Yasmina Borhani, Peter Watkinson, David Mole and the staff of the Oxford Main Dialysis Unit. Our research nurse, Sheera Sutherland, deserves a special mention for her tireless and exemplary work both at the frontline and behind the scenes: without her, this project would not have been possible. Moreover, I owe a great debt to my supervisors, Professors Chris Pugh and Lionel Tarassenko, for their patience, guidance and inspiration throughout. I would also like to thank my husband Stephen West for his support, advice and useful expertise in mathematics and computing! Most importantly of course, we are forever grateful to our amazing patients for their selfless and enthusiastic participation in our research, for the benefit of others.

Abbreviations

AAMI	US Association for the Advancement of Medical Instrumentation
ANOVA	Analysis of Variance
AUC	Area Under the Curve
AVF	Arterio-venous Fistula
BHS	British Hypertension Society
BMI	Body Mass Index
CVD	Cerebrovascular Disease
DBP	Diastolic Blood Pressure
DTI	Diffusion Tensor Imaging
ECG	Electrocardiogram
ESRF	End-Stage Renal Failure
CVVHDF	Continuous Veno-Venous Haemodiafiltration
CVVHF	Continuous Veno-Venous Haemofiltration
FFT	Fast Fourier Transform
GLM	Generalised Linear Model
HD	Haemodialysis
HDF	Haemodialfiltration
HRV	Heart Rate Variability
KDOQI	Kidney Disease Outcomes and Quality Initiative
KS	Kolmogorov-Smirnov
IDH	Intradialytic Hypotension
IHD	Ischaemic Heart Disease
MAP	Mean Arterial Pressure
MCA	Middle Cerebral Artery
MMSE	Mini-Mental State Exam
MRI	Magnetic Resonance Imaging
NIBP	Non-invasive Blood Pressure
NIRS	Near Infra-Red Spectroscopy
NPV	Negative Predictive Value
OR	Odds Ratio
PET	Positron Emission Tomography
PHQ-9	Patient Health Questionnaire
3MS	Modified Mini-Mental State Exam
PPG	Pulse Plethysmography
PPV (physiology)	Pulse Pressure Variation
PPV (statistics)	Positive Predictive Value
PTT	Pulse Transit Time

PVD	Peripheral Vascular Disease
RBV	Relative Blood Volume
RBF	Radial Basis Function
rSO2	Regional oxygen saturation
RTF	Return to Flow (calibration)
RWMA	Regional Wall Motion Abnormality
SBP	Systolic Blood Pressure
SPECT	Single Photon Emission Computer Tomography
SQI	Signal Quality Index
TTB	Trails Test B

Chapter 1

Introduction and Background

1.1 Objectives

The primary objectives of this thesis are:-

- To model the dynamic relationship between blood pressure, real-time symptoms, and downstream organ ischaemia during haemodialysis, in order to identify the most physiologically grounded, prognostic definition of intra-dialytic hypotension.
- To predict the development of intra-dialytic hypotension and/or cerebral ischaemia using personalised, probabilistic models of multivariate, continuous physiological data, ultimately working towards an early warning system for intra-dialytic adverse events (as defined in part one).

Secondary objectives include:-

- To quantify deterioration in cognitive function over time in haemodialysis patients and make a preliminary estimate of whether this is associated with intra-dialytic hypotension or cerebral desaturation.
- To assess the agreement between Finometer- and oscillometer-derived measures of blood pressure in haemodialysis patients.
- To assess the agreement between Finometer-derived and other potential non-invasive measures of continuous blood pressure (e.g. pulse transit time) in haemodialysis patients.

1.2 Background

The prevalence of end stage renal failure (ESRF) in the UK is 861 per million population[1]. Almost 50% of these patients are supported with haemodialysis (HD), which is often the modality of choice for the increasing number of frail elderly patients with multiple comorbidities, who are not fit for transplantation. Despite advances in technology, many patients experience drops in blood pressure during treatment, often with symptoms suggestive of end-organ hypoperfusion such as dizziness or chest pain. This phenomenon is known as intra-dialytic hypotension (IDH). The pathogenesis of IDH has yet to be fully elucidated. However, factors implicated include excessively rapid ultrafiltration (fluid removal) with inadequate refilling of the intravascular space; suboptimal compensation for ultrafiltration due to autonomic and cardiac dysfunction; and a rise in body temperature with subsequent vasodilation, due to the use of warmed dialysate and the intrinsic generation of heat during dialysis [2].

IDH is certainly a problem: from the patients' perspective, it is associated with disabling symptoms, and from the nursing perspective, it increases workload. However, proving that it is associated with hard outcomes has been problematic. The internationally accepted Kidney Disease Outcomes and Quality Initiative (KDOQI) definition requires an acute drop of 10mmHg in mean arterial pressure (MAP), or 20mmHg in systolic blood pressure (SBP), temporally associated with relevant symptoms: however, this definition has not been proven to correlate with patient outcomes [3].

Only one definition of IDH has been decisively linked with an independently increased risk of mortality, namely an intradialytic SBP nadir below 90mmHg regardless of symptoms, and this from a retrospective review of datasets with limited blood pressure and symptom data [4] . This is likely a surrogate measure for the most severe hypotension. Two earlier epidemiological studies did not prove an independent relationship with any measure of hypotension and mortality [5, 6]. One of these was a large, observational study of Japanese prevalent HD patients: non-invasive blood pressure (NIBP) data was recorded from a single HD session, and then patients were followed up for two years. The authors did report that SBP nadir was significantly associated with mortality, but they did not control for other comorbidities, particularly cardiovascular disease: the paucity of physiological and demographic data available limited any conclusions [5].

Tisler et al performed a similar prospective study in prevalent HD patients, but with superior method-

ology, assessing intra-dialytic stability with data gathered over a 10 month period rather than a single session. IDH was defined a priori as a sudden drop in SBP to <90mmHg or of >30mmHg from baseline, associated with symptoms and necessitating resuscitation. After sound adjustment for confounders, no independent relationship was found between frequency of IDH and mortality. Similarly, a large, multi-centre randomised controlled trial of haemodiafiltration (HDF) versus HD found that whilst the former modality significantly reduced the risk of IDH (SBP <90mmHg, or symptomatic drop in SBP >25mmHg requiring intervention), this did not translate into reduced morbidity or mortality over the subsequent 3 years [7].

Why has it proven so difficult to define the level of hypotension that causes harm? Firstly, haemodynamic status is known to vary considerably between sessions and over time, and in particular there is a different pattern after the "long break" (i.e. 3 as opposed to 2 days) from HD [8]. A surprising majority of studies have attempted to make models and predictions using haemodynamic data from only one treatment, and patients may have been incorrectly classified by these methods.

Secondly, accurate measurement of blood pressure outside critical care is a challenge: most studies of IDH have relied on NIBP, which has a large measurement error, especially in the context of real-world practice, and can only provide very intermittent data [9, 10, 11, 12]. SBP is the most used blood pressure index amongst nurses and clinicians outside anaesthetics and critical care, as reflected by the number of IDH definitions and studies which have focused near exclusively on it [6, 5, 13, 14, 15, 16]. However, non-invasive SBP has a far greater measurement error than non-invasive MAP when compared to intra-arterial readings, and is particularly sensitive to changes in cuff size and position [10, 9, 12]. This may be partly because NIBP devices measure MAP directly, and SBP is then estimated using a manufacturer-specific algorithm. Finger pulse wave methods of estimating blood pressures (e.g. the Finometer) similarly suffer from greater error for systolic readings, as systolic pressures change most between central and peripheral arteries, and to highly variably degree depending on individual vessel stiffness. Systolic pressures are unduly affected by changes in arterial stiffness, which will alter pulse pressures but not necessarily change downstream perfusion pressure. Whilst pulse pressure and systolic pressures may be more prognostic as regards complications of long term hypertension in the elderly, MAP is a more appropriate measure of adequate organ perfusion pressure during hypotension, yet has been relatively ignored in the IDH literature [17, 18].

Thirdly, it must be remembered that blood pressure is not the real index of interest. Returning to physiological principles, measuring blood pressure is useful because it is a surrogate for downstream tissue perfusion pressure, which is a surrogate for adequacy of cellular oxygen supply. Any increase in mortality would be due to repeated end-organ ischaemia: leading to complications such as cardiac failure, cognitive impairment, bacterial translocation across the gut, and ultimately mortality. However, the relationship between systemic blood pressures and tissue oxygen balance is not straightforward. Reductions in regional blood flow may occur without any change in systemic blood pressure, due to compensatory changes in arteriolar and venous tone, and this has been demonstrated even in the HD population [19, 20]. Moreover, reduced regional blood flow does not necessarily lead to cellular ischaemia: this depends on the extent of the fall, the oxygen content of the blood, the functional capillary density, position on the oxygen dissociation curve, cellular oxygen demand and mitochondrial health (i.e. capacity for aerobic respiration) among other factors [21]. Any threshold for ischaemia is likely to vary between organs, and between patients, depending on factors such as intact regional autoregulation.

1.3 Tissue Perfusion

Techniques to bypass systemic blood pressure and look directly at the adequacy of tissue oxygenation are in early stages of development. There have been an explosion of studies investigating the microcirculation and cellular/tissue oxygenation in the critical care literature, including key publications investigating the relationship between MAP, tissue oxygenation and ultimately organ dysfunction or mortality [22, 21]. These studies are generally in the context of animal models or septic shock in critically ill patients [23, 24, 25, 26]. The situation may be different in the outpatient HD population, who are more likely to have intact endothelial function, autonomic function and autoregulation. Given that most methods of measuring the microcirculation (or indeed macroscopic organ function) are invasive, expensive, intermittent or highly operator-dependent, it is likely that blood pressure monitoring will be the standard for routine outpatient HD treatment for the foreseeable future. Bearing this in mind, is it possible to identify which blood pressure thresholds, if any, are associated with end-organ ischaemia or dysfunction in HD patients, in order to find a more physiological and prognostic definition of IDH? There are a paucity of studies which have examined the relationship between systemic blood pressure and either tissue oxygenation, end-organ dysfunction or regional blood flow in HD patients; here I review the existing literature.

1.3.1 Cardiac Perfusion

The majority of relevant studies have chosen the heart as the indicator downstream organ, using direct and indirect measures of cardiac perfusion including ECG, myocardial perfusion scintigraphy, single-photon emission computed tomography (SPECT), echocardiography, PET (positron emission tomography) and MRI. Early studies using continuous ECG monitoring as a rough surrogate for adequate coronary perfusion found that asymptomatic ST depression during HD was a common phenomenon, even in patients with normal coronary arteries [27, 28, 29]. One such study combined online ECG monitoring with SPECT in 10 patients, scanning before and after the HD session, as well as at the onset of any ST depression. They found that asymptomatic ST depression correlated with MAP; however, perfusion defects appeared to have no relationship with either ST depression or blood pressure, frequently being present at baseline, and in some cases resolving during dialysis. Similar results were reported from a crossover study in 20 patients, where scintography was used assess myocardial perfusion during HD as compared to HDF (which generally affords greater haemodynamic stability) [30]. Again most patients had perfusion defects at baseline, which tended to increase in number and size during treatment (regardless of modality) but sometimes resolved. There was no association between perfusion defects and blood pressure. The small numbers and sparse haemodynamic data (infrequent NIBP) limits conclusions from both these myocardial perfusion studies.

In a series of small, single centre studies, a UK group have demonstrated that regional wall motion abnormalities (RMWAs) frequently develop during HD, and that this may be associated with magnitude of blood pressure change [13, 14, 15, 16]. In the largest and most useful study, 70 prevalent patients underwent monitoring with NIBP and two hourly echocardiography for a single dialysis session [13]. Maximum reduction in SBP was significantly associated with the development of RWMAs, along with pre-dialysis (not post-dialysis) troponin, ultrafiltration volume and age. Pre-dialysis troponin and age are likely to be markers of sicker patients with underlying cardiovascular disease, who may be prone to both hypotension and to RWMAs independently. Knowledge of the temporal relationship between these outcomes would be invaluable, but unfortunately echocardiograms and NIBP can only be performed intermittently: therefore, it is equally possible that the RWMAs preceded rather than followed the blood pressure changes. The majority of these patients underwent a second monitored session 12 months later:

it was found that intra-dialytic RWMA development (though not specified if during the baseline or follow up session) was associated with deteroration in resting ejection fraction at 12 months, as well as the composite outcome of mortality and cardiovascular events. Though tantalising, the study was not powered for hard outcomes (only 9 deaths occurred and 3 cardiovascular events, which were not defined), and these outcomes certainly could not be attributed to hypotension.

Two further studies from this group were crossover trials in 10 and 11 patients respectively looking at the impact of cooling dialysate, with each patient being monitored during one session with dialysate at 35 degrees and another at 37 degrees [16, 14, 31]. Within the limits of the small numbers and single level statistical methods (myocardial segments within the same individual being treated as independent entities), cooling was associated with reduced RWMAs, but it was not clear that this was due to greater systemic haemodynamic stability: serious and symptomatic hypotensions were not different between groups, though minor instability with asymptomatic >10% drops in SBP (regardless of pre-dialysis SBP) occurred more frequently in control sessions [16, 14].

Similarly, a number of small studies utilising cardiac MRI or MRI-PET have shown both global and regional drops in myocardial perfusion during dialysis without evidence of haemodynamic instability, though the study patients were few in number [20, 32]. It is possible that cardiac perfusion deficits, however measured, are simply markers of sicker patients with underlying cardiac dysfunction, rather than being a consequence of intra-dialytic hypotension. The relationship of RWMAs with pre- rather than post-dialysis troponin supports this hypothesis [13].

In summary, whether blood pressure changes are necessary or sufficient for RWMA development, or whether any associated hypotension represents cause or effect, remains unclear. The role of the myocardium in generating blood pressure confounds its utility as an indicator organ for hypotension-induced ischaemia.

1.3.2 Cerebral Perfusion

There has long been speculation that haemodynamic instability during HD leads to repetitive cerebral ischaemia and consequent cognitive decline. Whilst there is certainly an association between duration

of HD, ischaemic white matter changes and cognitive dysfunction, the evidence is of causation is weak. Cognitive impairment and white matter abnormalities are independently associated in a dose-related fashion with renal impairment per se, likely due to increasing burden of cerebral small vessel disease disease [33, 34, 35, 36]. Patients with cardiovascular disease may be both unstable on dialysis and prone to subcortical cerebrovascular disease independently. It has been shown that HD patients with subcortical white matter hyperintensities are at significantly greater risk of all cardiovascular events, independent of traditional risk factors [37].

Validated cognitive function tests are be a convenient, non-invasive and clinically important measure of end-organ damage. A recent cross-sectional study found no independent association between intra-dialytic blood pressure (using data from 12 sessions) and current cognitive function [38]. Another cross-sectional study using data from the Frequent Hemodialysis Network trials reported similar findings: whilst cognitive impairment and in particular executive dysfunction was common in HD patients, there was no independent link with intra-dialytic haemodynamic measures [39].

An alternative approach to functional testing is cerebral imaging. A number of studies have found an association between HD vintage and the burden of white matter abnormalities on MRI, particularly subtle changes on diffuser tensor imaging (DTI) [40, 41, 42, 43]. Promising data comes from a single-centre trial where 38 incident dialysis patients were randomised either to dialysis at 37 degrees or at 0.5 degrees below core body temperature, and followed up for the development of white matter abnormalities [43]. They underwent DTI MRI and continuous blood pressure monitoring (for a single session) at baseline, and again after 12 months of HD. The patients who had not undergonecooling had significantly more white matter ultrastructural abnormalities relative to their personal baseline. Whilst cooling is expected to improve haemodynamic stability by increasing peripheral vasoconstriction and venoconstriction, no difference was seen in blood pressure between groups in the monitored sessions, even using the very sensitive definition of a drop of SBP of >10% from baseline. However, there was limited haemodynamic data, and it cannot be assumed that the single monitored session at baseline was representative of the subsequent 155 treatments, on average, to which each patient would have been exposed during the intervention period. The clinical significance of these white matter changes was not assessed.

Proving a causative relationship between white matter ultrastructural abnormalities and IDH is dif-

ficult: these imaging techniques do not allow real-time/continuous monitoring, corresponding haemodynamic data is typically sparse, and most studies are cross-sectional. Moreover, whilst DTI is very sensitive and specific for detecting ultrastructural changes in white matter, it cannot give an indication as to pathogenesis: the indexes derived from DTI, e.g. fractional anisotropy, indicate a loss of structural integrity of nerve axons, which can be the end result of diverse processes including demyelination, inflammation, oedema or ischaemia [40, 44]. Most studies have not explored the clinical significance of any radiological abnormalities detected, though some have been able to demonstrate an association between DTI detected white matter changes and measures of executive function and processing speed in HD patients [41, 44].

In a different approach, Kobayashi et al looked directly at regional cerebral blood flow in 54 prevalent HD patients using SPECT, and correlated this with cognitive function. They reported a general reduction in blood flow compared to healthy controls, which worsened with HD vintage. Unfortunately, there was no intra-dialytic physiological data to indicate whether this was associated with blood pressure changes [45]. Mini mental state exam (MMSE) score did not correlate with blood flow, but this is not a sensitive test for cognitive impairment in HD patients, in whom the dysfunction is largely executive [46, 47].

Some investigators have assessed the relationship between blood pressure and cerebral blood flow during dialysis with transcranial Doppler (applied by a skilled operator over the middle cerebral artery (MCA)), with mixed results. Most, but not all, studies report a decrease in MCA blood flow velocity with HD [48, 49, 50, 51]. A major confounding factor is ultrafiltration-induced haemoconcentration, which will alter velocity independently of oxygen carrying capacity. Another weakness of transcranial Doppler is that measurements are usually intermittent, due to the requirement for a trained operator and careful positioning of the probe. Two investigators have successfully performed transcranial Doppler continuously throughout dialysis, finding that velocity is highly correlated with ultrafiltration volume and blood volume changes, but not with blood pressure. [52, 53].

Near-infra-red spectroscopy (NIRS) is a continuous, non-invasive and automatic technique for measuring tissue oxygenation which has existed for decades, but has only recently come into its own following improvements in technology and awareness. Cerebral oximetry, or cerebral NIRS, relies on the fact that

infrared light can penetrate the skull: changes in haemoglobin oxygen saturation in the frontal cortex are estimated from the absorption of different wavelengths of near-infrared light by oxygenated and de-oxygenated haemoglobin [54]. NIRS has been shown to correlate well with more invasive or operator dependent measures of cerebral perfusion, including transcranial Doppler and functional MRI [55, 56]. To date, there has been limited data on the use of NIRS in dialysis patients. In agreement with SPECT studies, baseline tissue oxygenation as measured by cerebral NIRS has been found to be significantly lower in dialysis patients than normal controls, and may correlate with HD vintage [57, 58, 59]. A case report described the use of real-time cerebral NIRS in a HD patient with carotid stenosis [60]. Cerebral tissue oxygenation was found to drop in tandem with blood pressure until surgical revascularisation. Only one other study has monitored cerebral NIRS during HD, for a single session in 18 consecutive patients: cerebral oxygenation was unchanged and did not appear to be associated with blood pressure, but there was no haemodynamic instability (and again only infrequent NIBP measurements) [57].

1.3.3 Splanchnic perfusion

The gut has been used as another "indicator" organ of hypoperfusion during HD. The splanchnic circulation may be compromised early in order to direct blood to more vital organs such as the brain and heart. In a crossover study using radiolabelled erythrocytes, Yu et al demonstrated contraction of the splanchnic circulation during rapid ultrafiltration on dialysis, but not during dialysis without fluid removal [61]. This was a small study of 8 prevalent HD patients, and there was no haemodynamic instability in any sessions.

There has been speculation that elevated endotoxin levels in HD patients may be due to asymptomatic gut ischaemia during treatment, leading to bacterial translocation across the gut wall. If confirmed, this would be a convenient, non-invasive marker of end-organ ischaemia, which could be retrospectively correlated with blood pressure. However, endotoxin levels may be influenced by a myriad of factors beyond gut ischaemia; renal impairment itself is associated with endotoxaemia, possibly due to phagocyte dysfunction (reduced clearance), fluid overload (with gut oedema), and increased incidence of cardiovascular disease [62]. Once established on HD, the dialysis water serves as a second source of endotoxin [63]. This, together with reduced residual renal function, is likely to account for a reported jump in endotoxin levels in 18 incident HD patients [64]. A cross-sectional study reported that pre-dialysis, but not post-dialysis, endotoxin levels were associated with the development of RWMAs and maximum SBP or DBP drop

(assessed by NIBP) [64]. This suggests confounding by comorbidities: pre-existing cardiac dysfunction, vascular disease, fluid overload or reduced residual renal function may predispose to both endotoxaemia and haemodynamic instability on HD. Moreover, peritoneal dialysis patients, whose treatment does not involve haemodynamic changes, had equally high levels of endotoxin [64]. Therefore it would appear that endotoxin levels are not a reliable marker of gut hypoperfusion.

A study by Jakob et al has provided rare and invaluable direct measurements of splanchnic blood flow and oxygen extraction during dialysis, albeit in acute renal failure [19]. Pulmonary artery, femoral artery, femoral vein, radial artery and hepatic vein catheters were inserted into 9 haemodynamically stable patients undergoing HD in a critical care environment. Splanchnic blood flow was estimated by infusing indocyanine green dye via the femoral artery, resampling at the hepatic vein and radial artery, and applying the Fick principle (see [65] for method). Cardiac output was estimated using thermodilution (Fick principle) via the pulmonary artery catheter. Systemic and regional oxygen consumptions were estimated as the product of the relevant blood flow and arterio-venous oxygen difference. In addition, the adequacy of tissue oxygenation was simultaneously estimated using gastric tonometry. Gastric tonometry is essentially a method of measuring gastric CO2 levels, which reflect mucosal PCO_2 levels. When there is inadequate mucosal perfusion, cells switch to anaerobic respiration, with accumulation of lactic acid: the excess of hydrogen ions translate to a rise in tissue CO2 production. Arterial pH and PCO_2 are measured to adjust for any systemic changes. The authors found that stroke volume and splanchnic blood flow fell during dialysis but blood pressure was maintained, reflecting a compensatory increase in venoconstriction and peripheral vasoconstriction, and possibly redirection of blood elsewhere. Elegantly demonstrating that reduced blood flow or perfusion does not necessarily equal ischaemia, splanchnic oxygen consumption and gastric tonometry measures did not change. There is one other study of gastric tonometry in dialysis, which concluded that HD patients significantly higher baseline gastric CO2 compared to controls (controlling for systemic pH), but there was no corresponding haemodynamic data [66].

1.3.4 Other

Hinchliffe et al performed continuous transcutaneous oxygen tension on the dorsum of the foot of 10 diabetic patients, and found a non-significant trend to reduced oxygenation during haemodialysis, but no haemodynamic data was gathered. [67].

1.3.5 Section Summary

In summary, the existing dialysis literature is of limited guidance in developing an evidence-based definition for IDH, and has not reliably identified a blood pressure threshold associated with either tissue ischaemia or hard outcomes such as mortality. Notably, the role of symptoms as a potentially valuable indicator of tissue hypoxia has not been investigated at all. The limitations of NIBP frequently impact on the quality of research in this area, and an affordable method of non-invasive continuous blood pressure measurement is highly desirable. Techniques to bypass systemic blood pressure and look directly at the adequacy of tissue oxygenation are in early stages of development, and with the possible exception of NIRS, they would not be suitable for routine outpatient dialysis monitoring.

1.4 Preventing adverse events on haemodialysis

There are various potential strategies to both predict and prevent hypotension during dialysis, most of which have been extensively reviewed in recent literature [68, 69]. Interventions to counteract haemodynamic instability include varying the dialysate sodium concentration, cooling the dialysate, reducing the speed of ultrafiltration or adding in a convective component to treatment (i.e. HDF). If frank decompensation occurs, the patient is usually lowered into the Trendelenberg position and given a fluid bolus. Ideally intervention should occur before this point, and a number of physiological parameters have been investigated for their potential to offer early warning of deterioration. Variables which have been reported to predict intra-dialytic haemodynamic instability include relative blood volume (RBV), variability of peripheral saturations, heart rate variability (HRV), amplitude of the pulse plethysmogram (PPG), blood pressure trend, or non-invasive surrogates for continuous blood pressure including pulse transit time (PTT) [70, 71, 72, 73, 74, 75, 76]. RBV is essentially the change in haematocrit from baseline, and reflects intravascular refilling from the interstitial space in response to ultrafiltration. Of these predictors, only RBV and blood pressure have been prospectively tested in patients; the others remain theoretical, derived using machine learning techniques applied retrospectively to small databases. Patient and event heterogeneity are problematic: for example, the RBV at which decompensation occurs is hugely variable, certainly between (and probably within) patients, and can be confounded by other

physiological factors [70].

There have been a number of trials of "biofeedback dialysis", where an input signal with information about the patient's physiology is used to adjust the dialysate conductivity or ultrafiltration rate accordingly, in order to prevent overt hypotension [76]. The input is occasionally blood pressure (which problematically becomes both predictor and outcome) but more commonly RBV, which can be measured online and continuously. There is considerable disagreement as to the predictive value of RBV changes [70, 77]. Nevertheless, a recent meta-analysis of existing biofeedback trials found that overall, biofeedback dialysis did appear to improve haemodynamic stability (albeit very variably defined), but warned that the studies were small and of poor quality, with no hard outcomes [76].

Cooled dialysate and convective modalities can improve cardiovascular stability compared to standard diffusive dialysis with dialysate temperature at 37 degrees [78, 69]. The improved haemodynamic stability seen with convective techniques is probably due to a cooling effect [79]. Cooling and online HDF are not more expensive than standard dialysis [80] . Although cooling is generally well tolerated, some patients will develop unpleasant symptoms related to falling body temperature. Cooling and convection are slow acting interventions, and thus cannot easily be applied in response to deterioration as part of a biofeedback loop: rather they are set as part of the fixed dialysis prescription and applied throughout treatment, regardless of physiological information.

Similar to the biofeedback techniques, both HDF and cooling reduce rather than abrogate adverse events [81, 7, 69]. For example, a real-world, prospective, observational study comparing cooled dialysis to HDF found that 16.5% and 25.9% of sessions respectively were still affected by IDH [81]. In addition, as with biofeedback dialysis, HDF and cooling have not been shown to improve hard outcomes. This may be because most studies have looked at preventing hypotension rather than preventing ischaemia or organ dysfunction, which might be expected to correlate more closely with morbidity and mortality. The exceptions are the small cooling trials discussed above, whose primary outcomes were markers of end-organ damage, but these were not powered to examine long term morbidity or mortality [43, 14, 16, 31].

The heterogeneity of the underlying pathogenesis of dialysis-induced hypotension and/or ischaemia may be responsible for the mixed results in the predictive and interventional studies. Any one physio-

logical variable is unlikely to reliably anticipate hypotensive/ischaemic events in every session in every patient, and similarly any one intervention is unlikely to be appropriate for all adverse events. It is unrealistic to prevent all IDH, given that intra-dialytic fluid gains (reflecting patient salt intake) may sometimes be too large to allow safe removal over 4 or 5 hours by any technique. Cooling may particularly benefit patients with impaired autonomic function, who are sensitive to heat-induced vasodilation, whereas reduced ultrafiltration would be more suitable for patients that have become truly intravascularly deplete. The physiology of these two groups of patients would be quite distinct. The ideal would be a system that could detect early deviation from the expected, compensated physiological trajectory for a given ultrafiltration volume in a given patient, using multiple physiological inputs.

A precedent for this approach is a so called "data fusion" algorithm developed in the Institute of Biomedical Engineering at Oxford University, which may have value in the early identification of critically ill patients [82]. This algorithm fuses five vital signs (blood pressure, pulse, respiratory rate, oxygen saturation, skin temperature) and compares the distributions of these vital signs (in a five dimensional space) with a pre-defined normal zone: when a threshold deviation from normality is reached, an alert is generated, allowing pre-emptive medical intervention. Preliminary clinical data suggests that the combination of physiological inputs provides an earlier and more sensitive warning of patient deterioration [83, 84]. As HD is a relatively reproducible physiological event that takes place in the same patient multiple times, it should be possible to identify which physiological patterns are normal for an individual patient, and which precede the occurrence of symptoms and clinical events.

1.5 Summary

Intra-dialytic haemodynamic instability is a common and disabling problem which increases nursing workload, but there is no definition which consistently or strongly associates with hard patient outcomes. There are interventions which can prevent intra-dialytic instability, but to optimise performance they need to anticipate the onset of hypotension, and be tailored to the underlying physiological abnormality. A number of approaches have been taken to predict the onset of hypotension using univariate physiological parameters at the population level, but results have been mixed.

A more physiological approach would be to look beyond intra-dialytic blood pressure at intra-dialytic

organ perfusion and oxygenation, which would be expected to correlate more closely with morbidity and mortality. Given the ease and familiarity of measuring blood pressure over the complexity and expense of measuring tissue oxygenation, it would be ideal if the blood pressure threshold typically associated with downstream tissue hypoxia in HD patients could be identified. However, the literature investigating end-organ ischaemia or dysfunction during HD is sparse, and there is not enough data for such an estimate. Moreover the threshold is likely to vary substantially between patients, particularly given the huge heterogeneity of the dialysis population. The ideal would be to anticipate and prevent end-organ ischaemia itself rather than its surrogate hypotension. There are precedents to suggest that a multivariate physiological model, particularly one personalised to the individual patient, would have superior predictive power to the current univariate approaches.

To recap the primary objectives of this thesis, therefore:-

- To model the dynamic relationship between blood pressure, real-time symptoms, and downstream organ ischaemia during haemodialysis, in order to identify the most physiologically grounded, prognostic definition of intra-dialytic haemodynamic instability.
- To predict the development of intra-dialytic hypotension and/or cerebral ischaemia using personalised, probabilistic models of multivariate, continuous physiological data, ultimately working towards an early warning system for significant intra-dialytic adverse events (as defined in part one).

Chapter 2

Generic Methods and Data collection

2.1 Trial Structure

All patients were eligible provided they had been established on HD for at least a month, were over 18 years of age, and were able to give consent. In total, 60 patients were recruited. The majority of patients (39) were unstable, defined as the need for nursing intervention (regardless of symptoms) on at least two occasions in the month preceding the study. The remainder were recruited as more stable controls for comparison and underwent slightly less monitoring, as outlined below. Continuous physiological data was prospectively gathered from each patient on consecutive HD sessions for a month, aiming for a minimum of 9 monitored treatments per patient. Ultimately, data was gathered from 635 HD sessions in 58 of patients: 85% of unstable patients and 81% of stable patients had successful data collection from 9 or more sessions.

At baseline all patients underwent physical assessment of dry weight, cognitive assessment using the modified mini-mental state test (3MS) and the Trail Making Test B (TTB), and screening for depression using the Patient Health Questionnaire (PHQ-9). Demographic data gathered included: age, sex, HD access (central line (Tesio) or arterio-venous fistula (AVF)), HD vintage, ESRF vintage, renal diagnosis, presence/duration of diabetes, cerebrovascular disease (CVD, i.e. previous transient ischaemic attack or stroke), known ischaemic heart disease (IHD, categorized into medically managed, need for angiographic intervention and need for surgical intervention), presence of peripheral vascular disease (PVD), current medications, erythropoetin responsiveness (index based on dose/weight), alcohol and smoking history, education level, socioeconomic class, marital status, exercise tolerance, independence of activities of daily

living and dialysis prescription. Laboratory data included serum albumin, haemoglobin, calcium, and dialysis adequacy (kt/V, a dimensionless measure of clearance normalised to body water volume).

All patients were followed up for two years after enrolment, with short cognitive tests repeated at 12 months if still alive.

All patients underwent monitoring of:

- Continuous blood pressure (volume-clamp method, Finometer Pro or Finometer Midi, Finometer Medical Supplies)
- Continuous cerebral tissue oxygenation (Cerebral NIRS, INVOS system, Covidien)
- 30 minute NIBP (Oscillometry, BBraun)
- Continuous RBV and access saturations (Crit-Line, Fresenius)
- Continuous dialysis machine parameter monitoring including access pressures, ultrafiltration rate/volume, blood flow and dialysate flow (Nexadia software, Braun).

The unstable patients were additionally monitored for:

- Continuous cardiac output (Finometer Pro, calibrated by ultrasound dilution performed at baseline and 2 hours, Transonic HD03 monitor, Kimal)
- Respiratory rate, ECG, PPG, PTT and pulse oximetry (Visi Black Shadow, Stowood Scientific Instruments)
- Real-time recording of type, onset and offset of symptoms, with a patient-friendly computer interface and response pad (Cedrus handset with Superlab software)

Any symptoms in the stable group were recorded on paper notes. If the Finometers failed for any reason, NIBPs were taken every 15 minutes until resolution. If patients required nursing attention or intervention for symptoms, they were able to attract the attention of their dialysis nurse with their call

bell as usual. Dialysis nurses made medical records as per standard practice on a purpose-designed flow sheet: data gathered included nursing interventions (e.g. saline infusion, bed tipping, slowing down ultrafiltration rate), symptoms reported and any concerns about the patient. As part of a related study, the unstable patients were also filmed during dialysis with a high resolution camera. One computer was used as a time server to all other devices in order to ensure that the multiple data streams were tightly synchronised. The Crit-Line monitor alone could not be linked into the multiple computer network, but was synchronised with the time server every morning. Any paper-recorded symptoms alone had potential for error, but where accompanied by an intervention, the timestamp could be confirmed from changes in dialysis machine parameters.

2.1.1 Dialysis procedures

Outpatient HD or HDF treatments on our unit are performed Monday to Saturday with three slots every day: the morning group starts at 7am, the afternoon group at 12 noon, and the twilight group at 5pm. Eight individuals underwent HDF and the remainder HD, all with Dialog+ Haemodialysis Systems, (BBraun). For HD we used high flux BBraun Diacap polysulfone dialysers, either the PS18 High (membrane area 1.8m^2, K_{UF} 55 ml/hr/mmHg, K_0A 911 ml/min) or PS20 High (membrane area 2.0m^2, K_{UF} 58 ml/hr/mmHg, K_0A 1005 ml/min) depending on clearance requirements. For HDF we used the Fresenius polysulfone FX100 dialyser (membrane area 2.2m^2, K_{UF} 73 ml/hr/mmHg, K_0A 1351 ml/min).

No alterations were made to usual dialysis prescriptions: blood flow (Qb), dialysate flow (Qd), acid concentrate, and the filter itself were individualised according to patient characteristics and monthly bloods, including KT/V. Qd was 500-800ml/min in all cases. Qb for tesios was usually 250-300ml/min, and for arteriovenous fistulae 250-400ml/min depending on fistula characteristics and clearance requirements. The acid concentrates in use (BBraun) could provide a dialysate sodium 135-140mmol/L, potassium 2-4mmol/L, ionised calcium 1.25-1.75mmol/L, magnesium 0.5-1.0mmol/L, acetate 2-3mmol/L, chloride 100-116mmol/L, and glucose 1g/L. Bicarbonate was provided with the BBraun Sol-cart B cartridge, which produced a dialysate bicarbonate of 32-36mmol/L. The temperature of the dialysate was matched to the temperature of the patient (measured using ear probe at the start of each session) except for those with repeated intra-dialytic hypotension, in which case it would be set to 1°C lower than body temperature. For patients undergoing HDF, replacement fluid was given pre-dilution at a starting rate

of 30% of Qb, increased up to 60% of Qb if needed for clearance. The main reason for switching from HD to HDF in our unit is refractory intra-dialytic hypotension despite cooling of dialysate, usually in those with severe cardiovascular disease.

Clinical staff and patients were blinded to all data except RBV and NIBP, so this could not influence symptom reporting or intervention. Oscillometry was performed automatically every 30 minutes and displayed on the front of the dialysis machine.

2.2 Measurement techniques

2.2.1 Finometer

Continuous blood pressure monitoring was achieved using Finometer devices, which detects blood pressure using volume clamp technology [85]. The patient wears a finger cuff which incorporates an inflatable bladder in combination with an infra-red plethysmograph. The point of maximum arterial unloading is determined, i.e. when cuff pressure equals intra-arterial pressure so that transmural pressure across the arterial walls is zero. The arterial diameter at this cuff pressure is estimated from the absorption of infra-red light. The artery is then "clamped" at this diameter by varying the cuff pressure so as to dynamically unload the finger arterial walls: the cuff pressure is therefore an indirect measure of intra-arterial pressure. There are regular automatic recalibrations of arterial size to compensate for changes in smooth muscle tone and haematocrit, so-called Physiocal calibrations. The interval between calibrations is determined by the signal quality and stability. A transforming function is applied to the finger arterial pressure waveform to estimate the brachial arterial pressure waveform, and a height sensor corrects for position of the finger relative to the heart. The Finometer devices have been extensively validated against intra-arterial measurements in several populations [86, 87, 88, 89, 90, 91, 92, 93]. They have also been used by a number of groups to monitor continuous blood pressure in the dialysis population, in whom readings correlate reasonably well with blood pressures measured by non-invasive oscillometric techniques [20, 94, 95, 31]. The more recent Finometer models use "Return to Flow" (RTF) calibration to refine the absolute systolic estimate, which has the most error (due to differences in pulse pressure between patients). An upper arm cuff occludes the brachial artery completely, and the arm cuff pressure at which flow returns to the finger signals the systolic intra-arterial brachial pressure, allowing adjustment of the

Finometer estimate. All unstable patients in the trial underwent regular RTF calibrations. Although most of the stable patients used an earlier model of the Finometer, absolute mean and diastolic pressures (as well as trends for all indices) have been shown to meet British Hypertension Society (BHS) and US Association for the Advancement of Medical Instrumentation (AAMI) standards even without RTF calibration [87].

The Finometer gives an estimate of continuous cardiac output measurement derived from a pulse contour analysis algorithm, with estimation of aortic diameter refined by demographic data [85]. However, the Finometer is better at detecting relative changes in cardiac output, and a gold standard method is still needed to obtain absolute values [96, 97]: we therefore used ultrasound dilution to calibrate the Finometer cardiac output, as outlined below.

In this trial, the Finometer finger cuff was sized to the individual patient, and positioned on the non-AVF arm. Hand warmers were used when necessary to improve signal. Fingers were rotated for patient comfort.

2.2.2 Transonic monitor

In dialysis patients dialysing via an AVF, ultrasound dilution (measured using a Transonic device) is a validated technique for acquiring accurate absolute values for cardiac output, but it can only be done intermittently [98]. The blood flow through the dialysis circuit is set at a fixed rate (200ml/min). A known volume of warmed saline is injected into the dialysis venous line, just before re-entry into the patient's circulation. This bolus then circulates through the patient, mixing fully in the left atrium, and returning to the dialysis arterial line. Doppler is used to measure the speed of blood flow in the venous and arterial lines over a minute following the injection. Reduced haematocrit resulting from a fluid bolus will proportionally increase the speed of flow depending on how much the fluid has diluted the blood. For the blood returning to the arterial line, this depends on the flow of blood at the point of maximum mixing, i.e. the cardiac output. Comparing the signal at the arterial and venous lines allows the ratio of dialysis circuit flow to cardiac output to be calculated. This technique can only be used where there is no access recirculation, i.e. a well functioning arteriovenous fistula. In suitable patients, we used ultrasound dilution to calibrate the Finometer cardiac output readings at 0 and 2 hours into each session.

2.2.3 Near-infrared Spectroscopy

Cerebral NIRS (Covidien, INVOS device) was used as a continuous, non-invasive measure of cerebral tissue oxygenation during HD, providing a measure of the adequacy of major organ perfusion downstream from blood pressure. Cerebral NIRS relies on the fact that infra-red light can penetrate the skull: changes in haemoglobin oxygen saturation in the frontal cortex are estimated from the absorption of different wavelengths of near-infra-red light by oxygenated and deoxygenated haemoglobin [54]. The INVOS device uses two wavelengths of light at 730 and 810 nm, either side of the isosbestic point (the wavelength absorbed equally well by oxygenated and deoxygenated haemoglobin). In addition, it uses two photodiode detectors at a distance of 3 and 4 cm, a technique called spatially resolved spectroscopy. The light reaching the proximal detector has taken a shallower course through the more superficial tissues such as the scalp and skull, whilst the signal at the distal detector has passed through both superficial and deep tissues: by subtracting the proximal from the distal signal, the oxygen saturation from cortical tissues can be isolated. Scattering of light by the skull and other tissues means that the true path length of light is not known, therefore it is difficult to estimate absolute values of oxygenated haemoglobin, though there are a number of algorithms in use to model scattering.

Cerebral NIRS has been shown to correlate well with more invasive or operator dependent measures of cerebral perfusion, including transcranial Doppler and functional MRI [55, 56]. Moreover desaturation detected by NIRS is associated with hard outcomes. In surgical populations, the length and severity of intra-operative cerebral desaturation as measured by cerebral NIRS correlates with post-operative decline in cognitive function, as measured by the MMSE and similar tests [99, 100, 101, 102]. In addition, cerebral desaturation appears to correlate with measures of other organ failure (eg length of intensive care stay, cardiac events, ventilator days and acute kidney injury) suggesting that the brain may serve as a useful index organ, in other words, that cerebral tissue oxygenation is a marker of a more widespread systemic insult [103, 104, 105, 106]. There are not enough randomised controlled trials yet to be certain that improving NIRS-measured tissue oxygenation improves outcomes, but summated results are promising [107]. There is increasing experience with cerebral NIRS as a monitor of cerebral oxygenation in non-surgical situations, eg after stroke or traumatic brain injury, during exercise, and at altitude [108, 109].

The INVOS sensor was placed on one side of the forehead, after cleaning of the skin. If the case of previous anterior circulation stroke, the non-affected hemisphere was chosen. All patients underwent clinical examination for carotid stenosis at baseline, and if positively identified, the opposite hemisphere was used. There was a large range of baseline cerebral oxygenation values. Therefore we did not use absolute but relative change in oxygenation from baseline to allow comparison across the population.

2.2.4 Visi Black Shadow

The Visi Black Shadow (Stowood Scientific Instruments) is a small portable monitor which was used to gather continuous three lead ECG, finger PPG, pulse oximetry and respiratory rate (using an individually fitted inductance belt). PTT was also outputted using an algorithm based on the distance from the R wave to the PPG upstroke.

2.2.5 Cognitive function tests

The 3MS is a test of global cognitive function including concentration, language, praxis, and memory. The TTB is a test of executive function, cognitive flexibility and processing speed. The PHQ-9 is a validated screening tool for depression, which may affect performance on the 3MS and TTB. Most investigators have found that cognitive dysfunction in dialysis patients is largely executive, eg. planning, managing time and space [35, 47]. Although the MMSE and 3MS have been widely validated as measures of global cognitive function, with components for orientation, language, attention and memory, they are less sensitive for detecting executive dysfunction. Conversely, the Trails Tests specifically assess executive function and processing speed. All of these assessments have been employed extensively in the dialysis population [110, 111, 47, 39]. They are not significantly different before and after dialysis, and repeatability is reasonable [46, 112, 113].

2.3 Signal Quality Indexes (SQI)

2.3.1 Finometer SQI

The Finometer waveform (data recorded at 200Hz) was divided into 30 second windows, with a sliding interval of 5 seconds. Physiocal calibrations were detected by searching for a square wave signal. The interval between Physiocal calibrations depends on the quality and stability of the PPG signal, and each calibration takes approximately 2 seconds. If more than 7.5 seconds in a given window consisted of calibrations, an SQI of 0 (poor) was assigned. The remaining windows underwent removal of outliers (+/- 3 standard deviations from the mean amplitude for each window): if there was more than 0.5 seconds of outlying values, an SQI of 0 was assigned. A peak detector was then applied using a maximum/minimum threshold technique, with an initialisation period of 1.5 seconds to detect a sample peak and trough: subsequent peaks were discounted if they did not reach 40% of the preceding peak-trough amplitude. Windows with a physiologically implausible heart rate were assigned an SQI of 0. The waveform quality of remaining windows was assessed with a correlation method: the minimum acceptable average correlation coefficient was set at 0.8.

2.3.2 Belt SQI

The SQI for the belt waveform was based on the combination of two methods for assessing the degree of sinusoidality, and was originally designed by Dr David Clifton at the IBME, Oxford University, with some adaptations for the current data. The belt waveform was detrended and subject to a low pass filter, after removal of extreme outliers (+/- 2 standard deviations from the mean amplitude for an entire session recording). The waveform was analysed in 60 second windows. The 4096 point discrete Fourier transform (FFT) for each window of filtered waveform was calculated (belt data recorded at 64Hz, so there are 3840 data points over 60 seconds, and the next power of 2 is 4096). Cut-off points were chosen as the frequencies corresponding to breathing rates between 8 and 35. The spectrum between these cut-offs was divided into 0.0624Hz intervals (roughly 4 breaths per minute), and the power summed for each interval. The interval with the maximum summed power was selected, and the summed power for this interval was divided by the total summed power for all intervals. This was the first signal quality indicator (SQI-FFT). The waveform was then downsampled to 2 Hz using spline interpolation, and the autoregression spectrum and poles (using order 7) found for each downsampled window. The breathing rate was taken

as the dominant pole between frequencies corresponding to 8 and 35 breaths per minute. The autoregression calculation was repeated using order 5 in order to establish the two most dominant poles. The second quality measure was the amplitude of the dominant pole (i.e. the estimated the breathing rate) divided by the amplitude of the second largest pole (SQI-AR). The combination of an SQI-FFT >0.3 and SQI-AR >1.1 and <2.7 was required for a window of belt waveform to be assigned an SQI of 1 (good).

2.3.3 PPG SQI

The PPG waveform was analysed in 15 second windows, with a 5 second sliding interval. Extreme outlying values were removed (+/- 2 standard deviations from the mean amplitude for an entire session recording). A peak detector was then applied using a maximum/minimum threshold technique, with an initialisation period of 1.5 seconds to detect a sample peak and trough: subsequent peaks were discounted if they did not reach 30% of the preceding peak-trough amplitude. Windows with a physiologically implausible heart rate were assigned an SQI of 0. The quality of the waveform of remaining windows was assessed with a correlation method: the average correlation coefficient between beats had to be 0.8 or above for the window to be assigned an SQI of 1.

2.3.4 ECG SQI

The ECG was analysed in 120 second windows, with a 30 second sliding interval. The raw ECG was band pass filtered between 3-25Hz to remove low and very high frequency noise (mains frequency, muscle tremor). Although the cardiac frequency falls below the lower limit, any QRS complexes are sufficiently large by comparison to the baseline wander that they are attenuated rather than removed. The filtered data was then differentiated, squared and integrated to exaggerate the signal from QRS peaks. A peak detector based on a modification of the Hamilton-Tomkins algorithm was used [114]. Once peaks were detected on the filtered ECG signal, the amplitude and width of the associated QRS complex was compared to that expected for a QRS complex in that patient. If the peak passed this assessment, the morphology of the QRS complex was compared to previous complexes. Only if the correlation was sufficient was the peak deemed to be a true "R". QRS complexes that were too wide, too high, or otherwise failed the correlation criteria were labelled as low quality complexes. Peaks in the signal that were three times higher than the maximum expected for a QRS were labelled as artefact (likely to be due to movement).

If a 120 second window was identified as having more than 10 low quality complexes , or more than 10 physiologically implausible or outlying RR intervals (more than 2.58 standard deviations away from the mean for that window), then that window was not used for analysis.

2.4 Demographics

The demographics and baseline parameters for the 60 recruited patients are shown in Table 2.1.

2.5 Statistics and Modelling Overview

Statistical modelling and analysis was all done with the programmes Matlab and R. The detailed methodology for each individual question is outlined in the relevant results chapter, but an overview is given here.

In all cases, statistical significance was considered to be a p value of 0.05 or less. Correlation statistics, linear regression and Bland-Altman plots were used to assess the agreement between different methods of measuring the same physiological variable. For simple comparison of means of normally distributed continuous variables, the appropriate Student's t test was used. If the variable was continuous but not normally distributed, the Wilcoxon rank sum or Kolmogorov-Smirnov test was used to detect location shift. The Pearson's chi squared test was used to compare counts of categorical variables between groups. Performance of binary classifiers was assessed using ROC curves (sensitivity and specificity) and recall-precision curves (sensitivity and positive predictive value (PPV)), e.g. MAP threshold to classify presence or absence of cerebral ischaemia.

Linear regression was used to model continuous outcome variables, after appropriate transformation of covariates to ensure a linear relationship with the dependent variable. Ordinary least squares was used to estimate covariates. Goodness of model fit was initially assessed with the adjusted R^2 measure (essentially the proportion of total variance which is explained by the model, adjusted for the number of covariates). Checks were performed to ensure normal distribution and homoscedasticity of residuals. Competing models were compared for goodness of fit to the data using the log likelihood ratio statistic, tested against a chi square distribution. Where there were multiple measures within the same patient, multilevel linear regression was tested.

Table 2.1: Demographics

Age [years (median, IQR)]		60.0 (51.5-76.0)
Sex (% male)		76.7
Race (% Caucasian)		86.7
Duration ESRF [years (median,IQR)]		20.5 (7.5-42)
Duration HD [months (median, IQR)]		19 (5-41)
Renal Diagnosis (%)	Diabetic Nephropathy	21.7
	Hypertensive/Renovascular Disease	16.7
	Glomerulonephritis	31.7
	Polycystic Kidney Disease	3.3
Access (%)	Tesio	26.7
	Fistula	73.3
Regular Alcohol Consumption (%)		15.4
Current Smoker (%)		20.0
Marital Status (%)	Married/Partner	46.7
	Widowed/Separated	33.3
	Single	20.0
Education (%)	O level/equivalent or above	60.0
	A level/equivalent or above	35.3
	University level	16.7
Socioeconomic class* (%)	Class 1-2	26.7
	Class 3	28.3
	Class 4-5	45.0
Known CVD (%)		15.0
Known IHD (%)		30.0
Known PVD (%)		8.3
Diabetes (%)	Any form	38.3
	Insulin dependent	16.7
	Type 1	10.0
Anti-hypertensives (%)	ACE/ARB	20.0
	Beta Blocker	21.7
	Other	40.0
Darbopoetin Dose (%)	Responsive (<0.45 mcg/kg/week)	55.0
	Intermediate	35.0
	Resistant (>1 mcg/kg/week)	9.9
Statin use (%)		65.0
Anti-platelet use (%)		50.0
Haemoglobin [g/dL (median, IQR)]		11.05 (9.2-12.8)
Total Calcium [mmol/L (median, IQR)]		2.30 (2.22-2.39)
Total Albumin [g/L (median, IQR)]		38.0 (35.0-40.0)
KT/V (median, IQR)		1.51 (1.23-1.66)

*based on occupation, NS-SEC [115]

Generalised linear models (GLMs) were used for categorical outcome variables, with an appropriate link function (usually logit or Poisson depending on the distribution of the dependent variable). Iteratively re-weighted least squares was used to find the maximum likelihood estimates for covariates. Goodness of model fit was initially assessed with Akaike's Information Criteria and the residual deviance. Competing models were compared for goodness of fit to the data using the log likelihood ratio statistic, tested against a chi square distribution. Where there were multiple measures within the same patient, mixed modelling was used.

For the comparison of probability distributions of univariate physiological data from normal and eventful HD sessions, Kullback-Leibler or Kolmogorov-Smirnov tests were applied. For multivariate analysis, data fusion techniques were used to create multidimensional probabilistic models of normality. The neuroscale algorithm, a radial basis function neural network, was used to map the multidimensional data to a two dimensional space, for ease of visualisation [116]. The neuroscale method first represents input data (here the data from normal HD sessions) as a Gaussian mixture model with a set number of "centres", determined by the Expectation-Maximisation algorithm. Each centre then becomes the centre for a Gaussian radial basis function. Essentially each input data point "activates" each centre according to distance from that centre. The final two dimensional output of the network is a linear combination of weighted outputs from the radial basis functions, the weights being determined by Sammon mapping to minimise the "stress" (basically Euclidean distance) between the multi-and two-dimensional representations of each data point. New data (i.e. from a new HD session) can then be fed into the neural network, and plotted against the "normal" map . In this way, early deviations from the predefined zone of normality for a given patient at a given stage of HD could be detected.

Chapter 3

Association of blood pressure with cerebral ischaemia and symptoms during haemodialysis

3.1 Introduction

As discussed in the Introduction chapter, it has proved difficult to prove that IDH is associated with hard outcomes. To date, only one definition of IDH has been linked with an independently increased risk of mortality, namely an intradialytic SBP nadir below 90mmHg, and this in a retrospective review of datasets with limited blood pressure and symptom data [4]. Rather than looking at epidemiological data, we have taken a complementary, physiological approach to the problem, and prospectively and continuously monitored blood pressure, real-time symptoms and cerebral NIRS in a large number of haemodialysis sessions. As outlined in the Methods chapter, cerebral NIRS is not only a validated measure of regional cerebral tissue oxygenation (rSO2), but has been shown to correlate with ischaemic impairment of other organs [103, 104, 105, 106]. Our objective was to assess the relationship between blood pressure, symptoms, and downstream organ ischaemia in order to 1) identify which if any blood pressure threshold, absolute or relative, best predicted tissue hypoxia during dialysis on the population level, and 2) identify whether the presence of symptoms improved this prediction.

3.2 Methods

See the Methods chapter for details of the trial and data collection. Continuous blood pressure monitoring was performed using the Finometer device. The beat-to-beat blood pressure data was processed by removal of extreme outliers (3 standard deviations from mean or more) and low pass filtering (Hamming window based with cutoff 0.083Hz) to attenuate high frequency noise. Data was discarded if it did not meet the standards of an SQI based on waveform quality, as described in the methods chapter. Missing segments were not interpolated. Blood pressure data was downsampled to a frequency of 0.0167Hz (i.e. one data point every minute) for the analyses in this chapter. For stable patients with the older Finometer model, baseline blood pressure was defined as the median value from a window beginning 2 minutes after recording start (to allow time for Physiocal calibration) and ending at the point of bleed-out, i.e. when the patient's blood enters the dialysis circuit and treatment commences. For the unstable patients with the Finometer Pro, the start point of the window was instead completion of RTF calibration.

Cerebral rSO2 was measured with the INVOS NIRS device, sampled at 5 second intervals. Data was processed with removal of extreme outliers (4 standard deviations from mean or more) and application of a low pass filter (Hamming window based with cutoff 0.083Hz) to attenuate noise. Data was downsampled to a frequency of 0.0167Hz for the analyses in this chapter. Baseline rSO2 was taken as the median of good quality data spanning the first 2-6 minutes of recording.

There is no consensus on the rSO2 cutoff value which should be considered abnormal or harmful. Healthy baseline values in the general population range from 60 to 80%. Thresholds for cerebral ischaemia have included absolute rSO2 ranging from 40 to 60%, absolute drops from baseline ranging from 15 to 25%, and relative drops from baseline ranging from 20 to 30% [117, 118]. However, some have suggested that an absolute drop of 10% should be the point for intervention, given that there appears to be definite harm once a 15% drop occurs [117]. In our dialysis population, although baseline rSO2 was still normally distributed, it was markedly shifted to the left: the 5th and 95th percentiles for rSO2 were 35% and 67% respectively, with mean 52%. An absolute drop of 10% is likely to have different significance for a population with a mean baseline rSO2 of 70% and a population with a mean baseline of 52%, representing a 14% and a 27% relative change in oxygenation respectively. Therefore, accepting the limitations of any arbitrary threshold, we chose a relative drop of 15% of the baseline value as the cutoff for potential cerebral ischaemia.

3.2.1 Analysis 1: Overview of association between MAP thresholds and adverse events

For the first part of the analysis, we identified drops in MAP below predefined thresholds, and then looked for temporally related symptoms, interventions or new onset cerebral desaturation. The aim of this analysis was to get an overview of the frequency of MAP drops, and temporally associated consequences. The thresholds were either absolute (e.g. 90mmHg, 80mmHg, 70mmHg, 60mmHg, 50mmHg ,40mmHg) or relative to baseline (e.g. -10mmHg, -15mmHg, -20mmHg, -25mmHg, -30mmHg, -40mmHg), and had to be sustained for a minimum of 2 minutes. Recovery was defined as the sustained return of MAP to above the threshold, again for a minimum of 2 minutes. New onset ischaemia was defined as a sustained (2 minutes minimum) drop in rSO2 below the 15% threshold within a window of -10 to +20 mins around the MAP change. If oxygenation had already dropped 15% or more from baseline before start of this window, temporally related ischaemia was defined as a further 5% drop, e.g. from 20 to 25%. Symptoms had to occur within a window of +/-20 minutes. These windows include a short anticipatory period as the thresholds are arbitrary, and in addition, symptoms may precede a decompensation. This strict protocol was designed to assess the temporal relationship between phenomena. For comparison, data segments of the same length (30 minutes) where the MAP did not fall below the given threshold were used as controls. The control segments were taken from sessions where the MAP remained above the threshold throughout, or from sessions before the first drop occurred.

3.2.2 Analysis 2: Sensitivity, specificity and predictive value of MAP changes for cerebral ischaemia

The key event for this analysis was the achievement of rSO2 threshold rather than blood pressure threshold. We identified the time of onset of new cerebral ischaemia, defined as above. The median MAP from a window of +/-5 minutes minutes around the time of rSO2 threshold achievement was taken as the blood pressure threshold at which ischaemia occurred. For comparison, any NIBP measurements in the 20 minute period preceding ischaemia onset were identified. Symptoms were deemed to be temporally associated if they occurred within +/-20 minutes of ischaemia onset. The MAPs at which ischaemia occurred were binned into 5mmHg categories. The cumulative occurrence of cerebral ischaemia at or

below each 5mmHg threshold, and above each threshold, was calculated. Control segments were taken from sessions where the rSO2 remained above the threshold throughout, or from sessions before the first drop occurred. Confusion matrices were constructed to compare sensitivity, specificity, PPV and negative predictive value (NPV) of different MAP thresholds (with or without contemporaneous symptoms) for predicting cerebral ischaemia. PPV is important as ischaemic segments were relatively rare compared to the number of control segments: in this situation, specificity may be misleadingly high due to the large number of correctly identified true negatives, masking the number of false positives.

3.2.3 Analysis 3: Modelling total ischaemia AUC during a haemodialysis session

Creating artificial categories can lead to the loss of important information. In addition, achievement of the ischaemia threshold is probably not as important as the time spent below the threshold, and how far below the threshold, i.e. the area under the curve (AUC). For each session, the AUC below the cutoff of a relative 15% drop was calculated, known hereafter as the ischaemia AUC (min*%). There was a huge excess of zeros, i.e. most dialysis sessions remained above the threshold throughout. For those that did cross the threshold, the square root of the ischaemia AUC resembled a Poisson function (see Figure 3.1). The most appropriate model for this data is a zero-hurdle Poisson GLM, with the option of adjusting for random effects (repeated measures within patients). The zero-hurdle model is essentially a two part model: the first part (zero part) predicts the binary outcome of whether the ischaemia threshold is achieved or not using logistic regression; the second part (count part) models the depth and duration of the ischaemia once the threshold is crossed, using a truncated Poisson model with a log link function (with the ischaemia AUC rounded to the nearest integer to generate counts).

The AUCs below different MAP thresholds, relative and absolute, were calculated for each session. MAP AUC values were highly positively skewed with an excess of zeros: in order to minimise the impact of extreme positive values and create a more interpretable scale, they were transformed by square root. They were then tested in turn as univariate covariates (+/- adjustment for baseline MAP) in both parts of the model, in order to identify the blood pressure measure which provided most information. Goodness of fit was compared with the log likelihood ratio, tested against a chi square distribution.

Symptom data was then added to see if this improved model fit over blood pressure alone. Finally

a select number of demographic and dialysis parameters were tested as additional covariates, including age, HD vintage, ultrafiltration volume and presence of vascular disease (i.e. history of IHD, PVD or CVD). These were chosen on the basis of biological plausibility for increasing vulnerability to cerebral ischaemia. After the models were calculated, count model covariates were transformed to express their relationship to ischaemia AUC rather than the square root of ischaemia AUC. MAP AUC coefficients were back transformed so that odds ratios (OR) were in units ofmmHg*min rather than the square root ofmmHg*min. The delta method was used to find the relevant back-transformed standard errors.

To validate the findings, avoiding any arbitrary categories for ischaemia, we constructed a mixed linear model to predict the rSO2 nadir, using the same covariates.

Figure 3.1: Counts for cerebral desaturation AUC ((%* minutes below threshold)$^{0.5}$) for sessions where ischaemia threshold was reached

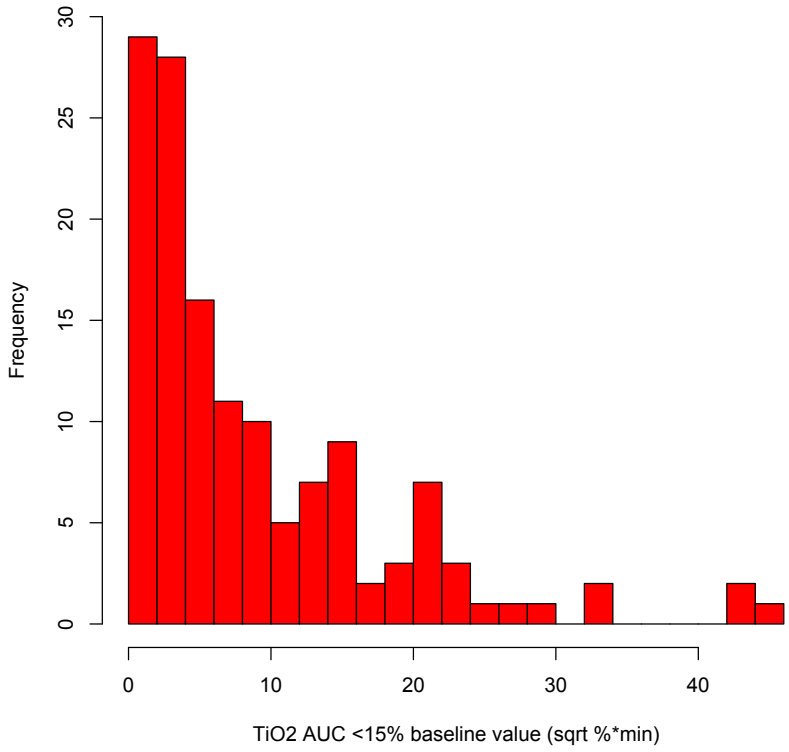

3.2.4 Analysis 4: Predicting symptoms during a haemodialysis session

Multilevel logistic regression was used to identify significant predictors of symptoms during a HD session: separate models were made for cramp symptoms and non-cramp symptoms as it became apparent that

these were quite distinct groups. Covariates included a number of demographic and dialysis parameters including maximal blood pressure change, maximal cerebral desaturation, age, diabetes vintage, HD vintage, ultrafiltration volume and difference in serum and dialysate electrolytes (calcium, sodium and magnesium).

3.3 Results

There was physiological data on 635 dialysis sessions in 58 patients. Two patients were found to have such severe vascular disease that the Finometer could not detect a finger pulse, and only NIBP measurements were available. Two other patients declined cerebral NIRS. In total, 576 sessions had Finometer monitoring, 583 NIRS monitoring and 521 had both. Demographics are summarised in the methods chapter.

3.3.1 Analysis 1: Overview of association of between MAP and adverse events

Sustained hypotensive episodes were extremely common. Using the KDOQI blood pressure threshold of a drop in MAP of 10mmHg from baseline, there was 889 events in 502 sessions, of the 576 with Finometer monitoring (see table 1). As expected, most of these hypotensions were not detected with 30 minute NIBPs. The proportion of Finometer hypotensions that were detected within -10 to +20 minutes by NIBP was approximately 20% for all blood pressure thresholds; either there was no NIBP measurement in this window, resolution had occurred in the time lag to the next NIBP, or there was disagreement between the measurement methods.

There were 166 interventions in total, of which 43% were associated with symptoms. 25 interventions occurred at times when the MAP was within 10mmHg of baseline: 12 of these were associated with symptoms (mainly cramp and feeling hot), and 11 were in response to an asymptomatic NIBP reading which was not confirmed by the Finometer.

In total, 24.9% of sessions featured symptoms, including 10.9% cramp, 8.8% nausea or sweating, 7.6% dizziness and 3.6% headache or back pain. In addition, 23.5% of sessions had at least one episode of cerebral ischaemia as defined above. The temporal association of relative changes in MAP with symptoms,

interventions and cerebral desaturation is shown in table 3.1; the equivalent for absolute MAP thresholds is shown in table 3.2.

Although there was an highly significant linear relationship between relative thresholds of MAP and incidence of temporally related ischaemia, it was not of large magnitude. On simple univariate linear regression, there was a 3% increase in cerebral desaturation per 10mmHg drop from baseline, p <0.001, R^2 0.87 (see figure 3.2). For absolute MAP thresholds, the relationship was better described by a negative exponential, with a sharp increase in cerebral desaturation below MAP 60mmHg (see figure 3.3). On simple univariate linear regression (with log transformation of cerebral desaturation incidence), every 20mmHg drop was associated with a doubling of the rate of ischaemia, p <0.001, R^2 0.88.

The onset of a sustained drop of MAP of 10mmHg or 10% from baseline, the KDOQI definition, was associated with new ischaemia in 38/889 incidences (4.7%), rising to 20/116 (17.2%) for a change of 40mmHg (see table 3.1). For comparison, 10.8% of sustained drops in MAP below 60mmHg were associated with new onset ischaemia, rising to 35.3% for a MAP below 40mmHg (see table 3.2).

There was also a highly significant linear relationship between relative thresholds of MAP and incidence of symptoms, but the effect size was again not large (4% increase per 10mmHg drop from baseline, R^2 0.89, p <0.001, see table 3.1). Absolute thresholds of MAP again had a more exponential relationship with symptoms, with a sharp rise in incidence below 60mmHg (doubling in symptom incidence per 24mmHg drop in MAP, R^2 0.69, $p = 0.021$, see table 3.2). The symptom breakdown revealed that dizziness, nausea and feeling hot or sweaty correlated most closely with blood pressure changes. In fact, there was no significant correlation between cramp and absolute blood pressure thresholds. The adjusted relationship between symptom type and physiology is fully explored in analysis 4, and confirms this overview.

Table 3.1: Events associated with MAP change from baseline

Threshold MAP change from baseline [mmHg, (number of episodes)]	Incidence new onset cerebral ischaemia (%)	Incidence symptoms	Incidence ischaemia when MAP change with symptoms (%)	Intervention rate (%)	Symptoms Reported (%)			
					Cramp	Hot/ nauseous	Headache, back or limb pain	Dizzy
No change (1770)	2.4	2.5	0	2.8	1.2	0.7	0.3	0
-10 (889)	4.7	7.2	13.1	4.4	2.7	1.7	0.7	2.6
-15 (744)	6.9	9.5	13.2	4.0	3.0	2.0	1.1	2.3
-20 (571)	8.1	10.2	19.2	5.6	3.5	2.5	1.8	3.7
-25 (430)	7.4	10.8	23.8	6.5	2.6	2.6	0.7	5.1
-30 (314)	8.4	11.0	18.7	5.7	2.9	4.5	0.3	4.5
-35 (192)	11.4	15.1	18.5	8.9	4.2	7.8	0	4.7
-40 (122)	17.2	20.5	24.0	13.1	5.7	11.5	0	9.8

Table 3.2: Events associated with absolute MAP

Threshold absolute MAP [mmHg, (number of episodes)]	Incidence new onset cerebral ischaemia (%)	Incidence symptoms	Incidence ischaemia when MAP change with symptoms (%)	Intervention rate (%)	Symptoms Reported (%)			
					Cramp	Hot/ nauseous	Headache, back or limb pain	Dizzy
>100mmHg (910)	3.1	3.9	6.5	1.5	0.7	1.8	1.0	0.7
100 (655)	4.6	3.4	0	2.4	1.1	1.1	0.5	1.1
90 (619)	4.2	5.2	6.3	3.1	2.1	1.0	0.8	1.8
80 (548)	6.8	7.3	7.5	3.7	3.1	1.8	0.4	2.4
70 (379)	7.8	7.7	13.2	8.2	7.7	3.4	0.1	4.2
60 (181)	10.8	4.4	21.7	8.8	4.4	3.3	0	5.5
50 (57)	29.8	21.1	58.3	17.5	1.8	5.3	1.8	10.5
40 (17)	35.3	23.5	75.0	17.7	5.9	11.8	0	5.9

Figure 3.2: Univariate relationship between relative MAP threshold and onset of cerebral desaturation

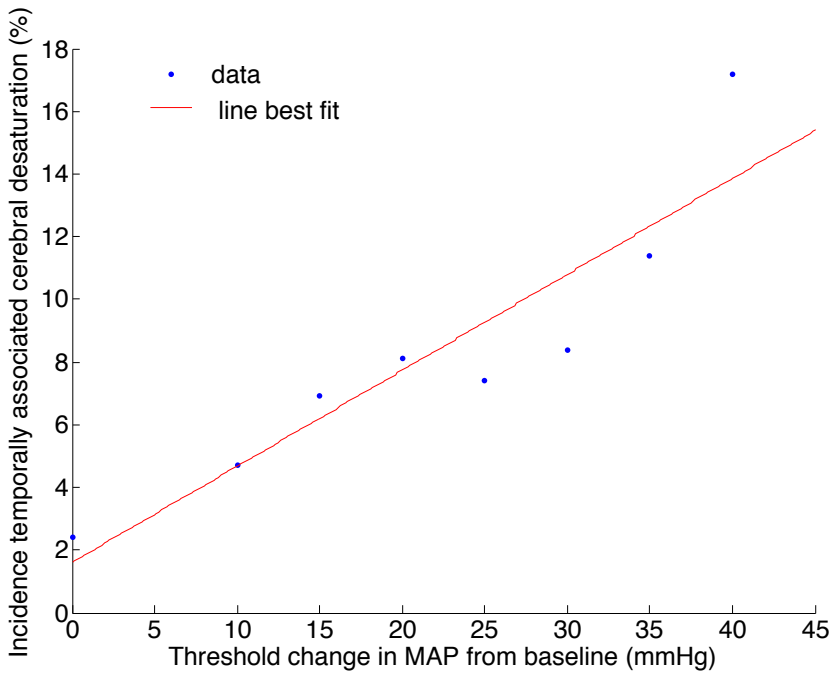

Figure 3.3: Univariate relationship between absolute MAP threshold and onset of cerebral desaturation

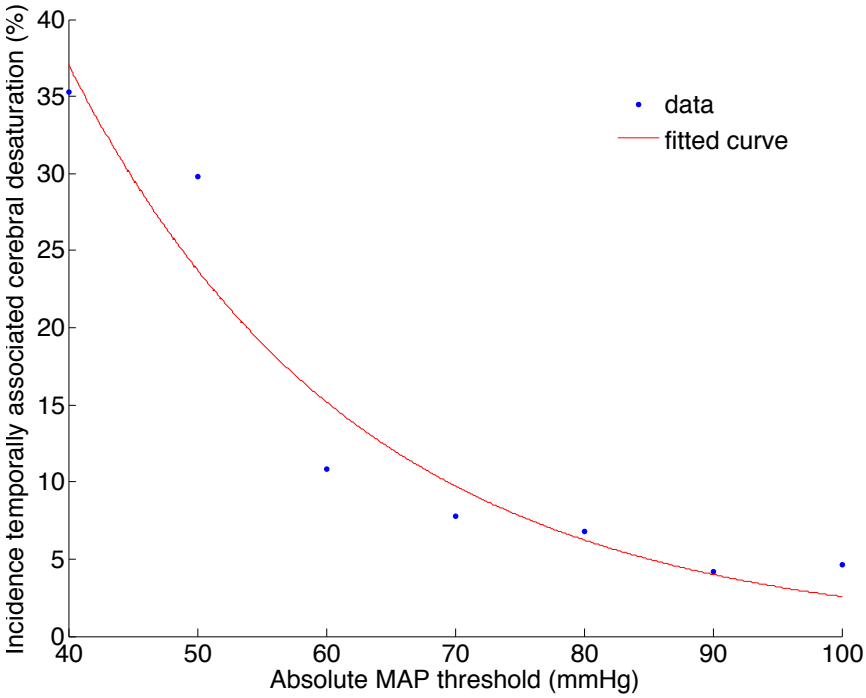

3.3.2 Analysis 2: Sensitivity, specificity and predictive value of MAP changes for cerebral ischaemia

The sensitivity, specificity, PPV and NPV of different MAP thresholds for predicting cerebral desaturation, independent of symptoms, are shown in tables 3.3 and 3.4. The sensitivity and specificity are depicted visually in figures 3.4 and 3.5. The sensitivity, precision and specificity of MAP thresholds combined with non-cramp symptoms are shown in tables 3.5 and 3.6. The number of false positives is dramatically reduced by the requirement for symptoms, but at the expense of sensitivity, i.e. non-cramp symptoms are useful when present, but most cerebral desaturations appear to be asymptomatic.

Table 3.3: Sensitivity and specificity of change in MAP for predicting cerebral desaturation

Change in MAP (mmHg)	Sensitivity	Specificity	PPV	NPV
Any fall	0.88	0.18	0.05	0.97
>10	0.69	0.50	0.06	0.97
>15	0.57	0.63	0.06	0.97
>20	0.44	0.74	0.07	0.97
>25	0.33	0.83	0.08	0.97
>30	0.26	0.88	0.09	0.96
>35	0.18	0.92	0.10	0.96
>40	0.13	0.95	0.10	0.96
>45	0.08	0.97	0.12	0.96

Table 3.4: Sensitivity and specificity of absolute MAP for predicting cerebral desaturation

Absolute MAP (mmHg)	Sensitivity	Specificity	PPV	NPV
<90	0.74	0.57	0.05	0.98
<85	0.66	0.66	0.06	0.98
<80	0.55	0.75	0.06	0.97
<75	0.50	0.82	0.07	0.97
<70	0.41	0.87	0.08	0.97
<65	0.33	0.92	0.09	0.97
<60	0.27	0.95	0.12	0.97
<55	0.19	0.98	0.13	0.96
<50	0.14	0.99	0.21	0.96
<45	0.08	0.99	0.24	0.96

Table 3.5: Sensitivity and specificity of change in MAP with symptoms for predicting cerebral desaturation

Change in MAP (mmHg)	Sensitivity	Specificity	PPV	NPV
Any fall	0.13	0.98	0.25	0.96
>10	0.12	0.99	0.28	0.96
>15	0.10	0.99	0.28	0.96
>20	0.09	0.99	0.27	0.96
>25	0.07	1.0	0.28	0.96
>30	0.06	1.0	0.31	0.96
>35	0.04	1.0	0.29	0.96
>40	0.03	1.0	0.29	0.96
>45	0.02	1.0	0.39	0.96

Table 3.6: Sensitivity and specificity of absolute MAP with symptoms for predicting cerebral desaturation

Absolute MAP (mmHg)	Sensitivity	Specificity	PPV	NPV
<90	0.12	0.99	0.26	0.97
<85	0.11	0.99	0.27	0.97
<80	0.11	0.99	0.28	0.97
<75	0.11	0.99	0.29	0.97
<70	0.11	0.99	0.32	0.97
<65	0.11	0.99	0.36	0.97
<60	0.10	1.0	0.47	0.97
<55	0.06	1.0	0.52	0.96
<50	0.05	1.0	0.68	0.96
<45	0.04	1.0	0.77	0.96

Figure 3.4: Sensitivity and specificity of change in MAP for predicting onset of cerebral ischaemia

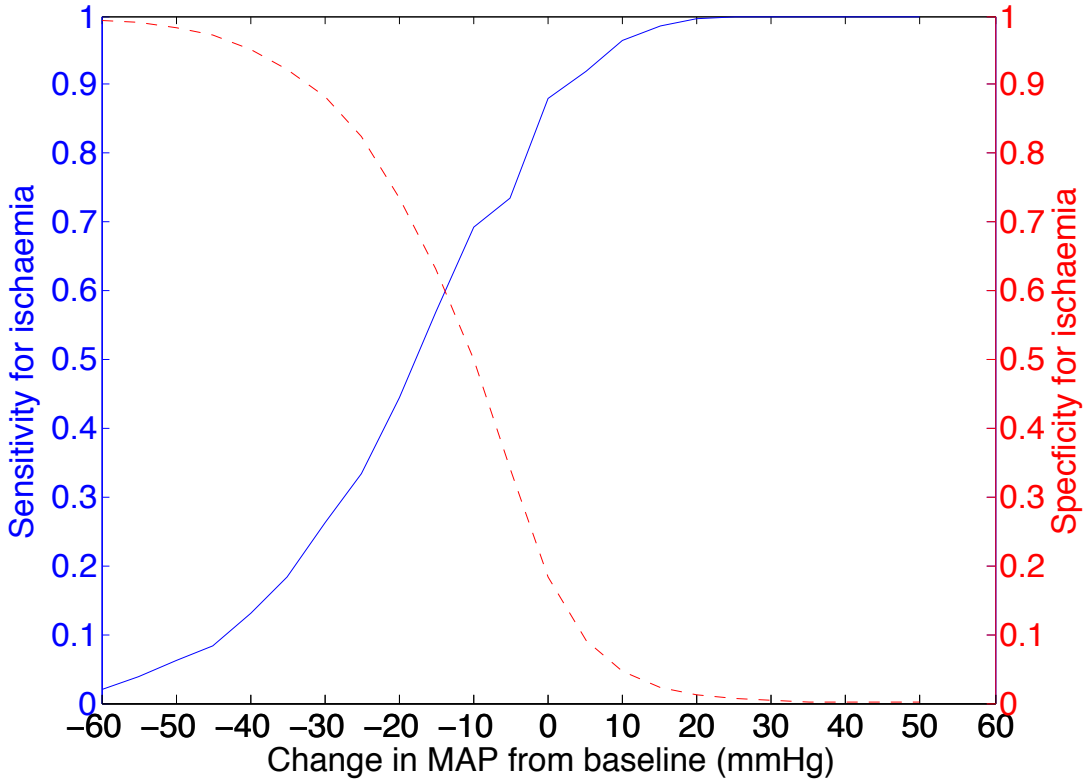

Figure 3.5: Sensitivity and specificity of absolute MAP for predicting onset of cerebral ischaemia

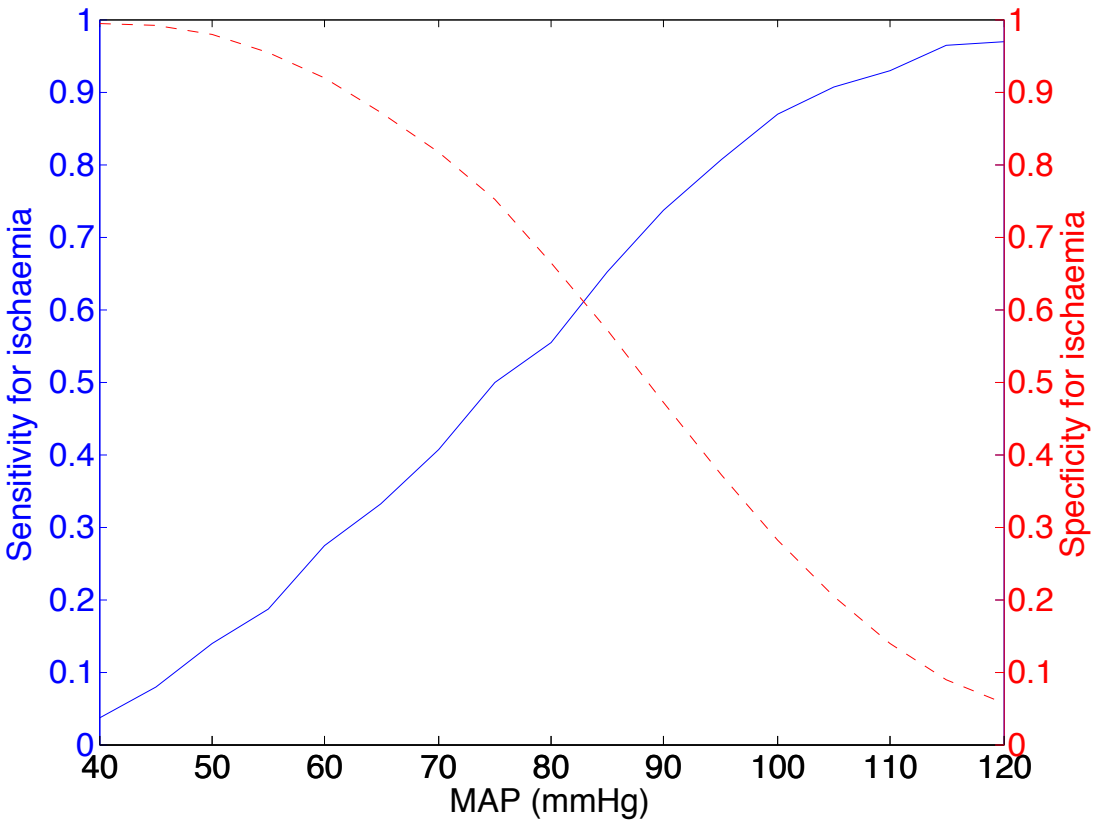

3.3.3 Analysis 3: Modelling total ischaemia AUC during a haemodialysis session

The most appropriate model for the outcome distribution of cerebral ischaemia AUC was a mixed two part model, essentially a multilevel zero-hurdle Poisson GLM, as explained in the methods. Blood pressure indices tested included AUCs below absolute MAP 50mmHg, 60mmHg and 70mmHg, and AUC below δMAP of 10mmHg, 20mmHg, 30mmHg and 40mmHg from baseline.

At the population level, univariate analysis suggested that relative MAPs were more closely associated with cerebral ischaemia. Univariate analysis was performed with adjustment for repeated measures and for baseline MAP (according to three simple categories, <80mmHg, 80-100mmHg, and >100mmHg). For both parts of the model, i.e. the zero part (achieving the threshold for ischaemia or not) and the count part (the depth and duration of ischaemia once threshold crossed), AUC below δMAP 40mmHg provided the best fit. AUC below absolute MAP of 60mmHg provided a very similar fit.

On multivariate analysis, again AUC below δMAP 40mmHg resulted in the best fit, followed closely by AUC below absolute MAP <60mmHg. Non-blood pressure terms which were significant included non-cramp symptoms, diabetes vintage and ultrafiltration volume: these covariates were significant only for the zero part of the model, i.e. the binary outcome of whether the cerebral ischaemia threshold was reached or not, but not the severity and duration of ischaemia. RBV, though not in itself significant, substantially improved the model fit. Patient specific intercepts significantly improved the model, indicating that there were further, unidentified patient-level variables determining susceptibility to cerebral ischaemia. The final model using AUC below δMAP 40mmHg is shown in Figure 3.6, and the variation in patient-level intercepts (i.e. individual variation in presence and severity of ischaemia after taking into account other covariates) in Figure 3.7.

The model using AUC below MAP 60mmHg had the same non-blood pressure covariates with nearly identical coefficients. This is unsurprising, as the two indices contained overlapping information, with correlation 0.17 (p <0.001). The odds ratios (OR) for every additional min*mmHg below 60mmHg were as follows: for baseline MAP <80mmHg, OR 1.02 zero part, OR 1.01 count part; for baseline MAP 80-100mmHg, OR 1.03 zero part, OR 1.02 count part; for baseline MAP >100mmHg, OR 1.16 zero part, OR 1.03 count part.

A linear mixed model predicting maximum drop in rSO2 (to avoid the arbitrary ischaemia threshold of 15% which we had chosen) confirmed the same significant covariates, though this time AUC below a MAP of 60mmHg slightly outperformed AUC below δMAP 40mmHg. Again, RBV was not significant in itself but contributed significantly to the best model. Exploratory analyses using the linear mixed model structure confirmed that SBP indices were inferior to MAP indices for modelling.

Figure 3.6: Best two part model for total cerebral ischaemia during a HD session

Count model covariates (predicting total cerebral ischaemia in %*min once threshold crossed)		**Coefficients (incidence rate ratio)**	**95% confidence intervals**	**p value**
ΔMAP >40 mmHg AUC (per mmHg*min)	Baseline MAP<80mmHg	1.04	1.01-1.08	0.005
	Baseline MAP 80-100mmHg	1.03	1.02-1.04	< 0.001
	Baseline MAP >100mmHg	1.01	1.01-1.02	< 0.001
Zero hurdle model covariates (predicting if ischaemia threshold is reached or not)		**Coefficients (odds ratio)**	**95% confidence intervals**	**p value**
UF volume (normalised to dry weight, per ml/kg)		1.05	1.02-1.08	0.003
Non-cramp symptoms (present at any time during session)		2.69	1.38-5.21	0.003
Diabetes vintage (per years)		1.05	1.01-1.08	0.009
Relative blood volume per (% decrease)		1.03	1.00-1.06	0.112
ΔMAP >40 mmHg AUC (per mmHg*min)	Baseline MAP<80mmHg	21.13	0.29-112.00	0.165
	Baseline MAP 80-100mmHg	1.18	0.98-1.38	0.060
	Baseline MAP >100mmHg	1.08	1.02-1.14	0.008

Figure 3.7: Patient specific intercepts for (a) the count and (b) the hurdle parts of the model, with 95% confidence intervals (log odds)

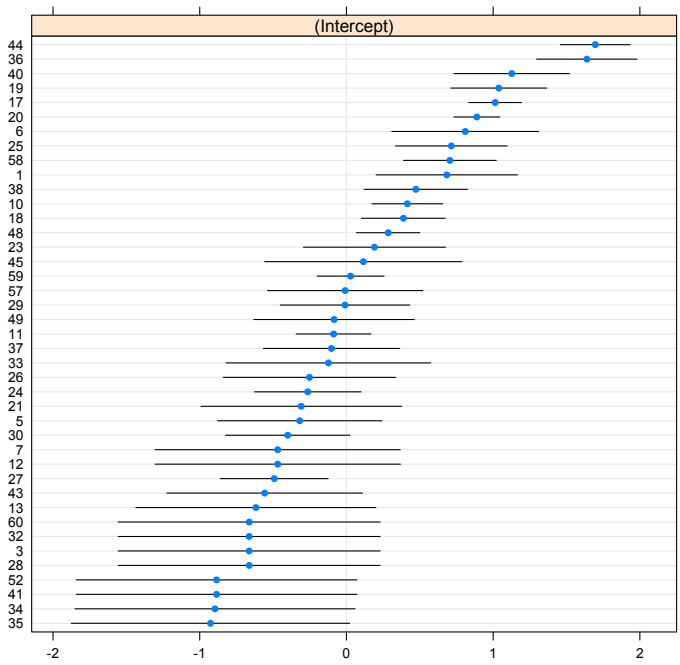

(a) Count part(binomial GLM) part

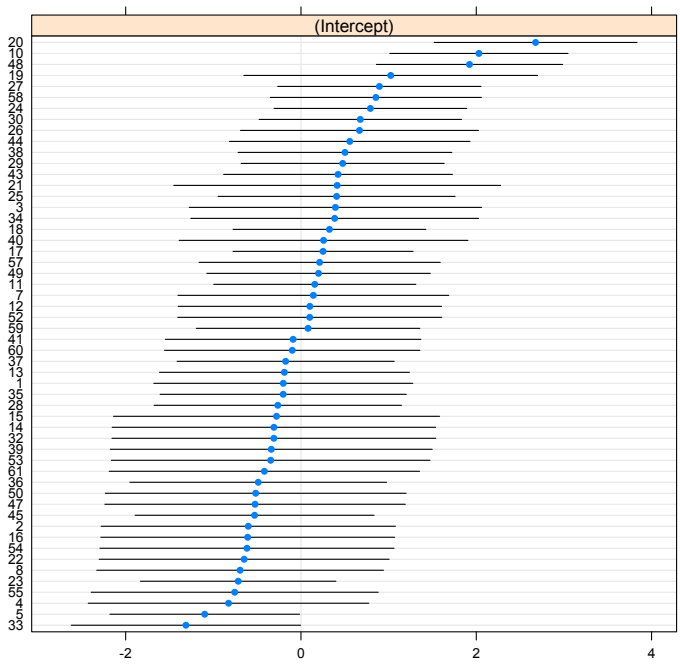

(b) Hurdle part (Poisson GLM) part

3.3.4 Analysis 4: Predicting symptoms during a haemodialysis session

We investigated symptomatology with multilevel logistic regression, looking for covariates which distinguished sessions featuring symptoms from those without symptoms. Significant predictors of non-cramp symptoms were found to be maximum drop in MAP, maximum drop in rSO2, age and years on HD. MAP nadir could be substituted for δ MAP, and resulted in a near identical model, with marginally inferior fit. SBP indices again were inferior to MAP indices. HD vintage and age were actually mitigating factors, i.e. younger patients who were new to HD were more likely to report symptoms. The final equation was:

$$Y_{ij} = \frac{e^{1.96+\mu_{0j}+0.02*\text{MAP_nadir}+0.05*\delta\text{rSO2}-0.04*\text{Age}-0.02*\text{HD_Vintage}}}{1+e^{1.96+\mu_{0j}+0.02*\text{MAP_nadir}+0.05*\delta\text{rSO2}-0.04*\text{Age}-0.02*\text{HD_Vintage}}} \tag{3.3.1}$$

where Y_{ij}=probability of non-cramp symptoms; j indicates the patient and i the HD session; MAP_nadir is the minimum MAP during the dialysis session inmmHg; δrSO2 is the maximum drop in cerebral oxygenation, measured as percent of baseline; HD_Vintage is years on HD; Age is patient age in years; and μ_{0j} is the patient-specific intercept.

The equivalent ORs are shown in table 3.7:

Table 3.7: Factors significantly associated with symptomatic HD

Covariate	Odds Ratio	95% Confidence Intervals	p value
Maximum drop in MAP	1.04 permmHg	1.01-1.06	0.003
Maximum drop in rSO2	1.06 per % baseline	1.02-1.10	0.005
Age	0.95 per year	0.92-0.98	<0.007
Dialysis Vintage	0.98 per year	0.96-1.00	0.052

On a single level model, ultrafiltration volume and difference between serum and dialysate sodium concentration were significantly associated with cramp. Once patient clustering was accounted for, ultrafiltration volume alone remained significant, with OR 1.67 (1.25-2.22) , p 0.023; the difference between serum and dialysate sodium concentration was borderline with OR 1.17 (0.98-1.39), p 0.08. Of the total residual variance, 44% was explained by between-patient variation, suggesting that important patient level factors were unidentified.

3.4 Discussion

As expected, we found a significant, temporal relationship between change in MAP and the onset of both end organ ischaemia and symptoms. It is clear that the lower the blood pressure, the greater the risk of both symptoms and cerebral desaturation: however, the majority of blood pressure drops were not associated with downstream tissue ischaemia or symptoms, even when they were severe. Conversely, in a small but important minority, ischaemia occurred without a drop in MAP.

There was no clinically useful compromise between sensitivity and specificity for predicting cerebral desaturation using blood pressure thresholds alone. Symptoms substantially improved specificity and precision, but nevertheless the majority of ischaemic episodes were asymptomatic. Relative MAP performed better than absolute MAP on ROC analysis, which is not surprising given the huge range of baseline MAPs across the population. In addition, a third of the patients had monitoring with the earlier Finometer model, which is better at detecting trends than absolute pressures (though for MAP and DBP it performs to internationally accepted standards).

Both before and after adjusting for relevant covariates and repeated measures, the duration and magnitude of excursions either below a δ MAP 40mmHg or absolute MAP of 60mmHg best predicted the ischaemia AUC for a given HD session. The median baseline MAP was 98.8mmHg, explaining the near identical models obtained with these MAP AUC indices. These indices, like the study of Flythe et al, likely represent the most extreme hypotension in the population [4]. A large epidemiological study of pulse pressure in HD patients has found that the relationship between MAP and SBP is well described by the equation[119]:

$$\mathrm{SBP} = 10.6 + 1.3 * \mathrm{MAP} \tag{3.4.1}$$

Therefore a MAP threshold of 60mmHg would on average be expected to correlate to a SBP of 88.6mmHg, close to the threshold identified by Flythe et al [4]. However, from the sensitivity and specificity tables 3 and 4, it can be seen that waiting until a MAP of 60mmHg for all patients would result in over two thirds of ischaemic events being missed over the whole population. Also, whilst specificity appears high, this is largely driven by the large number of true negatives (large predominance of both segments where the MAP was maintained over 60mmHg and segments without ischaemia) rather than a low number of false positives: looking at the precision in table 1, it can be seen that only 10% of

segments where the MAP dropped below 60mmHg featured new onset or worsening cerebral desaturation.

In agreement with the univariate sensitivity/specificity analysis, the presence of non-cramp symptoms, in addition to change in MAP, significantly improved the prediction of ischaemic events in the adjusted model. Previous studies that have not found symptoms helpful may have suffered from poor symptom recording and/or temporal resolution. Cramp is frequently included as a symptom consistent with muscle hypoperfusion and ischaemia. However, unlike symptoms such as dizziness, nausea and sweating, it was not associated with cerebral desaturation or even blood pressure once fluid and electrolyte changes had been taken into account. Conversely, cerebral desaturation was significantly associated with non-cramp symptoms. Despite being highly correlated with rSO2 nadir, change in MAP was also independently associated with non-cramp symptoms, albeit with a weaker relationship. As the patients were not blinded to NIBP blood pressure readings, it may be that knowledge of hypotension influenced symptomatology above and beyond actual tissue ischaemia. Moreover, the physiological processes involved in compensating for hypotension may themselves cause symptoms long before actual ischaemia occurs (e.g. tachycardia, sweating)

Many factors may affect the occurrence of symptoms. Firstly, the threshold for reporting symptoms, even using a bedside electronic system which does not require nurse attendance, will vary between patients. Younger people who are new to HD appear more likely to experience symptoms after controlling for blood pressure and rSO2 changes. This may partly reflect differences in expectations, anxiety levels or interpretation of physical sensations during HD. There was an inverse relationship between age and score on the PHQ-9 test, which screens for depression (Pearson's correlation coefficient -0.28, p 0.01). ESRF is likely to have a greater burden on career, family and finances in people of working and child-bearing age, and in addition there is less peer support for young HD patients; these factors may translate to greater psychological distress. It has been shown that low mood may be associated with increased sensitivity to acute ischaemic pain [120, 121, 122]. In addition, beliefs about the meaning of physical sensations can make a difference as to whether they are perceived as noxious or not [123]. Finally, ageing itself can modulate pain thresholds [124].

Other non-blood pressure indices which contributed significantly to the model included normalised ultrafiltration volume and RBV, which indicate respectively the magnitude and one facet of the response

(re-filling) to the challenge of fluid removal. These added information over and above blood pressure indices: blood pressure may be a late sign of decompensation, and it is possible that adverse effects at the tissue level occur before hypotension. The only demographic which added independently significant information to the model was diabetes vintage: this is likely a surrogate for autonomic dysfunction, and perhaps loss of the ability to autoregulate. Hypotension would be expected to have a more predictable adverse effect in the absence of autoregulation.

The relationship between systemic blood pressures and tissue oxygen balance is not straightforward. The results of this study explain why it has proven so difficult to link blood pressure changes (except for the most extreme hypotension) to hard outcomes, and highlights the shortcomings of current definitions of IDH. Any threshold for ischaemia is likely to vary between organs, and between patients, depending on factors such as intact regional autoregulation. In normotensive, healthy individuals, cerebral blood flow is held steady between systemic MAPs of 60 and 150mmHg; outside these limits cerebral blood flow varies linearly with MAP [125]. However, cerebral autoregulation thresholds vary substantially between individuals. Stratifying IDH thresholds for the presence or absence of cerebral autoregulation, or personalising thresholds according to the individual lower limit of autoregulation, may have much greater sensitivity and precision for predicting ischaemia and/or symptoms, and this will be the subject of our next analysis.

The key limitation of this study is that we looked at surrogate measures (rSO2) rather than hard patient outcomes, and moreover there is no consensus on what change in rSO2 is harmful. However, a convincing body of studies have now shown that rSO2 changes do correlate with morbidity and mortality in other populations [99, 100, 101, 102, 103, 104, 105, 106]. In Chapter 8, we furthermore demonstrate that decline in cognitive function in this population is associated with exposure to intra-dialytic cerebral ischaemia, as defined here.

3.5 Conclusions

At the population level, blood pressure thresholds alone have a poor trade off between sensitivity and specificity for predicting downstream tissue ischaemia during HD. Extreme drops in blood pressure (e.g. MAP below 60mmHg) and the presence of non-cramp symptoms have a reasonable PPV, but their absence does not rule out ischaemia. Other factors which provided predictive information over and above

blood pressure alone included diabetes vintage (autonomic function), ultrafiltration volume and RBV, which likely describe the cardiovascular challenge and response. Personalised models taking into account cerebral autoregulation thresholds are likely to be fruitful, and may allow the identification of clinically useful individualised or stratified MAP targets.

Chapter 4

Cerebral autoregulation and vulnerability to ischaemic insults

4.1 Introduction

In the last chapter we showed that, at the population level, blood pressure thresholds alone have a poor trade off between sensitivity and specificity for predicting cerebral ischaemia during HD. We further speculated that stratifying IDH thresholds for the presence or absence of cerebral autoregulation, or personalising thresholds according to the individual lower limit of autoregulation, would have greater clinical utility for the prediction and prevention of intra-dialytic ischaemic events.

Most physiology textbooks state that in normotensive, healthy individuals, cerebral blood flow is held steady between systemic MAPs of 60 and 150mmHg. However, in real world patients, cerebral autoregulation thresholds vary substantially between individuals, and the lower limit may be much higher [126, 125]. Early studies in human subjects used pharmacological or mechanical methods to induce large changes in blood pressure, and estimated simultaneous changes in cerebral blood flow [126]. One of the first such studies, in 19 normotensive adults, found that cerebral blood flow started to fall at a MAP as high as 80mmHg in some individuals [127]. However, oxygen uptake only became significantly impaired in a proportion of patients in whom the MAP fell below 60mmHg; the authors hypothesised that vasodilation and increased oxygen extraction offered some reserve, so that reduced blood flow did not immediately result in hypoxia. Finnerty et al employed a similar protocol in 44 patients of varying ages and baseline blood pressures, and found that clear symptoms of cerebral ischaemia developed at similar

cerebral blood flows in all patients, but that the MAP at which this occurred varied hugely: in those with malignant hypertension, the average MAP was 89mmHg, whereas in young, healthy patients, the average MAP was 35mmHg [128]. An analogous study in 10 patients with very severe hypertension found that the mean lower limit of autoregulation was as high as 120mmHg [129]. More recent studies using transcranial Doppler or NIRS to estimate cerebral blood flow have reported similar ranges [130, 131, 132].

It is clear that ischaemia does not necessarily result as soon as the lower limit is reached: this depends on other factors such as the ability to increase oxygen extraction. However, multi-organ morbidity and mortality have been shown to increase with AUC below the lower limit of cerebral autoregulation during cardiac surgery, suggesting it is a reasonable threshold to target clinically [106]. Other vascular beds may lose autoregulation at higher thresholds, with lower limits reported to be 70mmHg for coronary and renal circulations: in keeping with this, AUC below the cerebral autoregulation lower limit also appears to correlate with measures of other organ failure (eg length of intensive care stay, cardiac events, ventilator days and acute kidney injury) [103, 104, 105, 106, 133, 134]. Therefore it is likely to be beneficial to maintain MAP above the lower limit of cerebral autoregulation in settings where blood pressure is manipulated, including HD.

The objectives of this chapter are: 1) to characterise cerebral autoregulation in a population of HD patients; 2) to model the lower threshold of cerebral autoregulation using demographic and clinical factors (so that results may be generalised without the need to monitor each patient with NIRS); 3) to assess the specificity and sensitivity of the lower limit of cerebral autoregulation, when intact, for predicting tissue ischaemia during HD; 4) to identify the optimal MAP for patients without autoregulation.

4.2 Methods

See the Methods chapter for details of the trial and data collection. Continuous blood pressure monitoring was performed using the Finometer device. The beat-to-beat blood pressure data was processed by removal of extreme outliers (3 standard deviations from mean or more) and low pass filtering (Hamming window based with cutoff 0.083 Hz) to attenuate high frequency noise. Data was discarded if it did not meet the standards of an SQI based on waveform quality, as described in the Methods chapter. Missing segments were not interpolated. For stable patients with the older Finometer model, baseline blood

pressure was defined as the median value from a window beginning 2 minutes after recording start (to allow time for Physiocal calibration) and ending at the point of bleedout, i.e. when the patient's blood enters the dialysis circuit and treatment commences. For the unstable patients with the Finometer Pro, the start point of the window was instead completion of RTF calibration.

Cerebral rSO2 was measured with the INVOS NIRS device, sampled at 5 second intervals. Data was processed with removal of extreme outliers (4 standard deviations from mean or more) and application of a low pass filter (Hamming window based with cutoff 0.083 Hz) to attenuate noise. Baseline rSO2 was taken as the median of good quality data spanning the first 2-6 minutes of recording.

As discussed in the last chapter, there is no consensus on the rSO2 cutoff value which should be considered abnormal or harmful, and accepting the limitations of any arbitrary threshold, we again chose a relative drop of 15% of the baseline value as the cutoff for potential cerebral ischaemia.

4.2.1 Analysis 1: Cerebral autoregulation limits

Cerebral autoregulation curves were constructed for each patient and for the population as a whole. We first estimated autoregulation limits by fitting curves to the relationship between MAP and rSO2. This is a well-documented method which has been in use for decades, albeit more often with cerebral blood flow rather than cerebral oxygenation measurements [128, 129]. For this analysis, both NIRS and Finometer data were downsampled to a frequency of 0.0167 Hz (i.e. one data point every minute). The MAP data was grouped into 5mmHg bins (sliding every 1mmHg) and the mean of the corresponding rSO2 values were found for each bin. If there was less than half an hour of data for a given bin, it was discarded. For two patients in whom the Finometer could not read blood pressure due to severe vascular disease, MAP values were taken from NIBP measurements. There is a reasonable body of evidence that the cerebal autoregulation curve is best modelled with a third degree polynomial with positive first coefficient [135, 136, 137]. In comparison, the in the absence of autoregulation, regional blood flow and tissue saturation vary linearly with blood pressure. For the population as a whole, and then for each patient, we assessed whether the relationship between MAP and rSO2 was best modelled with an appropriate polynomial or an appropriate (i.e. positive gradient) straight line: goodness of fit was compared using the F test statistic (based on residual sum of squares for each model) against an F distribution. If the

polynomial provided a statistically significant better fit, then upper and lower autoregulation limits were estimated by drawing a horizontal straight line from the peak of the positive inflection and the nadir of the negative inflection respectively, and identifying where they intersected the ascending and descending limbs of the polynomial (see Figure 4.1).

For comparison, we also estimated the autoregulation limits using a recently described moving correlation method [55]. A low pass filter was applied to the beat-to-beat MAP data to remove information with period above 25 seconds. We then resampled both NIRS and MAP data at 0.1Hz, and calculated a moving correlation coefficient over 5 minute sliding windows, updated every minute. For each patient, and then for the population as a whole, we took the average correlation value for 5mmHg bins of MAP, again sliding every 1mmHg. Confidence intervals were calculated for each value. If there was less than half an hour of data for a given bin, it was discarded. Essentially a value of 0 indicates no relationship between blood pressure and perfusion, whereas a value of 1 indicates complete dependence of oxygenation upon blood pressure. Laboratory data suggests that a correlation of 0.3 and above is sensitive and specific for loss of autoregulation [55]. The lower and upper thresholds of autoregulation were defined as the points at either end of the range where the correlation value first rose to 0.3 or above. Absent autoregulation was defined as as a correlation uniformly above 0.3 at all pressures. The Pearson's correlation coefficient between the two methods was calculated.

Figure 4.1: Curve fitting method of determining limits of cerebral autoregulation

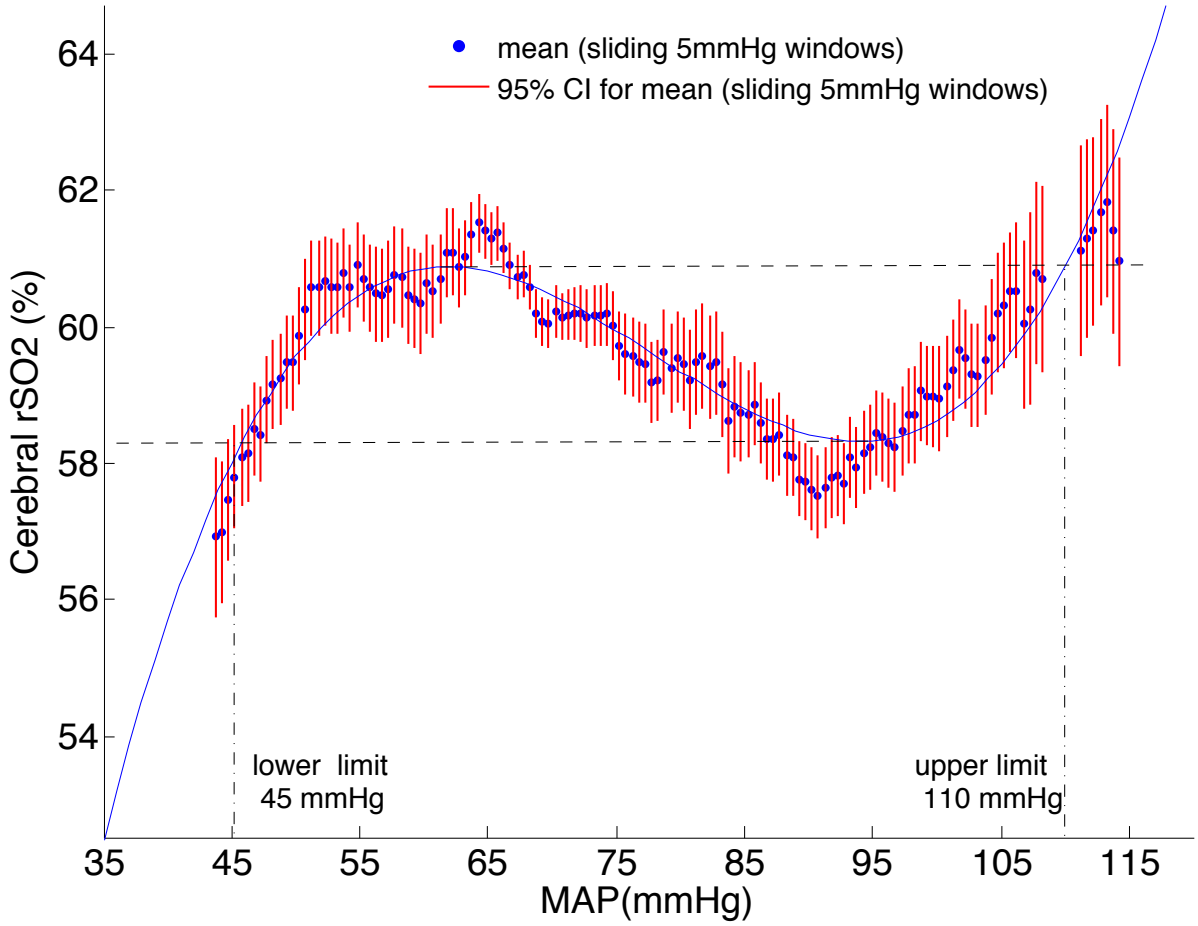

4.2.2 Analysis 2: Predicting presence of autoregulation and its lower limit

Logistic regression was used to model the binary outcome of present or absent autoregulation. Covariates were transformed as necessary to maximise the spread of data. Covariates tested were age, sex and comorbidities including diabetes vintage, HD and ESRF vintage, known IHD and CVD. For those with autoregulation, a linear model was constructed to predict the lower limit of autoregulation, with covariates including age, diabetes vintage, number of blood pressure medications and baseline MAP. All covariates in both models were chosen on the basis of biological plausibility and previous literature. The best model was selected using comparison of log likelihoods, against a chi square distribution.

4.2.3 Analysis 3: Sensitivity, specificity and predictive value of autoregulation lower limit for cerebral ischaemia

We identified the time of onset of new cerebral ischaemia, defined as above. The median MAP from a window of +/-5 minutes minutes around the time of rSO2 threshold achievement was taken as the blood pressure threshold at which ischaemia occurred. For those patients with autoregulation, the MAP was re-expressed as relative to the lower limit of autoregulation; for patients without autoregulation, absolute MAP was used. The MAPs at which ischaemia occurred were binned into 5mmHg categories. Two atypical individuals consistently developed ischaemia after bleedout (ie when the patient's blood first fills the dialysis circuit) in the absence of change in blood pressure. These events, by their number, risked dominating the population analyses, which were therefore performed with and without data from these patients. The cumulative occurrence of cerebral ischaemia at or below each 5mmHg threshold, and above each threshold, was calculated. Control segments were taken from sessions where the rSO2 remained above the threshold throughout, or from sessions before the first drop occurred. Confusion matrices were constructed to compare sensitivity, specificity, PPV and NPV of different MAP thresholds for predicting cerebral ischaemia in patients with and without autoregulation. PPV is important as ischaemic segments were relatively rare compared to the number of control segments: in this situation, specificity may be misleadingly high due to the large number of correctly identified true negatives, masking the number of false positives. As well as looking at sensitivity versus specificity at the population level, we looked at the individual patient level to see whether personalised MAP thresholds performed better.

4.3 Results

There was physiological data on 635 dialysis sessions in 58 patients. Two patients were found to have such severe vascular disease that the Finometer could not detect a finger pulse, and only NIBP measurements were available. Two other patients declined cerebral NIRS. In total, 576 sessions had Finometer monitoring, 583 NIRS monitoring and 521 had both. Demographics are summarised in the methods chapter.

4.3.1 Analysis 1: Cerebral autoregulation limits

Of the 56 patients who underwent cerebral NIRS monitoring, 37 had intact autoregulation (best fit third degree polynomial) and 18 had no autoregulation (best fit linear); the remaining patient had insufficient data, having only been monitored on one stable session. A typical curve for a patient with intact autoregulation is shown in Figure 4.2. In contrast, Figure 4.3 shows the relationship for a 90 year old patient, which is clearly linear. The alternative definition of absent autoregulation, a moving correlation value of >0.3 at all MAPs, occurred in none of our patients.

Using the curve fitting method (which also allowed parameters to be estimated for the two patients with only NIBP readings), a lower limit could be identified for 27 of the 37 patients. The remainder did not experience sufficient range of MAP to allow accurate modelling of the lower limit, but clearly had autoregulation. Using the moving correlation method, a lower limit could be identified for only 15 of the patients with intact autoregulation. The correlation between both methods of identifying the lower limit of autoregulation was 0.89, $p < 0.001$, though there was a small offset of approximately 5mmHg (moving correlation lower). The relationship between MAP and cerebral saturations for the whole population is shown in Figure 4.6. The moving correlation between continuous MAP and rSO2, plotted against median MAP, is shown for the whole population in Figure 4.5. For the remainder of the analysis we used the results from the curve fitting method, which appeared more appropriate to the monitoring methods. Mean lower limit of autoregulation was 74.1mmHg, with standard deviation 17.6mmHg (Figure 4.4). For a couple of young patients with chronically uncontrolled, severe hypertension, autoregulation was lost at MAP values as high as 105mmHg (Figure 4.7), representing extreme right shift.

Figure 4.2: MAP versus cerebral rSO2 in a patient with intact autoregulation, third degree polynomial fitted

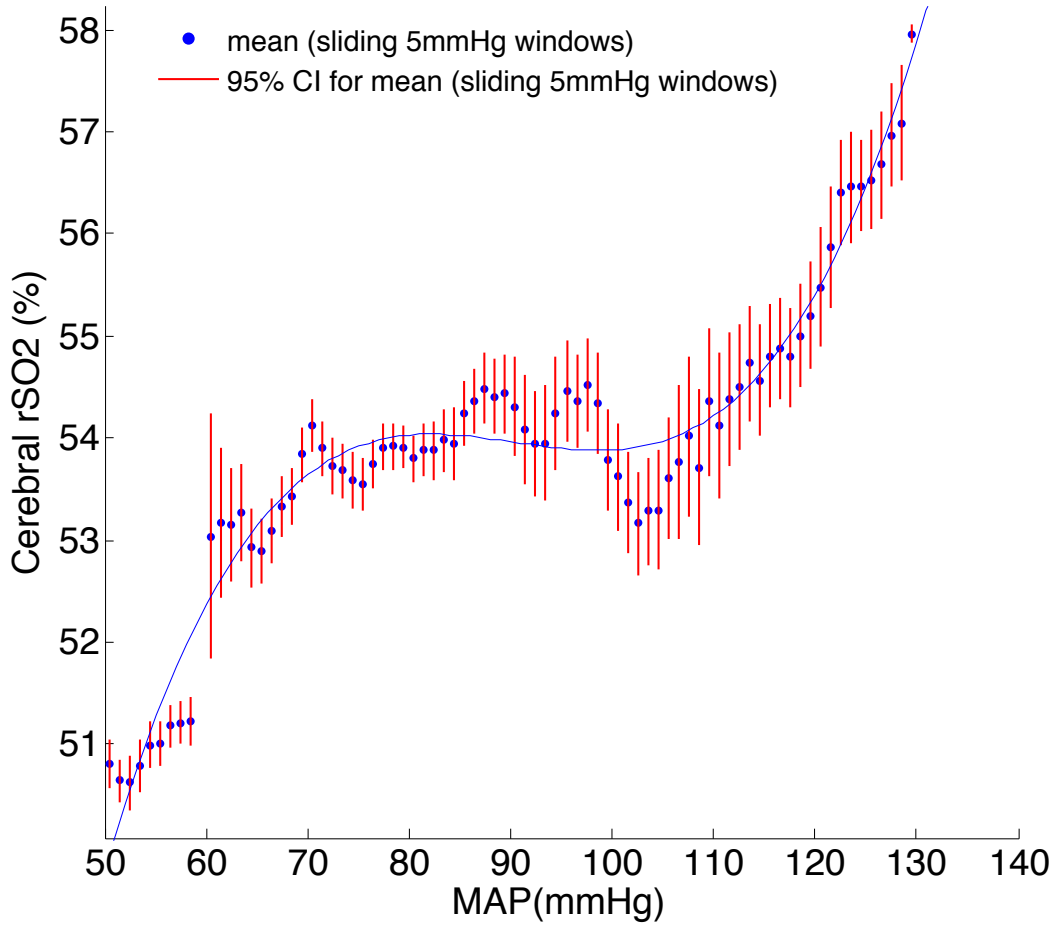

Figure 4.3: MAP versus cerebral rSO2 in a patient with no autoregulation, linear model fitted

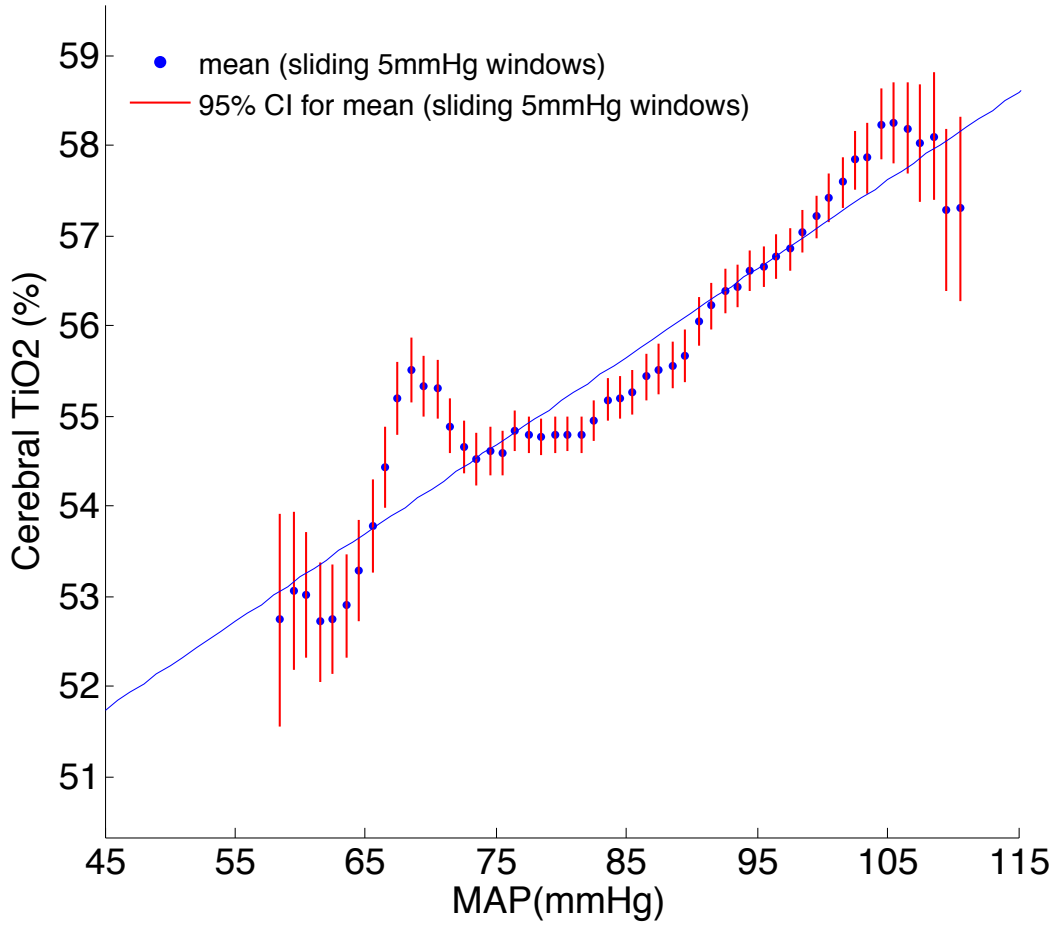

Figure 4.4: Histogram of probability densities for lower limit of cerebral autoregulation

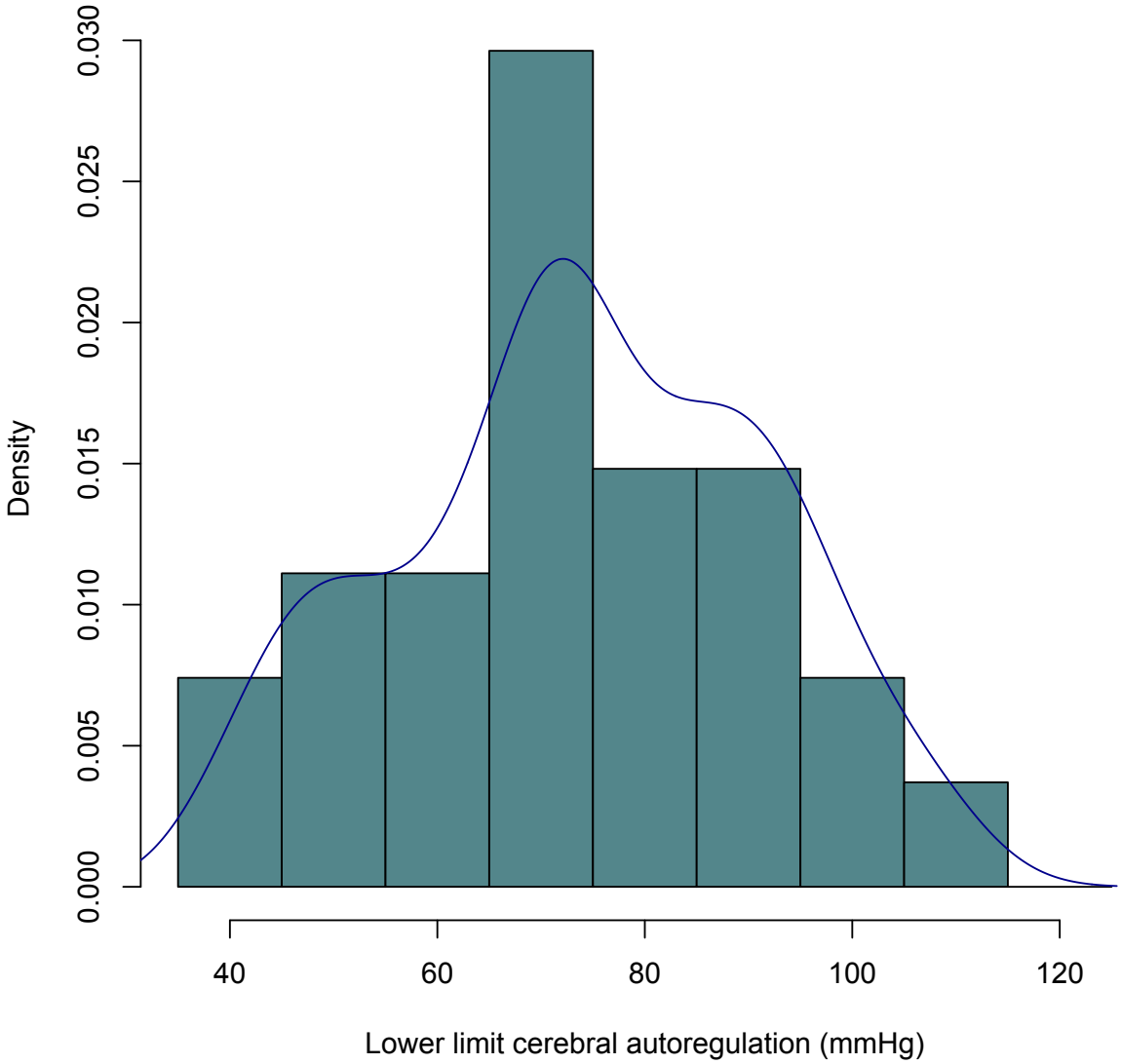

Figure 4.5: Relationship between MAP and COX at the population level

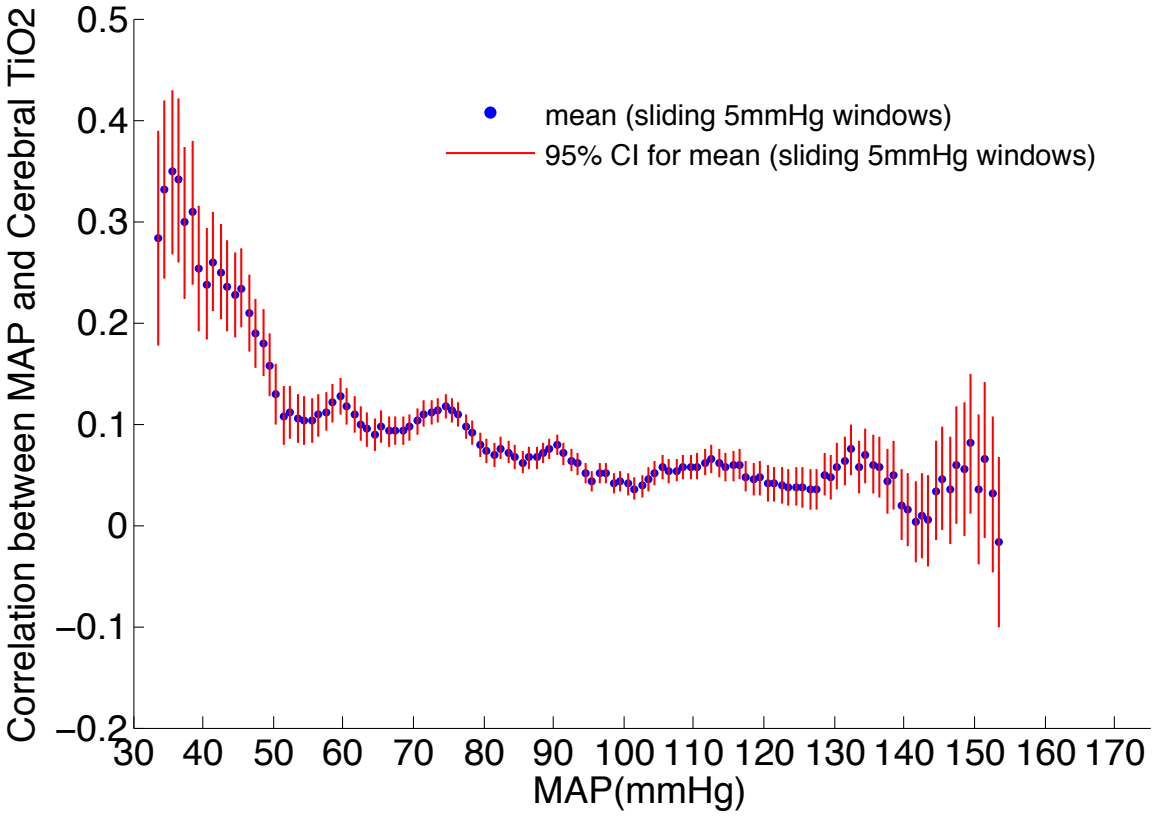

Figure 4.6: Relationship between MAP and cerebral rSO2 at the population level

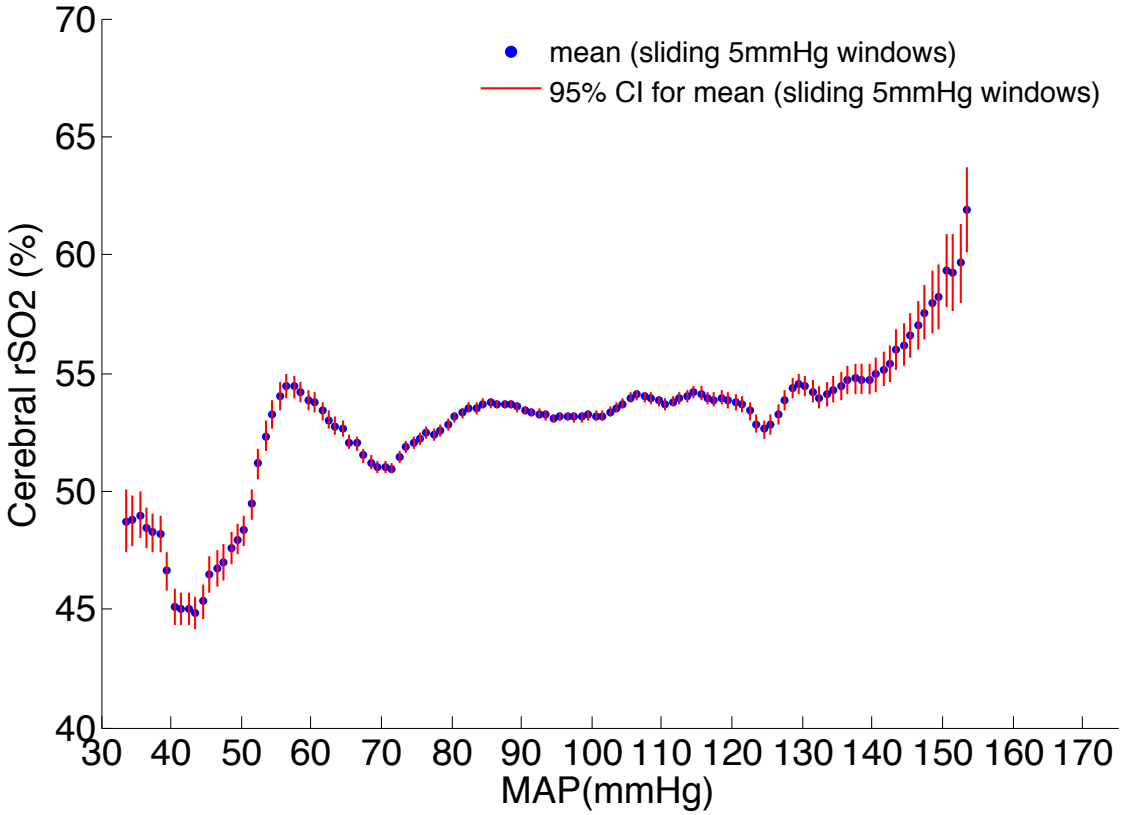

Figure 4.7: Example of a chronically hypertensive patient with loss of autoregulation at unusually high MAP

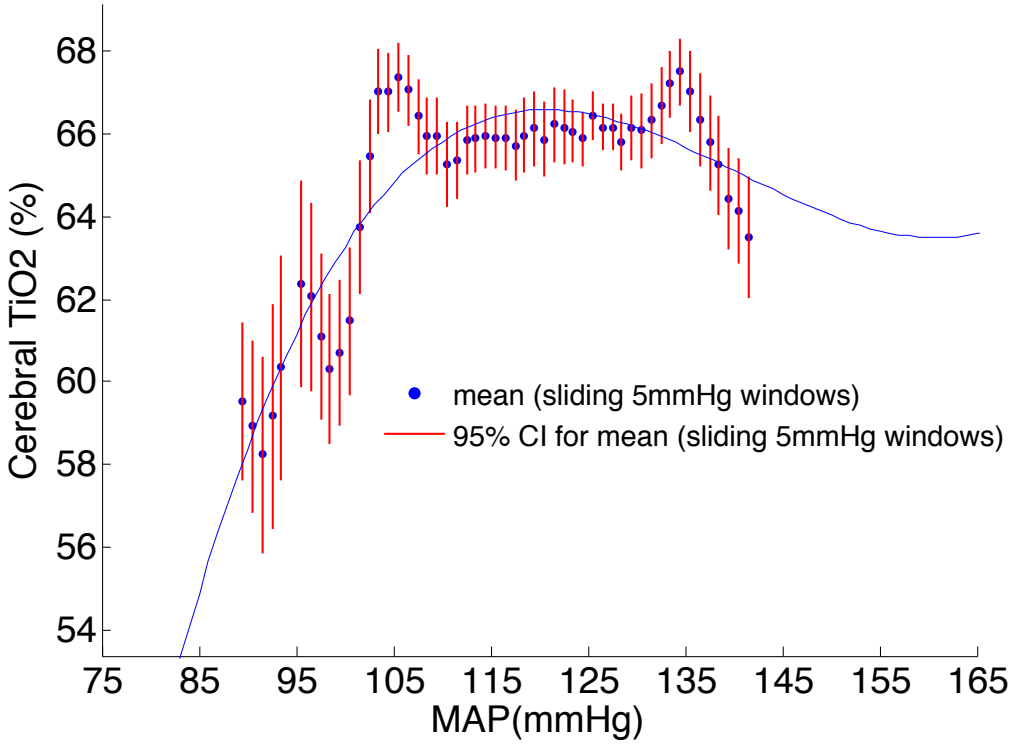

(a)

4.3.2 Analysis 2: Predicting presence of autoregulation and its lower limit

Factors which independently predicted loss of autoregulation on multivariate logistic regression were age with OR 1.08 per year (1.03-1.16, $p = 0.006$), and diabetes vintage with OR 1.07 per year (1.01-1.14, p =0.034). The model remained a fairly poor fit suggesting that there were a number of relevant variables which had not been accounted for.

For those patients with intact autoregulation for whom a lower limit could be identified (27 individuals), by far the most important factor in determining autoregulation limits was the baseline MAP. Figure 4.8 shows the unadjusted relationship between baseline MAP and lower limit of autoregulation (Pearson's correlation 0.73, p <0.001). In addition, increasing age was independently associated with shift of the lower limit to a higher MAP. This pattern was confounded by a distinct group of young patients with extreme hypertension: the best fitting model included an adjustment for the interaction between age and baseline MAP. The final equation was:

$$Lower_Limit = 2.69 * \text{Age} + 2.13 * \text{BP} - 0.02 * (\text{BP:Age}) - 162 \tag{4.3.1}$$

where BP is baseline MAP before bleedout, averaged over all sessions for that patient.

In other words, the autoregulation threshold increased by 2.69mmHg for every year of age (0.19-5.19, p 0.026), and 2.13mmHg permmHg increase in baseline MAP (0.87 -3.40, p 0.002).This was a reasonable model with R^2 0.62. The relationship between the predicted lower limit using this model, and the actual lower limit, is shown in figure 4.9.

Figure 4.8: Relationship between baseline MAP and lower limit of autoregulation (with line of best fit, Pearson's correlation 0.73)

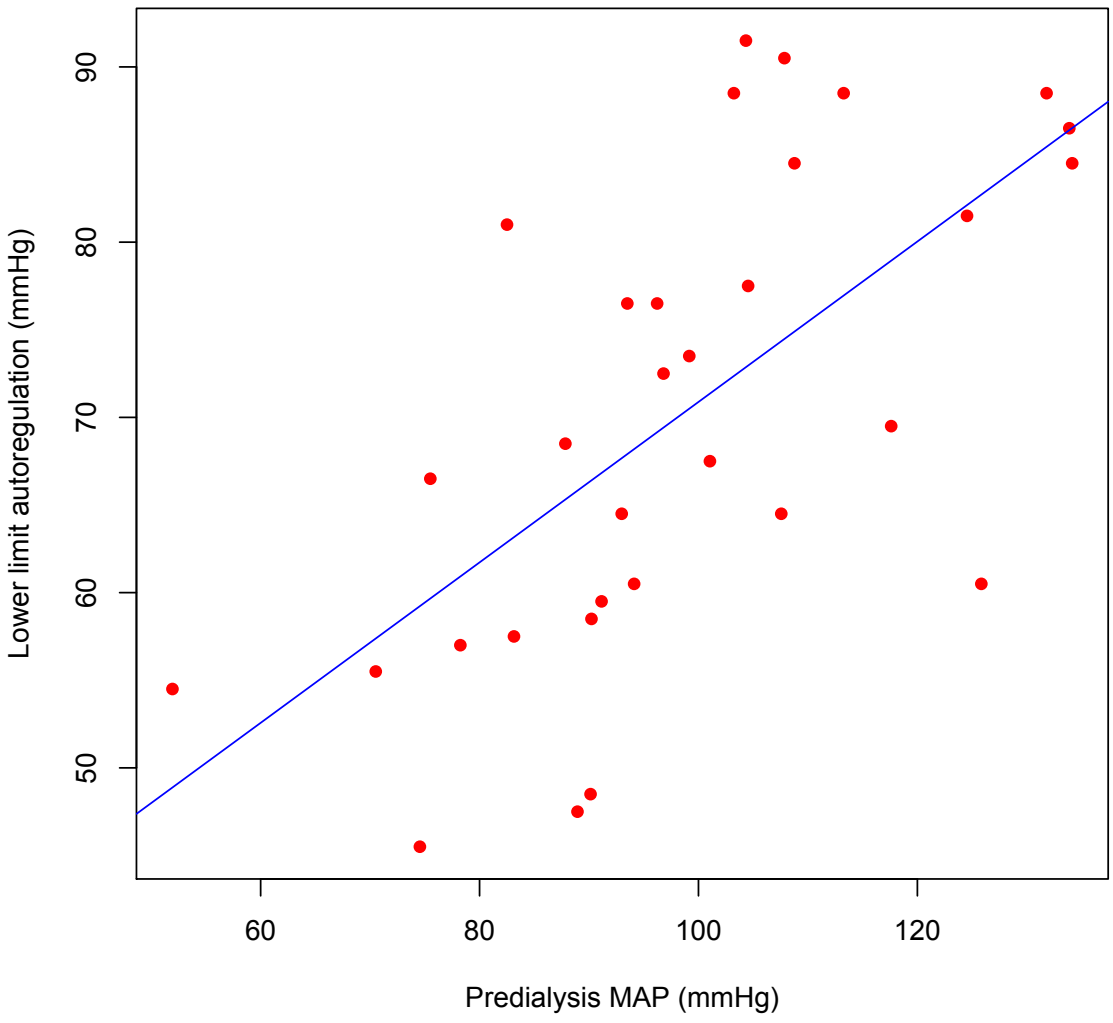

Figure 4.9: Predicted versus actual lower limits of autoregulation

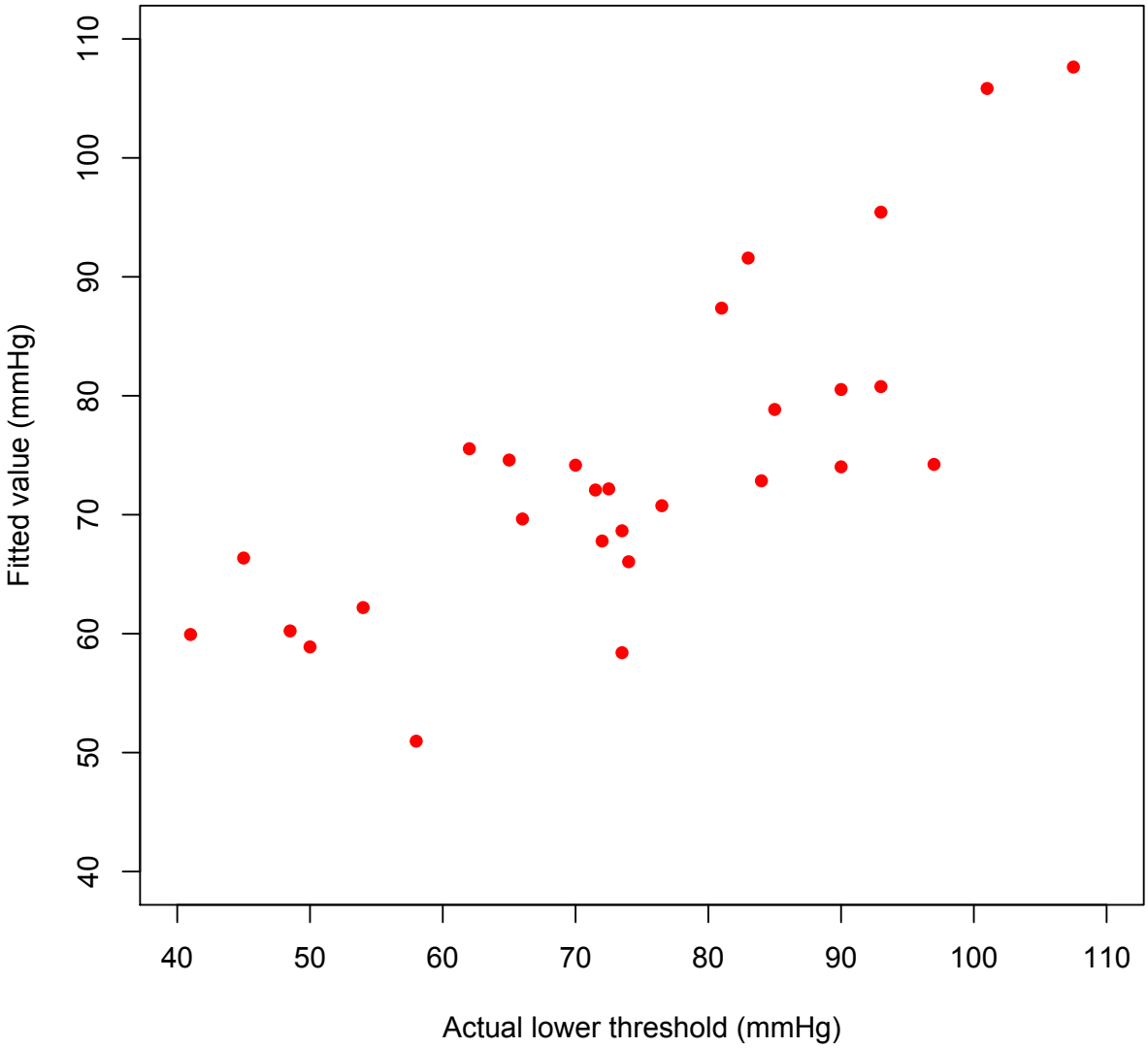

4.3.3 Analysis 3: Sensitivity, specificity and predictive values of autoregulation lower limit for cerebral ischaemia

The sensitivity, specificity, PPV and NPV of absolute MAP thresholds for predicting cerebral desaturation in patients WITHOUT cerebral autoregulation, independent of symptoms, are shown in table 4.1. The sensitivity and specificity for each MAP bin are depicted visually in Figure 4.10 and the ROC curve in Figure 4.11. It can be seen that the patients without autoregulation appear to be a much more homogenous group, and taking a MAP of 70mmHg as the threshold for intervention would have a sensitivity of 81% and specificity 74% for cerebral ischaemia. For the patients with identifiable autoregulation lower limits, the sensitivity and specificity of MAP thresholds relative to personalised lower limit are shown in table 4.2, and depicted visually in Figure 4.12. There is a clear improvement in sensitivity and specificity compared to models using MAP relative to baseline, or absolute MAP (see previous chapter). For example, if intervention occurred when MAP fell within 10mmHg of the predicted lower limit of autoregulation, 63% of ischaemic events would be prevented, with a 29% false positive rate. Including the two patients with atypical ischaemia at bleedout further lowered the sensitivity, as events were essentially occurring at baseline (not shown).

Table 4.1: Association of cerebral ischaemia with absolute MAP thresholds in patients WITHOUT autoregulation

Threshold MAP (mmHg)	Sensitivity	Specificity	Positive Predictive Value	Negative Predictive Value
<90	0.98	0.36	0.08	1.0
<85	0.98	0.45	0.09	1.0
<80	0.95	0.54	0.10	1.0
<75	0.91	0.65	0.11	0.99
<70	0.81	0.74	0.16	0.99
<65	0.67	0.80	0.18	0.98
<60	0.59	0.86	0.21	0.98
<55	0.45	0.89	0.20	0.97
<50	0.38	0.95	0.30	0.97
<45	0.29	0.98	0.42	0.96

Table 4.2: Association of cerebral ischaemia with MAP thresholds relative to lower autoregulation limit

MAP relative to lower limit (mmHg	Sensitivity	Specificity Value	Positive Predictive Value	Negative Predictive
+ 10	0.63	0.71	0.05	0.99
0	0.35	0.92	0.09	0.98
-10	0.15	0.98	0.15	0.98
-15	0.13	0.99	0.24	0.98
-20	0.11	1.0	0.62	0.98
-25	0.07	1.0	0.63	0.98
-30	0.06	1.0	0.67	0.98
-40	0.04	1.0	1.0	0.98

Figure 4.10: Sensitivity and specificity of absolute MAP thresholds for onset of cerebral ischaemia in patients WITHOUT autoregulation

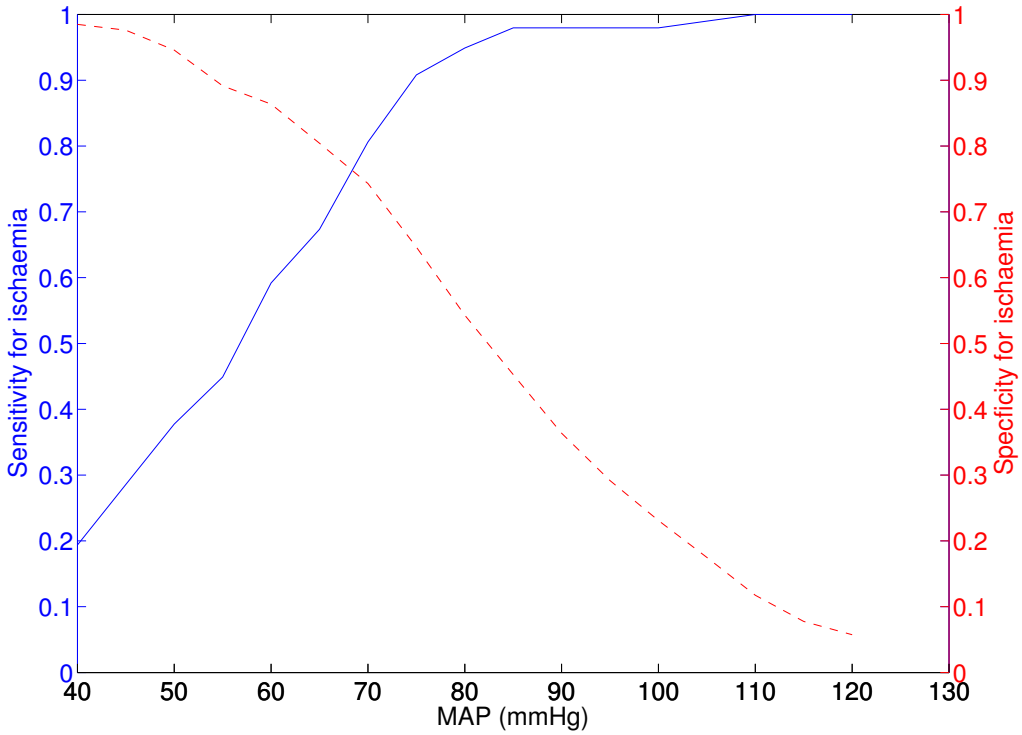

Figure 4.11: ROC curve: absolute MAP thresholds for predicting onset of cerebral ischaemia in patients WITHOUT autoregulation

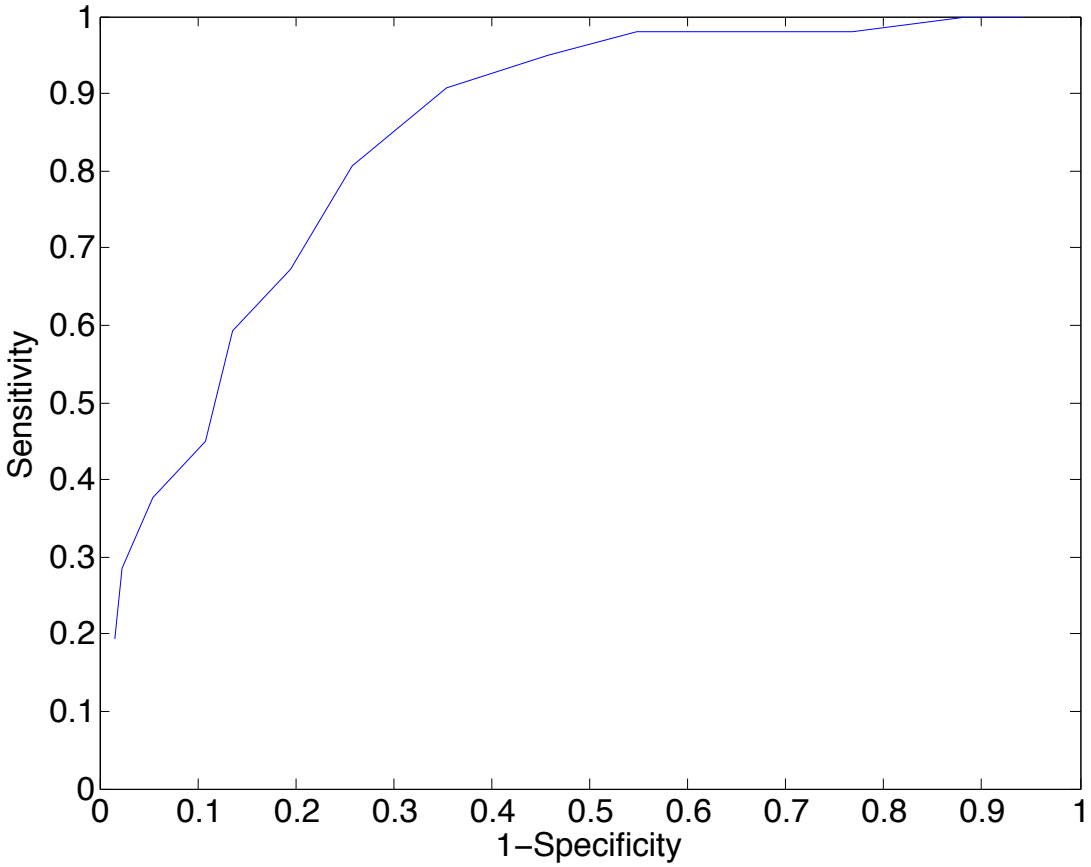

Figure 4.12: Sensitivity and specificity of MAP thresholds relative to lower autoregulation limit

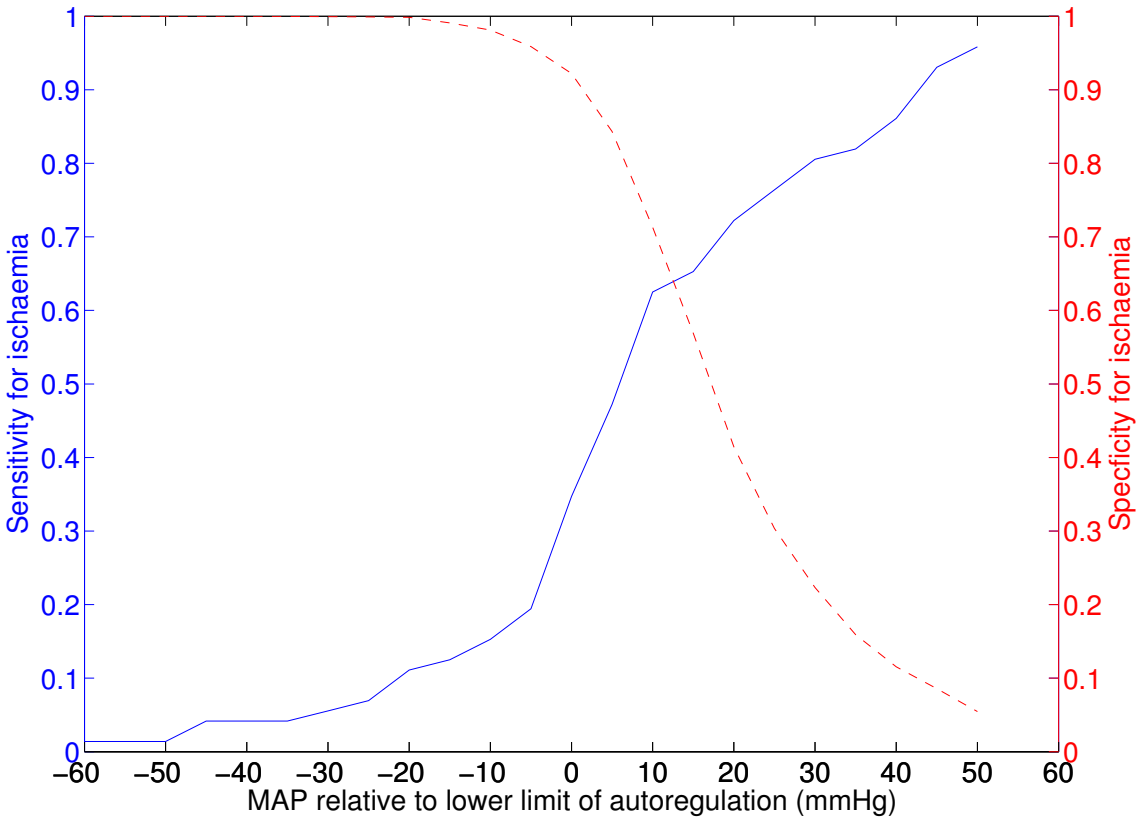

Performance of MAP as a predictor of cerebral desaturation was substantially better at the patient level, regardless of whether autoregulation was present or absent, i.e. personalised ROC curves had a larger AUC. MAP was less useful in the two patients who appeared to have recurrent ischaemic events independent of systemic pressures. Examples of personalised sensitivity and specificity curves for four very different patients are shown in Figure 4.13.

Figure 4.13: Performance of MAP for predicting cerebral desaturation: personalised models

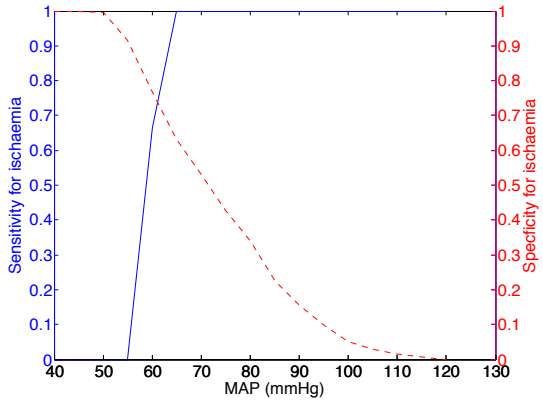

(a) 53 year old man with polycystic kidneys on transplant waiting list, intact autoregulation

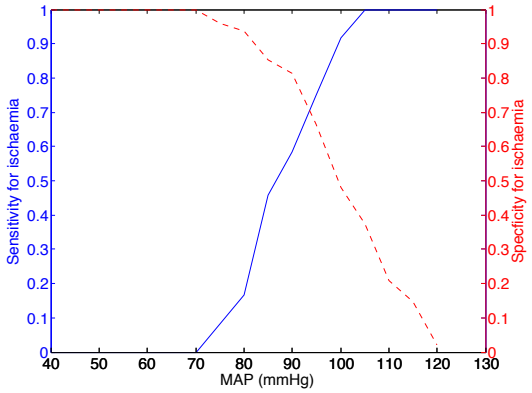

(b) 70 year old man with 30 years of ESRF, previous CVA, absent autoregulation

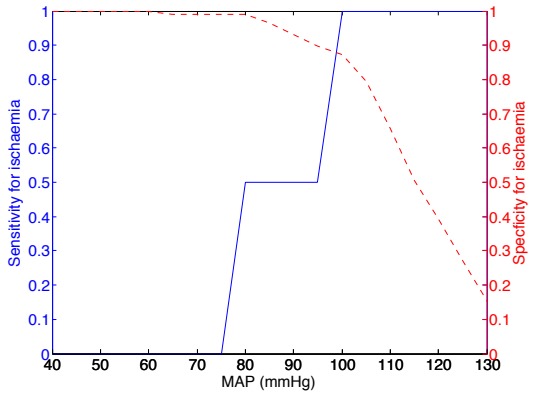

(c) 34 year old man with uncontrolled hypertension and fluid overload, intact autoregulation

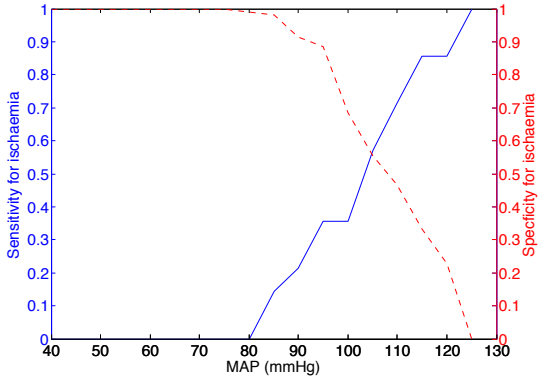

(d) 82 year old woman with unexplained cerebral desaturation at bleedout, independent of blood pressure

4.4 Discussion

Over a third of the HD patients sampled had absent autoregulation, according to the curve fitting method. The structure of the trial means that sicker, less stable patients were recruited more often, so this figure may be lower in the HD population as a whole. For comparison, patients undergoing cardiac surgery have been reported to have 20% incidence of absent autoregulation [138]. In contrast, the moving correlation definition of absent autoregulation (a correlation coefficient of greater than 0.3 at all pressures) was not achieved in any of our patients despite many having a clearly passive relationship between MAP and rSO2. The moving correlation method of assessing cerebral autoregulation was introduced in the mid 1990s, and is based on the relationship between spontaneous fluctuations in arterial blood pressure and cerebral blood flow, either in the time or frequency domain [139]. The main advantage of the moving correlation method is that it is dynamic, continuous, and in real-time. However, it requires a sensitive, continuous method of measuring both arterial pressure and cerebral blood flow (or a surrogate of blood flow such as tissue oxygenation) and has a small signal to noise ratio compared with methods that induce rapid and large changes in blood pressure [139]. Our data suggests that the substitution of the Finometer signal for an arterial line, at least in our awake and moving patients, reduces the true signal further. The correlation coefficient of 0.3 as a cutoff for absent autoregulation derives largely from animal studies and patients undergoing cardiopulmonary bypass, where subjects are anaesthetised and generally have intra-arterial lines, so the data is likely to be much cleaner [105, 55, 140].

For those patients with autoregulation, the mean lower limit was 74mmHg, but varied widely, with 95% confidence intervals from 38.9mmHg to 109.3mmHg. Estimations of autoregulation limits were similar for curve fitting and moving correlation methods, but more patients could be characterised with the former. This range is compatible with the results of the physiological studies described in the introduction, and highlights the inadequacy of using one target MAP for all patients [127, 128, 129, 130, 131, 132]. A contemporary study using cerebral NIRS and the moving correlation method found that the 95% confidence limits for the lower limit of cerebral autoregulation were 43 to 90mmHg (mean 66mmHg) in a comorbid population undergoing cardiopulmonary bypass [140]. This is very similar to the distribution in our population, albeit slightly left shifted, as expected with the higher incidence of hypertension in HD patients.

It has long been clinical practice for anaesthetists and intensivists to estimate the lower limit based

on age, comorbidities and pre-existing blood pressure, an approach which is likely to have large inaccuracies at the patient level [126]. It is now possible to measure real-time cerebral autoregulation limits using bedside techniques such as transcranial Doppler and cerebral NIRS, and this is an increasingly common approach in cardiac surgery and neurointensive care [139, 141] . However, it is not feasible to do this for all patients, particularly not in the outpatient dialysis setting, so a reasonably accurate method of estimating autoregulation limits using demographic and clinical factors would be useful. Our results suggest that baseline MAP is the key determinant of the lower limit in HD patients, with age also contributing independent information. These two variables accounted for most of the variation in this particular cohort, and the model was a good fit. Validation in an external cohort is needed, but it reassuring that several other studies have independently reported an excellent correlation between baseline MAP and lower limit of autoregulation, with the latter typically occurring after a drop of approximately 25% baseline value [126]. Joshi et al did not find evidence that any clinical factors, including baseline blood pressures, affected the lower limit in a population undergoing cardiac surgery, but used baseline SBP and pulse pressure instead of baseline MAP [140]. Other investigators have found that the use of ACE-inhibitors, but not beta-blockers, can alter the limits of cerebral autoregulation [142, 132]; we did not find any impact of anti-hypertensives in our study.

We took the approach of considering our patients in two broad groups: those with intact cerebral autoregulation, and those in whom cerebral oxygenation varied passively with MAP. Isolating patients without cerebral autoregulation resulted in a very respectable ROC curve for MAP alone as a predictor of ischaemic events. These patients appeared to be a much more homogenous group, and taking a MAP of 70mmHg as a cut off would result in a sensitivity of 81% and a specificity of 74% for the onset of cerebral ischaemia, a reasonable trade off. If the absence of autoregulation could be reliably predicted on the basis of demographic and clinical factors, without a the need for monitoring cerebral blood flow or oxygenation, this threshold could potentially be generalised to a substantial proportion of the HD community. Whilst age and diabetes were significant (and expected) risk factors for loss of autoregulation, this model did not explain most of the variation, and would be insufficient to classify patients. A myriad of factors have been shown to be associated with impaired autoregulation, including acute ischaemic stroke, diabetes, liver disease, traumatic brain injury and even dementia, but predicting intact cerebral autoregulation in an individual patient is more problematic [138, 125].

For those patients with intact autoregulation, there was a clear improvement in sensitivity and specificity using MAP relative to lower limit of autoregulation, compared to models using MAP relative to baseline, or absolute MAP. A caveat is that the lower limit determined by the curve fitting method is by definition likely to be associated with ischaemic events, but there was excellent agreement between the curve fitting and moving correlation results in the patients with the best quality data. Our definition of ischaemia was a 15% drop of the baseline rSO2 value for each session (variable even within a patient), whereas absolute rSO2 was used to construct the autoregulation curves. If intervention occurred when MAP fell within 10mmHg of the predicted lower limit of autoregulation, 63% of ischaemic events would be prevented, with a 29% false positive rate. It may not be possible to increase the sensitivity much further, as systemic blood pressure is only one of several factors that can determine tissue ischaemia: the final third of events may be related to changes in haemoglobin oxygen saturation for example. For this reason, including the two patients with atypical ischaemia at bleedout further lowered the sensitivity, as events were essentially occurring at baseline.

A major caveat is that, both for patients with and without autoregulation, specificity is heavily influenced by the large number of true negatives (ischaemia was a relatively rare event for most patients). Therefore the PPV, although improved, was still suboptimal. For example, in this population, amongst patients without autoregulation, intervening every time the MAP reached 70mmHg would result in 5 unnecessary treatments for every ischaemic episode prevented. Of course, if targeted at a higher risk population, i.e. individuals previously known to develop intra-dialytic cerebral ischaemia, performance would be much better. In addition, it may be deemed a worthwhile trade off, particularly if the intervention was simple and did not result in significant fluid loading, e.g. brief reduction in ultrafiltation rate alone.

Limitations of this study include the fact that the definition of ischaemia is essentially arbitrary: there is no consensus on what change in rSO2 is harmful, because rSO2 is a surrogate measure rather than a hard patient outcome. However, a convincing body of studies have now shown that rSO2 changes consistent with those seen in this study do correlate with morbidity and mortality in other populations [99, 100, 101, 102, 103, 104, 105, 106]. In Chapter 8, we furthermore demonstrate that decline in cognitive function in this population is associated with exposure to intra-dialytic cerebral ischaemia, as defined here. Another limitation is that we could not take into account factors that may have dynamically altered

the autoregulation threshold, particularly PaCO2 (which would be expected to rise with the bicarbonate load on dialysis). We had simultaneous data on respiratory rate and peripheral/access saturations, and these did not vary substantially in most patients during HD. Nevertheless, the occurrence of so many events in the 10mmHg window above the limit may point to inaccuracies in our estimates of the lower limit.

Overall, our results suggest that most promising approach of all would be personalised modelling. Even within the impaired autoregulation group there is considerable variation in the MAP at which ischaemia occurs. The ROC curves were generally far better when using a personalised absolute MAP threshold for each individual patient, both for patients with and without autoregulation. Given potential inaccuracies of predicting both the presence of autoregulation and its limits using demographic factors alone, this may require patients to undergo monitoring with cerebral NIRS for a number of dialysis sessions, sufficient to construct their individual autoregulation curve and estimate their personal threshold for onset of ischaemia. Whilst a method of continuous blood pressure monitoring would be ideal, we have shown that it is possible to construct autoregulation curves with NIBP measurements at 15 minute intervals. As the autoregulation limits can shift with time, this process would have to be repeated at intervals, e.g. if baseline blood pressure underwent significant changes. To temper the cost and inconvenience, this could be limited to incident or vulnerable patients, so that only one NIRS machine would be needed for a renal unit.

4.5 Conclusion

In summary, this is the first study to construct cerebral autoregulation curves for HD patients, and we have shown that this approach has utility in deciding the MAP threshold at which intervention should occur for an individual patient. The optimal MAP for patients without autoregulation, typically the elderly and longstanding diabetics, would appear to be 70mmHg or above. For the remainder of patients, a predicted lower limit of cerebral autoregulation can be calculated using baseline MAP and age: maintaining MAP above the lower limit plus 10mmHg would be expected to prevent two thirds of ischaemic episodes. Personalised ischaemia thresholds have the best performance, and would be most accurately determined by monitoring the patient with cerebral NIRS for several HD sessions.

Chapter 5

Comparison of oscillometric and finger volume-clamp blood pressure measurements in the haemodialysis population

5.1 Introduction

The gold standard measurement of arterial blood pressure measurement is that derived from an intra-arterial line, where arterial pressure is measured directly, usually at the radial or brachial artery. Central aortic pressure is the real index of interest, and so transducer position is adjusted to control for the impact of gravity at the measurement site relative to the level of the left atrium. Intra-arterial lines allow for waveform analysis, as well as direct measurement of systolic, mean and diastolic pressures. Outside the anaesthetic and critical care environment, such invasive monitoring is not practical, and the gold standard is ausculatory blood pressure monitoring. A mercury sphygmomanometer is used, with the cuff at heart level, and the practitioner listens over the brachial artery with a stethoscope whilst the cuff gradually deflates: the SBP is taken at the point where the pulse can first be heard as a clear tapping sound, and DBP as the point where silence returns. This requires a skilled operator present at the bed-side, and alternative automatic methods using oscillometry have become popular. Oscillometry is similar in that a cuff is placed around the upper arm at heart level, and pressure in the cuff is measured as it is slowly deflated: however, the primarily measure is the point of maximal oscillations, which correlates

with MAP. SBP and DBP are then estimated using an algorithm specific to the manufacturer.

In order to meet BHS standards, new oscillometric devices must be tested against ausculatory measurements made by trained practitioners. The agreement should be within 5mmHg for at least 50% of measurements, within 10mmHg for 75% of measurements, and within 15mmHg for 90% of measurements [143]. The AAMI standards use a similar distribution, specifying that the mean difference should be less than 5mmHg with standard deviation less than 8mmHg [144]. These generous acceptance limits are surprising given that changes as small as 5mmHg are used to make clinical decisions, and highlight the challenge of accurate blood pressure measurement.

Neither the BHS or AAMI make use of the ultimate gold standard of intra-arterial lines, for practical and ethical reasons [143]. Existing studies report relatively poor agreement between intra-arterial measurements and NIBP measurements (ausculatory or oscillometric), typical limits of agreement being +/- 20mmHg for MAP, and considerably wider for systolic and diastolic pressures [12, 11, 9, 10, 145]. SBP is generally underestimated by oscillometric techniques, and DBP overestimated. In everyday clinical practice there tends to be even larger errors, due to inappropriate cuff sizing or site, patient position, lack of training or difficult environments [9, 10, 11, 146]. A reasonably large, well-conducted trial demonstrated that ensuring the correct sized cuff, well-trained staff, ideal measurement conditions and a state of the art oscillometric device, improved the agreement for MAP to -2.4 +/- 11.8mmHg (oscillometric lower) [147]. The lack of agreement can be partly explained by the impossibility of obtaining simultaneous measurements of non-invasive and invasive blood pressures in the same limb, as all cuff methods require the cessation of arterial blood flow to the limb at the start of measurement. More importantly, NIBP monitoring is intermittent, giving just a single snapshot at a moment in time, whereas true blood pressure is a continuously varying, dynamic system.

There has been a large body of research over recent decades into reliable non-invasive methods of obtaining continuous arterial pressure measurements. Probably the most investigated to date are the Finometer devices, which use volume clamp technology [85]. The Finometer devices have been extensively validated against intra-arterial measurements in several populations, with generally very good results [86, 87, 88, 89, 90, 91, 92, 93]. Not unexpectedly, intra-arterial pressures appear to have closer agreement with Finometer readings than auscultatory readings, despite auscultation being considered the

non-invasive gold standard. Although volume-clamp technology has been used by a number of groups to monitor continuous blood pressure in the HD population, there are no published studies validating the Finometer against ausculatory, oscillometric or intra-arterial measurements in these patients [20, 94, 95, 31].

In unpublished thesis work, Hakim et al compared Finometer and oscillometric blood pressure measurements, performed sequentially in the non-access arm, in 25 HD patients [94]. They found a bias for SBP of 0.6mmHg (oscillometer higher) with limits of +/- 30mmHg, whereas bias for MAP was 1.44mmHg with limits of +/- 23mmHg. However, findings were limited by the following features: each patient only had two oscillometric measurements, resulting in a very small dataset of 50 paired measurements; there was no signal quality index for the Finometer waveform; there was an "approximately five minute" delay between Finometer and oscillometric readings; Finometer data for comparison was variably selected from the period before or after oscillometric measurement; repeated measures were not accounted for.

The objectives of this chapter are as follows: to examine the agreement between Finometer and oscillometric blood pressure readings during haemodialysis in a very large, robust dataset; to identify whether there is better agreement for trends in blood pressure relative to baseline than for absolute blood pressure; to look at patient specific factors that may impact on agreement.

5.2 Methods

See the Methods chapter for details of the trial and data collection. Continuous blood pressure monitoring was performed using the Finometer PRO (unstable patients, n=39) or Finometer MIDI (stable patients, n=19). The beat-to-beat blood pressure data was processed by removal of extreme outliers (3 standard deviations from mean) and low pass filtering (Hamming window based with cutoff 0.083Hz) to attenuate high frequency noise. Data was discarded if it did not meet the standards of an SQI based on waveform quality, as described in the Methods chapter. Missing segments were not interpolated. For stable patients with the older Finometer model, baseline blood pressure was defined as the median value from a window beginning 2 minutes after recording start (to allow time for Physiocal calibration) and ending at the point of bleedout, i.e. when the patient's blood enters the dialysis circuit and treatment commences. For the unstable patients with the Finometer Pro, the start point of the window was instead completion of RTF calibration.

All patients had oscillometric NIBP before and after dialysis, and at least every 30 minutes during the procedure itself. There was no pre-processing of the NIBP data. One computer was used as a time server to ensure all data streams were tightly synchronised. Both NIBP cuff and Finometer cuff were placed on the non-access arm. Inflation of the arm cuff led to brief cessation of blood flow to the fingers, and hence loss of Finometer waveform, but not for long enough that the Finometer stopped running. This impact of cuff inflation on the Finometer waveform was useful to confirm the timing and duration of the oscillometric measurements. The NIBP timestamp was outputted once the cuff had fully deflated and the waveform had returned to normal, approximately one minute after cuff inflation began. The earliest point that arm cuff inflation could start was therefore conservatively considered to be 80 seconds before the NIBP timestamp. The median of the 10 beats of Finometer data surrounding the -90 second point was taken as the "pre" measurement. If there was no data at the -90 point itself, the nearest data within the -150 to -90 second window was accepted. For comparison, the first Finometer timestamp to follow the NIBP timestamp was identified, and a median of the 10 beats surrounding this point was taken as the "post" measurement (provided there was not a gap of more than 60 seconds between the NIBP timestamp and the next Finometer timestamp). If the SQI for Finometer data at either the pre or post points indicated suboptimal data quality, these readings were discarded.

Bland-Altman plots were constructed for the agreement between absolute and relative to baseline SBP, DBP and MAP on the population level. Modified standard deviations were calculated to account for repeated measures within patients, using ANOVA as recommended by Bland and Altman [148]. In addition, plots were examined for each individual patient. Linear models were constructed to explain patient-level variability in agreement for MAP using clinical covariates including age, vascular disease (CVD, PVD or IHD), BMI, sex, median pre-dialysis oscillometric MAP, diabetes vintage and HD vintage.

5.3 Results

There was physiological data on 635 dialysis sessions in 58 patients. Two patients were found to have such severe vascular disease that the Finometer could not detect a finger pulse: in total, 576 sessions in 56 patients had Finometer monitoring. Demographics are summarised in the Methods chapter. Altogether, there were 4868 pairs of strictly time-matched pre-cuff inflation Finometer and oscillometer

measurements, and 4734 pairs of post-cuff inflation Finometer and oscillometer measurements. More of the pre-NIBP than post-NIBP Finometer readings met the stringent SQI criteria (3946 compared to 3125), largely because Physiocal calibrations became increasingly frequent in response to the waveform distortion and eventual loss associated with arm cuff inflation.

5.3.1 Population-level agreement between methods

The agreement between methods for absolute MAP, SBP and DBP are shown in table 5.1 (oscillometer minus Finometer for all calculations). It was apparent that the match between Finometer and oscillometer readings was highly variable from patient to patient, with some having a substantial bias in either direction. Hence, whilst the overall mean tended towards 0, there was a large standard deviation on the population level. Excluding the small number of patients with technical difficulties in blood pressure measurement (3 patients in whom an NIBP cuff of appropriate size could not be found due to body habitus, and 6 patients with upper limb peripheral vascular disease) improved the overall agreement meaningfully. The results excluding these patients are shown in table 5.2. These 9 patients not only had increased variability, but markedly outlying bias: the median patient bias for MAP in this subgroup was +12.2mmHg (in keeping with under-reading of Finometer due to vascular stenosis, or over-reading of NIBP due to an undersized arm cuff) . The remaining 47 patients had median bias of -3.4mmHg. The Bland-Altman plots for all patients and for the subgroup without technical difficulties in blood pressure measurement are shown in figures 5.1 to 5.3. Overall, MAP outperformed SBP for both bias and variation. In clinical practice, wide limits of agreement are more problematic than bias, and were considerably greater for SBP than MAP or DBP.

Other methods of assessing agreement between the methods include correlation and linear regression. A simple plot of Finometer (pre-arm cuff inflation) versus oscillometric MAP measurements, including all data, is shown in figure 5.4. The linear regression equation for the relationship between oscillometric and Finometer pressures is:

$$Finometer_MAP = 0.74 * NIBP_MAP + 24.01 \tag{5.3.1}$$

The R^2 for the linear model was 0.41. The correlation between absolute MAP as measured by os-

cillometric and volume-clamp methods was 0.68, p <0.001. Excluding patients who had not had RTF calibrations (i.e. who had been monitored with the Finometer MIDI rather than the Finometer PRO) did not improve agreement.

Table 5.1: Agreement between oscillometer and Finometer absolute blood pressure at population level, all patients

Index	Bias (Oscillometer-Finometer,mmHg)	Standard deviation (mmHg)
MAP (before arm cuff inflation)	-1.3	16.8
MAP (after arm cuff inflation)	0.5	17.4
DBP (before arm cuff inflation)	0.9	16.3
DBP (after arm cuff inflation)	2.0	16.4
SBP (before arm cuff inflation)	-3.1	23.4
SBP (after arm cuff inflation)	-1.4	23.4

Table 5.2: Agreement between oscillometer and Finometer absolute blood pressure at population level, excluding 9 patients where there were technical difficulties with measurement

Index	Bias (Oscillometer-Finometer,mmHg)	Standard deviation (mmHg)
MAP (before arm cuff inflation)	-3.5	14.0
MAP (after arm cuff inflation)	-1.0	14.8
DBP (before arm cuff inflation)	0.1	14.3
DBP (after arm cuff inflation)	1.9	14.2
SBP (before arm cuff inflation)	-6.9	19.6
SBP (after arm cuff inflation)	-4.4	20.3

Figure 5.1: Bland-Altman plots for difference between oscillometer and Finometer MAP

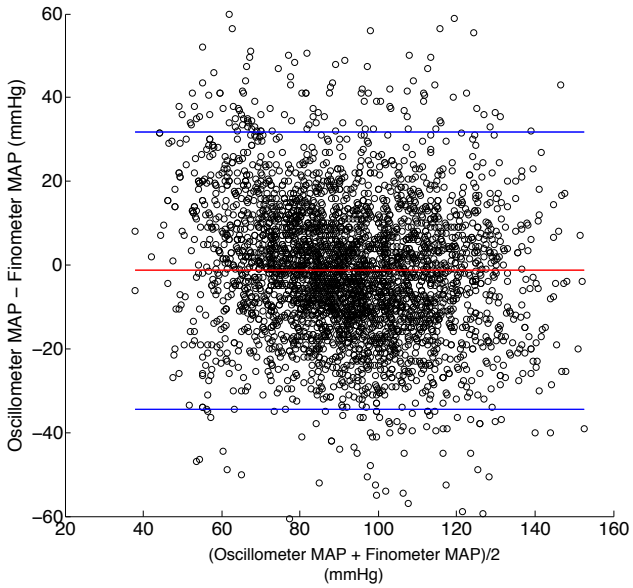

(a) All patients

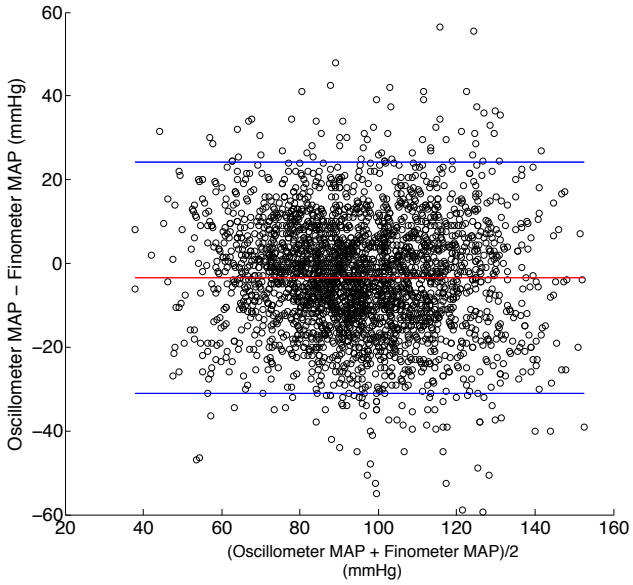

(b) Excluding those with technical difficulties in measurement

Figure 5.2: Bland-Altman plots for difference between oscillometer and Finometer SBP

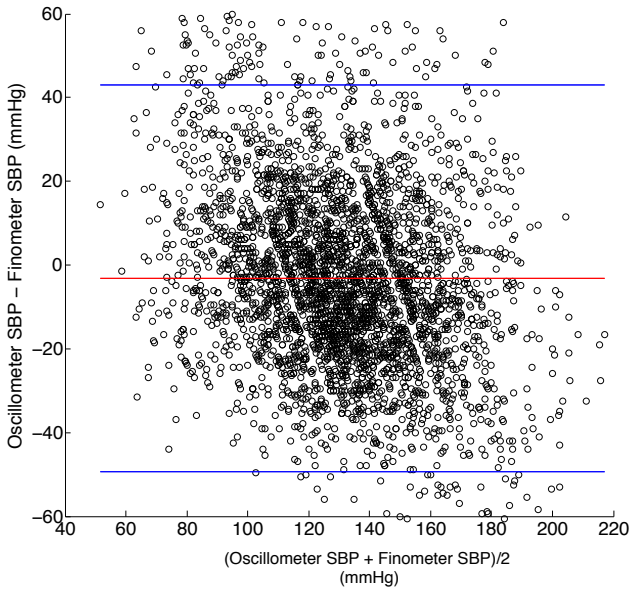

(a) All patients

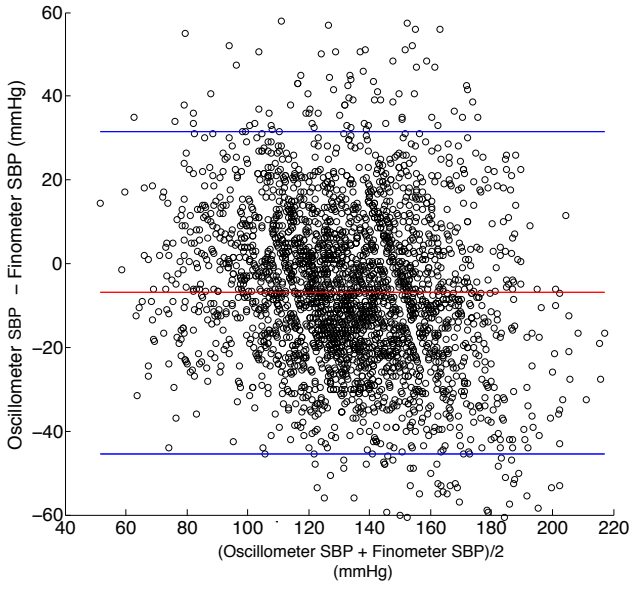

(b) Excluding those with technical difficulties in measurement

Figure 5.3: Bland-Altman plots for difference between oscillometer and Finometer DBP

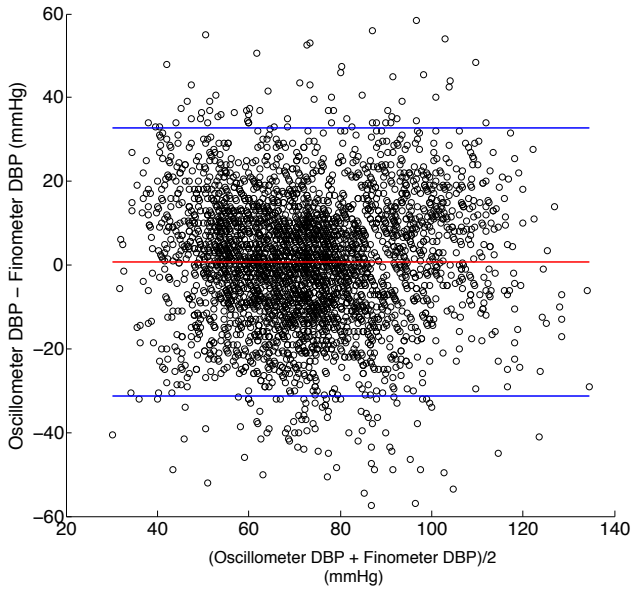

(a) All patients

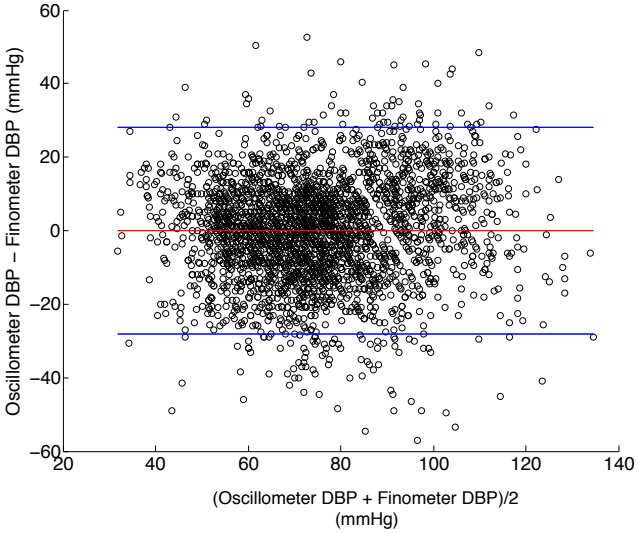

(b) Excluding those with technical difficulties in measurement

Figure 5.4: Finometer versus oscillometer MAP, all patients

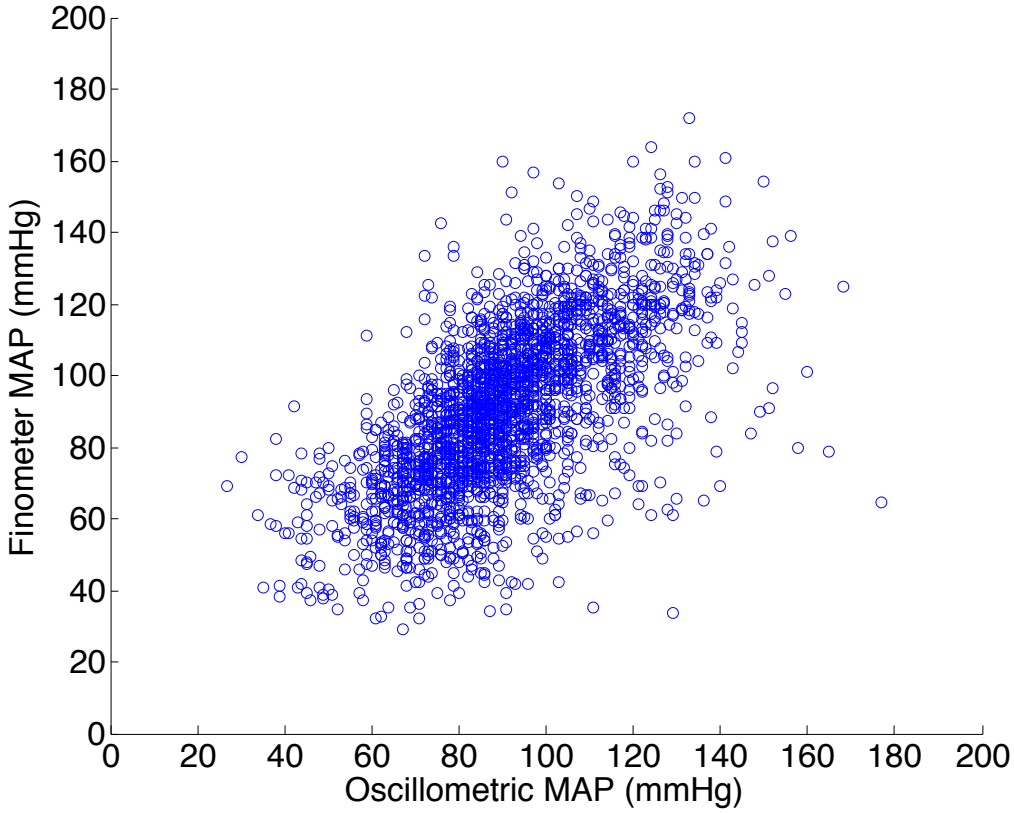

There was not an improvement in agreement using relative changes (i.e. trend) in MAP or SBP as shown in table 5.3 and table 5.4.

Table 5.3: Agreement between oscillometer and Finometer relative blood pressure at population level, all patients

Index	Bias (Oscillometer-Finometer,mmHg)	Standard deviation (mmHg)
MAP (before arm cuff inflation)	-3.8	17.8
MAP (after arm cuff inflation)	0.9	18.7
SBP (before arm cuff inflation)	-3.3	23.2
SBP (after arm cuff inflation)	0.1	24.1

Table 5.4: Agreement between oscillometer and Finometer relative blood pressure at population level,excluding 9 patients where there were technical difficulties with measurement

Index	Bias (Oscillometer-Finometer,mmHg)	Standard deviation (mmHg)
MAP (before arm cuff inflation)	-2.6	15.0
MAP (after arm cuff inflation)	0.4	15.3
SBP (before arm cuff inflation)	-3.4	20.3
SBP (after arm cuff inflation)	0.3	20.9

5.3.2 Patient-level agreement between methods

Even excluding the patients with technical difficulties in measurement, there was considerable patient-level variation in bias and limits of agreement, as depicted in figure 5.5. Linear models were constructed to investigate clinical factors determining bias and standard deviation of differences for a given patient (using MAP as index, and all patients included). For bias, as expected from the subgroup analysis, PVD, obesity and diabetes vintage increased positive offset (i.e. oscillometer greater than Finometer). Vascular disease was associated with an additional +8.74mmHg bias (0.93-16.55mmHg, p=0.029); BMI was associated with an increased +0.36mmHg per kg/m^2 (0.04-0.69mmHg, p=0.030); diabetes vintage was associated with an increased +0.19mmHg per year (0.00-0.38mmHg, p=0.049). However, approximately three quarters of the variance remained unexplained. Diabetes vintage also had a significant impact on the standard deviation of differences between Finometer and oscillometer: every year of diabetes increased the standard deviation by 0.12mmHg (0.04-0.21mmHg, p=0.006). In addition, those

patients with baseline blood pressures in the highest quartile showed more variability, with an increased 2.44mmHg in standard deviation compared to those in the interquartile range (0.33-4.55mmHg, p=0.024). Again the model was suboptimal, with 80% of variance unexplained.

It is perhaps unsurprising that higher absolute pressures should be associated with higher absolute variation, but overall there was no relationship between absolute blood pressure and agreement between methods. Within individual patients different patterns could be seen. Examples of BA plots for different patients are shown in figures 5.6; the axis limits are all identical to facilitate comparison. The first patient, a 53 year old man with polycystic kidneys and no major comorbidities, had a negative linear relationship between MAP and agreement (gradient of line of best fit -0.4), with the oscillometer tending to overestimate lower pressures and underestimate high pressures compared to the Finometer; bias was -1.6mmHg, with limits +/- 20.8mmHg. The next patient was morbidly obese (figure 6 (b)). In addition to cuff size issues, obesity introduces error because the oscillometric pulses become weaker and weaker with increasing arm circumference. It can be seen that there is a positive bias, presumably due to over-reading by an undersized arm cuff, and broad limits of agreement (6.8mmHg, +/- 34.2mmHg). There is also a positive linear relationship between MAP and agreement (gradient of line of best fit 0.6).

In contrast, the patient in figure 6 (c), who had no major comorbidities, shows no pattern between MAP and agreement, with good agreement throughout (bias -2.8mmHg and limits +/- 13.8mmHg). The patient depicted in figure 6 (d) had suspected upper limb vascular disease, and the plot supports a step change in blood pressure between the arm and the finger, with a strikingly positive bias of 22.9mmHg. There is a negative linear relationship between MAP and agreement, and particularly wide limits once MAP fell below 70mmHg, perhaps because of poor perfusion of the finger at lower driving pressures (+/- 34.2mmHg). Figure 6 (e) shows a patient with end stage cardiac failure, chronic hypotension and slow atrial fibrillation; again the agreement appears worse at extremely low pressures (-12.4mmHg, +/- 21.8mmHg). The final plot, figure 6 (f), is from a patient who started dialysis only a month previously with glomerulonephritis: he was hypertensive but had no non-renal comorbidities, and the agreement was equally good throughout all pressures (2.0 +/- 16.8mmHg). It can be seen that considering all measurements together at the population level may not be informative for the individual patient.

Figure 5.5: Patient-average means and standard deviations for difference between oscillometer and Finometer measurements

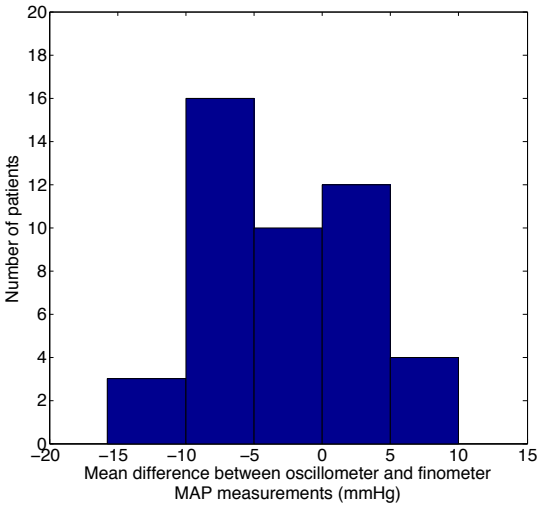

(a) Patient-average bias

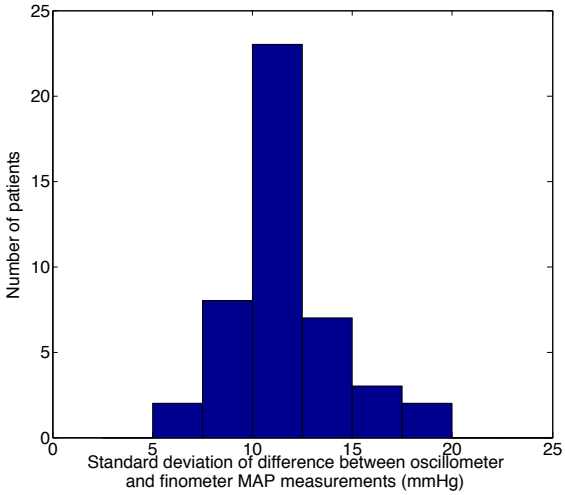

(b) Patient-average standard deviation of differences

Figure 5.6: Bland Altmann plots for individual patients

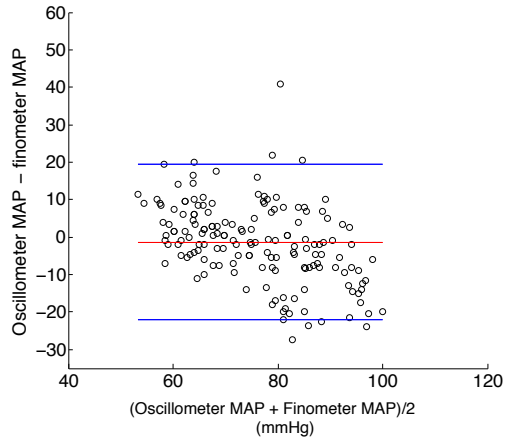

(a) 53 year old man with no major comorbidity

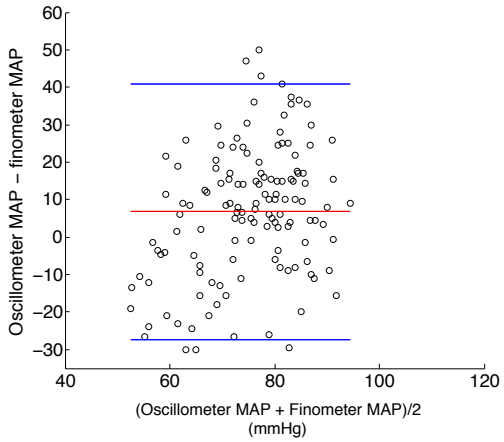

(b) Morbidly obese 60 year old lady with undersized arm cuff

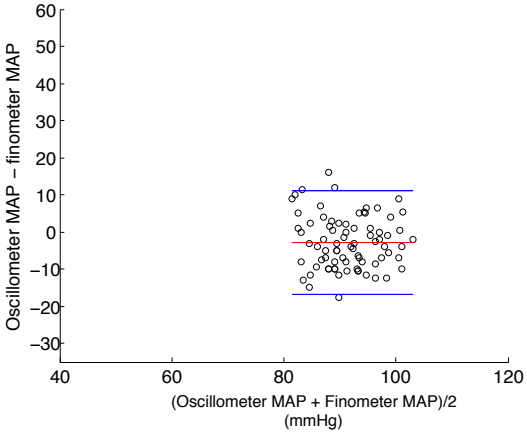

(c) 55 year old man with failed transplant, very stable on dialysis

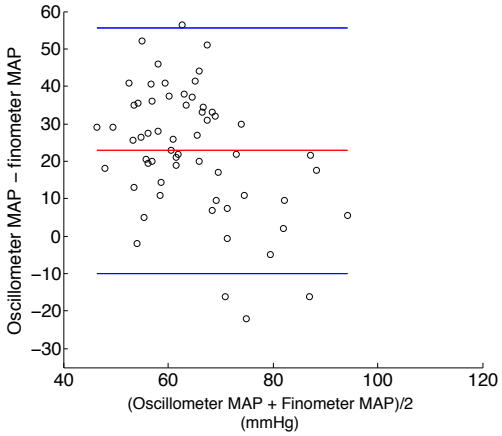

(d) 83 year old man with peripheral vascular disease

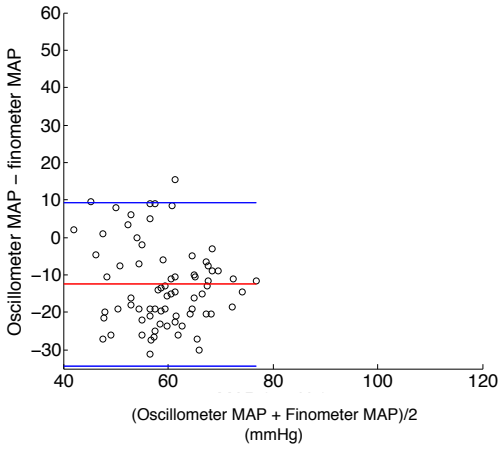

(e) 69 year old man with end stage cardiac failure and chronic hypotension

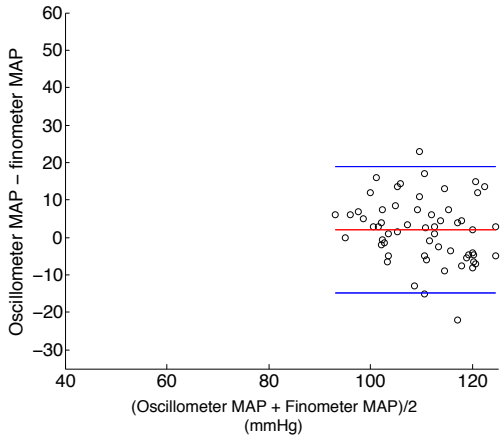

(f) Hypertensive 55 year old man with glomerulonephritis and no major comorbidity

5.4 Discussion

Accurate measurement of blood pressure outside critical care is a challenge: most studies of IDH have relied on oscillometry, which has a large measurement error compared to the true intra-arterial blood pressure, particularly in the context of real-world practice, and can only provide very intermittent data [9, 10, 11, 12]. We found that the agreement between oscillometer and Finometer measured blood pressures was suboptimal, though not much worse than that reported between oscillometer and intra-arterial line measurements, where typical MAP bias ranges from -2 to -5mmHg (oscillometer higher) with limits +/- 20mmHg [12, 11, 9, 10, 145]. Excluding the small number of patients with technical difficulties in blood pressure measurement, for MAP bias was -3.5mmHg (oscillometer higher), with limits of +/- 27mmHg. There was not improved agreement between methods at the population level when looking at trends rather than absolute values. This is expected, given that most of the error appeared to be random rather than systematic. It is a common misconception that a trend is easier to measure accurately than an absolute value: where there is random error (the majority of cases), the converse is true.

The limits of agreement are wider than those reported for oscillometer versus intra-arterial measurements. There are a number of potential reasons for this. Firstly, the Finometer is only a surrogate for intra-arterial measurements. Secondly, these studies were almost universally performed in a clinical trial setting, and moreover in a critical care environment where patients are sedated with one-to-one care. McMahon et al used real world data from an aeromedicine setting, and reported an agreement of +/- 23mmHg between oscillometry and intra-arterial line measurements [9]. Finally, none of these studies included renal patients, in whom blood pressure measurement may present particular challenges. There are a number of factors known to impact on the accuracy of oscillometry, which are particularly relevant for HD patients: these include arterial stiffness, diabetes, obesity and atrial fibrillation [149, 150, 151]. Moreover, HD is an outpatient environment, where patients are moving, talking and eating, and arm cuffs may be incorrectly sized and have to be placed over clothing. It has been shown that pre-dialysis blood pressure varies hugely between "usual care" oscillometric measurement, and "standardised" ausculatory measurement (sitting quietly, accurately sized cuff, skilled operator, repeated measures) [146].

Concerning the ESRF population specifically, there are only two studies to date which have validated NIBP against intra-arterial measurements, and none that have validated the Finometer in this population [150, 152]. Chen et al measured intra-arterial and oscillometric blood pressures in 41 HD patients and

found that non-invasive SBP was hugely inaccurate, with a bias of -30mmHg (oscillometer lower) +/- 20mmHg compared to the gold standard [150]. DBPs were reasonably similar, and MAP not reported. The extent of the SBP discrepancy was significantly associated with vascular disease, as indicated by peak carotid artery systolic velocity [150]. Lodi et al assessed the same oscillometer used in our trial, the Colin BX-100 (Colin Corporation, Aichi, Japan), which is incorporated into the Braun dialysis machines [152]. As a substudy, they compared the oscillometer against intra-arterial measurements on 11 HD patients in a critical care environment. The agreement was reasonable, being 3.4 +/- 19.6mmHg for SBP, but conclusions were limited by the fact there were only 16 paired measurements, done under ideal conditions in sedated patients.

We found substantial differences between patients in bias, agreement limits, and relationship between absolute MAP and agreement. On linear models, some of this could be explained by diabetes vintage (which increased both bias and variability), as well as obesity and PVD (which predominantly affected bias). Neither of the methods used in this study represent the true gold standard, an intra-arterial line, so it is not possible to say which method accounted for most of the measurement error, or which method was most affected by these clinical conditions. However, in existing literature, the Finometer performs better against intra-arterial lines than either sphygmomanometers or oscillometers. Indeed, obesity, vascular disease or diabetes are all factors which are known to impact on the accuracy of oscillometric measurements. Diabetes and vascular disease are also likely to impact on the quality of blood pressure waveform detected in the finger, though we used a robust SQI on the Finometer data. Obviously it is not possible to apply an SQI to NIBP readings - from the NIBP data alone, it cannot be ascertained, for example, whether the patient was moving, or the cuff had slipped down the arm.

In agreement with previous literature, we found that bias and limits of agreement were much worse for SBP than MAP, being -6.9mmHg and +/- 38mmHg respectively. SBP is the most used blood pressure index amongst nurses and clinicians outside anaesthetics and critical care, as reflected by the number of IDH definitions and studies which have focused near exclusively on it [6, 5, 13, 14, 15, 16]. However, non-invasive SBP has a far greater measurement error than non-invasive MAP when compared to intra-arterial readings, and is particularly sensitive to changes in cuff size and position [10, 9, 12]. This may be partly because NIBP devices measure MAP directly, and SBP is then estimated using a manufacturer-specific algorithm. Volume clamp methods similarly suffer from greater error for systolic readings, as

systolic pressures change most between central and peripheral arteries, and to a highly variably degree depending on individual vessel stiffness. Arterial stiffness will alter pulse pressures but not necessarily change downstream perfusion pressure. Whilst pulse pressure and SBP may be more prognostic as regards complications of long term hypertension in the elderly, MAP is probably a more appropriate measure of adequate organ perfusion pressure during hypotension [17, 18].

5.5 Conclusion

There were substantial differences between oscillometer and Finometer blood pressure measurements in HD patients, though the discrepancy was not much greater than that seen between oscillometer and intra-arterial line measurements in non-renal populations. It is likely that much of the error comes from the oscillometer, given the findings in previous literature, and the particular clinical factors that were associated with increased bias and variability. However, direct comparison of Finometer against intra-arterial measurements in the HD population is needed for any definitive conclusions. In agreement with other studies, MAP appears to involve substantially less measurement error than SBP.

Chapter 6

Cardiac Output Measurement

6.1 Introduction

The Finometer devices use volume clamp technology to estimate continuous blood pressure non-invasively. Whilst they have been validated in many patient groups, including the elderly and those with vascular disease, they have never been tested against gold-standard (an intra-arterial line) in the ESRF population. Therefore the validity of secondary measures derived from the blood pressure trace, e.g. baroreflex sensitivity and cardiac output, is even more questionable in this patient group.

Cardiac output is estimated by the Finometer using a pulse contour analysis algorithm known as the Modelflow approach. Modelflow estimates aortic flow via a three-element model (aortic characteristic impedance, arterial compliance, and systemic vascular resistance), with estimation of aortic diameter refined by demographic data [85]. A number of studies have tested the Modelflow approach against gold standard Fick principle methods (e.g. thermodilution, dye indication, ultrasound dilution) and found that trend in cardiac output can be accurately estimated in most situations [85]. However, the Finometer is better at detecting relative changes in cardiac output, and a gold standard method is still needed to obtain absolute values [96, 97].

In dialysis patients with AVF, it is possible to obtain intermittent gold-standard absolute cardiac output measurements using ultrasound dilution (using the Transonic device) [98]. To date, only one study has taken advantage of this in order to validate the Modelflow approach in HD patients, and reported not only a substantial absolute error, but also a lack of correlation between Finometer and ultrasound-

dilution measurements over time [153]. However, this was a very small study with only 50 measurement pairs in 25 patients undergoing HD: the aim of this chapter is to assess the agreement between ultrasound dilution and Finometer estimates of cardiac output for both absolute and relative values in a larger cohort.

6.2 Methods

See the methods chapter for full details on trial structure and data collection, including ultrasound dilution protocol.

Continuous blood pressure and cardiac output monitoring was performed using the Finometer device. The beat-to-beat blood pressure data was processed by removal of extreme outliers (3 standard deviations from mean or more) and low pass filtering (Hamming window based with cutoff 0.083 Hz) to attenuate high frequency noise. Data was discarded if it did not meet the standards of an SQI based on waveform quality, as described in the methods chapter. Missing segments were not interpolated.

Ultrasound dilution measurements were done on the unstable subset of patients ("study" patients, see Methods chapter) who were undergoing haemodynamic monitoring with the Finometer Pro. Ultrasound dilution requires a well-functioning AVF with no recirculation, which meant that some patients in this group were excluded. The first Transonic measurement was done shortly after bleedout and was used to calibrate the Finometer reading. The Finometer cardiac output at the time of ultrasound dilution read-out was recorded as a spot value. For as many eligible sessions as possible depending on availability of equipment, a second Transonic measurement was taken 2 hours into HD, and again compared to the simultaneous Finometer reading. This allowed paired measurements of both absolute and relative cardiac output. For the purposes of assessing Finometer performance against the standards proposed by Critchley and Critchley, the median of the SQI-filtered Finometer-measured cardiac output over the 2 minutes preceding each spot value was used, to eliminate the impact of poor quality data.

Correlation and Bland-Altman statistics were used to assess agreement between methods. Modified standard deviations were calculated to account for repeated measures within patients, using ANOVA as recommended by Bland and Altman [148]. In accordance with previous literature, the difference between measurements was expressed both as an absolute value, and as a percentage of the mean of each

measurement pair. ANOVA was used to look for significant differences in agreement between patients. Linear mixed models were constructed to identify factors which could explain session-level and patient-level variation in agreement. Covariates for baseline (absolute) agreement included age, HD vintage, diabetes vintage, baseline MAP, PVD, IHD, ultrafiltration volume (i.e. degree of fluid overload) and recent KT/V (as a measure of haemodialysis dose). Covariates for mid-dialysis agreement (relative, as post calibration) included the above, plus the following intra-dialytic parameters: maximum change in blood pressure, maximum change in RBV. Models were compared using the log-likelihood ratio, tested against a chi square distribution.

6.3 Results

There were 27 patients in total who both had AVF access and were monitored with the Finometer Pro. Three of these patients had recirculation and were excluded. Unfortunately the Transonic monitor was unavailable for two months of the study period due to equipment breakdown, and at other times was not always available for research use. In total there were 177 paired ultrasound dilution and Finometer measures of cardiac output, 124 of which were at baseline (pre-calibration) and 53 mid-dialysis (post-calibration, i.e. a measure of trend). For most analyses, there was little difference between simultaneous spot Finometer values and median averaged Finometer values; as spot values were used for real-time calibration, results displayed here are based on spot rather than filtered values unless specified.

6.3.1 Baseline values

There was a remarkably wide range of baseline cardiac output values. Adjusting for patient clustering, the significant predictors of baseline cardiac output were age (-0.05 L/min per year), fluid overload (+0.32 L/min per litre over dry weight), anaemia (+0.34 L/min per g/dl fall in Hb) and fistula flow (+1.53 L/min per litre). These are physiologically expected covariates.

At baseline, the median difference between Finometer and ultrasound dilution measurements was 1.74 L/min (interquartile range -0.18 to 3.67 L/min). Expressed as a percentage of the mean value of each measurement pair, the median error was 23.9% (interquartile range -3.4 to 53.2%). The correlation between absolute measures of cardiac output by the two methods was 0.26, $p<0.001$. Bland-Altman plots

for differences in baseline cardiac output between the two measurement methods are shown in figures 6.1 and 6.2.

For two patients with probable upper limb vascular stenosis, who had a substantial offset between the brachial cuff pressure and finger pressure, the cardiac output was substantially underestimated by the Finometer. For the majority of patients, the Finometer overestimated the absolute cardiac output before calibration. There was substantial variation between patients ($p<0.001$ on ANOVA). Figure 6.3 illustrates patient-specific box plots for the agreement between Transonic and Finometer-estimated absolute cardiac output. A mixed linear model was constructed to determine factors affecting the agreement between baseline (absolute) measurements for each session. Covariates which significantly influenced the agreement of the two measurement methods before calibration included presence of PVD, haemodialysis vintage and age (with a term to adjust for the interaction between years on dialysis and years of age). 29% of residual variance was due to unexplained between-patient rather than within-patient factors. The final model was:

$$Y_{ij} = 72.5 + \mu_{0j} - 44.1 * \text{PVD} - 4.2 * \text{HD} - 1.0 * \text{Age} + 0.1 * \text{Age*HD} + \epsilon_{ij}, \qquad (6.3.1)$$

where Y_{ij}=% difference in cardiac output between methods (Finometer minus ultrasound dilution); j indicates the patient and i the dialysis session; μ_{0j} is the patient-specific intercept; PVD is 1 when PVD present, 0 otherwise; HD is years on haemodialysis; Age is years of age; and ϵ_{ij} is residual error.

Figure 6.1: Measurement differences between Finometer and ultrasound dilution cardiac output, expressed as percentage of absolute cardiac output

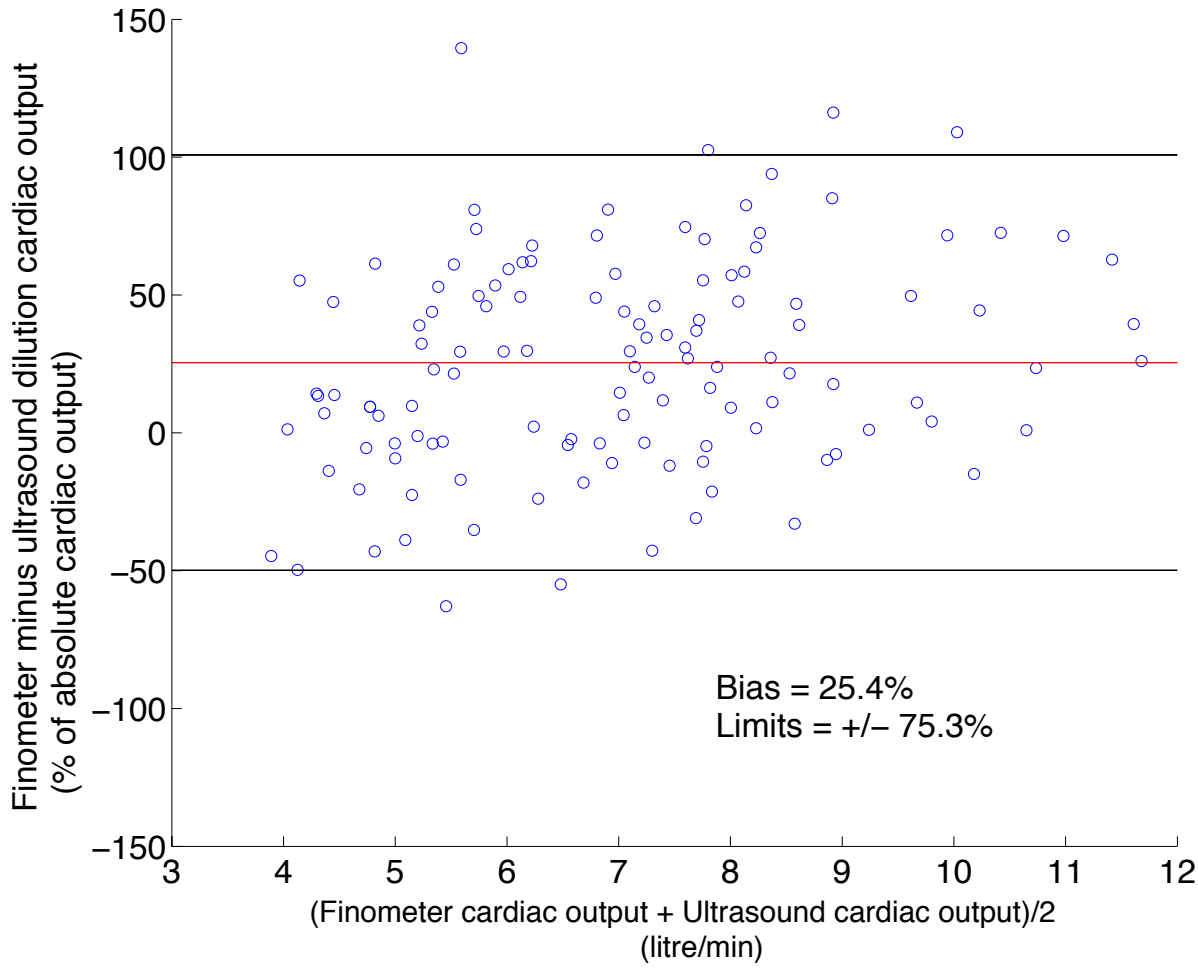

Figure 6.2: Measurement differences between Finometer and ultrasound dilution cardiac output, absolute values

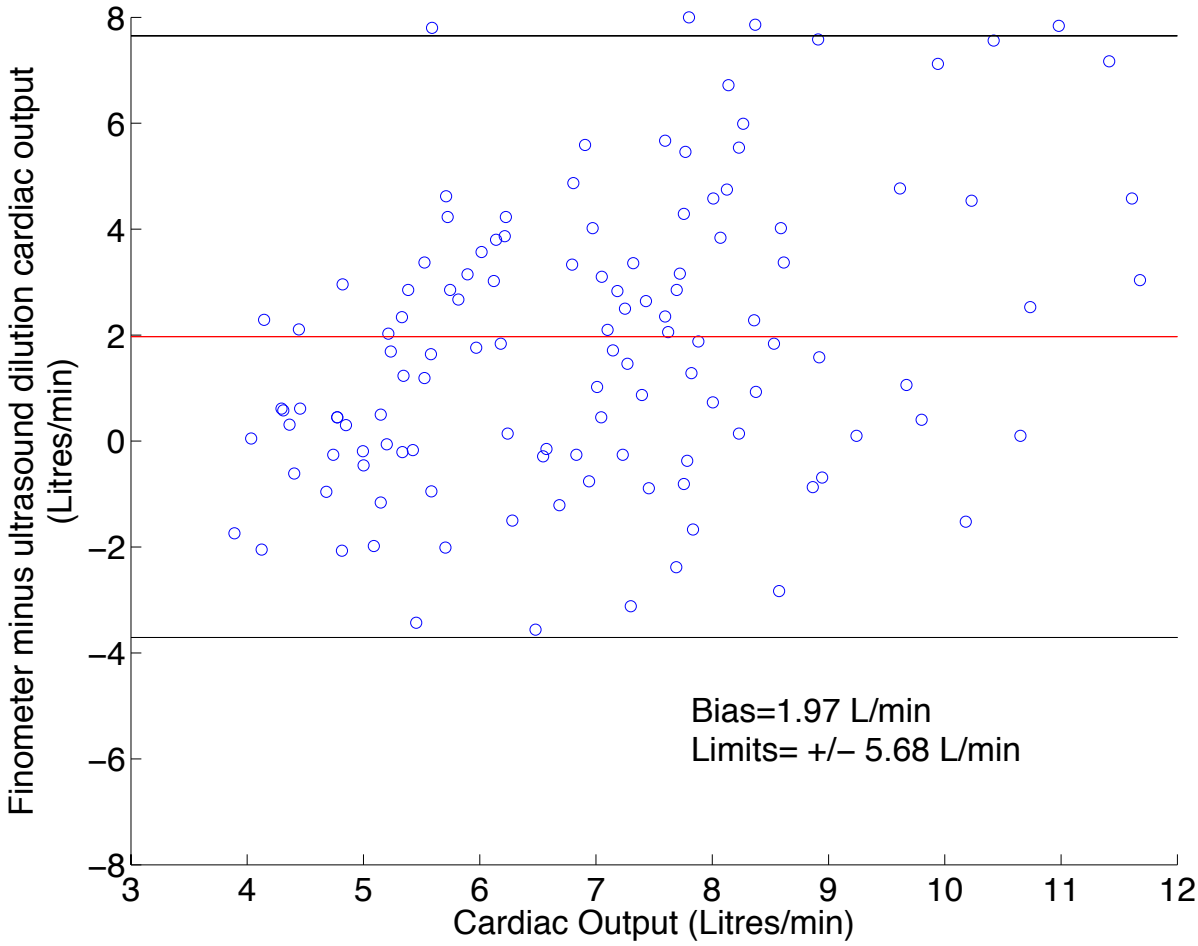

Figure 6.3: Box plots of within-patient differences between Finometer and ultrasound dilution cardiac output measurements

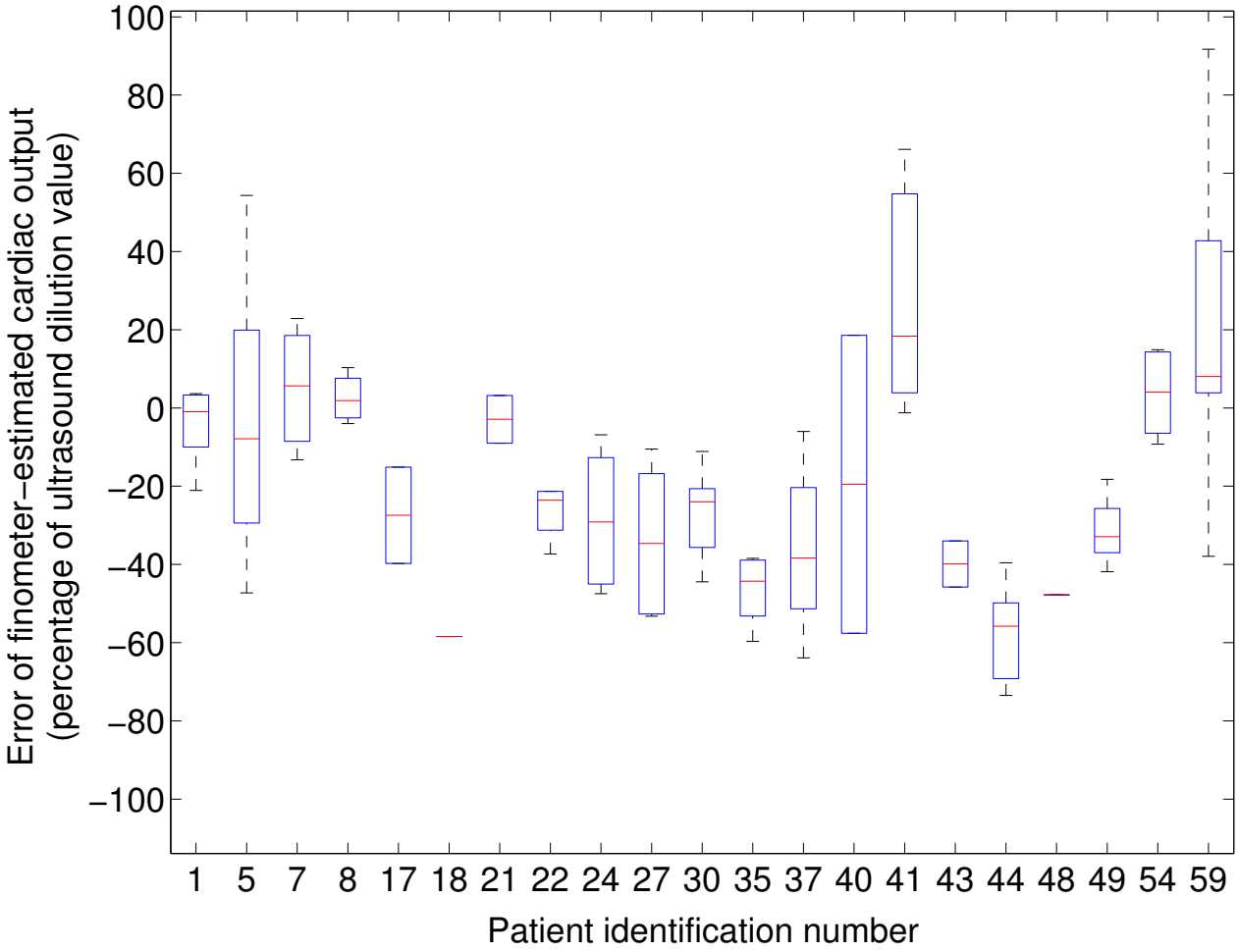

6.3.2 Trend over haemodialysis

For trends over a 2 hour period, agreement was much better. The median difference between calibrated Finometer and ultrasound dilution measurements mid-dialysis was -0.16 L/min (interquartile range -1.02 to 0.39 L/min). Expressed as a percentage of the mean value of each measurement pair, the median error was -3.9% (interquartile range -22.3 to 8.7%). The correlation between the two methods for absolute change from calibrated baseline was 0.60, $p<0.001$. The linear relationship between Transonic and Finometer-measured change from calibrated baseline is shown in figure 6.4. It can be seen, as expected, that cardiac output falls during haemodialysis in most cases.

Whilst bias, interquartile range and correlation were substantially improved when relative rather than absolute cardiac output was considered, the 95% limits of agreement on Bland-Altmann plots remained wide, suggesting a number of influential outliers. The acceptable 95% limits of agreement between gold standard and novel measures of cardiac output are conventionally +/-30% [154]. Using filtered, SQI-passed Finometer values instead of spot values (i.e. so that spot values taken from periods of poor quality data were censored), the mean bias in this study was -5.2%, with 95% limits of agreement +/-57.5%. Bland-Altmann plots for the differences in relative cardiac output between the two measurement methods (using SQI-passed Finometer values) are shown in figures 6.5 and 6.6.

A mixed linear model was constructed to determine factors affecting the agreement between mid-dialysis (relative) measurements for each session. ANOVA did not reveal significant differences between patients, and in keeping with this, a random effects term (i.e. to adjust for patient clustering) did not improve the model. Covariates which significantly influenced the agreement of the two measurement methods 2 hours after calibration included maximum change in MAP and ultrafiltration volume.

$$Y_{ij} = 1.7 - 15.1 * \mathrm{UF} - 0.8\delta * \mathrm{MAP} + \epsilon_{ij}, \tag{6.3.2}$$

where Y_{ij}=% difference in cardiac output between methods (Finometer minus ultrasound dilution); j indicates the patient and i the dialysis session; UF is the ultrafiltration volume in litres; δ MAP is the maximum change in MAP inmmHg; and ϵ_{ij} is residual error. However, it was a poor fitting model, with less than 10% of variance explained. Modelling was limited by small numbers.

Figure 6.4: Relative change in cardiac output between baseline and mid-dialysis

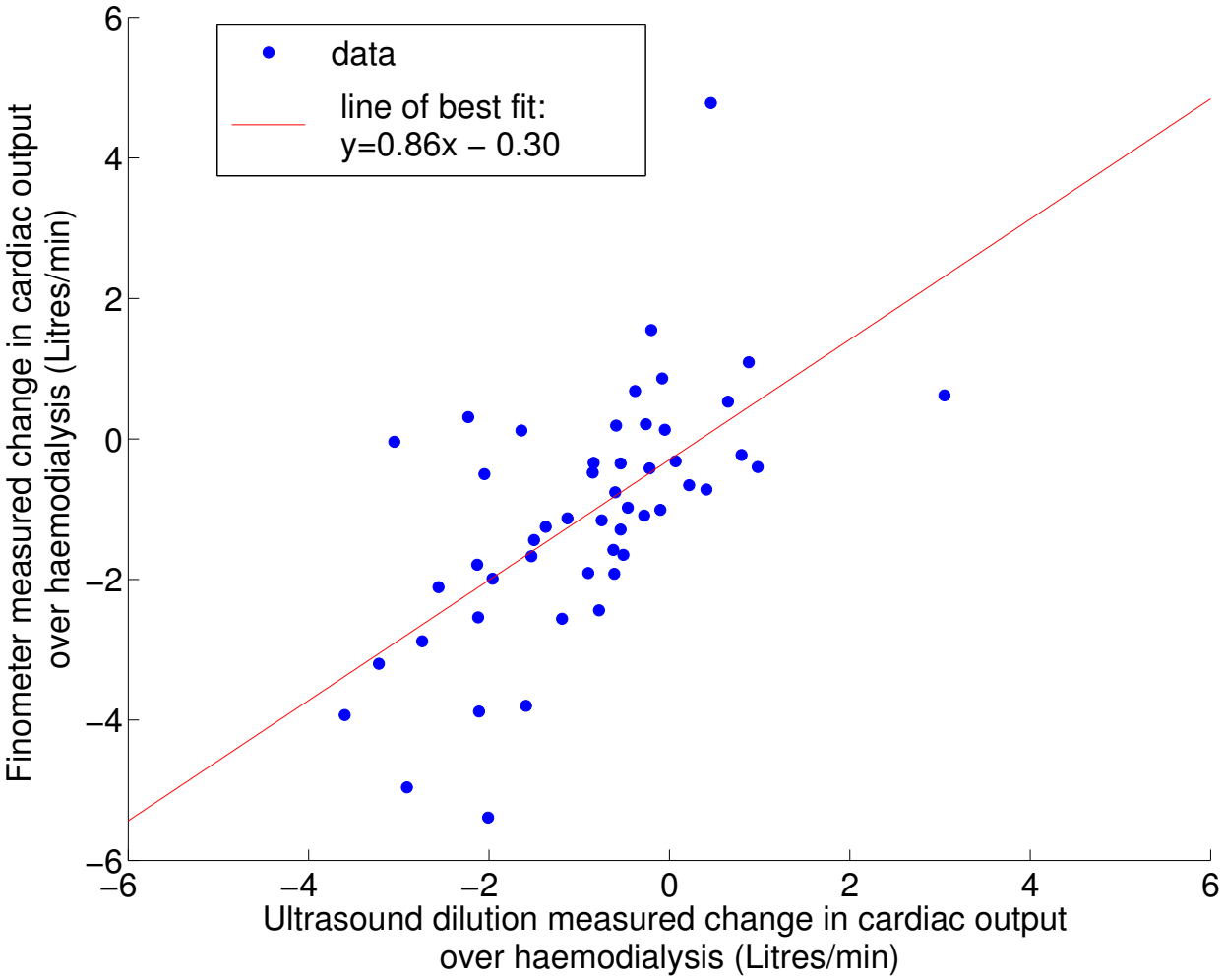

Figure 6.5: Measurement differences between calibrated Finometer and ultrasound dilution cardiac output, two hours after calibration (expressed as percentage of absolute cardiac output)

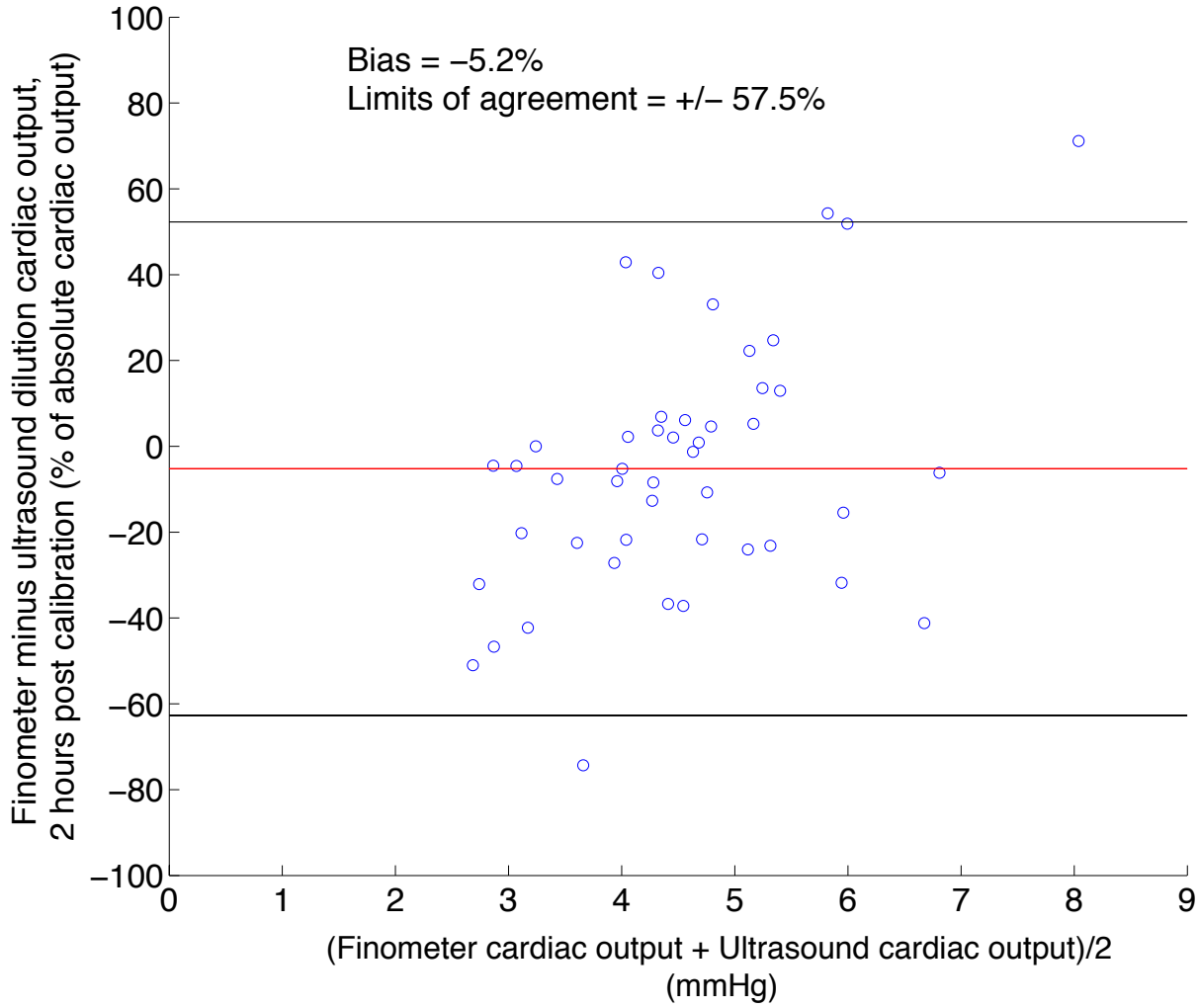

Figure 6.6: Measurement differences between calibrated Finometer and ultrasound dilution cardiac output, two hours after calibration (absolute values)

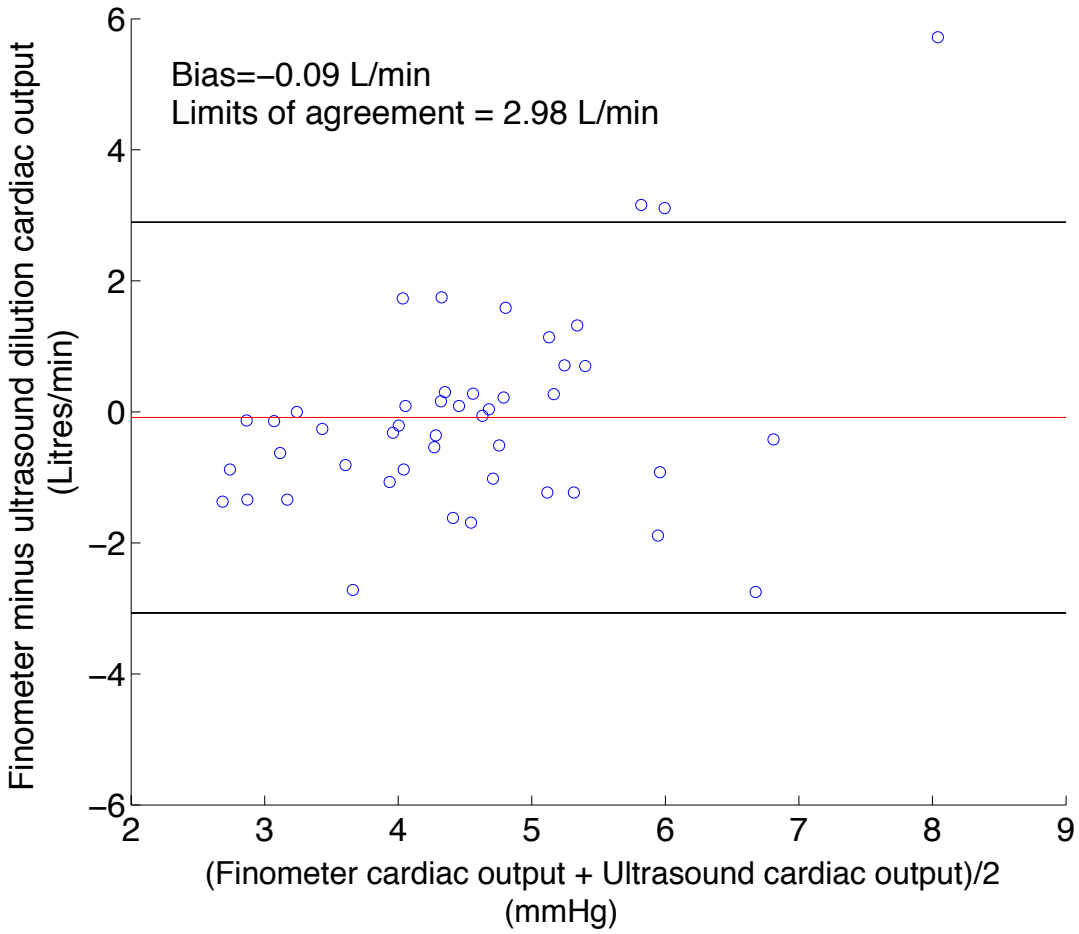

6.4 Discussion

In this population of HD patients, we found a large error, both random and systematic, in absolute cardiac output values obtained from the Finometer. There was minimal bias and reasonable correlation for trends, although limits of agreement remained suboptimal. The only other study to address this question in HD patients was performed by Cordtz et al [153]. These investigators looked at 25 HD sessions in 25 patients, who underwent continuous monitoring with the Finometer, plus ultrasound dilution measurements at baseline and mid-dialysis, i.e. 50 paired measurements [153]. We replicated this study with a much larger number of measurements, 177 pairs in total, from 21 patients, using the same methodology. Cordtz et al reported that the difference between absolute Finometer and ultrasound dilution measurements was 20% with 95% limits of agreement +/- 70%; we found similar results in our population, with bias 25% and limits +/- 75%. Cordtz et al did not repeat Bland-Altman analysis for trends, instead looking for correlation between Finometer and ultrasound dilution estimates of relative change, and found that there was no significant relationship [155, 148]. In contrast, we found a highly significant, moderately strong correlation between the methods for change in cardiac output. This discrepancy may be explained by our larger numbers and use of a robust Finometer SQI to exclude regions of poor quality waveform.

Correlation statistics have a number of weaknesses, and Bland-Altman methodology is preferable for comparing measurements. Bland-Altman analysis showed that post-calibration agreement was reasonable, with minimal bias, but the limits of agreement were too wide to meet clinical standards. Critchley and Critchley proposed that acceptable 95% limits of agreement between gold standard and novel measures of cardiac output were +/-30%, which allows for the error in gold standard measurements themselves [154]. In this study, the limits of agreement for change in cardiac output were +/- 57%, although the tails of the distribution were long, and in fact two thirds of relative measurements fell within the 30% bracket. Interestingly, change in fluid balance and blood pressure were significant predictors of greater error in trend; it is possible that these dynamic physiological changes introduced more drift. The heating effect of HD may also contribute to drift: a small study in normal volunteers has shown that warming core temperature by 1^oC introduced substantial error into Modelflow estimates of cardiac output trends [156].

On mixed modelling, HD vintage was predictive of greater error in absolute cardiac output estimates.

This is physiologically plausible as uraemia induces many changes in the cardiovascular system, including vascular calcification and endothelial dysfunction, as well as autonomic impairment. HD vintage was not significant for error in relative cardiac output estimates, but the numbers were much smaller for this analysis.

6.5 Conclusion

In this HD population, Finometer-derived measures of absolute cardiac output were insufficiently accurate for clinical use. Trend in cardiac output was estimated reasonably well in most cases, although the limits of agreement were wider than in other populations.

Chapter 7

Surrogate measures of continuous blood pressure

7.1 Introduction

Accurate measurement of blood pressure outside critical care is a challenge: most studies of IDH have relied on NIBP, which has a large measurement error, especially in the context of real-world practice, and can only provide very intermittent data [9, 10, 11, 12]. As shown in chapter 4, it is likely that intermittent methods will miss clinically important hypotensive episodes. However, continuous blood pressure measurement requires either an invasive intra-arterial catheter, or expensive equipment using volume-clamp technology or tonometry, neither of which are practical for routine outpatient dialysis. It is possible that surrogate measures of blood pressure could give useful information on trends, whilst being measured continuously, cheaply and non-invasively. The key objectives of this chapter are to assess the agreement between Finometer-derived and other potential non-invasive measures of continuous blood pressure in HD patients: the two major candidates are PTT and vascular access pressures.

PTT is the time taken for a pressure wave to travel from the heart to a given point in the peripheral vasculature. It is typically measured as the time from the R wave of the ECG to the upstroke of the PPG measured at the finger. PTT is related inversely to blood pressure as shown in the equation below:-

$$\mathrm{BP} = \frac{-2\ln \mathrm{PTT}}{\alpha} + \frac{\ln \frac{2r\rho L^2}{hE_0}}{\alpha} \tag{7.1.1}$$

where BP is blood pressure; PTT is pulse transit time; α is a constant; r is the inner radius of the blood vessel; ρ is density of blood; L is the path length; h is the thickness of the vessel wall; and E_0 is the zero pressure modulus of the vessel wall. Over the range of pressures seen in clinical practice, the relationship has been shown to approximate to inverse linear. When the PTT is calculated as the time delay between the foot of proximal and distal waveforms, PTT correlates better with diastolic pressures; when measured as the ECG R wave to PPG peripheral pulse upstroke, it generally has a closer relationship with changes in systolic pressures [157]. PTT has been extensively investigated as a method of tracking change in blood pressure in a wide variety of settings including HD, but as summarised in a recent systematic review, results have been variable and frequent recalibration may be required [157]. This is likely because the other variables in the equation may not remain constant for more than a few minutes, e.g. vessel tone is a dynamic process.

Access pressures are relatively unexamined as a source of haemodynamic information. AVFs are usually created by side-anastomosing an artery, usually the radial or brachial artery, to a reasonably sized vein. The segment of vein then has mixed venous and arterial blood flowing through it. Due to the higher inflow pressures, and the reduced peripheral resistance in the limb, the blood flow through the arterialised vein will increase over time: when sufficiently expanded, the vein can be needled to allow efficient HD, e.g. with circuit blood flows of 250-350 ml/min.

There are two small studies showing that directly measured intra-fistula MAP can track changes in systemic intra-arterial MAP [158, 159]. In the more recent study, Nakane et al threaded a pressure-transducing catheter through the arterial needle and into the fistula itself; intra-access pressure was continuously monitored and compared to femoral artery pressure, measured via an intra-arterial line. Numbers were very small, and the venous blood was returned to a site distant from the fistula, so the results are not entirely comparable to modern dialysis access. Nevertheless, the authors reported a fairly constant ratio between systemic MAP and fistula MAP over the course of haemodialysis. However, they also noted that in some patients the fistula pressure dropped far more than the systemic pressure, which they hypothesised was due to changes in intravascular volume. There are not only a number of anatomical and physiological variables affecting the relationship between systemic pressures and intra-fistula pressures, but there are yet more factors affecting the relationship between intra-fistula pressures and pressures measured in the dialysis circuit [160]. This is relevant because the arterial and venous

access pressures measured by dialysis machines are not actually the pressures at the needles, but in the dialysis circuit (at the pre-pump point and venous bubble trap respectively, see figure 7.2). Whether the contribution of systemic arterial pressure to the pressure eventually measured in the dialysis circuit is detectable and clinically useful has yet to be determined.

7.2 Methods

See the methods chapter for full details of the trial and data collection. Button-hole cannulation with 15G needles was used almost universally for AVF access. All patients with AVFs had undergone recent ultrasound dilution studies (measuring access flow and recirculation) as part of routine clinical care.

Patient movement has been shown to substantially compromise the performance of PTT as a measure of blood pressure: for this reason, and because PTT has been shown to be comparable between fistula and non-fistula limbs, we positioned the pulse oximeter on the access arm which was more likely to be held still [75]. For patients without AVFs who dialysed via Tesio lines (tunnelled dual lumen catheters in a central vein), pulse oximeter position was left to patient choice.

Blood pressure monitoring was performed using the Finometer PRO (unstable patients, n=37) or the Finometer MIDI (stable patients, n=19). The beat-to-beat blood pressure data was initially processed by removal of extreme outliers (3 standard deviations from mean) and application of an SQI based on waveform quality (see methods chapter).

7.2.1 Pulse transit time processing and analysis

PTT was calculated by the Black Shadow device (Stowood Medical Supplies) as the time between the peak of the ECG R wave and the mid-point (amplitude) of the PPG upstroke, as illustrated in figure 7.1. The PTT was initially processed by removal of extreme outliers (3 standard deviations from mean) and application of an SQI based on PPG waveform quality (see methods chapter). Beat-to-beat PTT proved too noisy for use. Therefore both PTT and Finometer data (after pre-processing as above) were subject to a low pass filter with cut off 0.083 Hz, i.e. high frequency noise with a period above 2 minutes was attenuated, and downsampled to one minute timestamps.

Figure 7.1: PTT was defined as the time between the R wave (point A) and the mid-point of the PPG upstroke (point B)

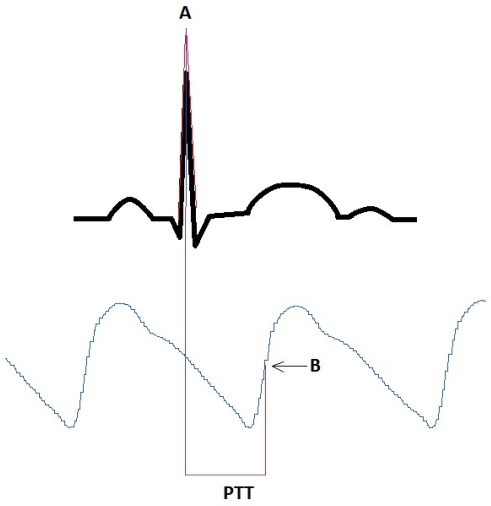

For each session, Pearson's correlation between PTT and both MAP and SBP was calculated. Factors influencing the correlation for each session were assessed using linear mixed models, taking into account patient clustering. Covariates included age, diabetes history, HD vintage, PVD, maximum change in MAP, baseline MAP, baseline pulse, use of beta blockers, baseline haematocrit, maximum change in RBV, and ultrafiltration volume.

For each patient, data from all sessions was then pooled. The Finometer-measured blood pressure (δMAP and δSBP) was plotted against the PTT, with both variables expressed as either absolute values or change from baseline. In all cases, baseline values were defined as the median of the first 5 values for which paired data was available. As the relationship between PTT and blood pressure is known to be inverse linear, simple linear regression was used to model the relationship between relative blood pressure and relative PTT, and absolute blood pressure and absolute PTT. The coefficient of variation (R^2) was used as a index of the proportion of variance explained. In addition, Pearson's correlation coefficient was calculated for pooled patient-level data, and linear regression was used to identify patient factors asso-

ciated with variation in correlation results. Covariates used included age, diabetes history, HD vintage, PVD, CVD, IHD (confirmed on angiography), typical baseline MAP, typical baseline pulse and use of beta blockers.

7.2.2 Access pressure processing and analysis

All patients with AVFs dialysed through 15G needles (1.8 mm diameter, 254 mm length). Arterial and venous access pressure values are recorded by the Braun dialysis machine only at one minute intervals. The arterial access pressure is actually the pressure before the blood pump in the dialysis circuit, and the venous access pressure is the pressure at the venous bubble trap before the blood is returned to the patient (see figure 7.2 [161]). In addition to systemic arterial pressure and intravascular filling, these pressures will be affected by pump speed, pump stops, haematocrit, any movement of the fistula limb or needles, and anatomical features of the anastomosis. Access pressure data from periods when the pump was not at the exact prescribed speed was discarded. In addition, extreme outliers (2 standard deviations from mean) and values which differed by more than 50mmHg from the preceding measurement were removed, being suggestive of artefact. In addition, discordant arterial and venous needle pressures (i.e. when one increased and the other decreased, suggesting that the change was not driven by systemic pressures) were identified and discarded.

Figure 7.2: Diagram of a basic HD circuit illustrating the sites of arterial and venous access pressure measurement [161]

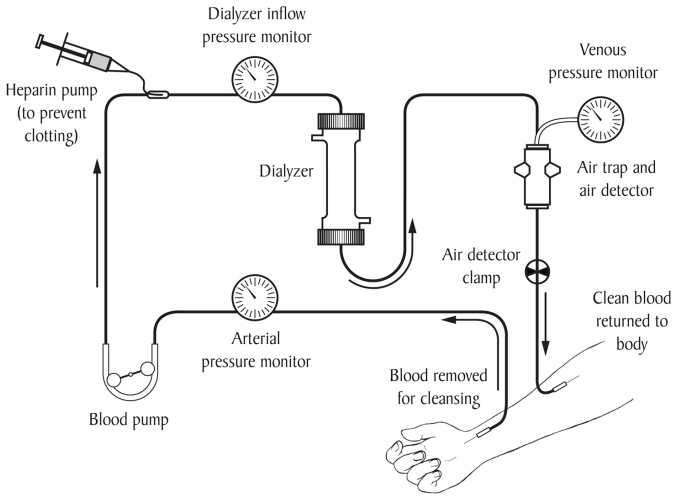

A problem with correlating Finometer and access data is that there is a major difference in temporal resolution between the two data streams. The Finometer will be sensitive to higher frequency fluctuations in pressure. Moreover, as continuous access pressure waveforms were not available for analysis, it was unknown whether the values provided by the Braun dialysis machine represented an average over the preceding minute, or a spot reading (in which case, the access pressures may vary substantially depending on whether the cardiac cycle is in systole or diastole). Simple downsampling of the Finometer data would therefore be insufficient to overcome these problems (this was confirmed by first running the analyses using only downsampling without filtering). Instead both data streams were filtered to ensure comparable resolution. Finometer data, after the pre-processing described above, was subject to a low pass filter with cut-off 0.0042 Hz, i.e. fluctuations in blood pressure with a period less than 4 minutes were attenuated. The access pressure data was subject to a moving average filter with a sliding window

of 4 minutes, to even out variations associated with the cardiac cycle and artefact. The Finometer data stream was then downsampled to 0.125 Hz to match the timestamps of the access pressure data.

Paired access pressure measurements for each NIBP recording were identified by taking the median of pre-processed needle pressures in a window +/- 5 minutes around the NIBP timestamp.

The change in Finometer-measured blood pressure (both δMAP and δSBP) was plotted against the change in access pressure (both δarterial and δvenous) for the population as a whole, and for access type subgroups, i.e. brachial AVF, radial AVF, any AVF or Tesio. In all cases, baseline values were defined as the median of the first 3 values for which paired data was available. Simple linear regression was used to model the relationship between each combination of systemic pressure index and access pressure index, and the coefficient of variation (R^2) was used as a index of the proportion of variance explained. Pearson's correlation coefficient was also calculated for each combination, i.e. the correlation between relative changes of pooled population data, regardless of session or patient. For comparison, change in NIBP-measured blood pressure was also plotted against change in time-matched access pressure measurements. Finally, Bland-Altman plots were constructed for the Finometer- or oscillometer-measured changes in systemic pressure (again both δMAP and δSBP) and the corresponding changes in needle pressure (both δarterial and δvenous). Both regression and Bland-Altman analyses were then repeated on the individual patient-level.

The Pearson's correlation coefficient between Finometer- or oscillometer-measured absolute pressures (MAP and SBP) and absolute access pressures was calculated for each session. Factors influencing the correlation for each session were assessed using linear mixed models, taking into account patient clustering. Covariates included age, diabetes history, PVD, access type, access flow, maximum change in MAP, baseline MAP, baseline haematocrit, maximum change in RBV, and ultrafiltration volume. Linear regression models were used to identify patient-level factors affecting the performance of access arterial pressures as a surrogate for Finometer-measured MAP. Covariates included age, diabetes history, PVD, access type, access flow, typical ultrafiltration volume, baseline haematocrit, and typical baseline MAP.

7.3 Results

7.3.1 Pulse transit time

Session-level analysis

A total of 397 sessions in 35 patients had Finometer and PTT data of sufficient quality for analysis. The median session-level correlation between absolute PTT and MAP was -0.15, interquartile range -0.44 to 0.11: a histogram of session-level results is shown in figure 7.3. The median correlation between absolute PTT and SBP was -0.15, interquartile range -0.47 to 0.11 (see figure 7.4). 31% of sessions had a statistically significant negative correlation of magnitude at least 0.3 between MAP and PTT (though 12% had a statistically significant positive correlation of 0.3 or above). 34% of sessions had a statistically significant negative correlation of magnitude at least 0.3 between SBP and PTT (though 11% had a statistically significant positive correlation of 0.3 or above). On mixed modelling, only baseline pulse rate significantly influenced the session-level correlation between PTT and blood pressure (either MAP or SBP), and there was a strong patient effect. For correlation between MAP and PTT, the coefficient for pulse rate was 0.007 per beats/min increase, i.e. a 10 beats/min increase strengthened negative correlation by -0.07 points. 24% of residual variance was at the inter-patient level. The patient-specific intercepts are shown in figure 7.9. Correlation statistics may undervalue the potential of PTT. Figures 7.5 to 7.8 show examples of sessions where, visually, the PTT tracks the blood pressure well. However, the correlation values vary widely, with the fourth example having a statistically significant positive correlation on account of long periods where both blood pressure and PTT do not change.

Figure 7.3: Session-level correlations between PTT and Finometer MAP

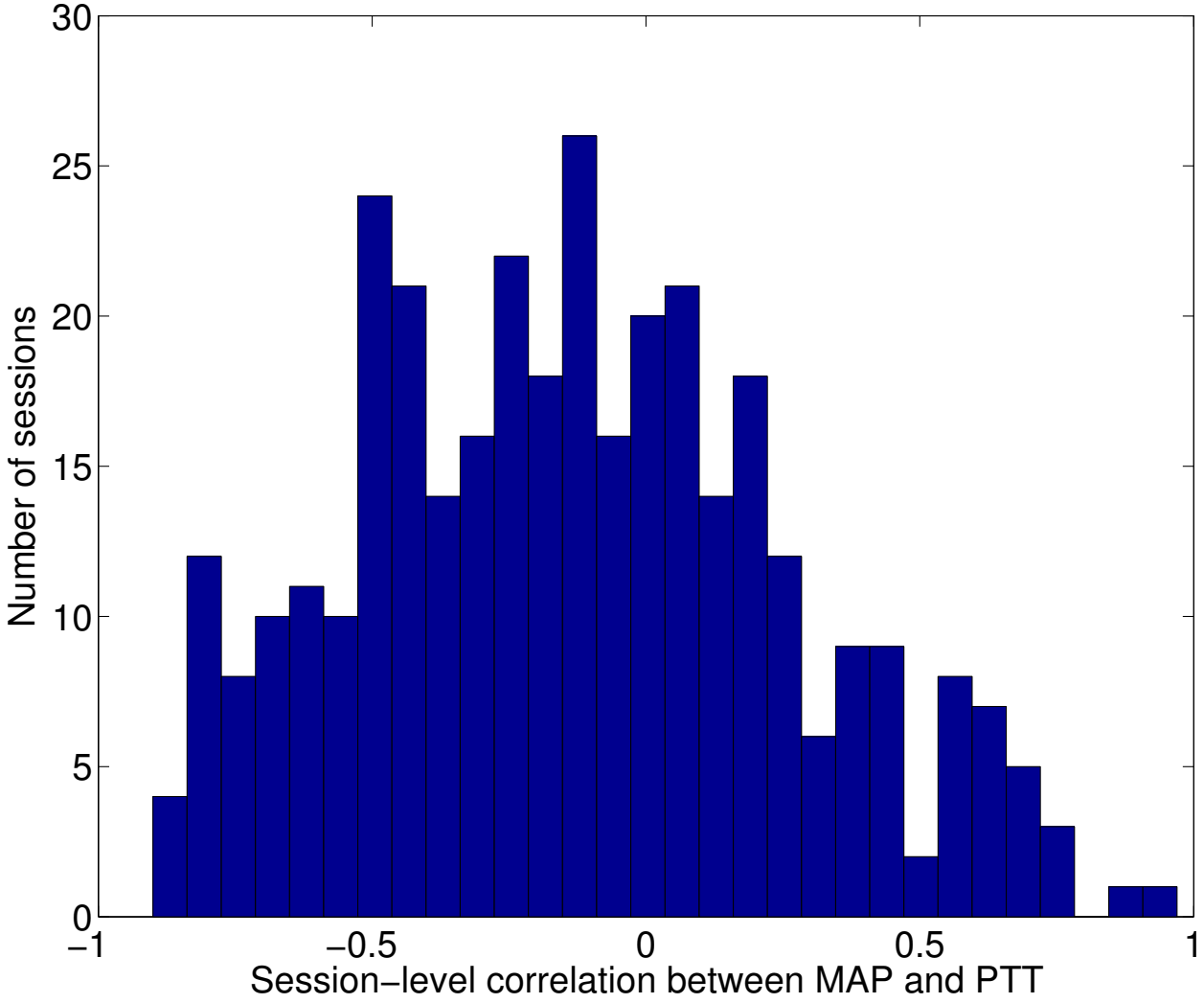

Figure 7.4: Session-level correlations between PTT and Finometer SBP

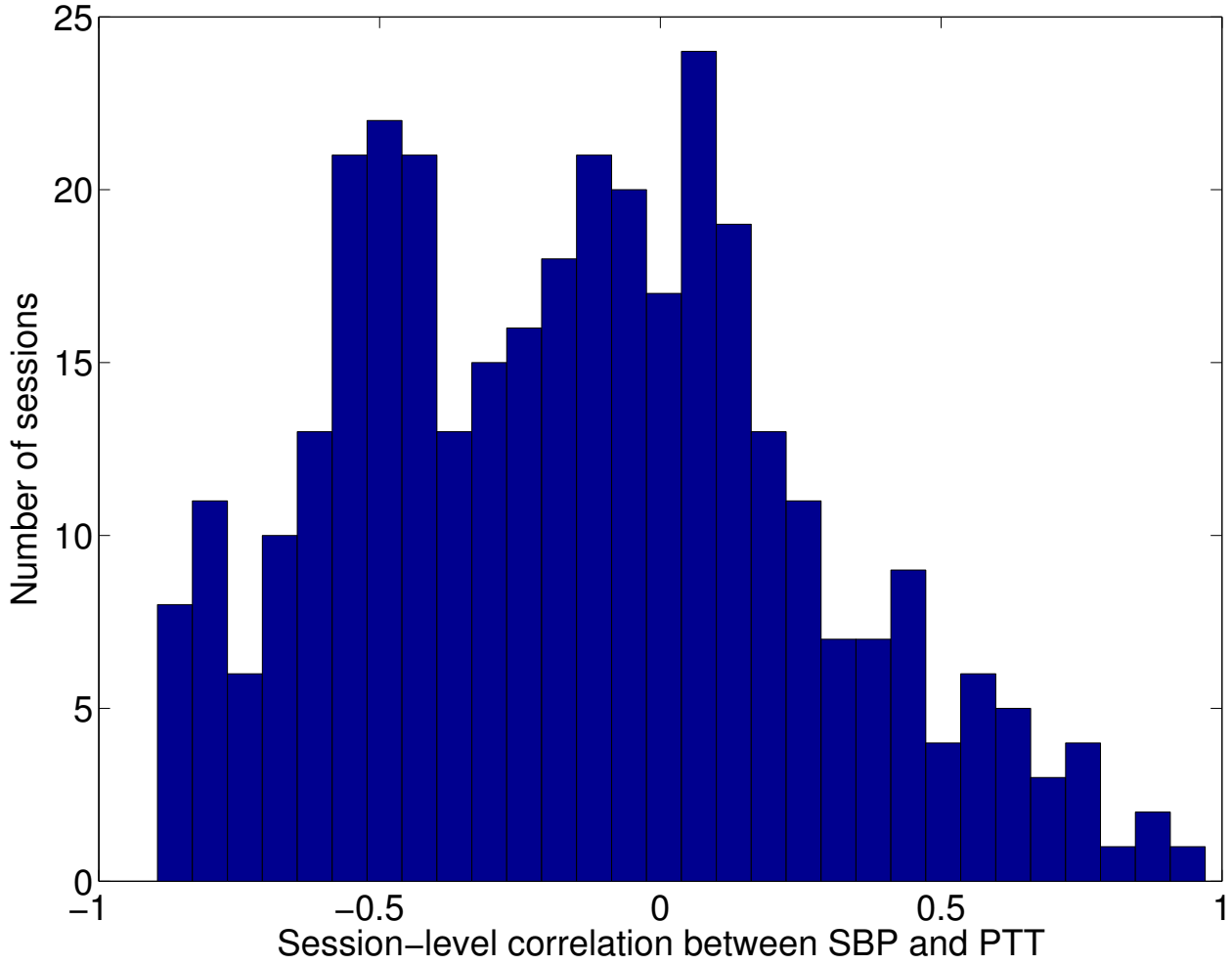

Figure 7.5: MAP versus PTT for a haemodialysis session in a 53 year old man with polycystic kidneys, R= -0.69, p <0.001

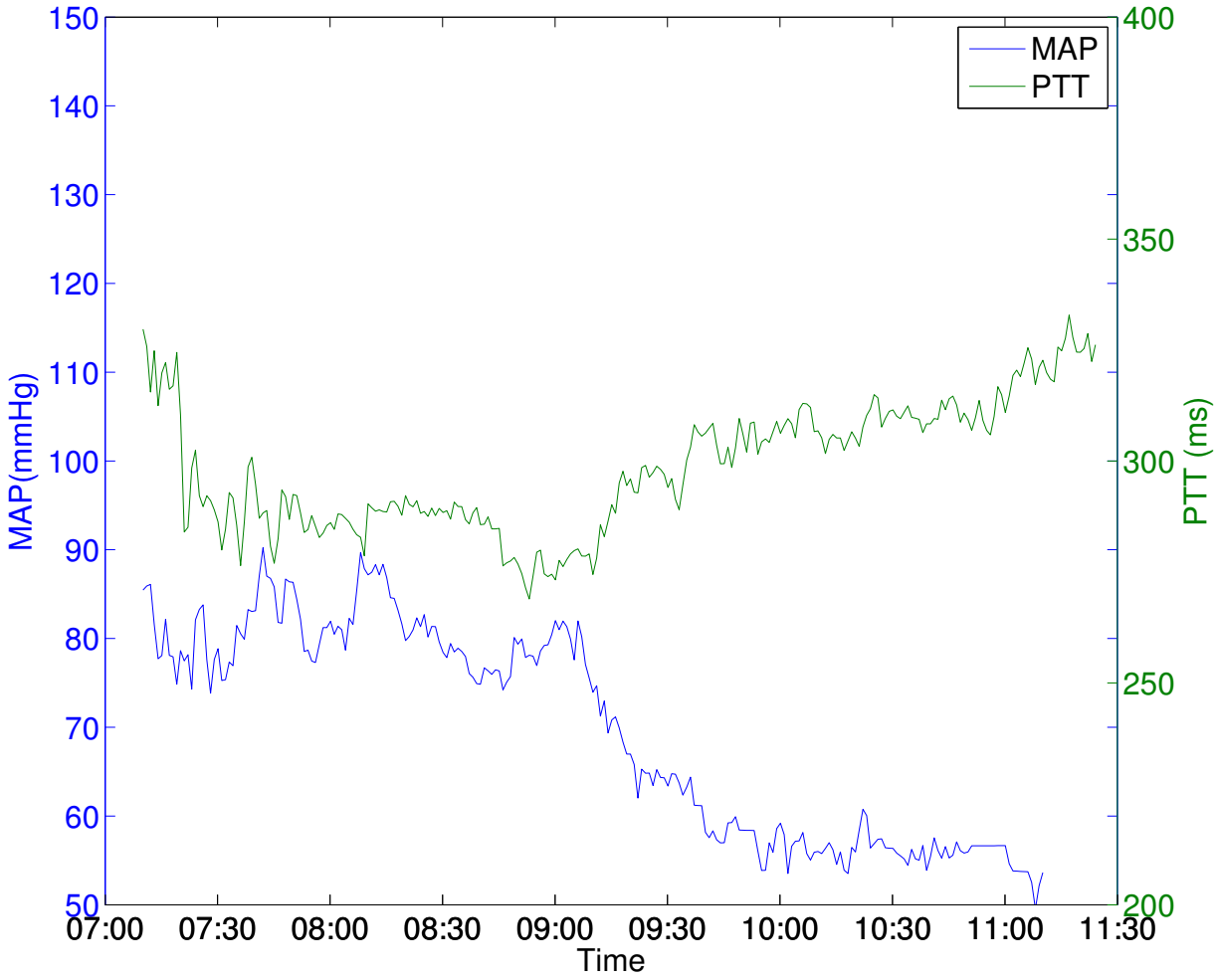

Figure 7.6: MAP versus PTT for a haemodialysis session in a 30 year old man with hypertensive renal disease and fluid overload, R= -0.76, p <0.001

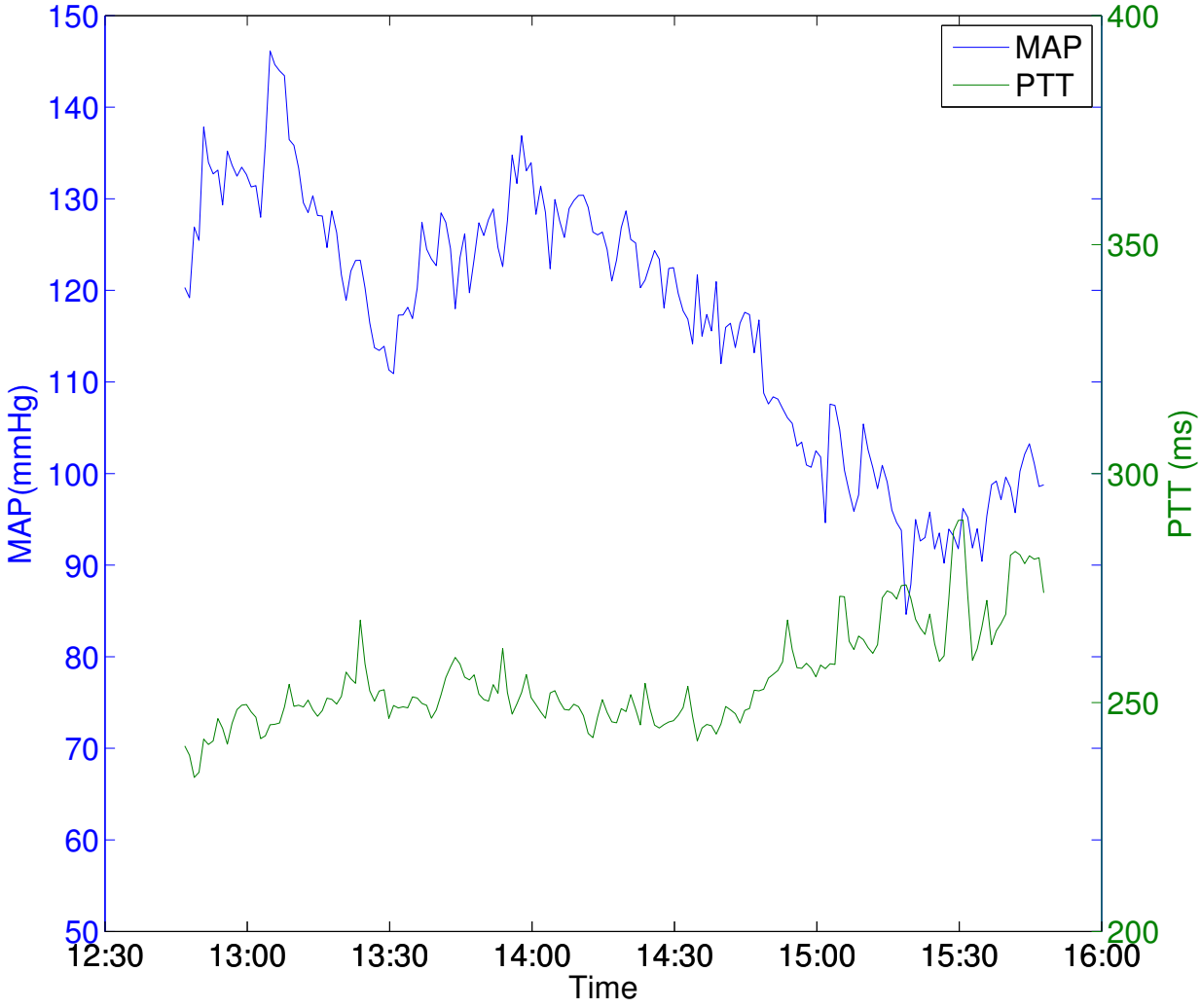

Figure 7.7: MAP versus PTT for a haemodialysis session in a 56 year old man with long-standing diabetes, R= -0.51, p <0.001

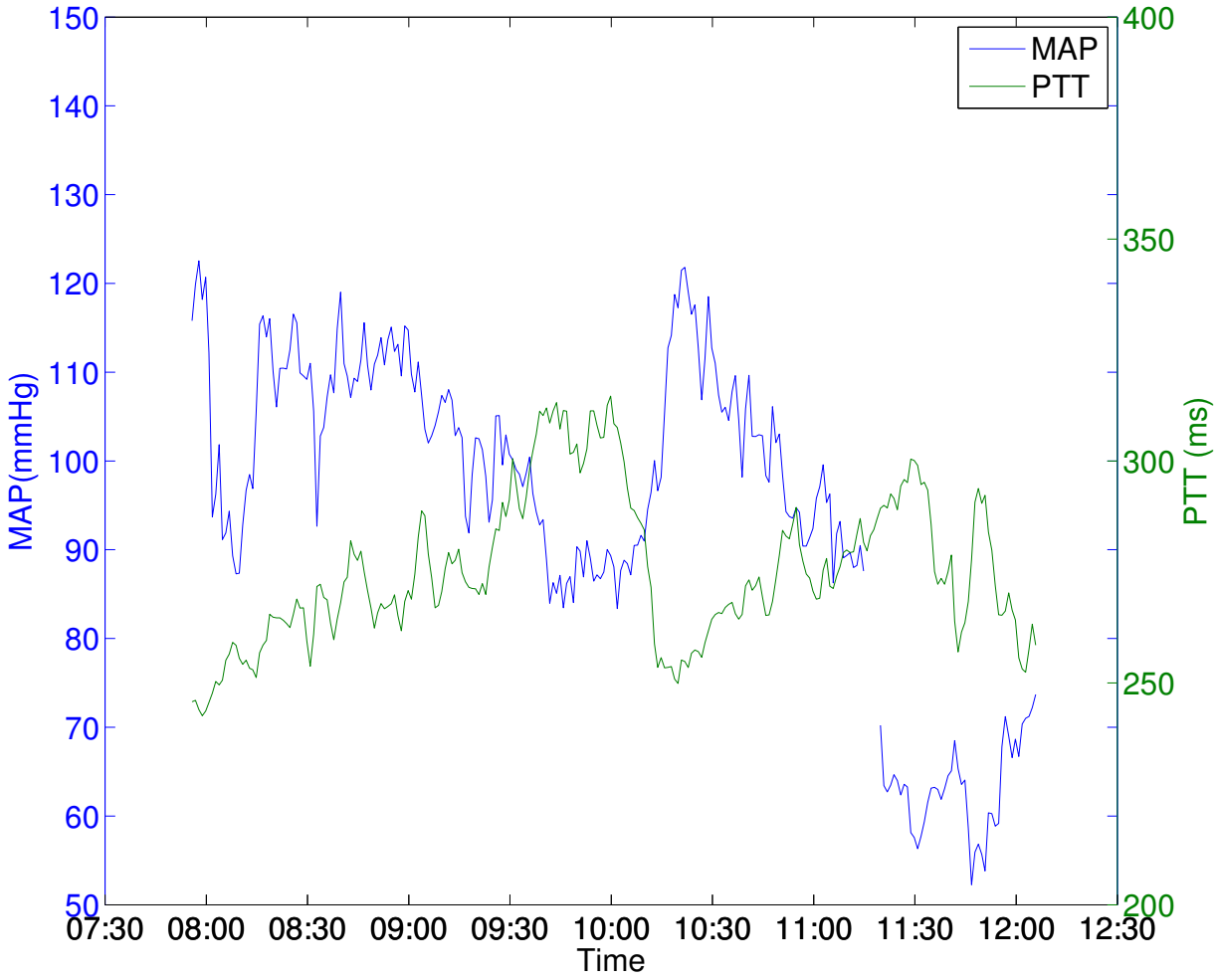

Figure 7.8: MAP versus PTT for a haemodialysis session in the same patient as figure 19, R= +0.20, p <0.002

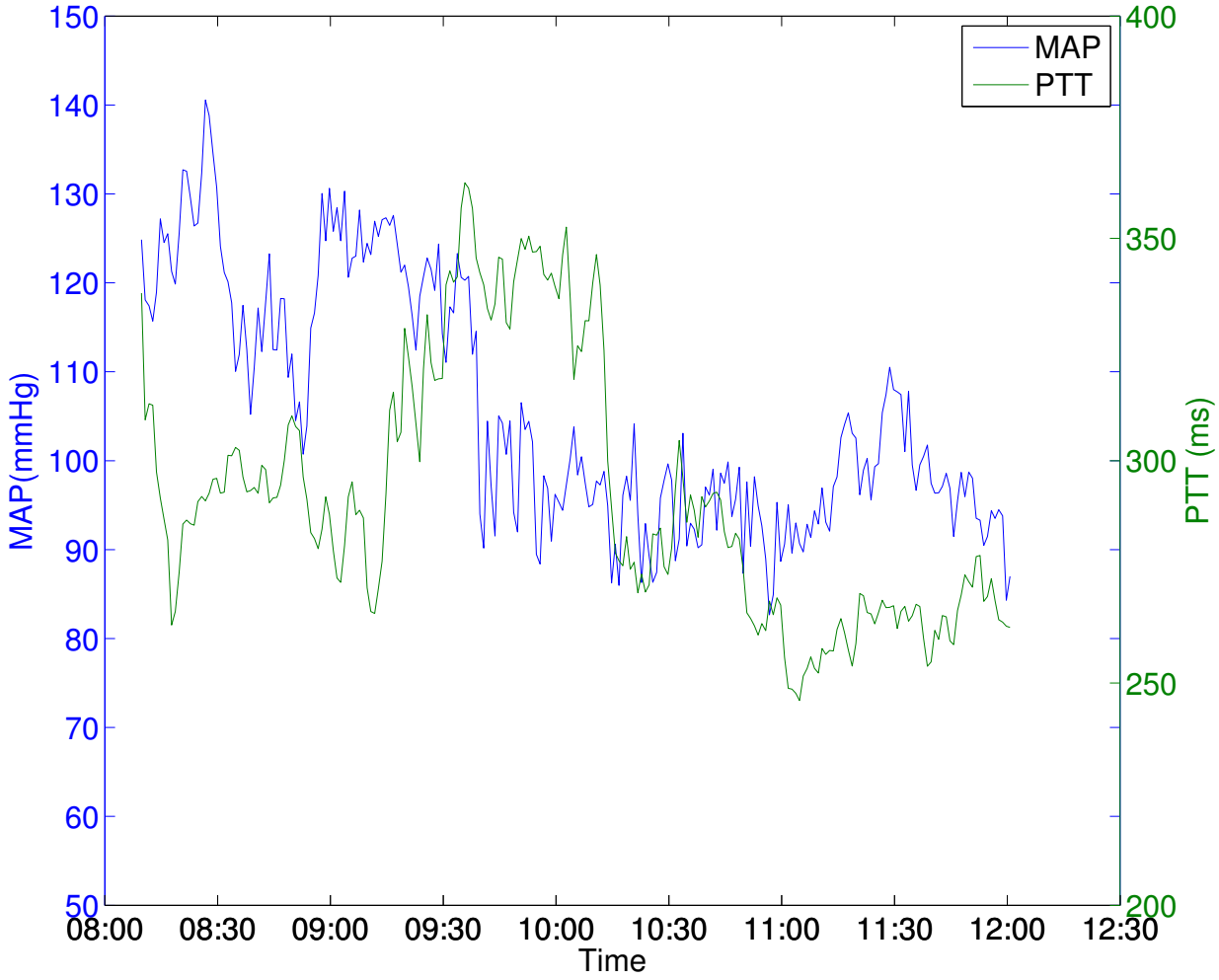

Figure 7.9: Patient-specific intercepts for session-level correlation between PTT and MAP

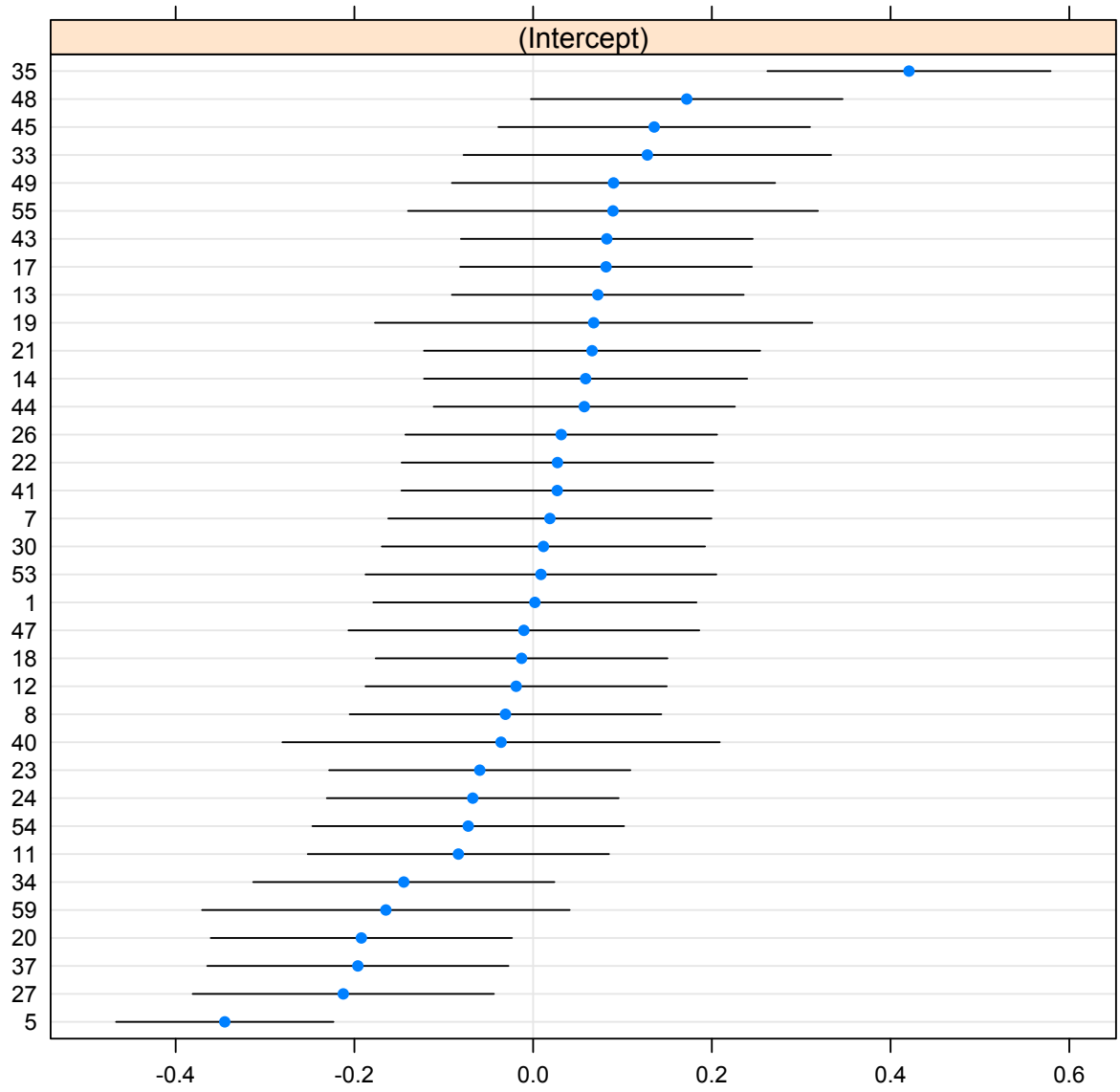

Patient-level analysis

Most patients showed a statistically significant negative linear relationship between absolute PTT and blood pressure, but all were relatively weak. The patient-specific linear model terms and goodness of fit for the relationship between PTT and MAP are shown in table 7.1. The linear models for the relationship between SBP and absolute PTT provided very similar goodness of fit to the MAP models in all patients; in all cases, the SBP model coefficient was approximately 0.63 times the MAP model coefficient, with a near identical constant. The regression plots for the patient with the best fit are shown in figures 7.10 to 7.13.

The median patient-level correlation for PTT and MAP (i.e. all data for each patient pooled) was -0.14, interquartile range -0.34 to 0.03. The median patient-level correlation between absolute PTT and SBP was -0.18, interquartile range -0.30 to 0.00. The patient-level correlations between relative PTT and relative blood pressure, i.e. data expressed as change from the baseline, were very similar (note not identical as each session had different baseline values). For 26 out of 35 patients, the relationship between δPTT and δ blood pressure was weaker than that for absolute values.

Linear modelling found that a third of the variance in patient-correlation between absolute PTT and absolute MAP could be explained by the presence of vascular disease and the use of beta blockers (an effect which interestingly was unrelated to average baseline pulse). PVD on its own was significantly predictive of less negative correlation; the presence of vasculopathy in at least two regions (PVD, IHD or CVD) was an even stronger predictor, with +0.44 less negative correlation, $p<0.001$. In addition, the use of beta blockers increased negative correlation by -0.21, $p=0.005$, presumably due to the reduction of pulse rate throughout dialysis sessions (the average baseline pulse gives no information about heart rate during the rest of the monitoring period).

We did not attempt to pool absolute data at the population level, as the absolute value depends on a large number of patient-specific factors beyond blood pressure. However, we did pool δ PTT and δ blood pressure, and found a highly significant but weak correlation of -0.1 using MAP, and -0.12 using SBP.

Table 7.1: Patient-specific linear regression terms for PTT=β MAP + constant (only patients with at least four sessions of data)

Patient (sex, age [years])	Linear model β	Linear model constant	Linear model R^2
M, 34	-0.44	336.15	0.29
M, 53	-0.42	331.9	0.16
M, 83	-0.39	308.0	0.08
F, 45	-0.21	284.7	0.04
F, 59	-0.73	319.4	0.14
M, 87	-0.09	265.3	0.01
M, 73	-0.52	345.9	0.11
M,47	0.06	349.2	0.00
M, 58	-0.87	407.9	0.26
M, 56	-0.05	273.1	0.00
M, 69	-0.06	336.9	0.00
M, 43	-0.33	332.3	0.06
M, 54	0.06	246.7	0.00
F, 60	-0.12	293.5	0.01
F, 72	0.14	364.5	0.00
M, 78	-0.26	400.6	0.02
M, 56	-0.27	361.4	0.02
F, 59	-0.41	316.0	0.11
M, 30	-0.30	289.2	0.12
M, 77	0.34	272.1	0.13
M, 60	-0.50	377.5	0.09
F, 79	-0.62	357.1	0.27
M, 83	0.70	374.6	0.03
M, 26	-0.55	318.8	0.10
M, 75	0.59	298.1	0.04
F, 35	-0.24	292.8	0.05
M, 50	-1.19	377.0	0.14
M, 39	0.11	296.6	0.01
F, 84	-0.20	314.2	0.02
M, 80	-0.12	280.3	0.00
M, 77	-0.37	299.1	0.16
F, 52	0.41	243.6	0.04
M, 63	-0.55	315.3	0.09

Figure 7.10: Absolute MAP versus absolute PTT for all sessions in a 34 year old male patient

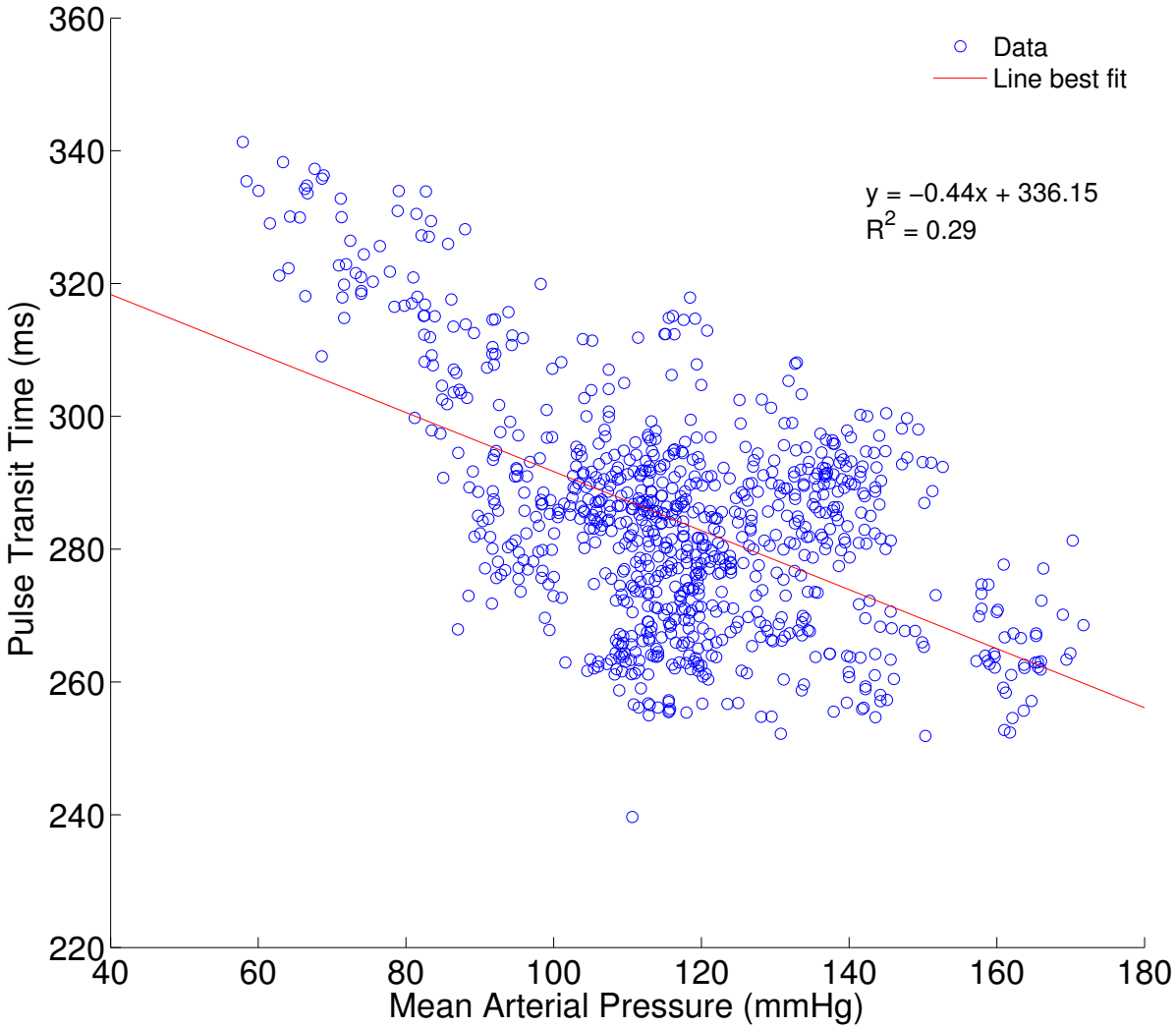

Figure 7.11: Relative MAP versus relative PTT for all sessions in a 34 year old male patient

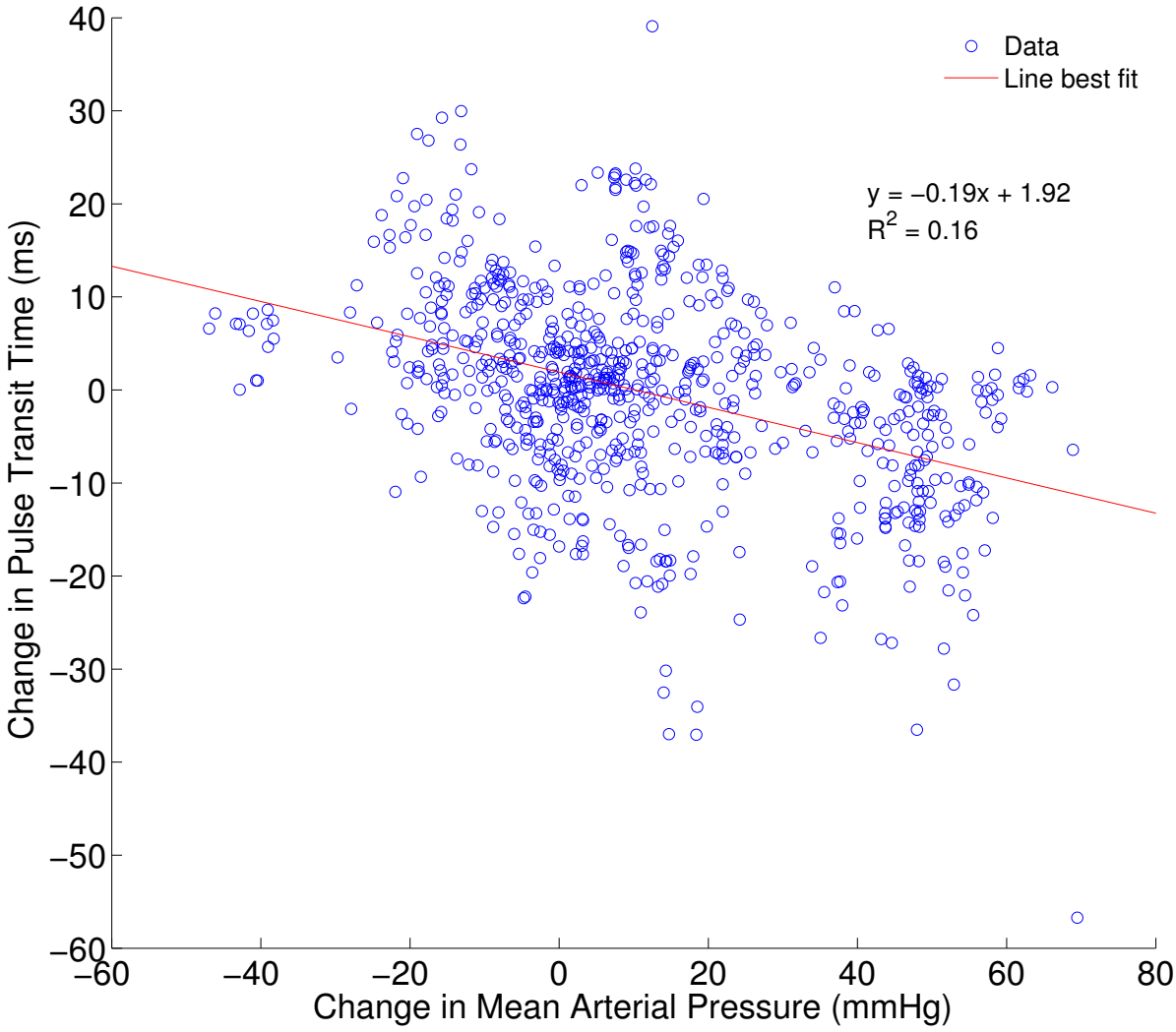

Figure 7.12: Absolute SBP versus absolute PTT for all sessions in a 34 year old male patient

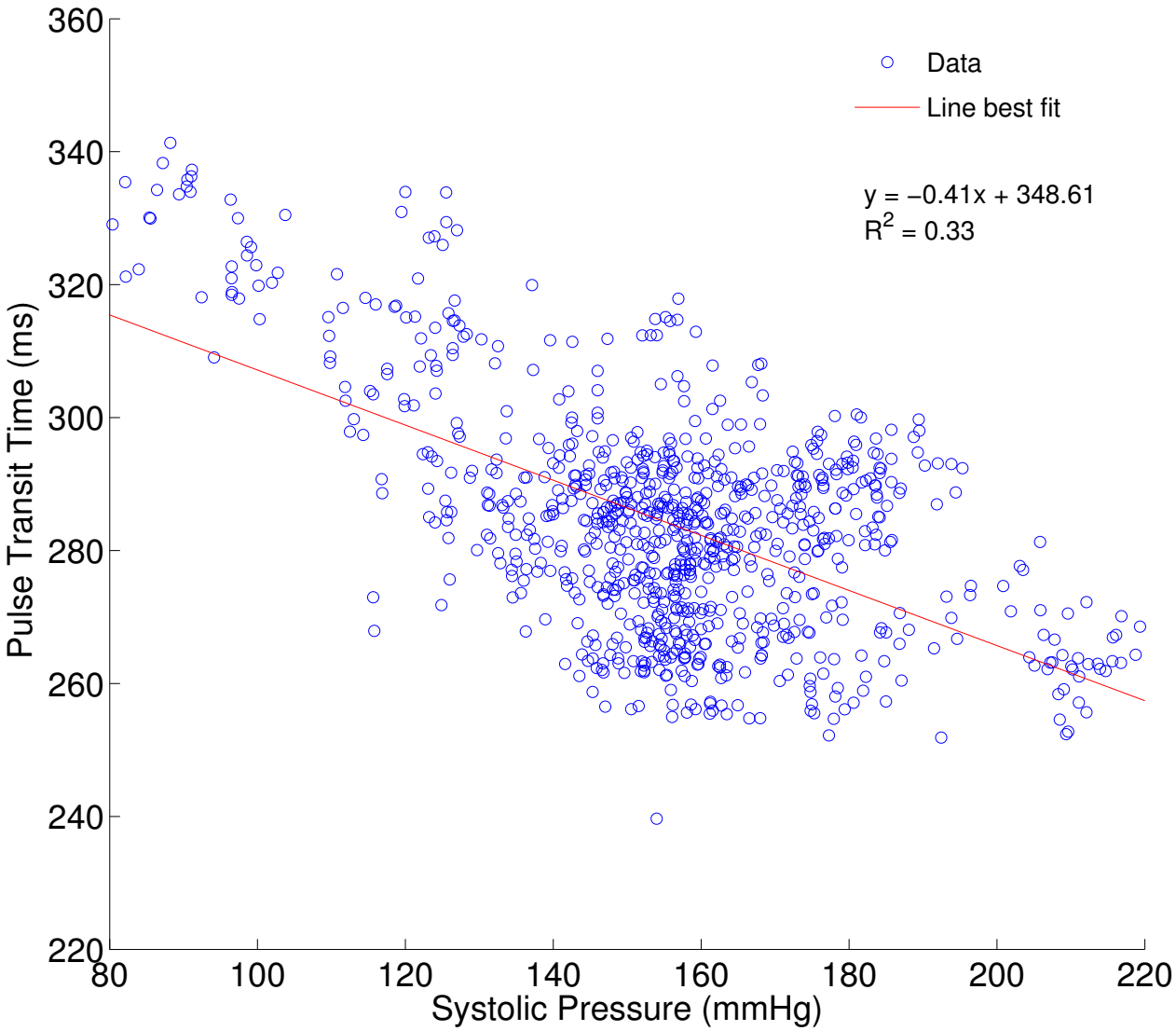

Figure 7.13: Relative SBP versus relative PTT for all sessions in a 34 year old male patient

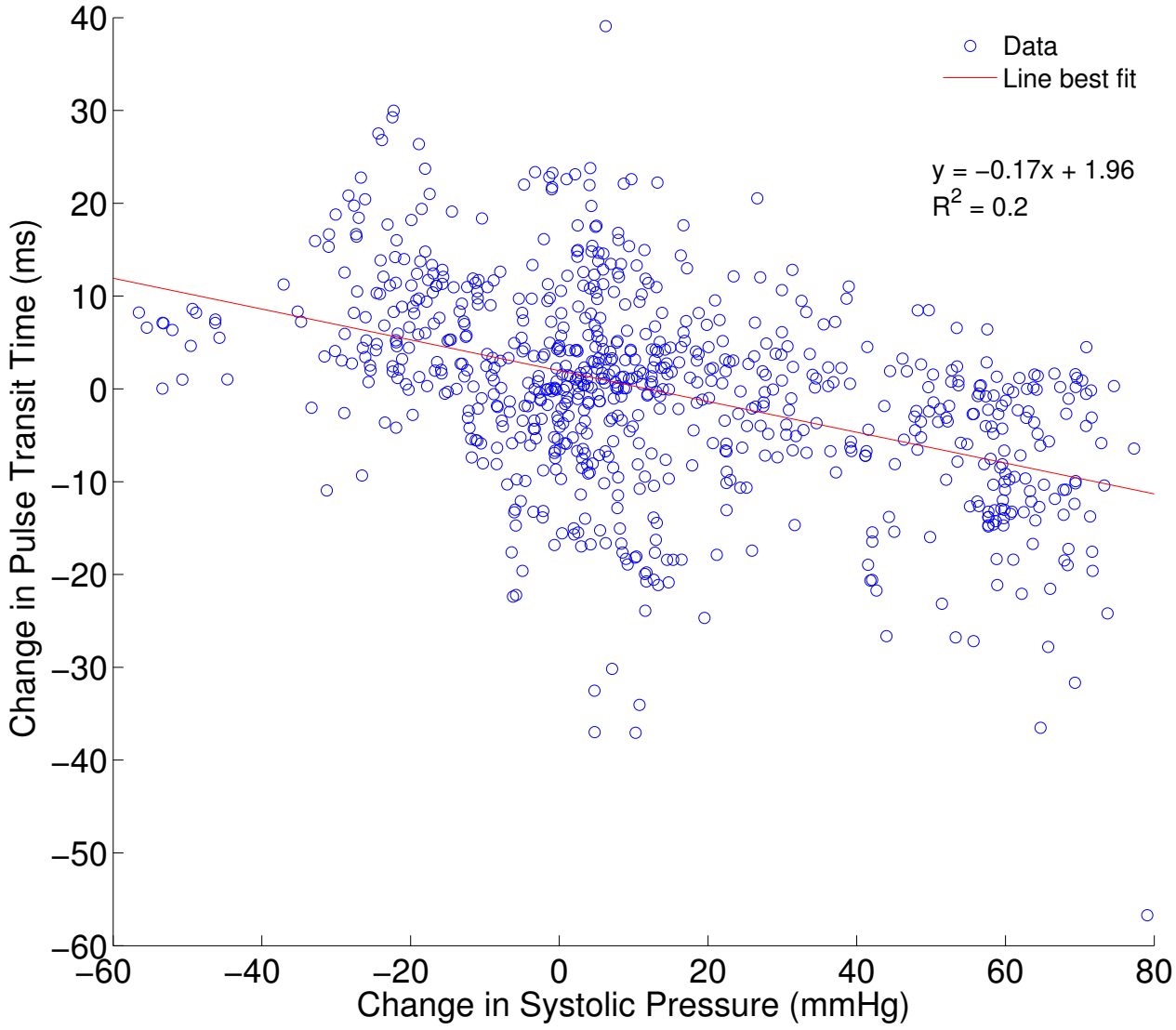

7.3.2 Access pressures

Pooled data statistics

There were 521 sessions with sufficient data to assess the relationship between Finometer pressures and access pressures: of these, 144 sessions used Tesio access, 142 radial AVFs and 235 brachial AVFs. Of the AVFs, two were PTFE grafts, both supplied by the brachial artery; one of these patients had no Finometer data for comparison due to severe PVD, and the other was considered in the brachial AVF group. On recent ultrasound dilution Doppler studies, 4 AVFs had been found to have at least some recirculation. The median access flow was 1635 ml/min for brachial AVFs and 1020 ml/min for radial AVFs. There were 436 sessions with at least 6 NIBP measurements which could be matched to a needle pressure within +/- 5 minutes: of these, 123 used Tesio access, 117 radial AVFs and 196 brachial AVFs.

Considering all data points from sessions using AVFs, there was a statistically significant but very weak correlation between δarterial pressures and Finometer-measured δMAP (R 0.14, $p<0.001$), and between δvenous pressures and Finometer-measured δMAP (R 0.10, $p<0.001$). Very little of the variation in needle pressures, even with the strict pre-processing described above, could be explained by changes in systemic blood pressure, and vice versa. For example, univariate linear regression predicting Finometer-measured δMAP from AVF δarterial pressures found an adjusted R^2 of 0.022 (i.e. only about 2% of variance explained by access pressures, see figure 7.14). Limiting analysis only to brachial AVFs provided only minimal improvement (see figure 7.15). A summary of linear regression models, R^2 and correlation coefficients for each comparison according to access is shown in tables 7.2-7.4. With the exception of Tesio line sessions, access pressures had a closer relationship to Finometer-measured than oscillometer-measured systemic pressures, and there was little difference between using MAP and SBP as the blood pressure index.

Bland-Altmann plots were constructed for all comparisons, grouped according to access type. Neither δarterial or δvenous access pressures showed useful agreement with any index of systemic blood pressure. The best agreement was seen for change in arterial needle pressure and change in Finometer-measured MAP: brachial AVFs performed slightly better than all AVFs (see figures 7.16 and 7.17). Tables 7.2-7.4 summarise the mean and standard deviation of differences between access and systemic pressures, grouped according to access.

Figure 7.14: Relationship between δarterial needle pressures and δMAP, all AVFs (regression terms for access pressures as covariate and MAP as dependent variable)

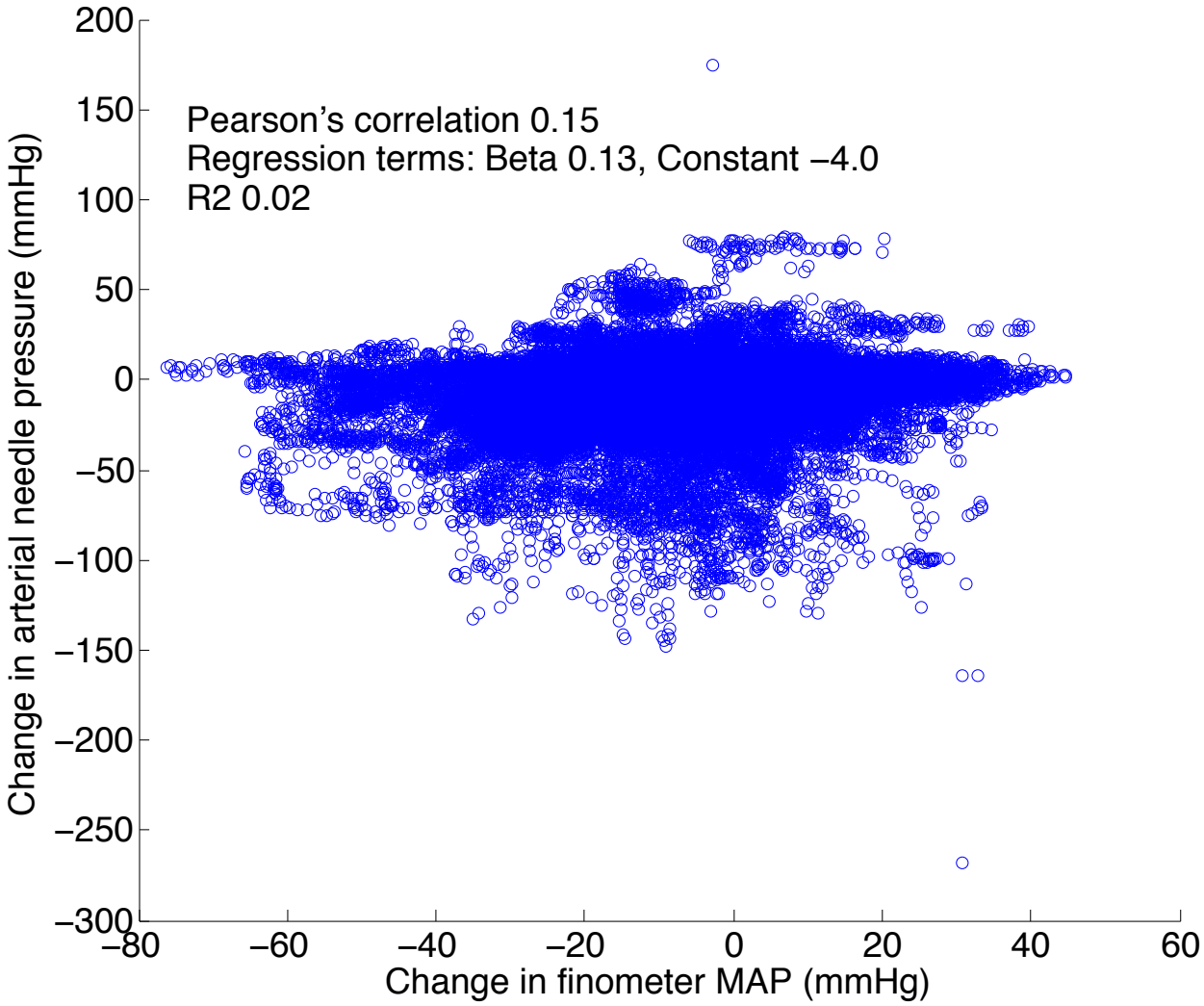

Figure 7.15: Relationship between δarterial needle pressures and δMAP, brachial AVFs only (regression terms for access pressures as covariate and MAP as dependent variable)

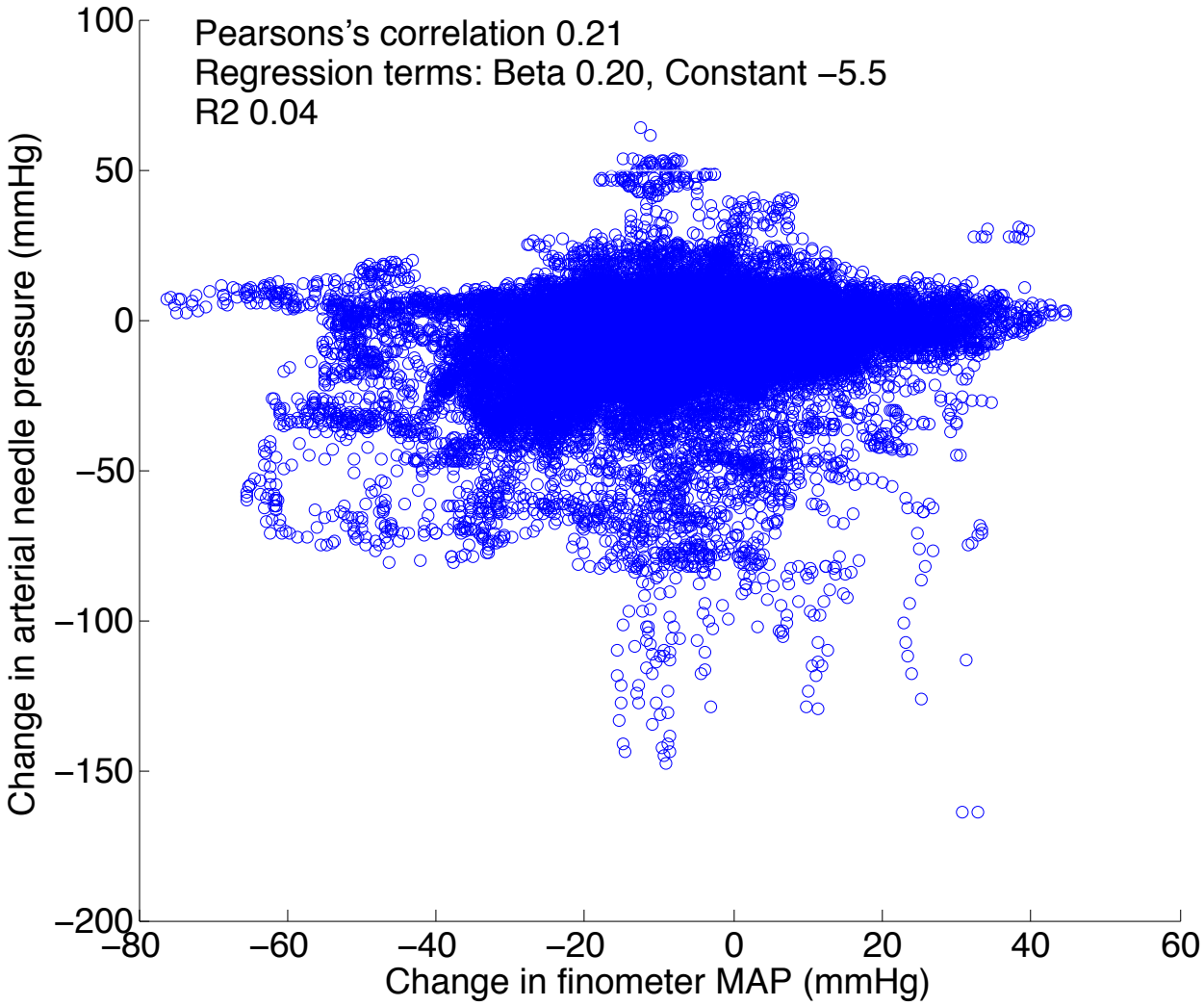

Figure 7.16: Measurement differences between δarterial needle pressures and δMAP, all AVFs

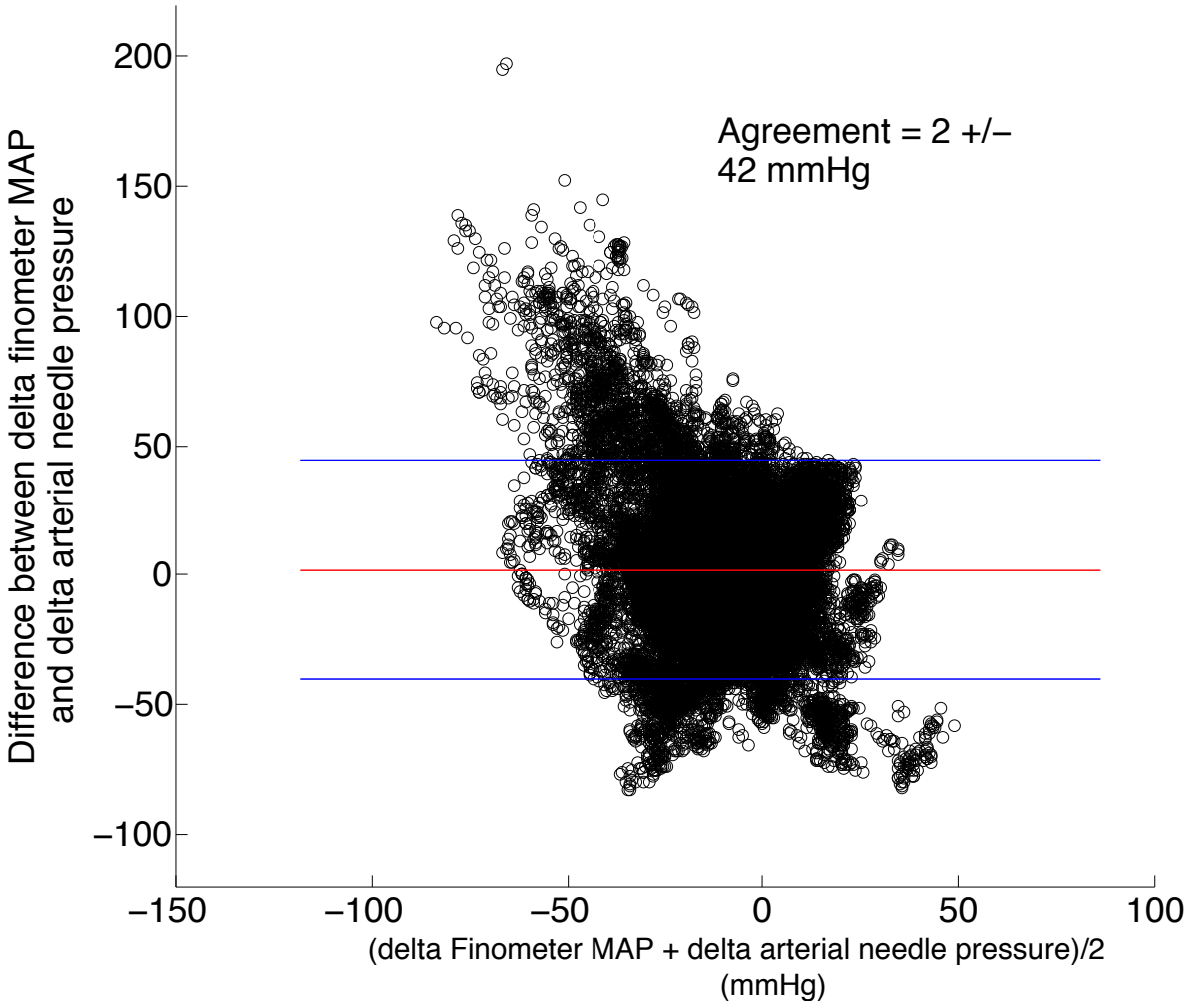

Figure 7.17: Measurement differences between δarterial needle pressures and δMAP, brachial AVFs

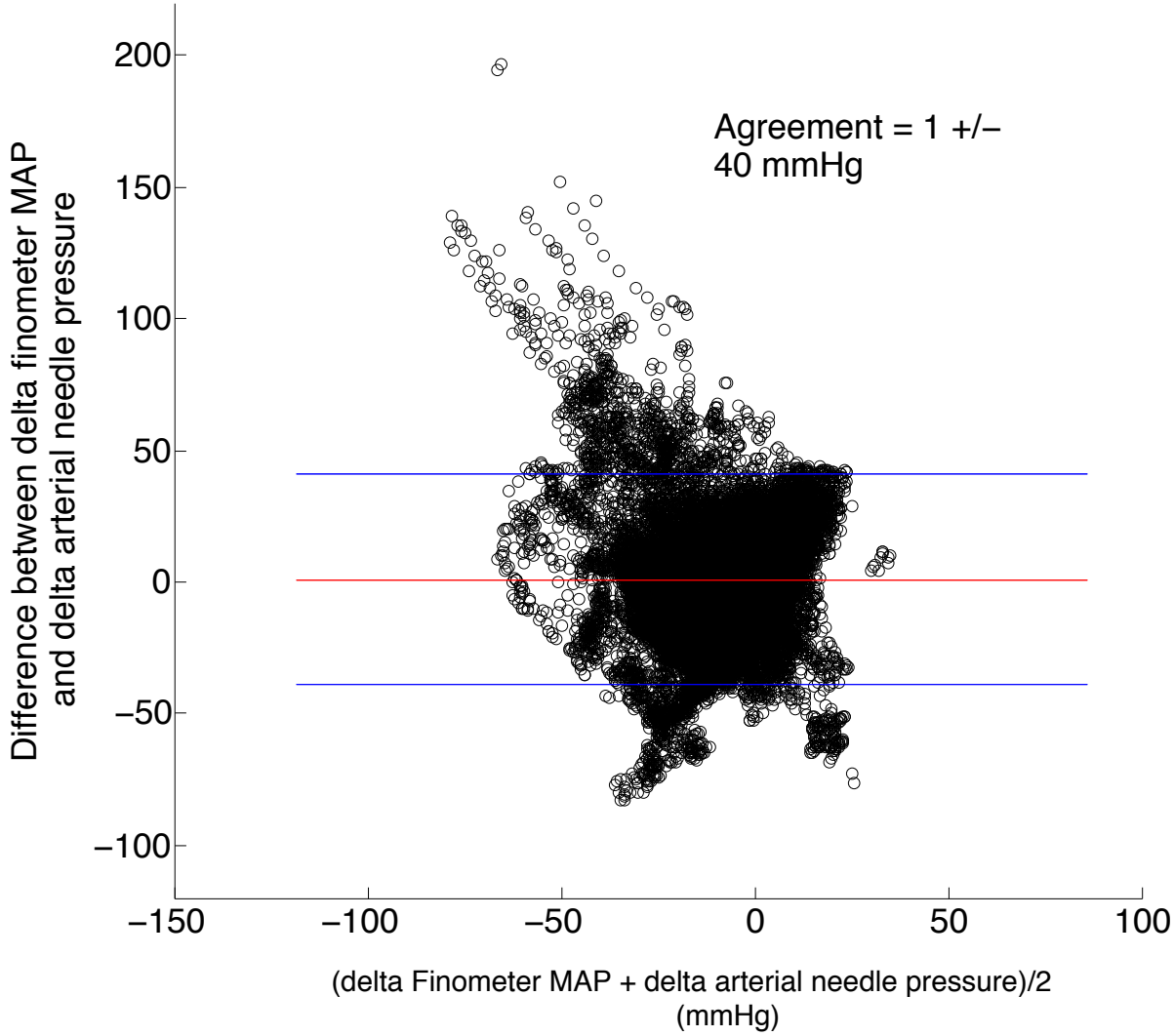

Table 7.2: Regression and correlation statistics, AVF sessions only

Blood pressure index	Access pressure index	Correlation (p value)	Linear model terms (β,Constant)	Linear model R^2	Bland-Altman Bias, SD
Finometer MAP	Arterial	0.14 (p<0.001)	0.12, -5.00	0.021	2.0, 21.6
Finometer MAP	Venous	0.10 (p<0.001)	0.08, -5.6	0.009	-3.5, 23.0
Finometer SBP	Arterial	0.16 (p<0.001)	0.12, -10.0	0.025	-2.5, 26.7
Finometer SBP	Venous	0.10 (p<0.001)	0.20, -8.9	0.010	-7.9, 28.3
Oscillometer MAP	Arterial	0.09 (p<0.001)	0.07, -4.9	0.008	-1.7, 26.3
Oscillometer SBP	Arterial	0.12 (p<0.001)	0.14, -7.7	0.014	-2.5, 26.6

Table 7.3: Regression and correlation statistics, brachial AVF sessions only

Blood pressure index	Access pressure index	Correlation (p value)	Linear model terms (β,Constant)	Linear model R^2	Bland-Altman Bias, SD
Finometer MAP	Arterial	0.21 (p<0.001)	0.20, -5.5	0.043	0.8, 20.5
Finometer MAP	Venous	0.13 (p<0.001)	0.11, -6.6	0.017	-4.0, 23.1
Finometer SBP	Arterial	0.20 (p<0.001)	0.30, -9.5	0.040	-4.1, 27.0
Finometer SBP	Venous	0.13 (p<0.001)	0.17, -11.2	0.016	-8.8, 29.3
Oscillometer MAP	Arterial	0.17 (p<0.001)	0.13, -2.5	0.030	-2.5, 25.0
Oscillometer SBP	Arterial	0.11 (p<0.001)	0.14, -9.3	0.012	-4.1, 26.8

Table 7.4: Regression and correlation statistics, Tesio sessions only

Blood pressure index	Access pressure index	Correlation (p value)	Linear model terms (β,Constant)	Linear model R^2	Bland-Altman Bias, SD
Finometer MAP	Arterial	0.09 (p<0.001)	0.11, -1.9	0.008	0.1, 16.7
Finometer MAP	Venous	-0.03 (p<0.001)	-0.02, -2.5	0.001	2.1, 23.6
Finometer SBP	Arterial	0.08 (p<0.001)	0.15, -3.0	0.007	-1.3, 21.7
Finometer SBP	Venous	-0.05 (p<0.001)	-0.05, -3.7	0.003	-1.0, 27.9
Oscillometer MAP	Arterial	0.17 (p<0.001)	0.13, -2.5	0.030	-2.0, 19.9
Oscillometer SBP	Arterial	0.15 (p<0.001)	0.14, -3.9	0.022	-1.3, 21.6

Session-level correlations

The median session-level correlation between Finometer MAP and AVF arterial needle pressure was 0.17 (interquartile range -0.15 to 0.54). The distribution of session-level correlations for Finometer MAP and AVF arterial access pressure is shown in figure 7.18. The equivalent for oscillometer MAP is shown in figure 7.19. As outlined in the discussion, the apparent improved performance of oscillometer MAP in this analysis alone likely represents methodological problems with using correlation statistics.

ANOVA revealed that the correlation varied significantly according to access, with mean correlation for sessions with Tesios 0.09, radial AVFs 0.13 and brachial AVFs 0.20 ($p = 0.008$). Due to the nature of correlation statistics, maximum change in MAP during a session is likely to increase the session-level correlation. A confounding factor is that maximum change in MAP also varied significantly according to access type: mean drop in MAP for sessions with Tesios -20.0mmHg, radial AVFs -22.5mmHg and brachial AVFs -27.2mmHg ($p<0.001$ on ANOVA). This is probably a chance association, although Tesios are more likely to be used in new starters who may have accumulated less comorbidity, and brachial fistulas are only created when radial access has been precluded by vascular disease. The session-level correlations varied substantially between patients: figure 7.20 shows the mean and 95 % confidence intervals for correlations for each patient (Finometer MAP and arterial access pressure). Once patient clustering had been taken into account, the only significant determinant of session-level correlation on mixed modelling was maximum change in MAP. This was a poor model, with the vast majority of variance remaining unexplained.

Figure 7.18: Session-level correlations between arterial access pressure and Finometer MAP, all AVFs

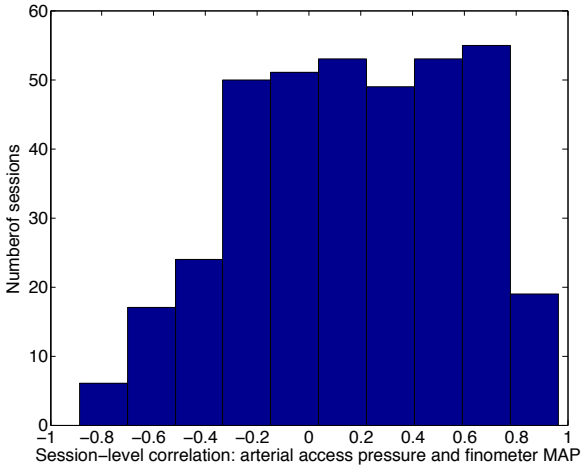

Figure 7.19: Session-level correlations between arterial access pressure and oscillometer MAP, all AVFs

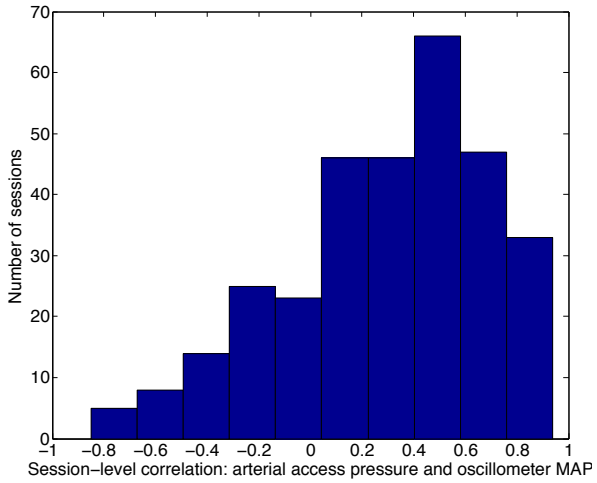

Figure 7.20: Variation in session-level correlations (x-axis) between patients (represented by numbers on y axis)

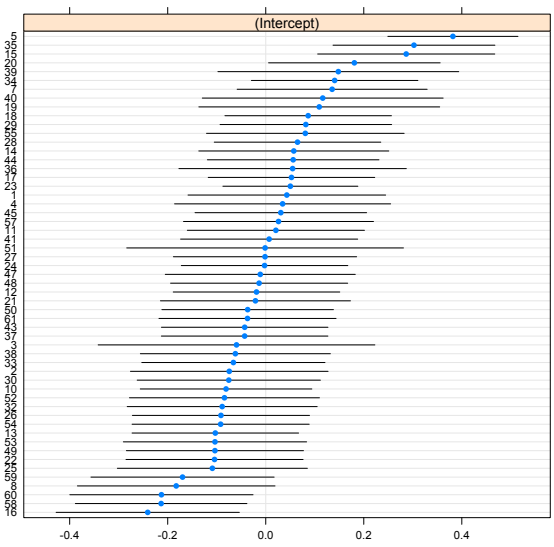

Patient level agreement

The agreement between δarterial access pressures and δMAP, as measured by Bland-Altmann methods, also varied substantially between patients. Figure 7.21 shows the standard deviation of the difference between measurement methods for each patient. Figure 7.22 shows the mean bias between measurement methods for each patient.

Figure 7.21: Standard deviation of differences between δarterial access pressure and δMAP (Finometer) for each patient

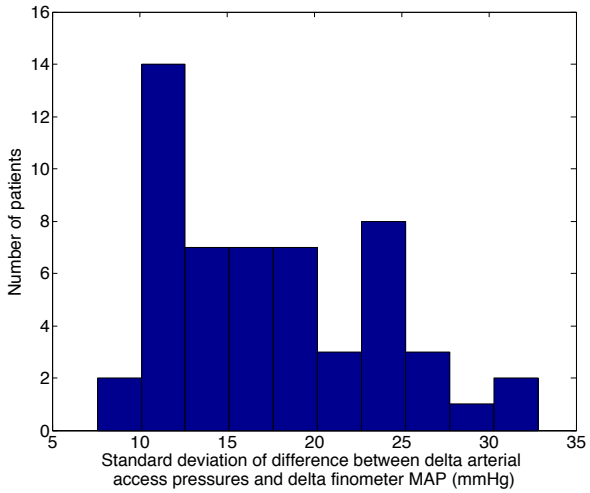

Figure 7.22: Mean difference between δarterial access pressure and δMAP (Finometer) for each patient

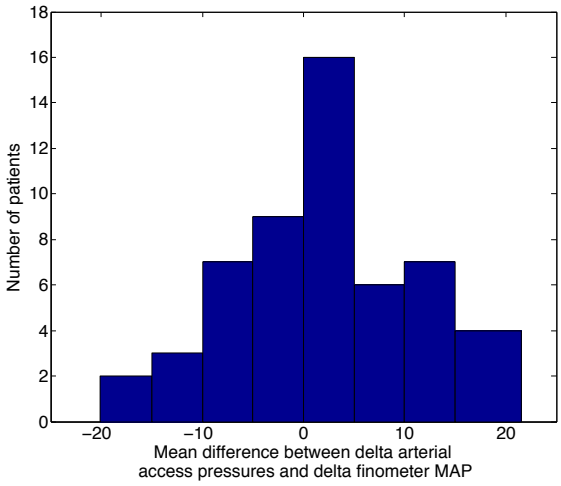

Even within access types, there was substantial variation: figure 7.23 shows box plots for the differences between all paired measurements within each patient, only for those with a brachial AVF. On linear regression, the factors significantly associated with standard deviation of the difference were as follows:

-Access type: +4.36mmHg for radial AVF compared to brachial AVF (p=0.015)

-Diabetes: +6.97mmHg for tablet controlled diabetes (p=0.017), +7.92mmHg for insulin controlled diabetes (p = 0.005) compared to no diabetes

-Typical UF volume: +2.28mmHg per litre (p=0.017)

This was a reasonable model, which met the assumptions of linear regression, and explained approximately a third of variance between patients. In contrast, none of the tested covariates were found to explain the patient differences in mean bias.

Figure 7.23: Box plots of within-patient differences between δarterial access pressure and δMAP (Finometer), brachial AVFs only

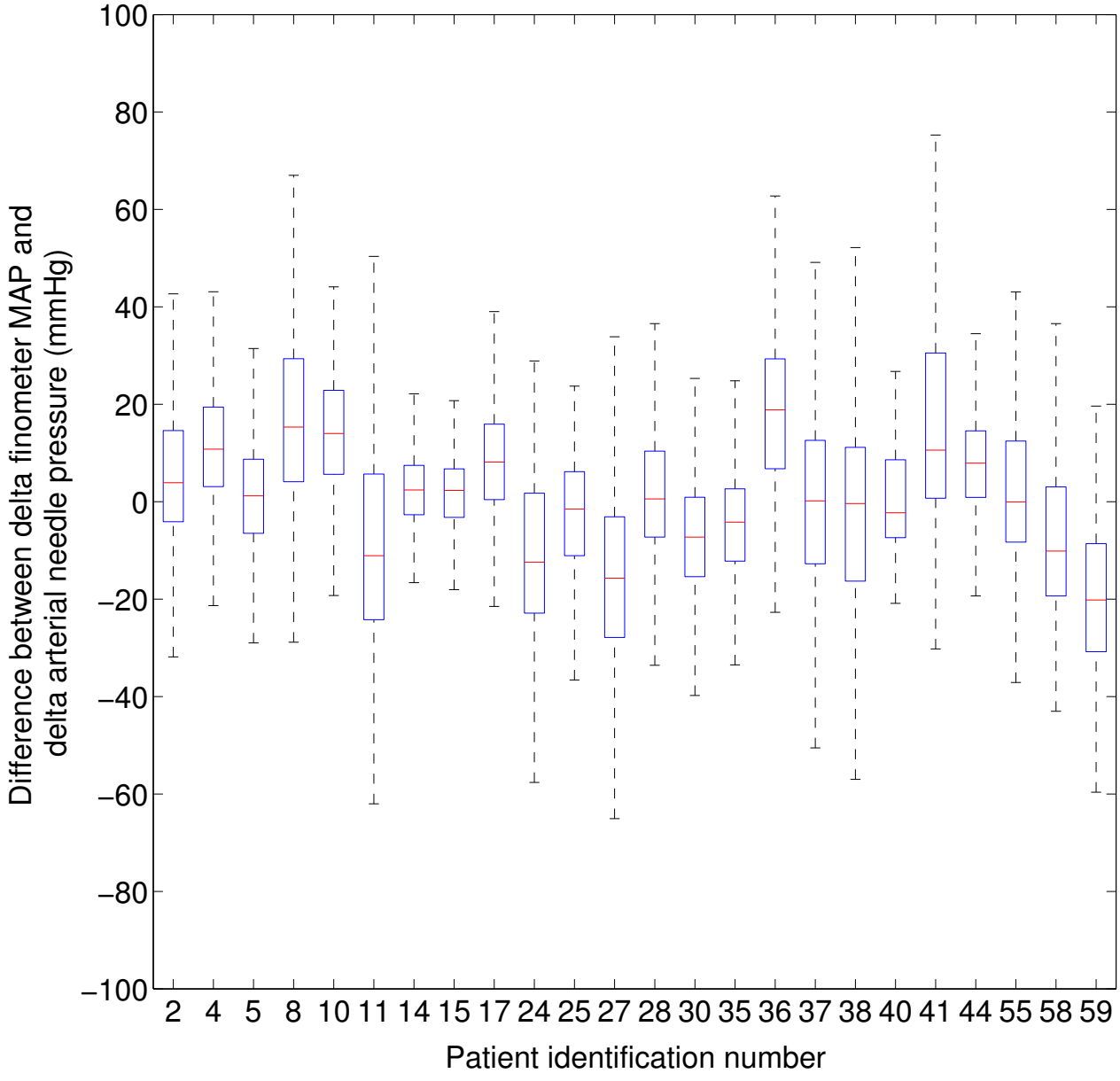

Despite the fact that access pressures performed much better in some patients than others as a surrogate of systemic pressures, even in the best example the agreement was not clinically useful. The patient with the best results was a non-diabetic 54 year old male with polycystic kidneys and minimal comorbidity, who had a large brachial AVF (patient 5 in figure 7.20). The scatter plot of δ arterial access pressures and δMAP for this patient is shown in figure 7.24, and the corresponding Bland-Altman plot in figure 7.25. The regression coefficients (access pressures as covariate and MAP as dependent variable) are β 0.72, constant -3.7, with R^2 0.41. Whilst promising, the BA plot show that the limits of agreement remain wide.

Figure 7.24: Plot of δarterial access pressure and δMAP for best example patient

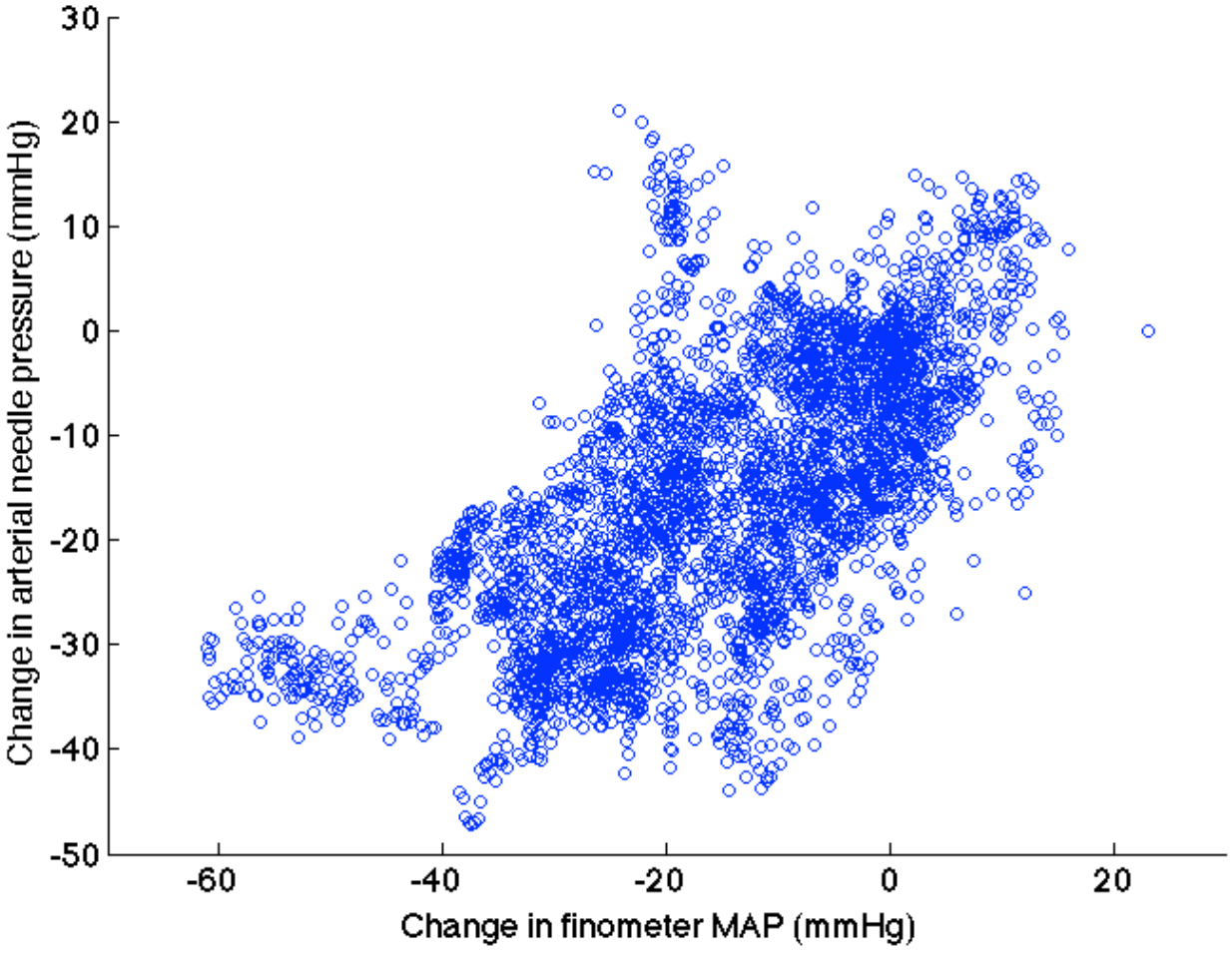

Figure 7.25: Measurement differences between δarterial needle pressures and δMAP for best example patient

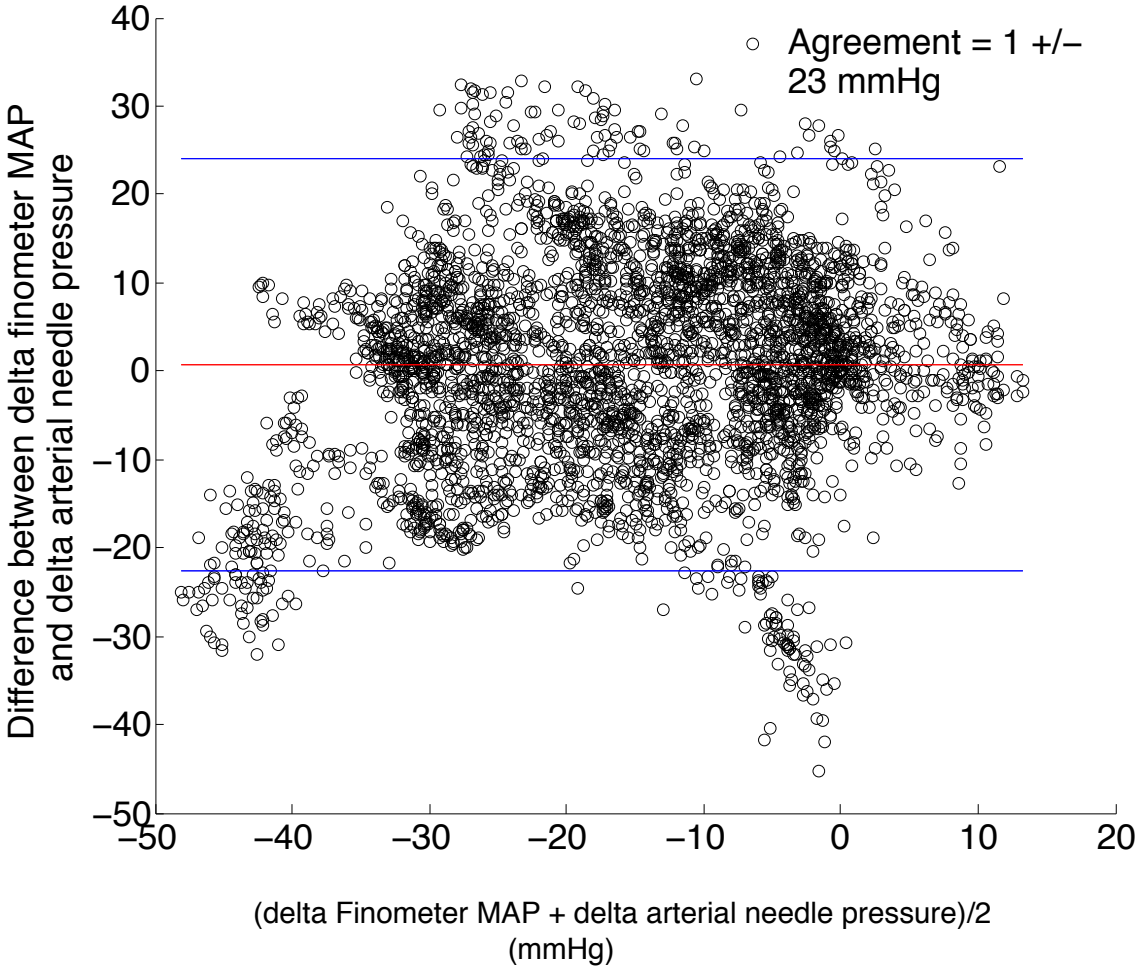

7.4 Discussion

PTT

We found that the majority of patients had a significant negative correlation between intra-dialytic PTT and blood pressure, but the strength of the relationship was generally weak, and not only variable between individuals, but between sessions within the same patient. The correlation at patient-level is expected to be less than the correlation at session-level, as even within the same subject, the relationship between blood pressure and PTT may vary from day to day, e.g. with the autonomic and mechanical vascular response to fluid retention. Even at session level, however, the correlation was generally weaker than that reported in other studies, regardless of blood pressure index used. A summary of studies which have used the R wave to PPG wave method of PTT to track blood pressure is presented in a recent review [157]. Pooling studies was not possible, due to different definitions of PTT, different perturbations (e.g. exercise, vasoactive drugs), different populations and different measurement periods. However, those defining PTT as we did (R wave to the mid-point of the PPG upstroke) reported average correlations for SBP ranging from -0.32 to-0.99, and -0.37 for MAP (only one study), whereas our median correlations were -0.15 for both MAP and SBP. The superior agreement in these studies reflects the much shorter time periods analysed, with change over minutes rather than hours. In addition, they used otherwise healthy patients or sedated patients, and some compared PTT to intermittent non-invasive blood pressure rather than continuous blood pressure [162, 163, 164]. Generally a smaller number of data points favours high correlation scores: dependence on the number of data points is one of the reasons that correlation can be misleading. Generally, linear regression with an R^2 is more useful when assessing the strength of the relationship.

Only one group to date have used PTT to track continuous blood pressure over entire dialysis sessions. Mambelli et al compared continuous PTT-derived blood pressure to continuous intra-arterial blood pressure in 4 patients undergoing HD on an intensive care unit using the Harmonized Alert Sensing Technology (HASTE) device [75]. This device estimates SBP using a linear equation: the coefficient and constant are initially selected based on values derived from 50 healthy individuals, and then updated based on frequent calibrations (every 5 minutes for the first 30 minutes, and then every 20 minutes). They found excellent correlation between intra-arterial SBP and HASTE-estimated SBP in this population, although notably the limits of agreement were wide at +/- 26.6mmHg. When they attempted to replicate results

in 14 outpatient HD sessions using an oscillometer as the reference, they found no significant relationship between HASTE-estimations of SBP and oscillometric SBP. This was attributed to substantial patient movement, and vascular disease resulting in a difference between upper arm and finger pressure, both issues that similarly affected our study. Moreover, our analysis was a retrospective examination of the raw relationship between PTT and blood pressure over an entire dialysis session, whereas the frequent calibrations with the HASTE device mean that Mambelli et al were essentially looking at the relationship over 20 minute blocks.

The relationship between PTT and blood pressure is altered by a number of factors, as shown in the equation in the introduction, including vessel inner diameter, vessel thickness, and blood viscosity. These factors change dynamically during HD as fluid is removed: in patients with an intact autonomic nervous system, vasoconstriction will alter vessel dimensions and stiffness. Therefore it is likely that frequent recalibration is going to be necessary to track blood pressure in this population. However, if calibration is required every 20 minutes or more, then arguably the PTT is not providing a great deal of extra information, unless the patient is prone to very rapid changes. It may be that the PTT is best suited for estimating short term changes, e.g. over general anaesthetic induction or during a cardiovascular challenge.

In terms of the ideal blood pressure index to track PTT, MAP and SBP appeared to perform similarly in this population. Interestingly, we found that the relationship between PTT and blood pressure was slightly stronger when absolute rather than relative values were used. This may be because we had sufficient data for each patient (typically 60 hours) to assess this relationship at the level of each individual, rather than having to pool data and assess at the population level.

The use of beta blockers and the presence of vascular disease explained a substantial amount of inter-patient variation. Beta blocker use could improve the performance of PTT as a surrogate measure of blood pressure by attenuating the autonomically-driven dynamic changes in vascular tone. This might perhaps allow PTT to track blood pressure changes over longer periods without the need for recalibration. This hypothesis would explain why the beta blocker term could not be replaced by a measure of average baseline pulse. Nevertheless, at the session-level, even adjusting for random effects, baseline pulse rate was a highly significant determinant of correlation score: lower pulse rates were associated with a

stronger relationship between PTT and blood pressure. It may be that this is confounding from the use of beta blockers, but beta blocker use was not a significant term in the model even if the pulse covariate was excluded. Alternatively, those with a low pulse rate at baseline may be fitter patients, with less fluid overload, who are less likely to undergo large changes in heart rate during dialysis. It is known that RR variability is related to changes in PTT, probably due to shared autonomic modulation rather than cause and effect [165]. Some investigators have shown that increasing heart rate appears to be associated with increasing pulse wave velocity in the absence of changes in blood pressure, i.e. increasing heart rate alters the relationship between PTT and blood pressure [166, 167]. It is possible that this phenomenon is an artefact of measurement method rather than a physiological process, but animal studies have shown that heart rate can indeed influence arterial elasticity [168].

Access pressures

Overall, it was not possible to reliably estimate changes in systemic blood pressures from dynamic access pressures. The δarterial access pressure measured from brachial AVFs showed the greatest relationship with systemic blood pressure changes, but the correlation was weak. The slight advantage of δMAP over δSBP for agreement may have been obviated by taking into account the magnitude of baseline values, though there is a rationale for access pressures correlating better with MAP: whether or not the access pressure values were spot measurements (i.e. at different times in the cardiac cycle) or averages over the preceding minute, they would have tended to the mean value over the cardiac cycle, particularly once the smoothing filter was applied. It is likely that brachial AVFs performed better as they are more proximal and tend to have larger anastomoses with greater blood flow, although access flow itself was not a significant covariate. Given the arterial needle is positioned closer to the anastomosis of the artery with the vein, it was expected that AVF arterial pressures would have greater agreement with systemic pressures than AVF venous pressures. However, this relationship unexpectedly also held true for Tesio lines, where both lumens are adjacent in the superior vena cava. In addition, the limits of agreement were narrowest for Tesios, despite the fact that this access type should only detect changes in central venous pressure. These may be chance findings, reflecting the smaller number of sessions with Tesio access. It may not be intuitive that the central venous pressure measured from a Tesio would correlate with systemic pressures at all: one explanation is that preload is a determinant of cardiac output.

There was a huge amount of inter-patient variation in all of the correlation, regression and agreement statistics, only some of which could be explained by the type of access. On multivariate linear regression, it appeared that a well as access type, ultrafiltration volume and diabetes history were significant predictors of wider limits of agreement. A physiological explanation for the ultrafiltration covariate is that haematocrit will rise as fluid is removed, and this has been shown to alter the relationship between dialysis circuit and access pressures. It is often more difficult to establish good vascular access in patients with diabetes due to atherosclerotic changes, and this may translate to poorer access blood flow. A weakness of the linear regression model reported is that access blood flow and needle size data was not gathered (though this would not have changed the results of the other analyses).

Session-level correlation statistics were sometimes at variance with agreement statistics, and this chapter highlights some of the issues with correlation measurements, namely that they are very sensitive to both the number of data points compared and the maximum change in the variable. As there was very few NIBP measurements per session, the session-level correlations were artificially higher, despite the fact that other, more robust measures of agreement suggested that NIBP provided a poorer surrogate for systemic pressures. Fluctuations in the Finometer MAP which did not strictly coincide with fluctuations in needle pressures would be penalised, whereas a very high correlation with NIBP could be achieved as long as the general trend was in agreement.

The fluid mechanics underlying fistula haemodynamics are complex, but there are two key areas where large and variable errors are introduced in the process of estimating systemic pressure changes from access pressure changes. First, there is the drop in pressure between the arterial system, e.g. brachial or radial artery, and the arterialised vein. The ratio of systemic to intra-access pressure has been proposed as a method of access surveillance, so has been well investigated [169]. A number of different anatomical features have been found to affect the relationship between arterial pressure and downstream access pressures, including the angle and diameter of the anastomosis, the outflow resistance, and whether the access is a native fistula or a graft [170, 171, 172]. If the systemic to intra-access pressure ratio is fixed, then the trend in systemic pressure could still be reliably estimated: however if the anastomotic diameter or flow patterns vary with arterial pressures, then the ratio may be variable. Nevertheless, two small historical studies found that directly measured intra-fistula pressures generally correlated with changes in femoral intra-arterial MAP [158, 159].

Secondly, there is the difference between the so-called "static" intra-fistula pressure and the pressures measured at the the pre-pump and venous bubble trap. When the pump is off, and the lines are clamped, there are only hydrostatic forces to consider. However when the pump is moving as in this study ("dynamic" pressures), interpretation becomes even more difficult [172, 173, 174]. Investigators have found that, in addition to actual intra-fistula pressure itself, the dynamic pressures are influenced by baseline haematocrit, ultrafiltration volume, tubing diameter and length, and needle size/orientation [173]. In fact, it is thought that dynamic venous and arterial pressures are largely a reflection of the hydraulics of the needles [174, 173]. Small changes in the position or angle of the needles during dialysis, e.g. due to patient movement or increased proximity of the needle tips to the vessel wall with reduction of intravascular volume, will change dynamic pressures independently of static pressures and independently of each other. In our unit, the arterial needle is positioned so that the bevel is facing away from the direction of blood flow, which is likely to confound estimates of true access pressures further. Considering all these factors, it is perhaps not surprising that we did not find dynamic needle pressures to be a useful surrogate for systemic pressures. Furthermore, it has been suggested that there is substantial inaccuracy in access pressures reported by dialysis machines [174].

It is possible that improved agreement could be found with increased resolution of access pressure measurements, limiting analysis to high flow brachial AVFs confirmed to be without recirculation, and the use of more sophisticated models to account for the myriad of factors determining the relationship between systemic blood pressure and dynamic access pressures.

7.5 Conclusions

Dynamic access pressures in this study did not show sufficient agreement to be used as a surrogate measure of trends in continuous systemic blood pressure, though there was considerable variation between patients. PTT showed promise in some patients as a method of tracking either MAP or SBP over the course of haemodialysis, but the relationship was much weaker than that reported by studies examining short term changes. Therefore, without frequent calibration, it is unlikely to have sufficient accuracy for clinical use.

Chapter 8

Relationship between deterioration in cognitive function testing and intra-dialytic physiology

8.1 Introduction

There has long been speculation that haemodynamic instability during HD leads to repetitive cerebral ischaemia and consequent cognitive decline. Whilst there is certainly an association between duration of HD, ischaemic white matter changes and cognitive dysfunction, the evidence of causation is weak. This is because cognitive impairment and white matter abnormalities are independently associated with renal impairment per se in a dose-related fashion, likely due to increasing burden of cerebral small vessel disease [33, 34, 35, 36].

To definitively answer the question of whether cerebral ischaemia occurs during HD, a continuous, non-invasive method of monitoring cerebral tissue oxygenation during a large number of dialysis sessions is needed. Methods of measuring tissue oxygenation are outlined in the Introduction chapter. As discussed, cerebral NIRS is the only option for uninterrupted, non-invasive monitoring of cerebral oxygenation on an outpatient dialysis unit, and has been shown to correlate well with more invasive or operator dependent measures of cerebral perfusion, including transcranial Doppler and functional MRI [55, 56]. To date, there has been limited data on the use of NIRS in HD patients.

We monitored 58 patients with continuous blood pressure and cerebral NIRS for 9-12 consecutive dialysis sessions each, in order to assess their typical exposure to cerebral ischaemia and hypotension, and then correlated this with change in cognitive function over 12 months. The primary objective was to quantify deterioration in cognitive function over time, and to make a preliminary estimate of whether this is associated with intra-dialytic haemodynamic instability or cerebral ischaemia.

8.2 Methods

See the Methods chapter for details of the trial and data collection. Continuous blood pressure monitoring was performed using the Finometer device. The beat-to-beat blood pressure data was processed by removal of extreme outliers (3 standard deviations from mean or more) and low pass filtering (Hamming window based with cutoff 0.083 Hz) to attenuate high frequency noise. Data was discarded if it did not meet the standards of an SQI based on waveform quality. Missing segments were not interpolated. For stable patients with the older Finometer model, baseline blood pressure was defined as the median value from a window beginning 2 minutes after recording start (to allow time for Physiocal calibration) and ending at the point of bleedout, i.e. when the patient's blood enters the dialysis circuit and treatment commences. For the unstable patients with the Finometer Pro, the start point of the window was instead completion of RTF calibration. Blood pressure data was downsampled to a frequency of 0.0167 Hz (i.e. one data point every minute) for these analyses. The AUCs below different MAP thresholds, relative and absolute, were calculated for each session.

Cerebral oximetry was measured with the INVOS device. Data was processed with removal of extreme outliers (3 standard deviations from mean or more) and application of a low pass filter (Hamming window based with cutoff 0.083 Hz) to attenuate noise. Data was downsampled to a frequency of 0.0167 Hz for these analyses. Baseline rSO2 was taken as the median of good quality data spanning the first 2-6 minutes of recording.

As discussed in the previous chapters, there is no consensus on the rSO2 cutoff value which should be considered abnormal or harmful, and accepting the limitations of any arbitrary threshold, we again chose a relative drop of 15% of the baseline value as the cutoff for potential cerebral ischaemia. . For each session, the AUC below the cutoff of a relative 15% drop was calculated, known hereafter as the

ischaemia AUC (min*%).

At baseline and at 12 months from study entry, patients underwent cognitive function testing consisting of the 3MS and the TTB, and screening for depression using the PHQ-9. All patients were assessed by the same individual, and strictly in accordance with published protocols. This included capping the TTB at 5 minutes if the patient had been unable to complete the task by this time. At baseline, all patients were assess on the dialysis unit, within the first two hours of treatment; at 12 months, some individuals had had transplants, and they were assessed either on the dialysis unit or outpatients, a similar environment.

The results of cognitive function tests at baseline were compared to reference values for the general population. At the time of the trial, the 3MS, TTB and PHQ9 were being piloted on the dialysis unit as part of a clinical audit: therefore, baseline data, including demographics, was available from an additional 16 patients outside the study. Linear modelling was used to identify significant predictors of baseline performance on the TTB and 3MS, with covariates including age, level of education, cerebrovascular disease, other vascular disease, diabetes vintage, HD vintage, PHQ score and baseline rSO2.

In order to adjust for the different exposure to intra-dialytic hypoxia during follow up that resulted from, for example, transplantation or increased frequency of treatment, the average session ischaemia AUC for a given patient was calculated, and multiplied by the number of sessions delivered during follow up. This was then entered as a covariate into a linear model predicting the percentage change in TTB score between baseline and 12 month follow up. Other covariates tested included relative and absolute hypotension AUC (with exposure calculated in the same way), age, level of education, CVD, other vascular disease, diabetes vintage, HD vintage, PHQ-9 score and baseline rSO2. Variables were transformed to maximise the linear relationship between predictors and outcome, and checks were performed on the residuals to ensure models were valid.

As there were more deaths than expected, and the number of patients was relatively small, the robustness of all results was tested with the boot strapping (resampling with replacement) and jack knifing (resampling without replacement).

Figure 8.1: Histogram of baseline cerebral rSO2

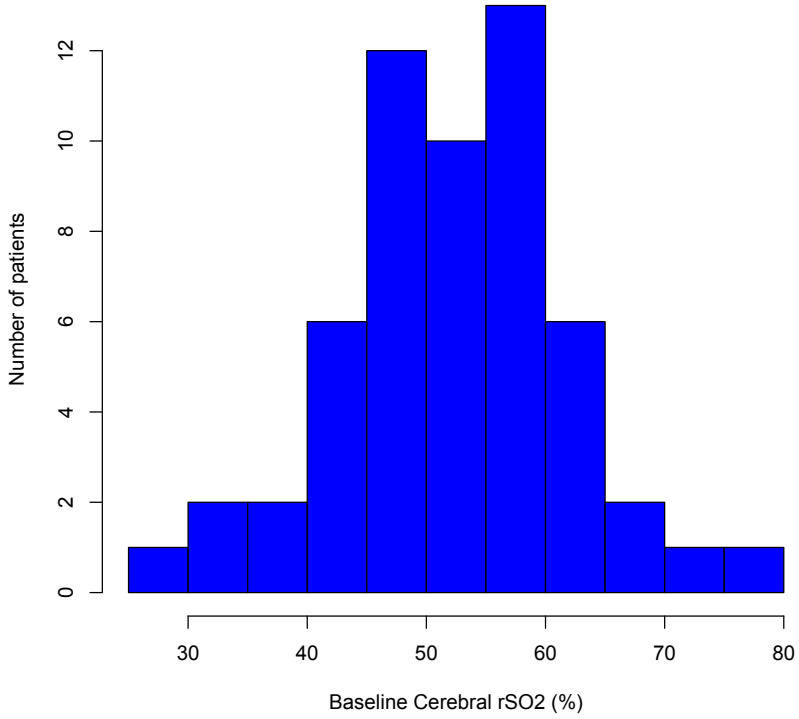

8.3 Results

8.3.1 Baseline cognitive function tests

Baseline cognitive function tests were available from all 60 recruited patients, and from 16 additional dialysis patients who had been assessed as part of a clinical audit. The median 3MS score was 92, interquartile range 88 to 96 (not significantly different when limited to study patients). Figure 8.2 shows the baseline 3MS scores against age, with lines drawn at the previously reported optimal cutoff points for both dementia and cognitive dysfunction [175]. For 3MS score, only age and educational level were significant (table 8.1).

The median TTB score was 122 seconds, interquartile range 83 to 185 (not significantly different when limited to the study patients). On linear regression, as expected, age and level of education were significant predictors of performance (see table 8.2). However, HD vintage, but not ESRF vintage, was also significantly associated with the score. The models did not change when restricted only to study patients. Table 8.3 shows TTB scores in this HD population compared to reference values for the general

population, stratified for age and educational level. The improved performance in the extremely elderly with high levels of education is likely to be a survival effect.

Figure 8.2: Baseline 3MS scores against age for this population

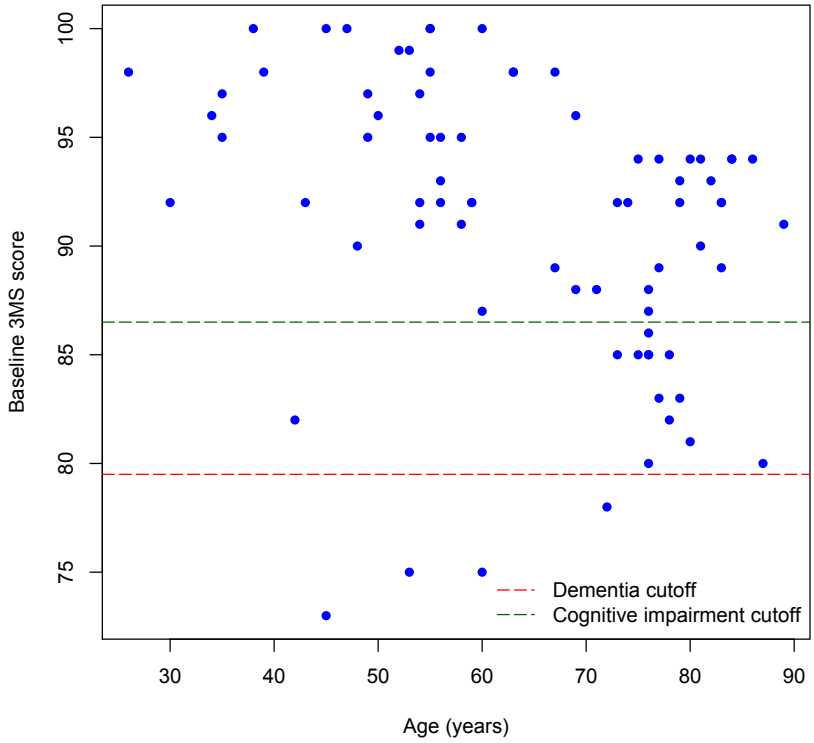

Table 8.1: Factors significantly associated with baseline 3MS score

Covariate	Odds Ratio	95% Confidence Intervals	p value
Age	-0.12 points per year	-0.03 to -0.21	0.009
Educational level*	2.09 points per level	0.50 to 3.79	0.010

*Possible levels: No qualifications, O level/equivalent, A level/equivalent or above

Table 8.2: Factors significantly associated with baseline TTB score

Covariate	Odds Ratio	95% Confidence Intervals	p value
Age	2.1 seconds per year	1.2 to 2.9	<0.001
Educational level*	-26.8 seconds per level	-11.1 to -42.1	<0.001
Haemodialysis Vintage	6.2 seconds per sqrt(years)	1.5 to 10.8	0.010

*Possible levels: No qualifications, O level/equivalent, A level/equivalent or above

Table 8.3: TTB scores for study population compared to reference values in red [176]

Age group (years)	TTB score, All educational levels (median, IQR)	TTB score O level/equivalent or less (median, IQR) (n=51)	TTB score A level/equivalent or more (median, IQR) (n=25)
≤ 40 (n=7)	67 (55-80) 50 (42-61)	NA*	NA*
41-55 (n=19)	86 (69-120) 64 (55-74)	NA*	NA*
56-70 (n=16	110 (78-152) 76 (66-98)	149 (89-176) 86 (73-114)	94 (67-133) 68 (60-74)
71-80 (n=23)	183 (159-229) 115 (74-156)	197 (157-255) 120 (94-162)	161 (158-170) 87 (63-134)
>80 (n=11)	138 (117-224) 138 (91-197)	213 (117-252) 143 (103-204)	134 (120-146) 121 (84-184)

*Education not expected to alter result under 55 years of age

8.3.2 Deterioration in cognitive function over 12 months

Of the 58 patients who completed physiological monitoring, follow up cognitive function testing was performed on 47 individuals. 2 patients had moved units and were not contactable, and 9 patients had died. Of the 47 available patients, 9 had undergone transplantation during the follow up period, and the remainder were still on outpatient haemodialysis. In two cases, there was insufficient rSO2 data (one in a transplanted patient, one in a patient still on dialysis), so in total, there were 45 cases available for modelling.

The mean change in TTB performance was +12.4 seconds, although the distribution had a long right tail, with median only +1 second, as shown in figure 8.3 . A separation was seen in those who had undergone transplantation (mean -6.9 seconds, i.e. an improvement) and those who remained on dialysis (mean +16.1 seconds), though due to small numbers and potential confounders (e.g. age), firm conclusions cannot be drawn from this. The mean change in 3MS score was -1 point, with substantial patient variation. Follow up 3MS scores against cut-offs for cognitive dysfunction are shown in figure 8.4.

Figure 8.3: Probability densities of follow up TTB scores against baseline TTB scores (the second peak results from the use of a cutoff when more than 5 minutes was required to complete the task)

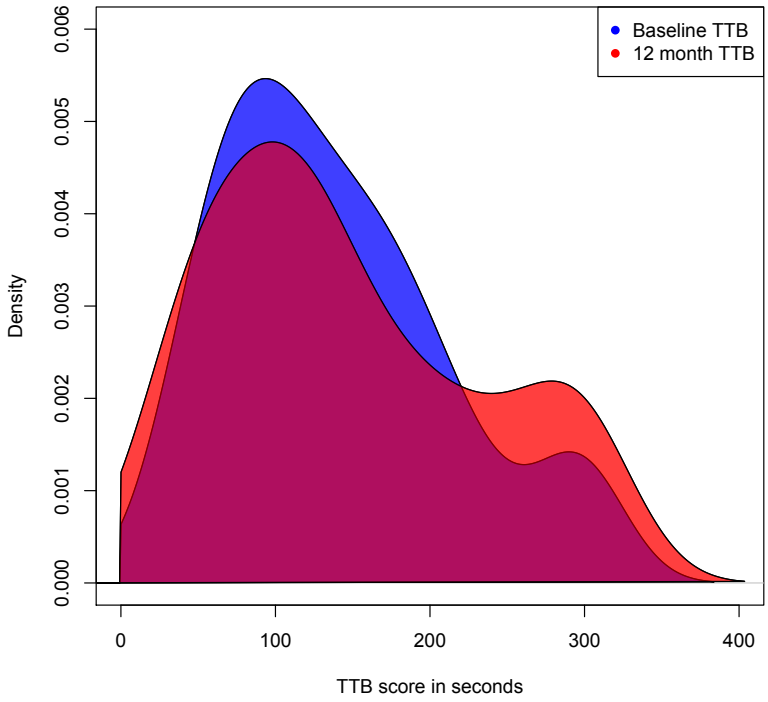

Figure 8.4: Follow up 3MS scores against age for this population

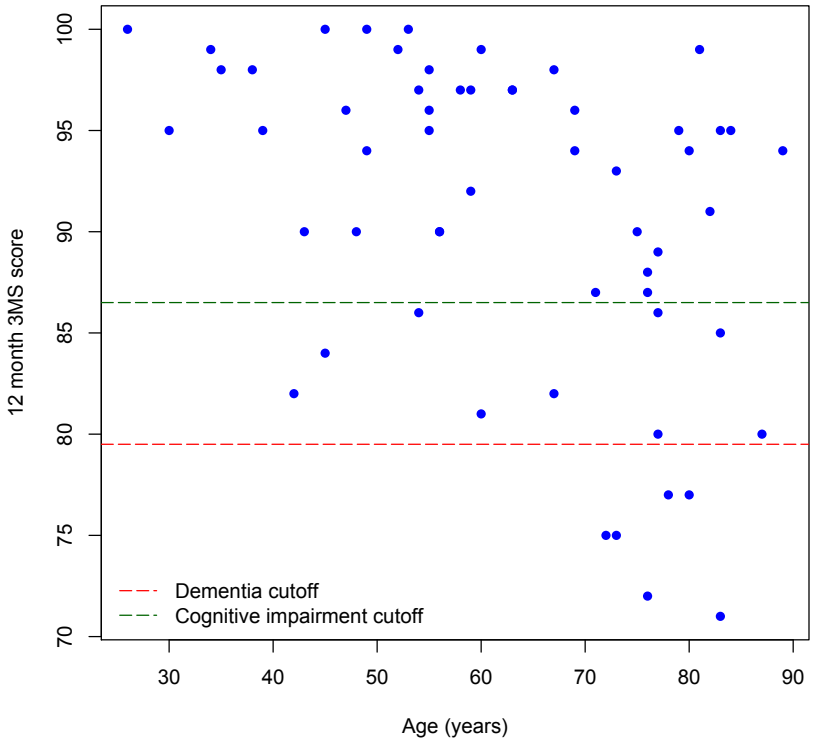

On multivariate linear modelling, with bootstrapping to check robustness and attenuate the impact of influential outliers, the only covariate that remained a significant predictor of deterioration in TTB score (expressed as percentage change from baseline) was total exposure to intra-dialytic hypoxia, as defined above. Similar results were obtained when the deterioration in TTB score was expressed in seconds. The only significant predictor of change in 3MS performance after bootstrapping was change in PHQ-9 score, with an increase of 0.26 points per unit improvement in depression score (p=0.03). The relationship between change in TTB and cumulative exposure to intra-dialytic hypoxia was not linear, with proportionally greater effect size occurring as exposure increased. To obtain a linear relationship for the purposes of linear modelling, total exposure was transformed with the power of 0.2. The final equation after bootstrapping was:

$$\delta\text{TTB} = -7.8 + 5.8 * \text{Hypoxia}^{0.2} \tag{8.3.1}$$

where δ TTB= percentage change in TTB over 12 months, and Hypoxia is the estimated AUC for cerebral ischaemia over the 12 months in %min.

The confidence intervals for the hypoxia coefficient were 0.5 to 11.1, p=0.036. Linear model assumptions were satisfactorily met, though the model was a poor fit with R^2 only 0.10. Two individuals had a consistently large Cook's distance for all analyses. Reassuringly, removing these two cases increased the significance of the relationship (hypoxia coefficient 5.9, bootstrap confidence intervals 1.9-9.7, p=0.004), and improved the fit to R^2 0.16. These two individuals had extremely low baseline rSO2 values (below 35%) so this may have influenced results, given that ischaemia was defined as a percentage of baseline.

8.4 Discussion

This is the first study measuring both continuous cerebral oxygenation and continuous blood pressure over a large number of HD sessions, including many with haemodynamic instability. The key finding was that cumulative intra-dialytic exposure to cerebral ischaemia, arbitrarily defined as less than 15% of baseline value, corresponded to change in executive cognitive function. Cerebral desaturation far outperformed relative or absolute blood pressure thresholds in terms of predicting decline in cognition.

In keeping with other investigators, we identified significant abnormalities in cognitive function in this HD population [34, 47, 35]. At all ages and education levels, the TTB scores were substantially lower than expected for the general population [176]. Most investigators have found that cognitive dysfunction in dialysis patients is largely executive, eg. planning and processing speed, areas specifically assessed by the TTB [35, 47]. Although the MMSE and 3MS have been widely validated as measures of global cognitive function, with components for orientation, language, attention and memory, they are less sensitive for detecting executive dysfunction. However, there were still detectable differences between the study population 3MS scores and those typically reported for the general population. There are not normative values as such for the 3MS, as it is mainly a screening test for cognitive impairment in the elderly, and has a ceiling effect. Nevertheless, for normal adults aged 60-69, one study has reported a median score of 95 (IQR 93-97), with median 94 (IQR 90-97) for patients aged 70-79 [177]. The equivalents in our study population were 96 (88-98) and 86 (85-92), i.e. a greater deterioration with age and more variable results. Some argue that adjustment for age or education leads to clinically important cognitive dysfunction being missed, and that the same cutoffs should be used for the whole population, e.g. 86 and below has been reported to have a sensitivity of 78% and specificity of 76% for cognitive impairment, and 79 or below a sensitivity of 85% and specificity of 84% for dementia [178, 175]. Using these cutoffs, at baseline 5% of the study population had dementia and a further 16% cognitive dysfunction.

In the general population, baseline rSO2 values have been reported to lie between 60-80%, with a normal distribution [179]. In this study population, we found a normal distribution shifted substantially to the left, with most values lying between 40-60%. This is in keeping with other studies which have shown that baseline tissue oxygenation as measured by cerebral NIRS has been found to be significantly lower in HD patients than normal controls, and may correlate with HD vintage [57, 58, 59]. In another approach, Kobayashi et al looked directly at regional cerebral blood flow in 54 prevalent HD patients using SPECT, and reported a general reduction in blood flow compared to healthy controls, which worsened with HD vintage [45].

There have been conflicting reports on inter-test reliability for both the 3MS and TTB [112, 113, 180]. Therefore the change in score that should be deemed to represent a genuine change in cognition is controversial. Small changes within an individual should be interpreted in the context of normal, short-term intra-individual variation. The coefficient of variation is an established method to assess test-retest reli-

ability, and is calculated by taking the standard deviation of the differences, and dividing by the mean value of the test. Day to day TTB performance has been reported to have fairly large coefficient of variation of 33% [113], though with this very short retest interval, it is unsurprising that there was a "practice" effect. In data derived from the Frequent Hemodialysis Network trial, the coefficient of variation was approximately 7% in the subset of patients for whom raw scores were given [39]. As regards 3MS, a large study also reported a 3 month coefficient of variation of approximately 7% (standard deviation of difference in score 6 points) [112]. Generally a change of greater than 5 points on the 3MS is considered clinically significant [180]. Notably, much of the inter-test variance can be attributed to inter-observer differences, and unlike previously published literature, both baseline and follow up tests were administered by the same individual in our study. In addition, with the 12 month interval in our study, any practice effect would be minimised.

The change in 3MS and TTB scores over 12 months in this study was very variable: overall there was a mild decline, but some patients showed a marked deterioration in performance, and others even improved. There is only one comparable study looking at longitudinal changes in TTB and 3MS scores in HD patients. Kurella-Tamura et al analysed change in TTB score over 12 months in patients enrolled in the Frequent Haemodialysis Network trial, and similarly found an overall deterioration with a mean change of approximately +9 seconds, but a wide range of results [181]. Indeed, 55% patients showed an improvement, although the change was expressed in absolute seconds rather than percentage of baseline, and so the clinical significance was likely to be variable. Compared to our study population, patients were younger, with mean age of 50 years. Change in performance was not related to frequency of HD or depression scores; alternative determinants were not explored. In our study, the only factors found to explain the variance in change in cognitive function were estimated exposure to intra-dialytic cerebral ischaemia over the 12 month period (TTB), and the severity of depression, as measured by the PHQ-9 (3MS).

This is also the first study to demonstrate that intra-dialytic physiology is associated with changes in cognitive function. Previous studies, as discussed in the Introduction chapter, have not found a relationship between intra-dialytic haemodynamic instability and either cognitive outcomes, or surrogates such as radiological changes. The small numbers mean that this study can at best be considered a pilot. Findings must be confirmed in a larger cohort of patients: bootstrapping and statistical techniques to

reduce confounding are no substitute for large numbers. Ultimately a controlled trial pairing continuous cerebral tissue oxygenation monitoring with interventions such as cooling or biofeedback dialysis might help to establish if such interventions can improve intra-dialytic cerebral perfusion; following up with robust functional tests would then allow detection of any clinically significant cerebral protection. Cerebral NIRS is likely to be the only suitable technology for this task. MRI techniques for assessing cerebral perfusion are not suited to continuous, real-time monitoring in a large number of patients, and also give no indication of oxygen balance.

Finally, another limitation arises from the assumption that the dialysis sessions during the study period were representative of those during follow up. However, we monitored many more sessions per patient than is typical in the literature. Finally, error may arise from the definition of cerebral ischaemia: there is no consensus on what change in rSO2 is harmful. We extrapolated from existing literature as far as possible, and the association with change in cognitive function provides some support for the threshold chosen.

8.5 Conclusions

Cumulative intra-dialytic exposure to cerebral ischaemia, arbitrarily defined as less than 15% of baseline value, corresponded to change in executive cognitive function. Cerebral desaturation far outperformed relative or absolute blood pressure thresholds in terms of predicting decline in cognition.

Chapter 9

Prediction of cerebral desaturation on haemodialysis using univariate variables at the population level

9.1 Introduction

Interventions to counteract intra-dialytic haemodynamic instability include varying the dialysate sodium concentration, cooling the dialysate, reducing the speed of ultrafiltration or adding in a convective component to treatment (i.e. HDF): however to optimise performance, they need to anticipate the onset of hypotension, and be tailored to the underlying physiological abnormality [68, 69].

A number of approaches have been taken to predict the onset of hypotension using univariate physiological parameters at the population level, but results have been mixed. Returning to physiological principles, measuring blood pressure is useful because it is a surrogate for downstream tissue perfusion pressure, which is a surrogate for adequacy of cellular oxygenation. It may therefore be more fruitful to anticipate and prevent end-organ ischaemia itself rather than its surrogate hypotension. Moreover, the underlying pathogenesis of dialysis-induced hypotension and/or ischaemia is likely to be very heterogeneous. It is possible that one physiological variable is unlikely to reliably anticipate hypotensive/ischaemic events in every session in every patient. Before abandoning univariate predictors at the population level altogether, it is important to explore the full range of potential covariates in a large and robust dataset: some data streams are likely to have more value than others. In addition, it is important to assess

whether the results depend on the type of event being predicted, eg tissue ischaemia, classic KDOQI event or other definition of hypotension. These are useful first steps in the progression to multivariate, personalised models.

The key objectives of this chapter are as follows: to identify which univariate physiological variables, on the population level, best distinguish normal dialysis sessions from those affected by symptoms, hypotension or cerebral ischaemia; to identify whether the most informative physiological variables vary according to the type of event being predicted; to confirm the need for multivariate, personalised models. The reasons for choosing the brain as the indicator organ are outlined in the introduction chapter, and include the availability of technology to monitor cerebral oxygenation in a continuous and non-invasive manner throughout dialysis, and the fact that validated cognitive function tests are a convenient, non-invasive and clinically important measure of end-organ damage.

9.2 Methods

See the methods chapter for full details of the trial and data collection. The following physiological and derived variables were assessed:

- MAP
- Cardiac output (relative to baseline)
- Heart rate (derived from ECG)
- LF power, normalised units (ECG derived)
- PPG amplitude (relative to baseline)
- Pulse pressure variability (PPV, derived from PPG and Finometer)
- Peripheral saturations
- Saturation variability
- Respiratory rate
- Access blood saturations (AVF or central venous)

- RBV
- Ultrafiltration volume
- Cerebral rSO2

9.2.1 Data pre-processing

Blood pressure monitoring was performed using the Finometer PRO (unstable patients, n=37) or the Finometer MIDI (stable patients, n=19). The beat-to-beat blood pressure data was processed by removal of extreme outliers (3 standard deviations from mean) and low pass filtering (Hamming window based with cutoff 0.083 Hz) to attenuate high frequency noise, followed by application of an SQI based on waveform quality (see Methods chapter). Cardiac output was derived from the Finometer waveform (patented Modelflow algorithm), with calibration by ultrasound dilution in patients being monitored with the Finometer PRO. Only cardiac output data from segments passing the Finometer SQI were considered, and extreme outliers were removed. As not all sessions were calibrated with ultrasound dilution, for the population analyses, cardiac output was expressed as percentage change from baseline value. For patients being monitored with the Finometer MIDI (n=19), baseline blood pressure and cardiac output were defined as the median values from a window beginning 2 minutes after recording start (to allow time for Physiocal calibration) and ending at the point of bleedout. For those patients being monitored with the Finometer PRO (n=37), the start point of the window was instead at completion of RTF calibration. The ultrasound dilution calibration could not be done until after bleedout: in applicable sessions, cardiac output values prior to this point were retrospectively transformed.

Cerebral rSO2 was measured with the INVOS NIRS device, sampled at 5 second intervals. Data was processed with removal of extreme outliers (4 standard deviations from mean or more) and application of a low pass filter (Hamming window based with cutoff 0.083 Hz) to attenuate noise. Data was downsampled to a frequency of 0.0167 Hz for the analyses in this chapter. Baseline rSO2 was taken as the median of good quality data spanning the first 2-6 minutes of recording.

Haematocrit and access blood saturations were measured continuously in all patients using the Crit-Line monitor (Fresenius). RBV was pre-processed by application of a median filter, and removal of values above +5% (which were artifactual due to fluid boluses, drugs or wash back at the end of dialysis). Access

blood saturations underwent minimal processing, beyond removal of values correlating with RBV above 5%.

The 37 unstable patients also underwent monitoring with the Visi Black Shadow (Stowood Scientific Instruments), which was used to gather continuous three lead ECG, finger PPG, pulse oximetry and respiratory rate (using an individually fitted inductance belt). The belt data and PPG data were pre-processed and subject to SQIs as described in the methods. Peripheral saturations from good quality PPG windows were selected, and extreme outliers were removed. Saturation variability was calculated as the standard deviation over the mean for each 60 second window, in accordance with previous literature [72].

For PPG-derived measures, the amplitude of each beat was taken as the difference between the PPG peak and the preceding trough, i.e. the PPG pulse pressure. PPG PPV was calculated for every 15 second window, using the variation in amplitude over 12 successive beats (estimated to cover one or two respiratory cycles, as we are looking for variation with respiration). The average difference between the two largest and two smallest peaks was found, and expressed as a percentage of the median pulse pressure in this window. For comparison, an identical process was performed on good quality segments of the Finometer arterial waveform, to give a second measure of PPV. In addition, PPG amplitude was considered as a continuous variable. As the units are arbitrary, PPG amplitude was expressed relative to baseline, defined as the median value of the data before bleed out (excluding the first 60 seconds after probe application, whilst calibration was occurring).

ECG heart rate was calculated using a peak detector based on a modification of the Hamilton-Tomkins algorithm [114], with application of an SQI as described in the Methods chapter. Once outliers had been removed, instantaneous heart rate was calculated based on each R wave to R wave interval (RR interval). For spectral analysis, each 120 second window of RR time series was first detrended (linear) and resampled at 2 Hz using spline interpolation. The window size of 120 seconds was chosen as this is the shortest time that allows the LF component to be assessed, and longer times are more likely to result in violation of stationarity [182]. A Hamming window function was applied to reduce spectral "leakage" and fast Fourier transforms were computed using the next power of 2 as the number of points. LF power was defined as the area under the curve for the spectrum between frequencies of 0.04 Hz to 0.15 Hz,

and HF power as the area between frequencies of 0.15Hz and 0.41Hz. LF normalised units (LFnu) were defined as the proportion of power in the range 0.04-0.41 Hz falling in the LF band, and HF normalised units the proportion falling in the HF band (together LFnu and HFnu add up to 1, or 100%, depending on how they are expressed). LF and HF power absolute measurements were log transformed in order to achieve a normal distribution of values for analysis.

After pre-processing and application of SQIs as described above, all data streams were resampled to a frequency of 1 Hz (i.e. one data point every second). Whenever a value was assigned to a window, the timestamp was taken as the centre of that window.

9.2.2 Determination of distance between normal and abnormal sessions

Sessions were divided into normal and abnormal groups based on the following events: KDOQI-defined event, i.e. 10mmHg drop in MAP with symptoms and nursing intervention (both within -10 to +20 minutes of the blood pressure threshold being attained); cerebral ischaemia, defined as an rSO2 drop of 15% or more of baseline value, sustained for at least 5 minutes; drop of MAP below 60mmHg, sustained for at least 5 minutes. Data after the first event in a session was discarded. As "normal" physiology is likely to depend on the stage of HD, data was sorted according to time point of treatment: pre-bleedout data was grouped together regardless of length; data between bleedout and hour 4 was divided into 30 minute segments; post-hour 4 data was grouped together regardless of length.

Visualisation

Each physiological variable was considered in turn, i.e. univariate analysis. The distribution of each variable was assessed visually and with a probability-probability plot. Data was transformed as required to achieve a normal distribution, and then the mean and standard deviation of the pooled "normal session" data, and the pooled "abnormal session" data, was found for each 30 minute segment. After back transformation, the trajectory of the mean and 95% limits of the abnormal sessions was then plotted against that of the normal sessions. As sessions were censored after an event, the abnormal data diminished with increased time on dialysis: once there were less than 6 abnormal sessions, data was discarded.

Statistical analysis

Each physiological variable was considered in turn, i.e. univariate analysis. There are a number of challenges in comparing data at the population level, including the wide range of normal (and abnormal) values, and clustering of data according to patient. As a preliminary investigation, the Wilcoxon rank sum (or two sample t test where appropriate) was used to compare the pooled data from normal and abnormal sessions for each hour of dialysis. One way analysis of variance was used to assess patient clustering to estimate the validity of results, as the rank sum and t tests do not take into account repeated measures.

Rather than the difference between pooled data, it is of more relevance whether individual data segments can be classified as belonging to normal or abnormal sessions. The two-sample Kolmogarov-Smirnov (KS) test is a non-parametric test which assesses the likelihood that two sets of data come from the same continuous probability distribution. Data was broken down into 5 minute windows, which were grouped according to hour of dialysis and whether they were from an abnormal or normal session. As normal data segments were hugely variable across the population, the traditional KS test cutoff returned the answer that essentially all normal segments were significantly different, making comparison of normal and abnormal segments meaningless. Therefore we aimed to define a customised KS test value for significant differences between normal and abnormal data segments, which took into account the large differences between normal segments. For a given hour, two randomly selected 5 minute segments from the normal sessions were compared using the using the KS test; this was repeated 10,000 times, and the distribution for test values was constructed (control distribution). This allowed an estimation of the typical "distance" between normal segments for a given variable. The process was then repeated for 10,000 pairs of 5 minute windows from normal and abnormal sessions. The distribution of resulting test values (test distribution) was compared to the control distribution. We identified the 95th percentile of the control distribution, and use this as the customised KS test value to distinguish significantly different data segments. The chi square test was used to compare the proportion of test values from the test distribution passing this point. As an alternative, the Wilcoxon rank sum test was used to look for a shift in the median KS test value.

9.3 Results

There was physiological data on 635 dialysis sessions in 58 patients. Two patients were found to have such severe vascular disease that the Finometer could not detect a finger pulse, and only NIBP measurements were available. Two other patients declined cerebral NIRS. In total, 576 sessions had Finometer monitoring, 583 NIRS monitoring and 521 had both. There was ECG, PPG and respiratory rate data on 388 dialysis sessions in 37 patients. Demographics are summarised in the methods chapter.

There was a substantial number of abnormal sessions as defined by the three different event types. There were 42 sessions in 22 patients with KDOQI-defined IDH: the median drop in MAP at the time of intervention was 25mmHg from baseline. There were 120 sessions in 23 patients with a sustained drop in MAP below 60mmHg. There were 119 sessions in 39 patients with a sustained drop in rSO2 of 15% of baseline: the median MAP at onset of ischaemia was 78mmHg.

9.3.1 Visual comparison of univariate physiological variables

Figures 9.1 to 9.15 show the trajectory of individual physiological variables over dialysis, according to whether the sessions were normal or affected by an event. The mean and 95% limits of the data for each group of sessions are displayed against each other. It should be noted that estimates for abnormal data become less robust as time of dialysis progresses, because sessions were censored at the time of the event. This is particularly evident for the KDOQI events, which were relatively few in number to begin with.

9.3.2 Haemodynamic variables

The trajectory of absolute MAP over normal and abnormal sessions, according to the three different definitions of events given above, is shown in figure 9.1. As expected, there is clear separation using the event definition of MAP <60mmHg, and this difference is apparent at baseline: patients who start at a lower MAP are more likely to drop below this absolute threshold. However, there is also a steeper gradient in the abnormal sessions. For other event types, there appears to be no substantial separation in MAP between normal and abnormal sessions. For comparison, the change in MAP from baseline is shown in figure 9.2. Again, as expected, the separation is greatest for sessions with and without MAP <60mmHg.

Heart rate, at the population level, appears similar in sessions with and without cerebral ischaemia or severe symptoms (figure 9.3). Heart rate is clearly lower throughout sessions affected by drop in MAP below 60mmHg. This was not found to represent clustering of patients on beta blockers. However, change in heart rate appears to be more informative (figure 9.4). The heart rate increases in sessions which go on to develop severe hypotension or symptoms, possibly representing an appropriate sympathetic response. Sessions with cerebral ischaemia are unique in that the heart rate overall appears to remain the same, or if anything decrease, over the HD session. In keeping with this, sessions with cerebral ischaemia appeared to have substantially less LF power, a marker of sympathetic tone, throughout dialysis, whereas sessions with severe symptoms were characterised by an increase in LF power (figure 9.5). Change in cardiac output as measured by the Finometer, and change in PPG amplitude (essentially a surrogate for cardiac output), did not distinguish eventful sessions (figures 9.6 and 9.7).

It is apparent that for several physiological variables, there is a pronounced change between pre-bleedout and immediate post-bleedout values, e.g. LF power, cardiac output. This may be artifactual, due to the decision to pool together all pre-bleedout data regardless of length, whereas all post-bleedout data was separated into 5 minute segments. However, it is physiologically plausible that the process of losing 150 mls of blood into the dialysis circuit over a minute could be associated with detectable autonomic and haemodynamic cardiac output, the nature of which would depend on intravascular status and position on the Starling curve. Venesecting as little as 250 mls can bring dramatic symptomatic relief to a patient in pulmonary oedema: it is possible that more subtle, subclinical changes could follow the sudden loss of 150 mls [183].

9.3.3 Indicators of volume status

On the population level, RBV or ultrafiltration volume, which are commonly used in clinical practice, did not appear to be useful predictors of events (figure 9.8, UF volume not shown). Another measure of intravascular depletion is PPV: perhaps as this showed less inter-individual variation in the threshold for events, this proved to be one of the most promising variables for predicting all types of events (figure 9). Pulse pressure variability as measured by the Finometer proved to be more useful overall than that derived from the PPG, perhaps due to differences in signal quality, or because the Finometer was measuring changes in arterial diameter rather than capillary diameter. On the population level, the range of values for PPG PPV was huge for both normal and abnormal sessions, making comparisons more difficult (not

shown).

9.3.4 Respiratory and oxygenation variables

Respiratory rate did not distinguish abnormal from normal sessions, regardless of event definition (figure 9.10). Peripheral saturations and AVF saturations were not substantially different between normal and abnormal sessions, with the exception that fistula saturations appeared higher throughout HD (figures 9.11 and 9.12). Central venous saturations applied only to a small proportion of the overall dataset , i.e. those with Tesio lines (16 patients). Central venous saturations were lower in abnormal sessions from baseline, regardless of event definition (figure 13). This was explained by clustering of events in one or two patients who had a lower baseline value, illustrating the problem with population modelling. In this case, the lower central venous saturations are just identifying the patients who have more comorbidities. In contrast, peripheral saturation variability emerged as a potentially useful predictor, particularly for cerebral ischaemia, as shown in figure 9.14. Change in cerebral oxygenation, as expected, was significantly greater in sessions which featured cerebral ischaemia, but also in sessions marked by KDOQI events and MAP <60mmHg, suggesting an overlap between the different definitions (figure 9.15).

Figure 9.1: Absolute MAP in normal and abnormal sessions

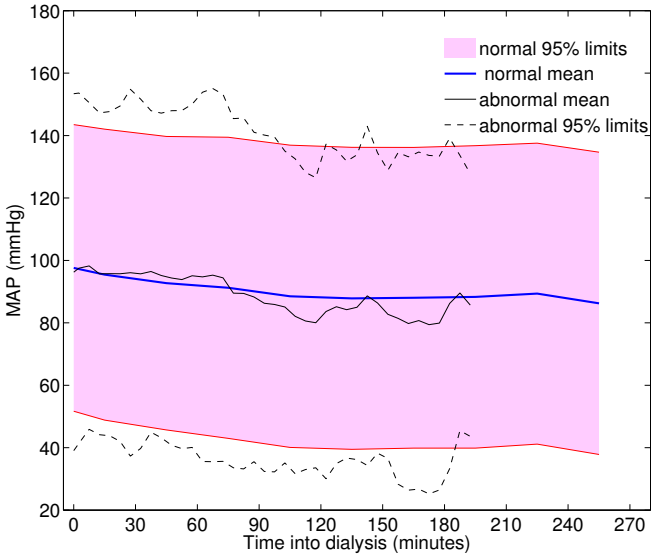

(a) KDOQI-defined IDH

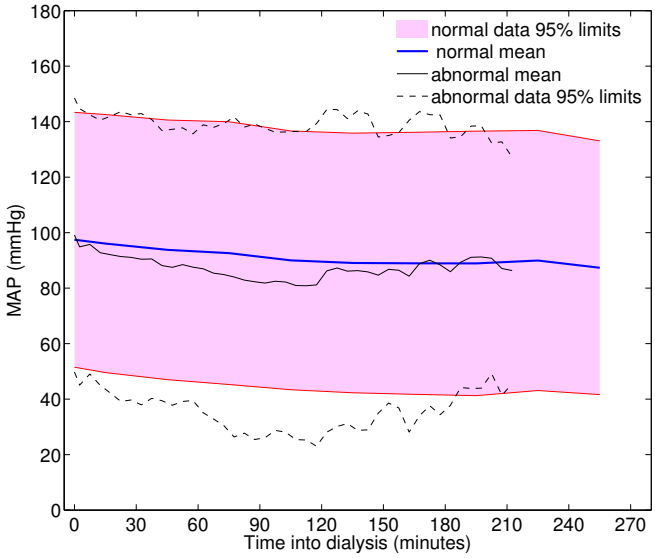

(b) Cerebral ischaemia (15% drop)

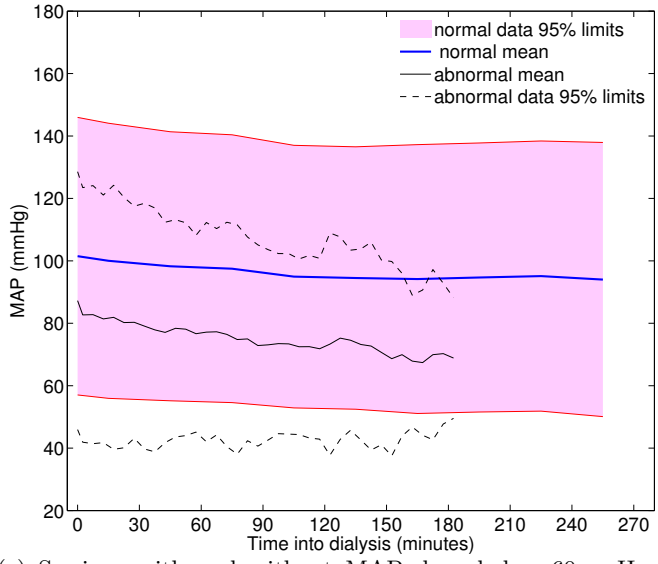

(c) Sessions with and without MAP drop below 60mmHg, population level

Figure 9.2: Relative MAP in normal and abnormal sessions

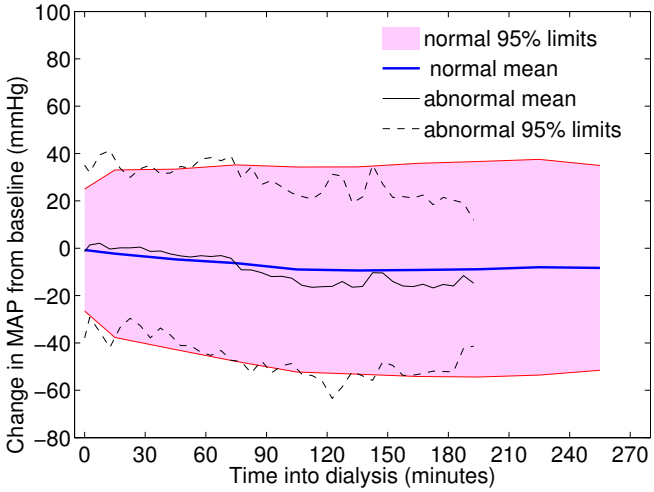

(a) KDOQI-defined IDH

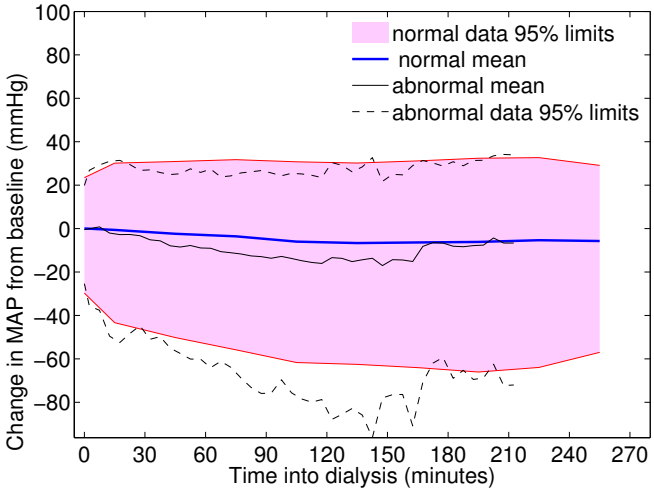

(b) Cerebral ischaemia (15% drop)

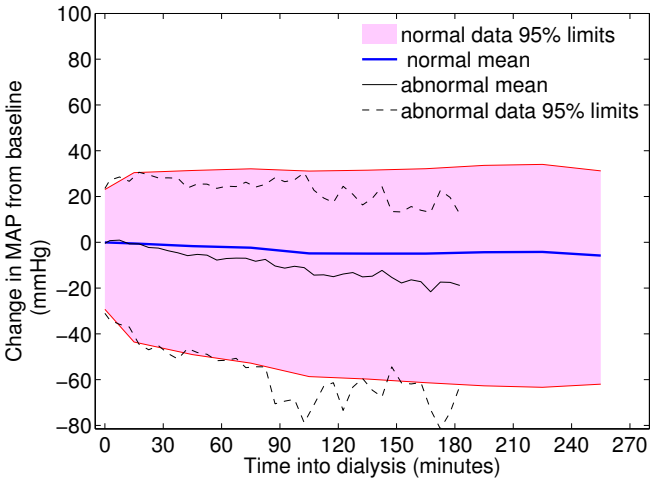

(c) MAP drop below 60mmHg

Figure 9.3: Heart rate in normal and abnormal sessions

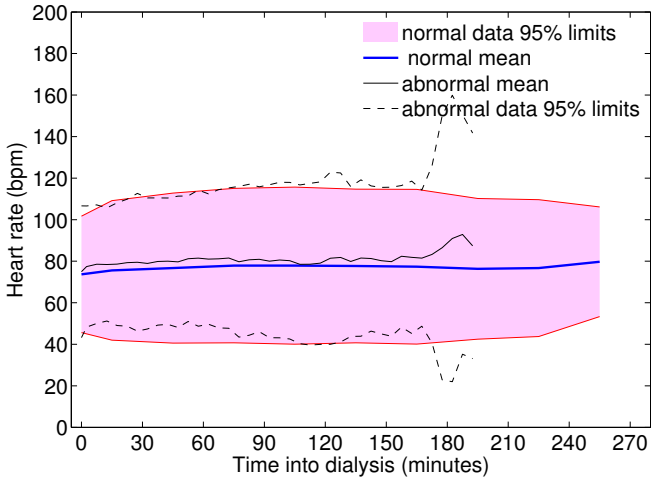

(a) KDOQI-defined IDH

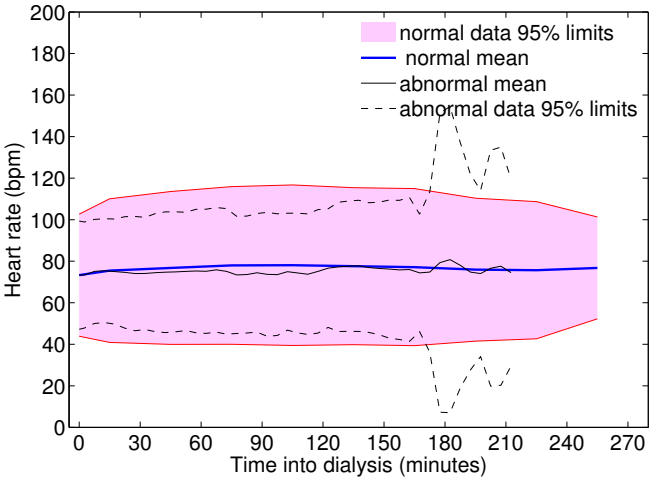

(b) Cerebral ischaemia (15% drop)

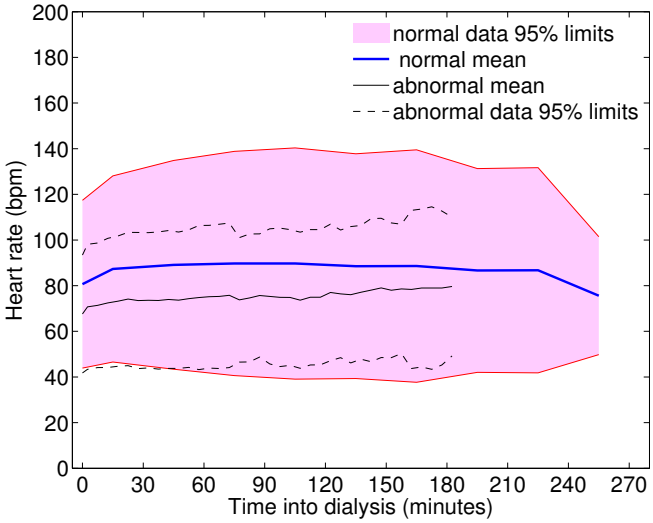

(c) MAP drop below 60mmHg

Figure 9.4: Change in heart rate in normal and abnormal sessions

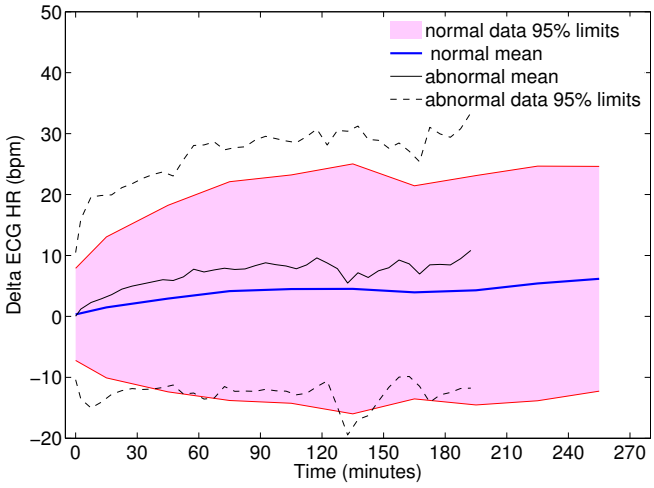

(a) KDOQI-defined IDH

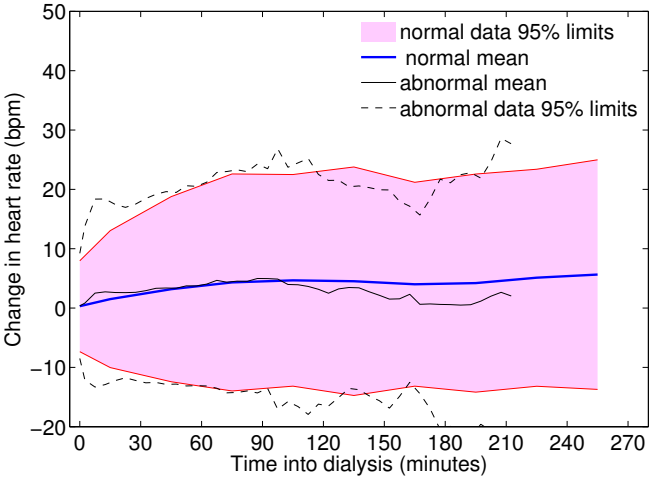

(b) Cerebral ischaemia (15% drop)

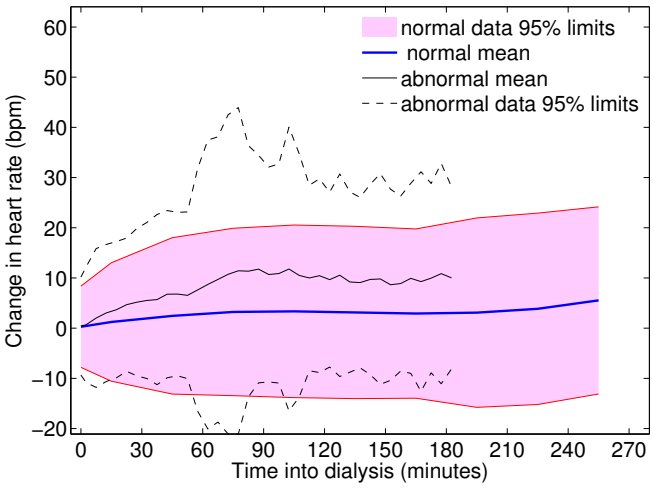

(c) MAP drop below 60mmHg

Figure 9.5: Normalised low frequency power in normal and abnormal sessions

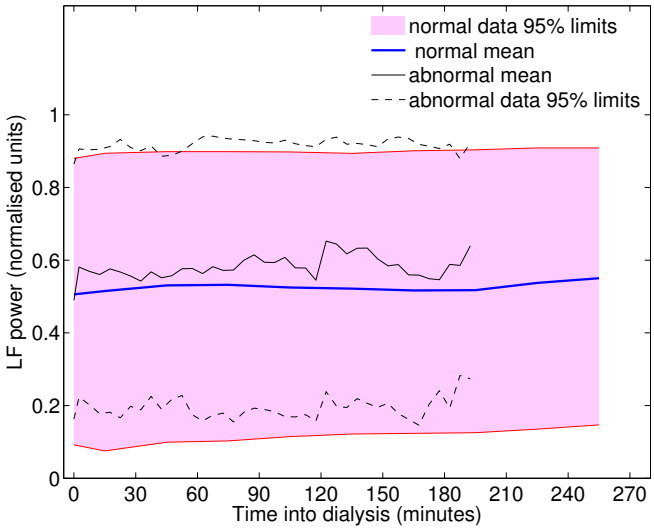

(a) KDOQI-defined IDH

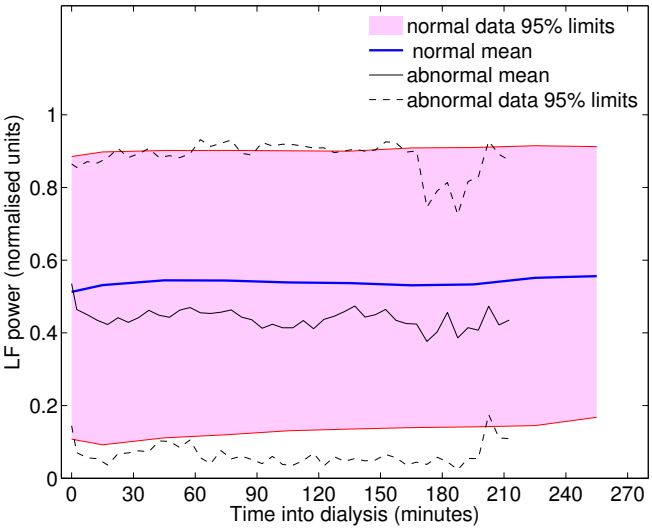

(b) Cerebral ischaemia (15% drop)

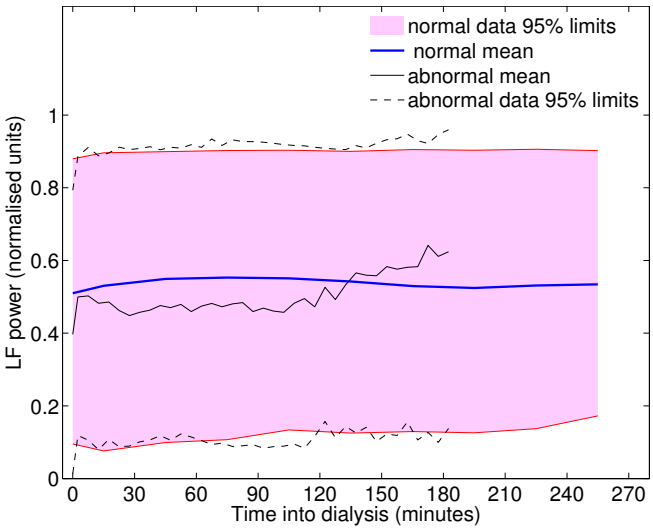

(c) MAP drop below 60mmHg

Figure 9.6: Cardiac output in normal and abnormal sessions

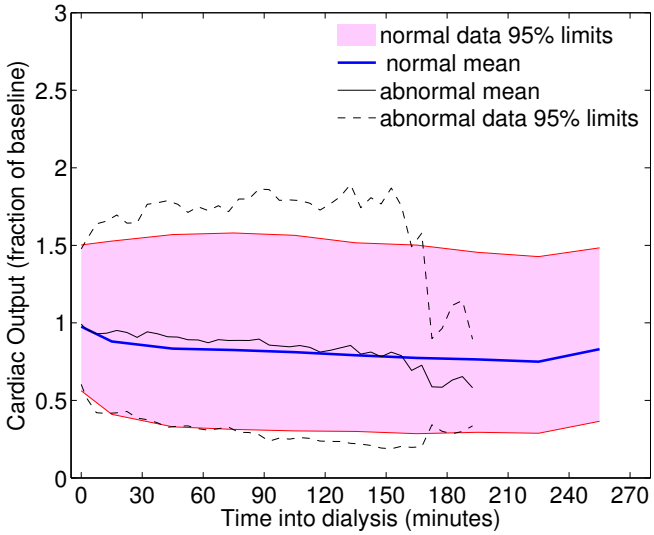

(a) KDOQI-defined IDH

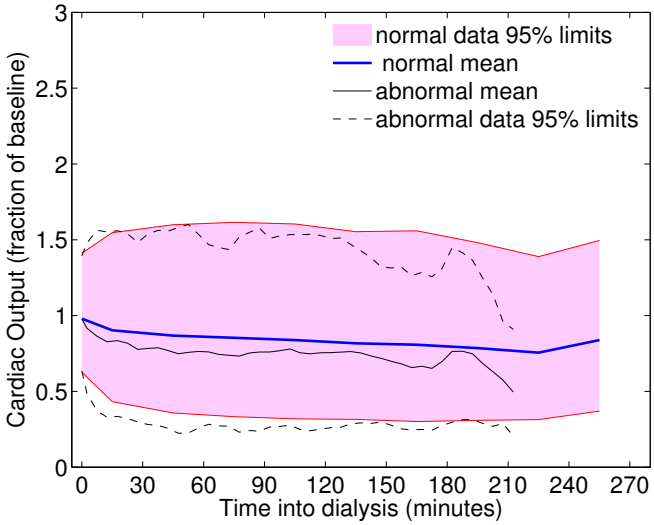

(b) Cerebral ischaemia (15% drop)

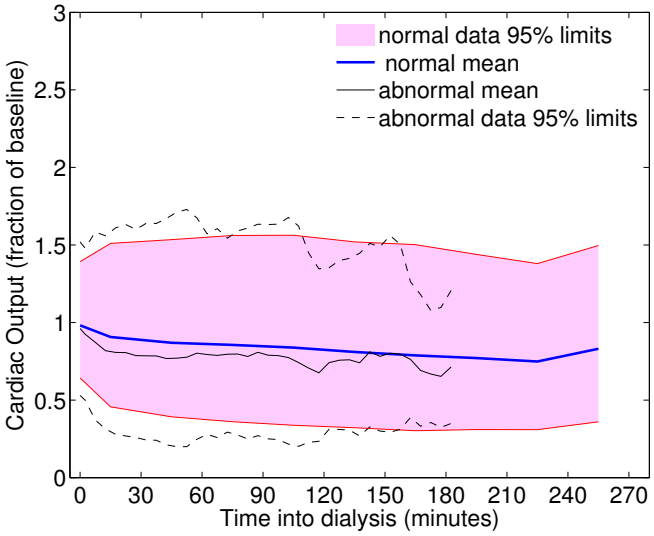

(c) MAP drop below 60mmHg

Figure 9.7: Change in PPG amplitude in normal and abnormal sessions

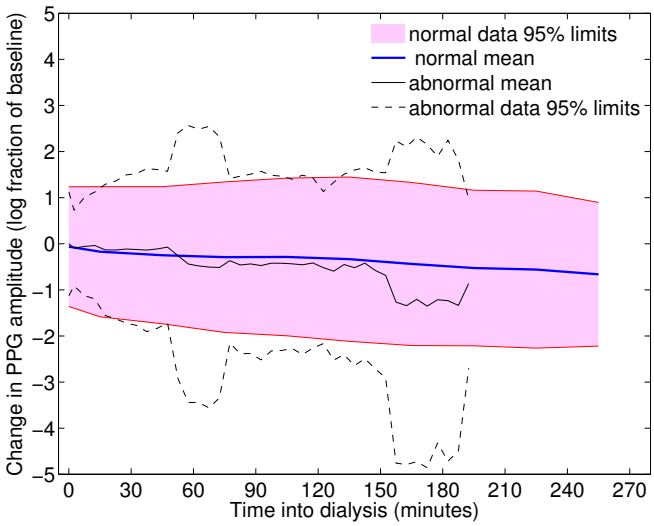

(a) KDOQI-defined IDH

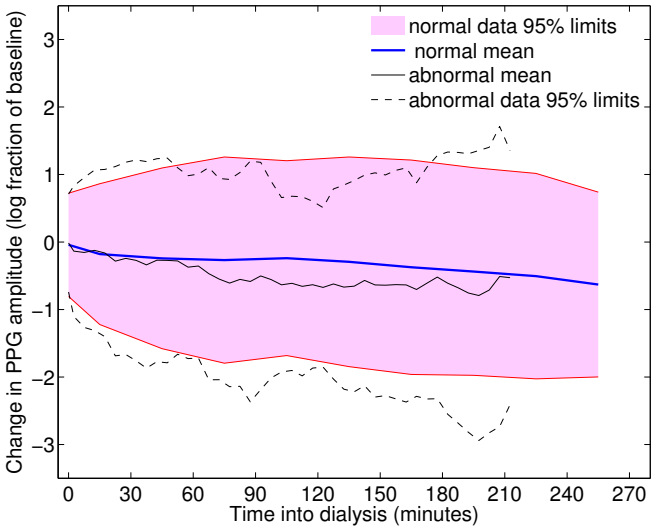

(b) Cerebral ischaemia (15% drop)

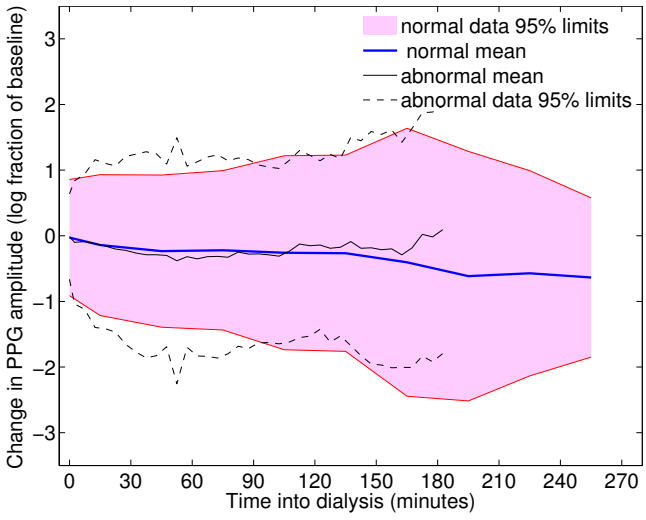

(c) MAP drop below 60mmHg

Figure 9.8: Relative blood volume in normal and abnormal sessions

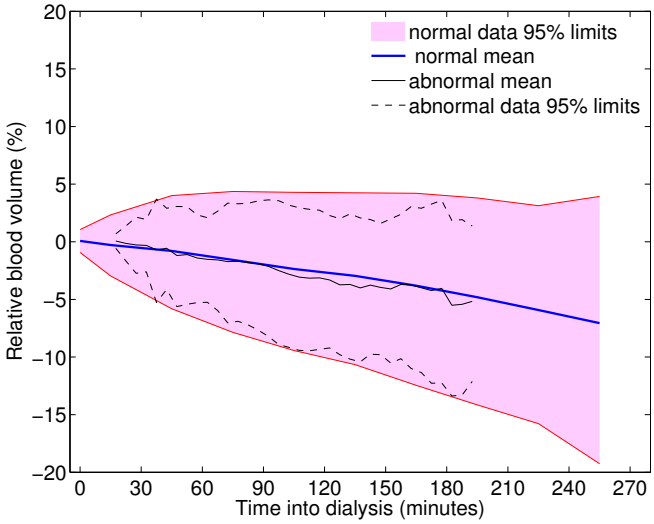

(a) KDOQI-defined IDH

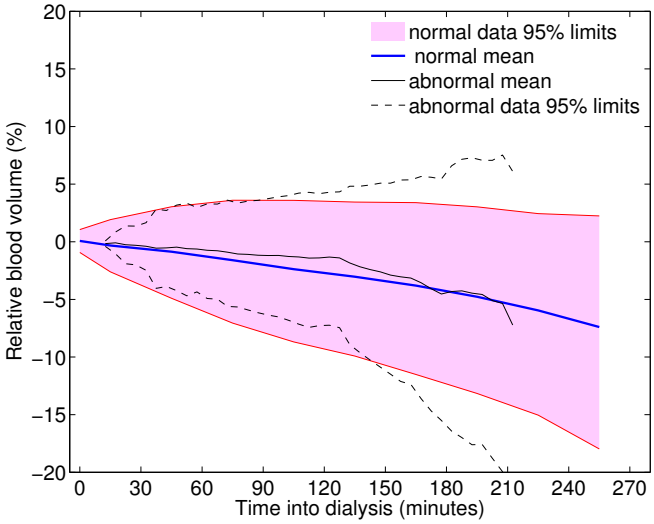

(b) Cerebral ischaemia (15% drop)

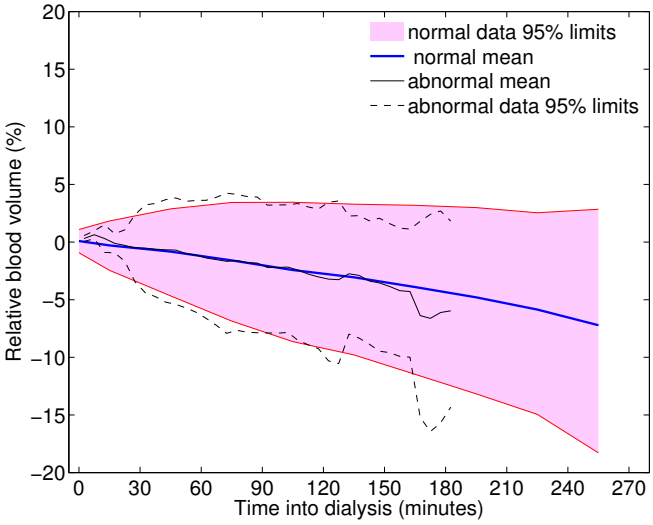

(c) MAP drop below 60mmHg

Figure 9.9: Finometer pulse pressure variation in normal and abnormal sessions

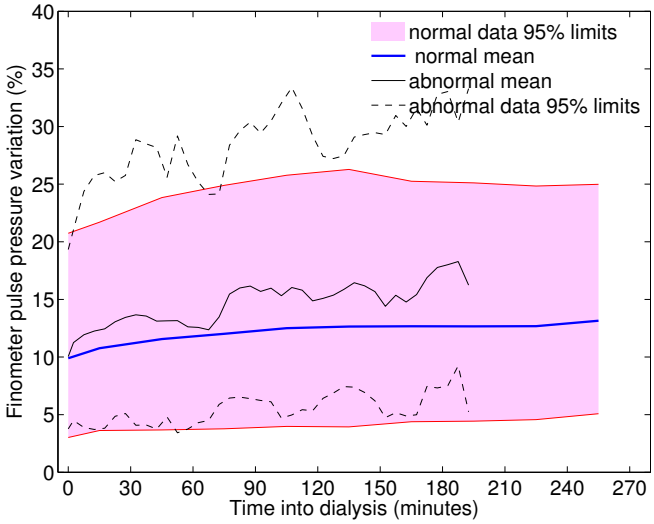

(a) KDOQI-defined IDH

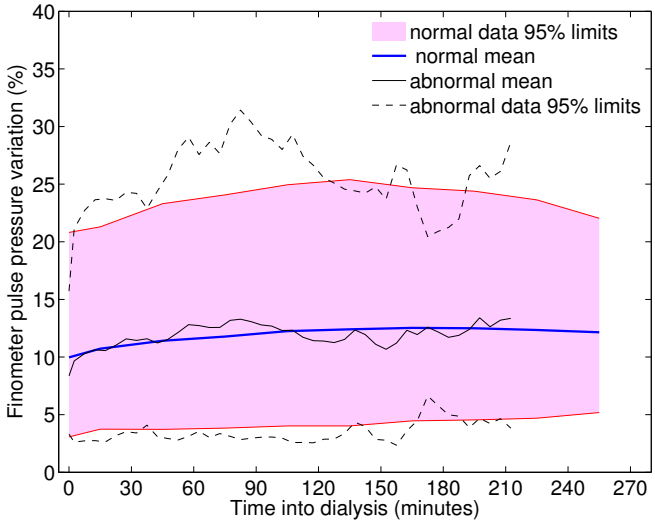

(b) Cerebral ischaemia (15% drop)

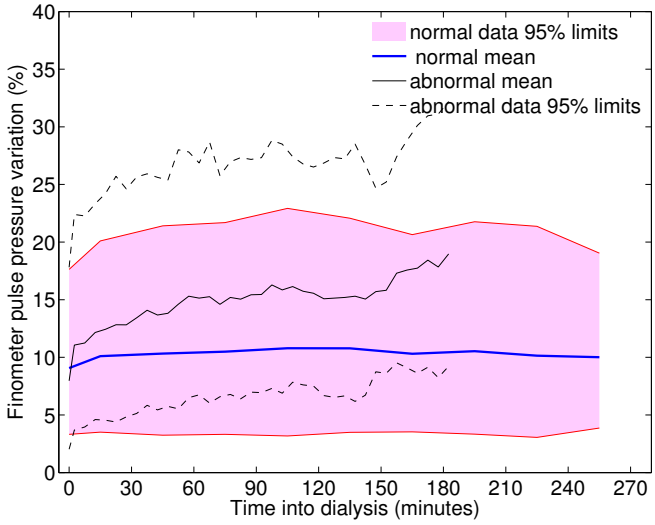

(c) MAP drop below 60mmHg

Figure 9.10: Respiratory rate in normal and abnormal sessions

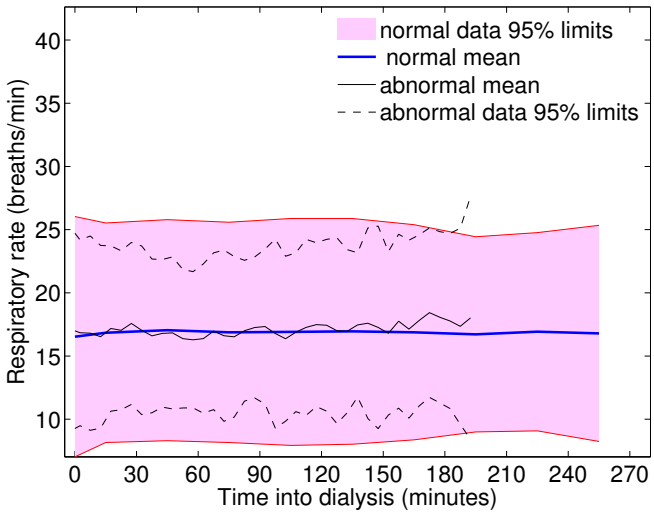

(a) KDOQI-defined IDH

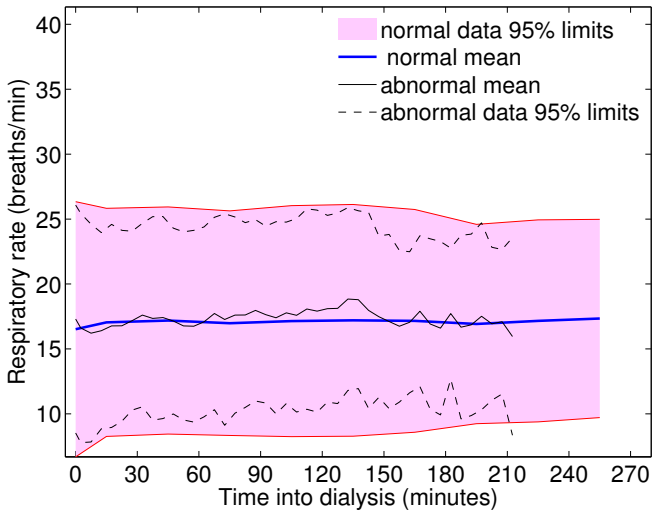

(b) Cerebral ischaemia (15% drop)

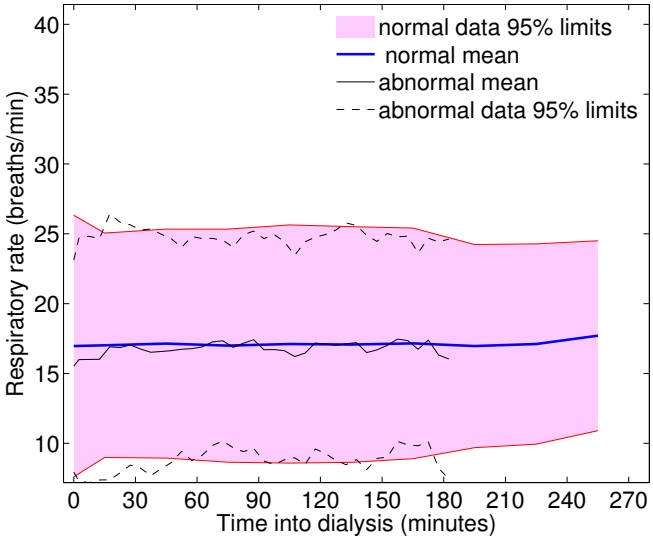

(c) MAP drop below 60mmHg

Figure 9.11: Peripheral saturations in normal and abnormal sessions

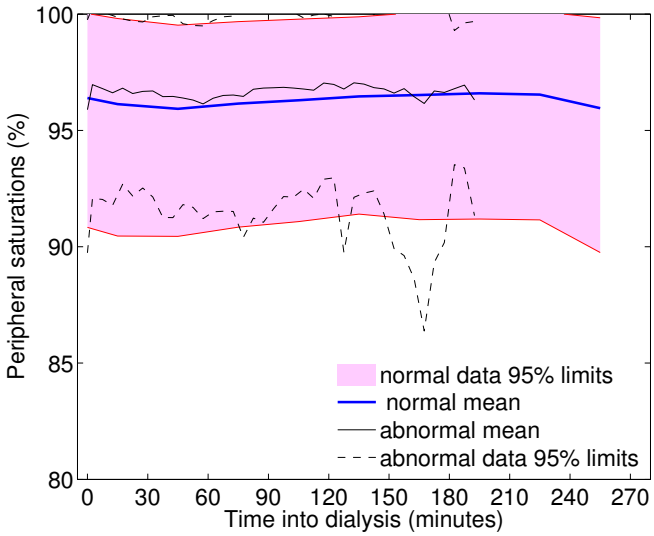

(a) KDOQI-defined IDH

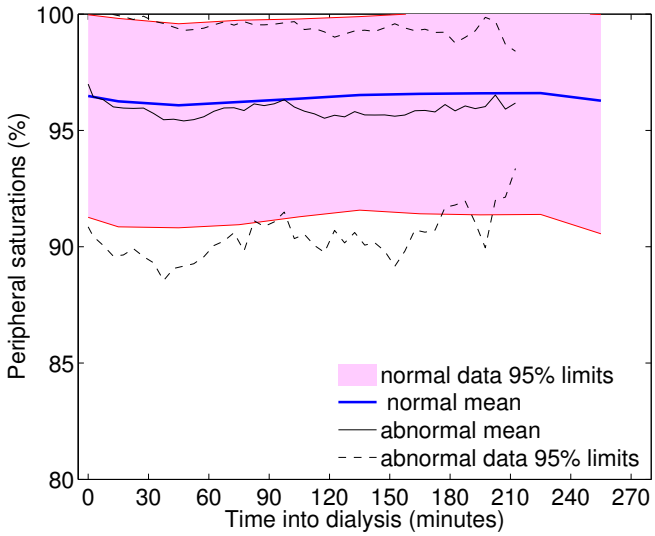

(b) Cerebral ischaemia (15% drop)

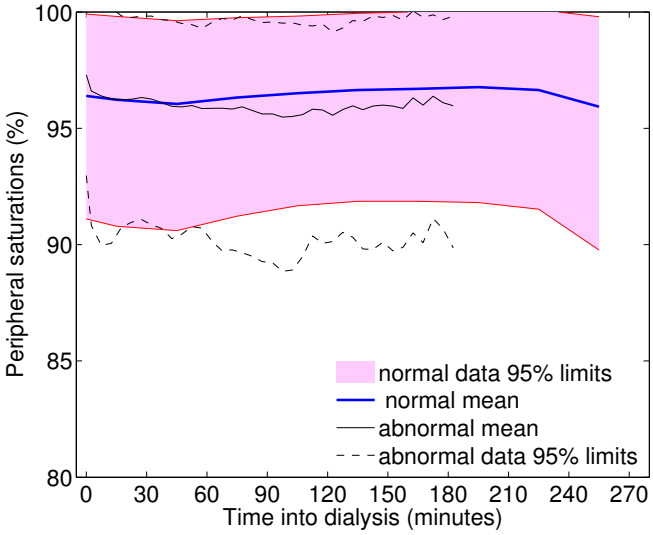

(c) MAP drop below 60mmHg

Figure 9.12: Fistula (arterialised) saturations in normal and abnormal sessions

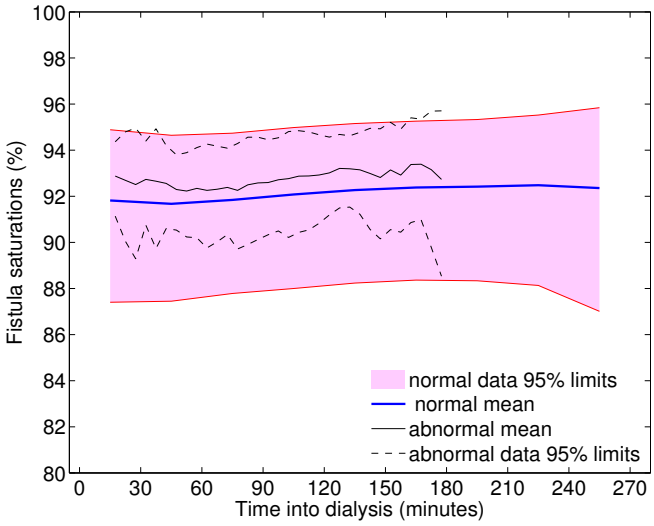

(a) KDOQI-defined IDH

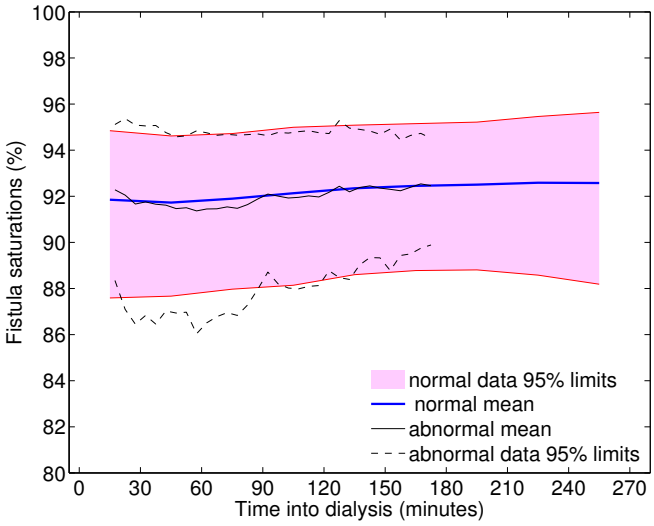

(b) Cerebral ischaemia (15% drop)

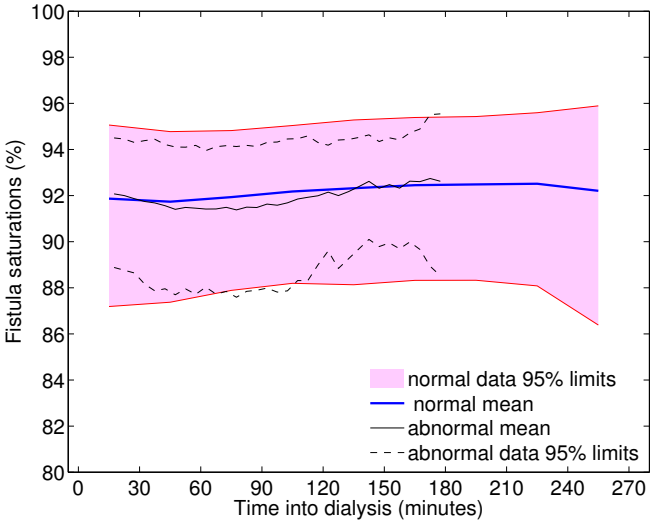

(c) MAP drop below 60mmHg

Figure 9.13: Central venous saturations in normal and abnormal sessions - patients with Tesio only

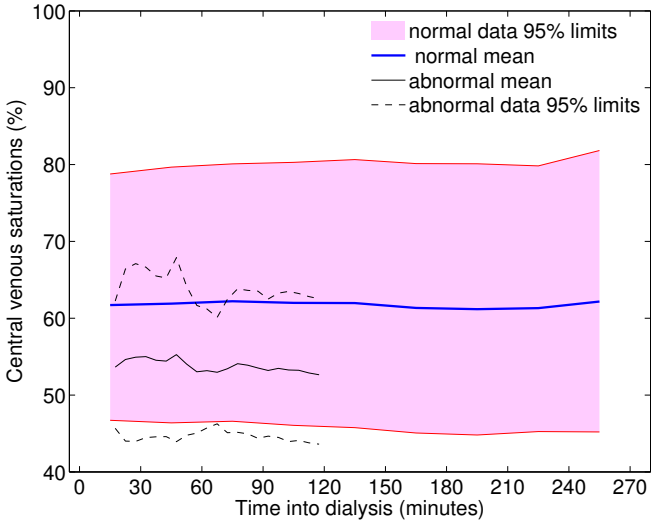

(a) KDOQI-defined IDH

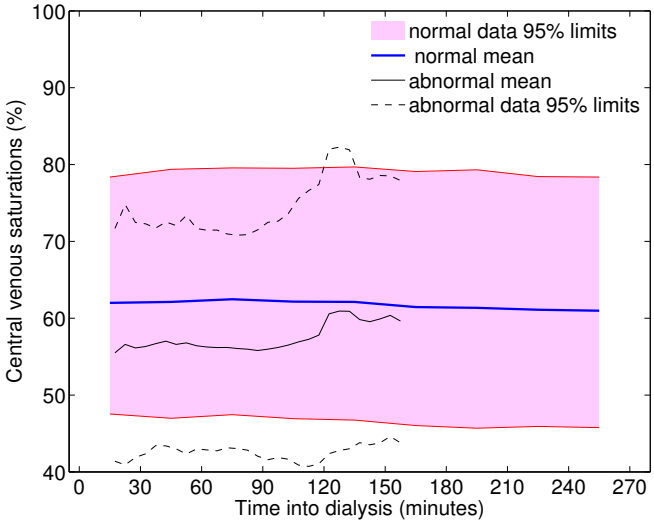

(b) Cerebral ischaemia (15% drop)

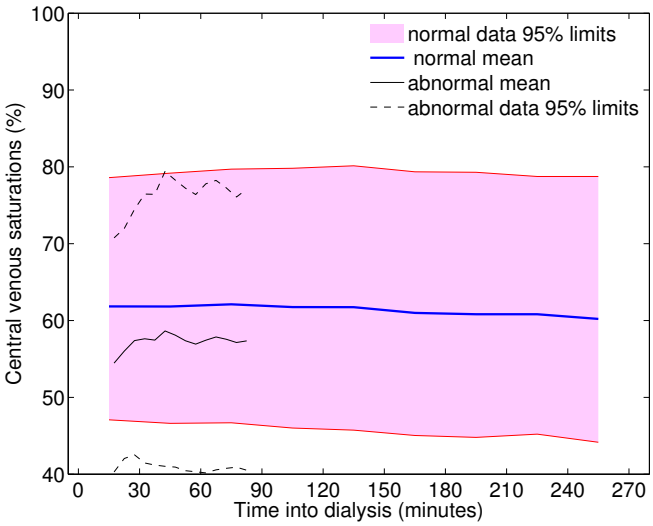

(c) MAP drop below 60mmHg

Figure 9.14: Peripheral saturation variability in normal and abnormal sessions

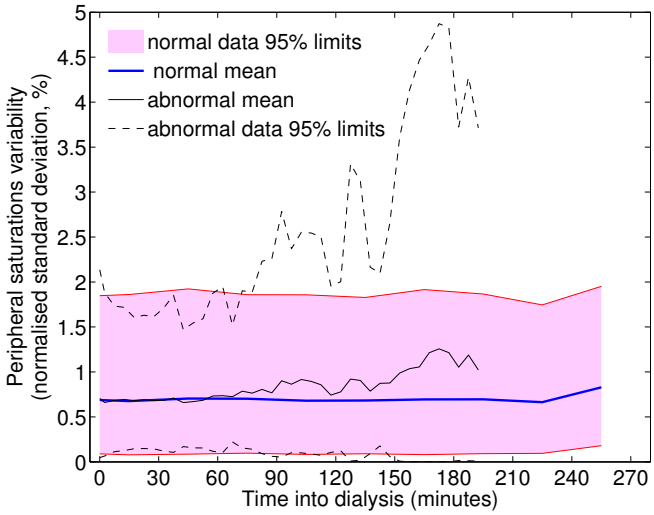

(a) KDOQI-defined IDH

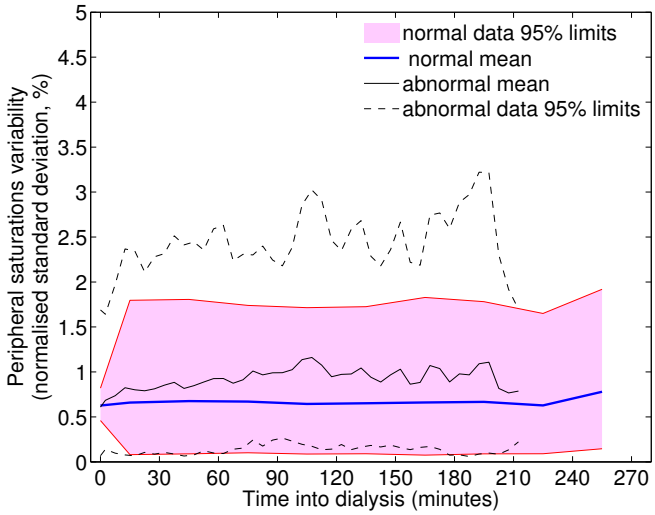

(b) Cerebral ischaemia (15% drop)

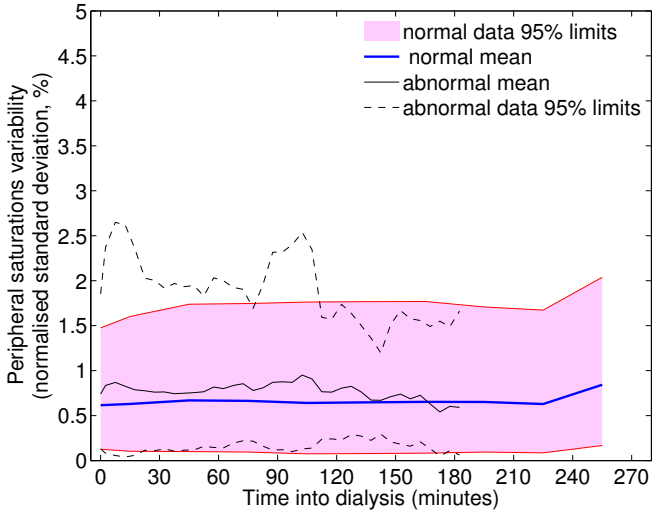

(c) MAP drop below 60mmHg

Figure 9.15: Change in cerebral oxygenation in normal and abnormal sessions

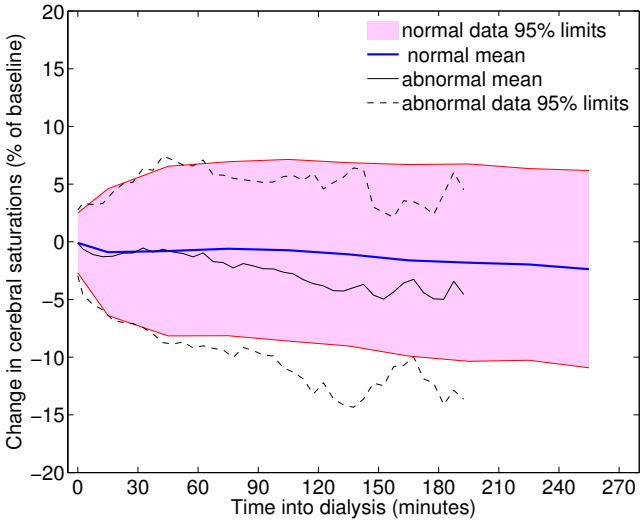

(a) KDOQI-defined IDH

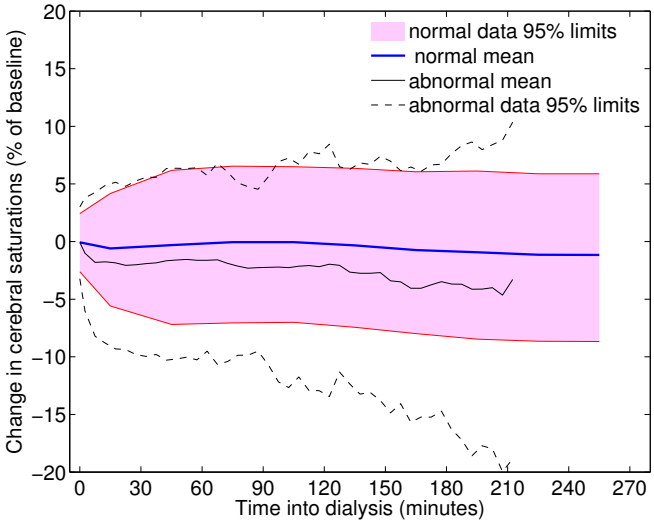

(b) Cerebral ischaemia (15% drop)

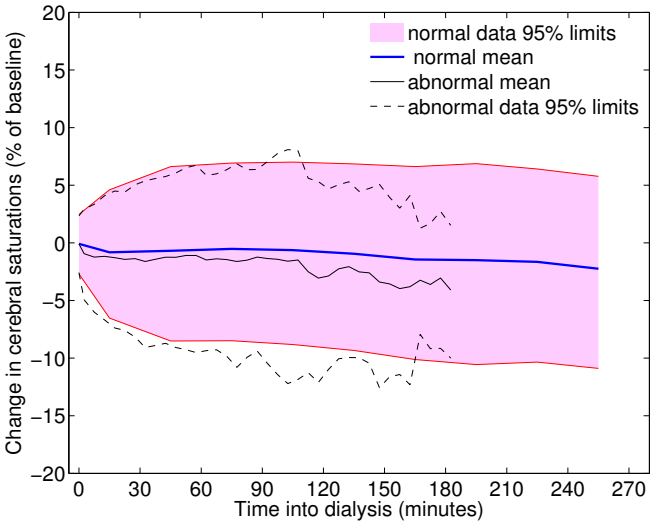

(c) MAP drop below 60mmHg

9.3.5 Statistical analysis

Comparing pooled normal and abnormal data for each hour using the Wilcoxon rank sum test (or two sample t test for normally distributed data) proved to be oversensitive, returning the result that every variable differed significantly at every hour between normal and abnormal sessions, however defined. This was partly because the rank sum test does not take into account patient clustering. One way analysis of variance was used to assess patient clustering, and confirmed strong evidence of substantial patient-level differences for every single variable. In addition, because of the large number of data points (1800 per 30 minute segment of dialysis session, with a total of 635 dialysis sessions, i.e potentially over a million data points for each segment), the rank sum test was powered to detect very small, clinically insignificant differences between normal and abnormal sessions.

As an example, the pooled data for RBV during the first hour of dialysis is shown in figure 9.16, with normal values (sessions without cerebral ischaemia) in blue, and superimposed abnormal values (sessions which later developed cerebral ischaemia) in red. This confirms the visual inspection in figure 8, that overall there is very little difference in the distribution of RBV values between sessions with and without ischaemic episodes. The median is -0.37% for normal sessions and -0.43% for abnormal sessions, a difference which would not be considered clinically significant, but which reached statistical significance due to the large number of data points. However the second part of the analysis, construction of control and test distributions of KS test values, confirmed that the abnormal segments did not differ from the normal segments more than the normal segments differed from each other, as shown in figure 9.17 (in fact there is more distance between the normal segments). The rank sum test also confirmed that there was no significant difference in the distribution of test scores.

For each physiological variable, test and control distributions of KS test scores were compared using 1) the Wilcoxon rank sum test on raw scores and 2) the chi square test on the proportion of scores passing the 95th percentile of the test distribution. For distinguishing sessions which did and did not go on to develop severe hypotension (MAP <60mmHg), absolute MAP and Finometer PPV were significant for at least two hours of dialysis on both tests. Absolute MAP and Finometer PPV values from sessions which did and did not go on to feature severe hypotension are compared in figures 9.18 to 9.21. For distinguishing sessions which did and did not go on to develop cerebral ischaemia, only PPG PPV was significant for at least two hours of dialysis (figures 9.22 and 9.23). No physiological variables could

distinguish sessions with and without KDOQI events.

These findings must be interpreted cautiously as the identification of a customised KS test value to separate normal and abnormal segments proved problematic. The KS test score caps at a value of 1, and for most variables even the normal segments were so dissimilar that the majority of comparisons resulted in the maximum test value, as shown in figure 9.17, 9.19 and 9.21 . Indeed, for the majority of variables, the 95th percentile of the control test score distribution was 1. This meant that the method was not very sensitive for differences, and may explain why some variables which appeared very promising on visual inspection, e.g. saturation variability and change in heart rate, did not reach significance. Another explanation is that differences in visual inspection of pooled data may be driven by a few patients, the impact of which is minimised by the repeated KS test methodology, i.e. these variables may be more useful on the patient level. The KS test was substituted by the Kullback-Leibler divergence test, another test for distance between data, with similar results (not shown).

Figure 9.16: RBV during hour 1 in sessions with and without later development of cerebral ischaemia

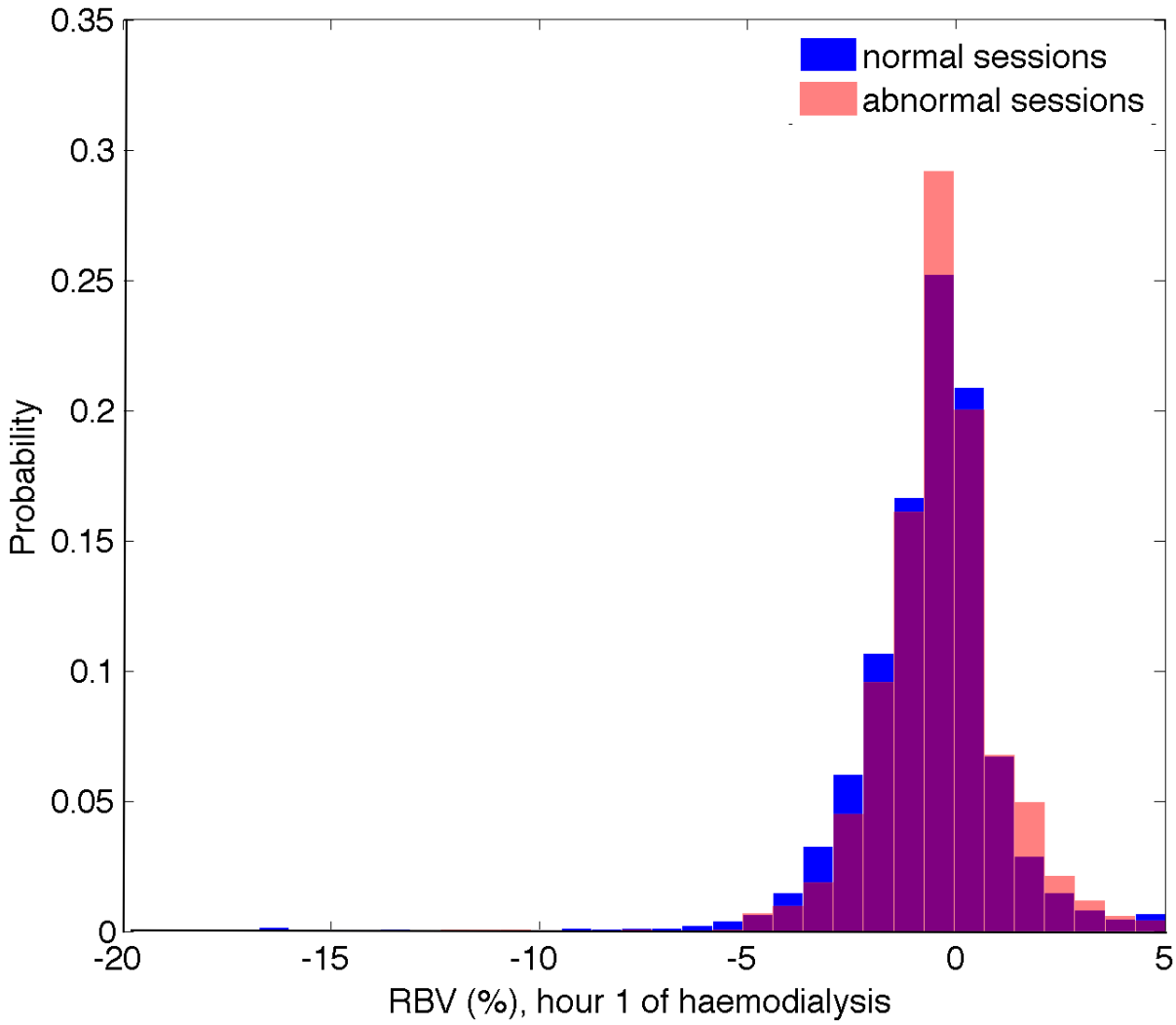

Figure 9.17: Comparison of RBV data from sessions with and without later development of cerebral ischaemia

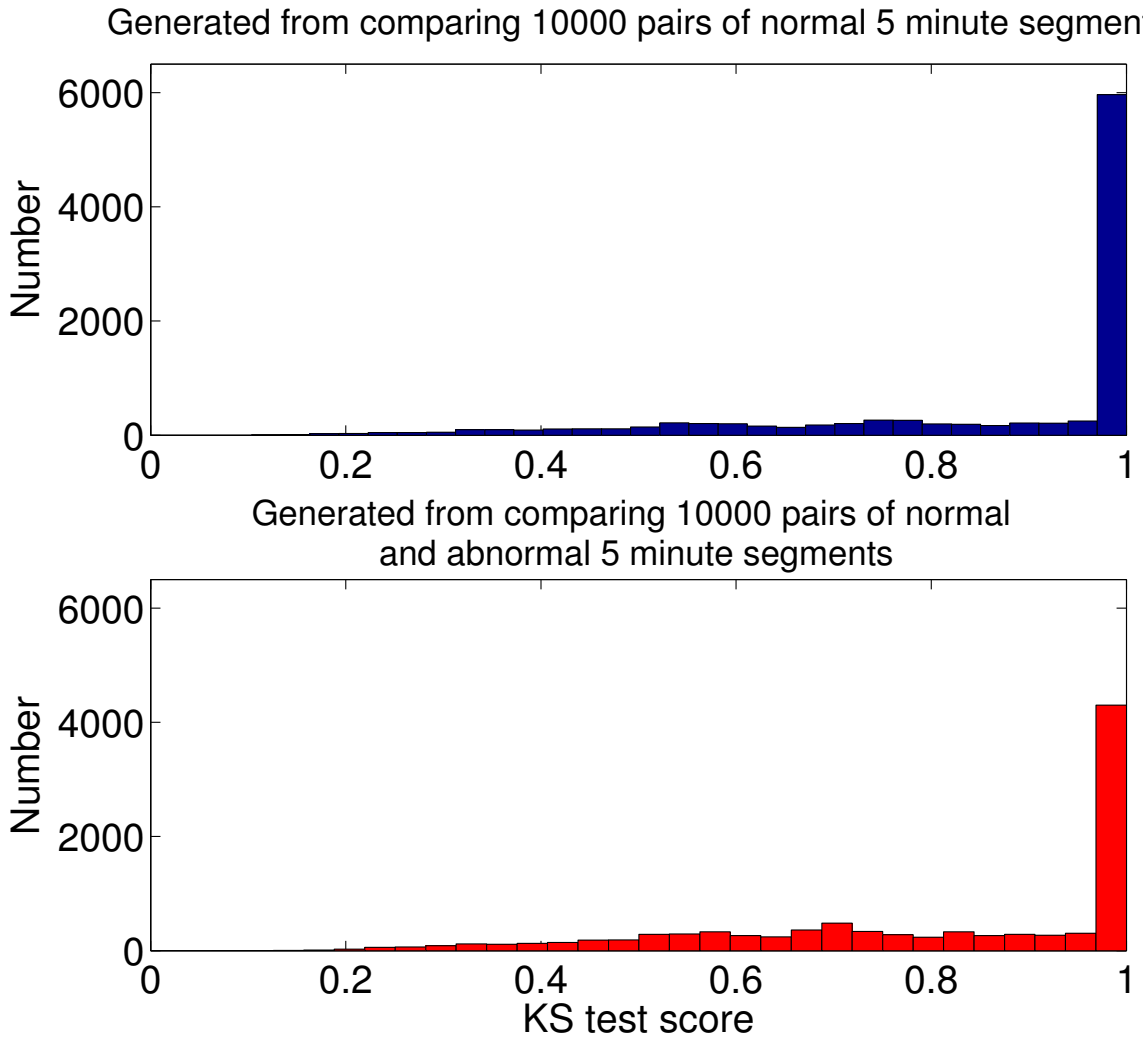

Figure 9.18: MAP during hour 3 in sessions with and without later development of severe hypotension

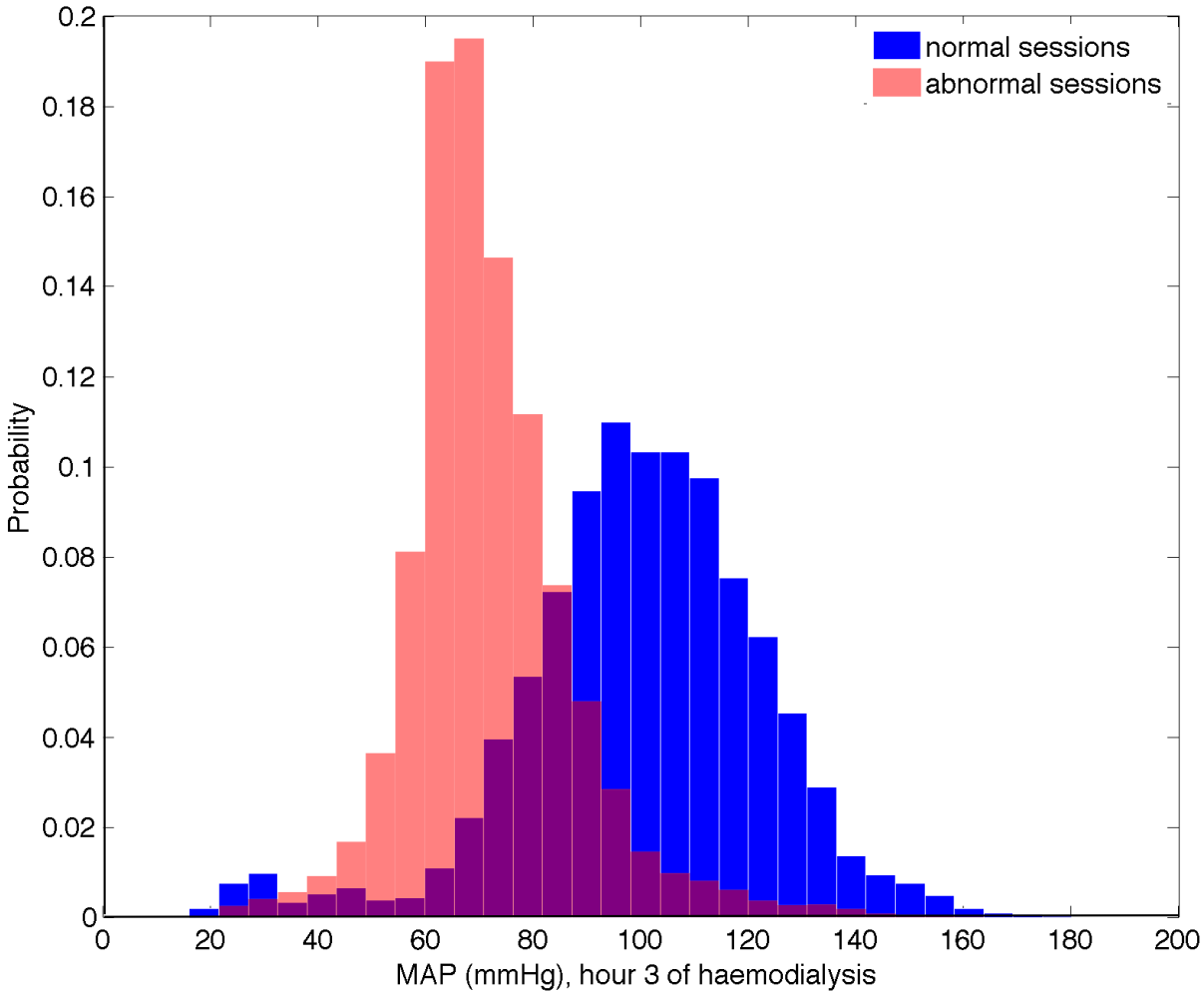

Figure 9.19: Comparison of MAP data from sessions with and without later development of severe hypotension

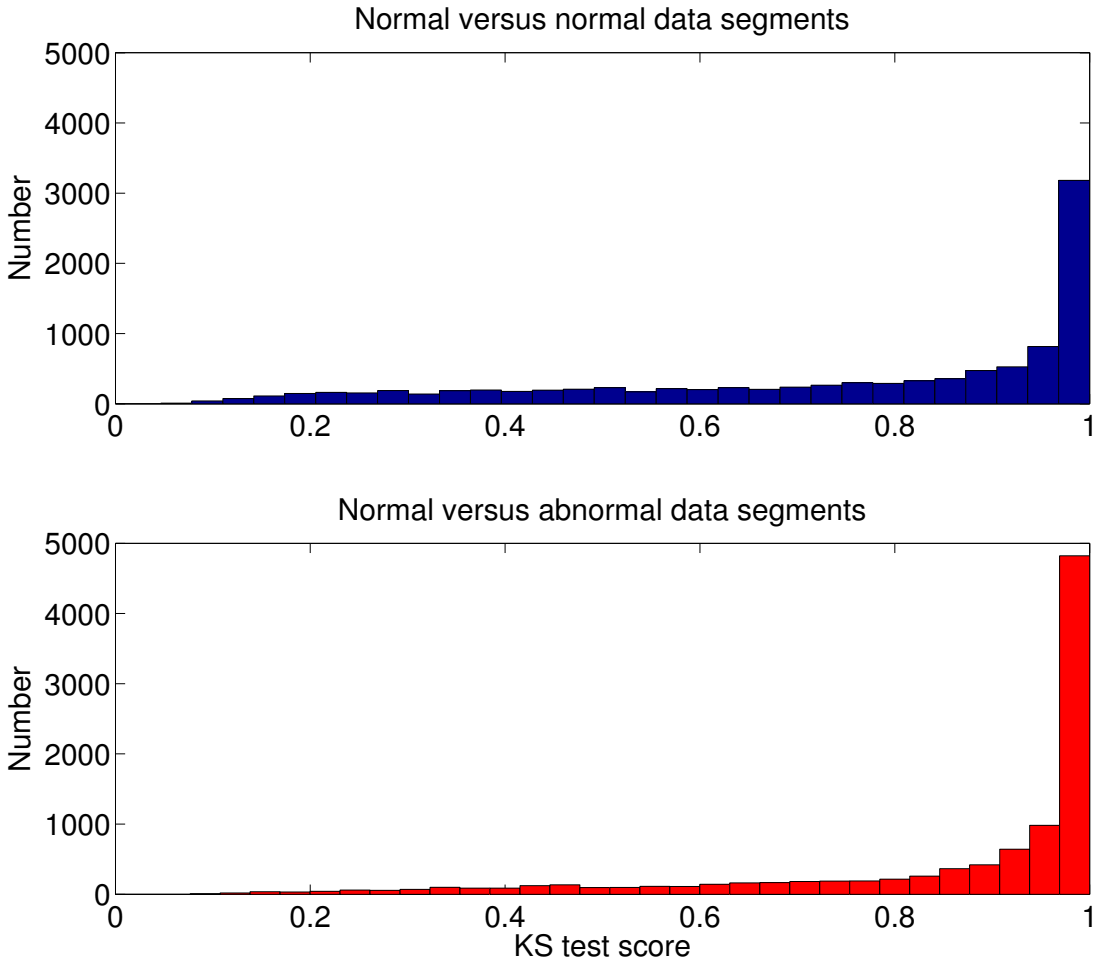

Figure 9.20: PPV during hour 4 in sessions with and without later development of severe hypotension

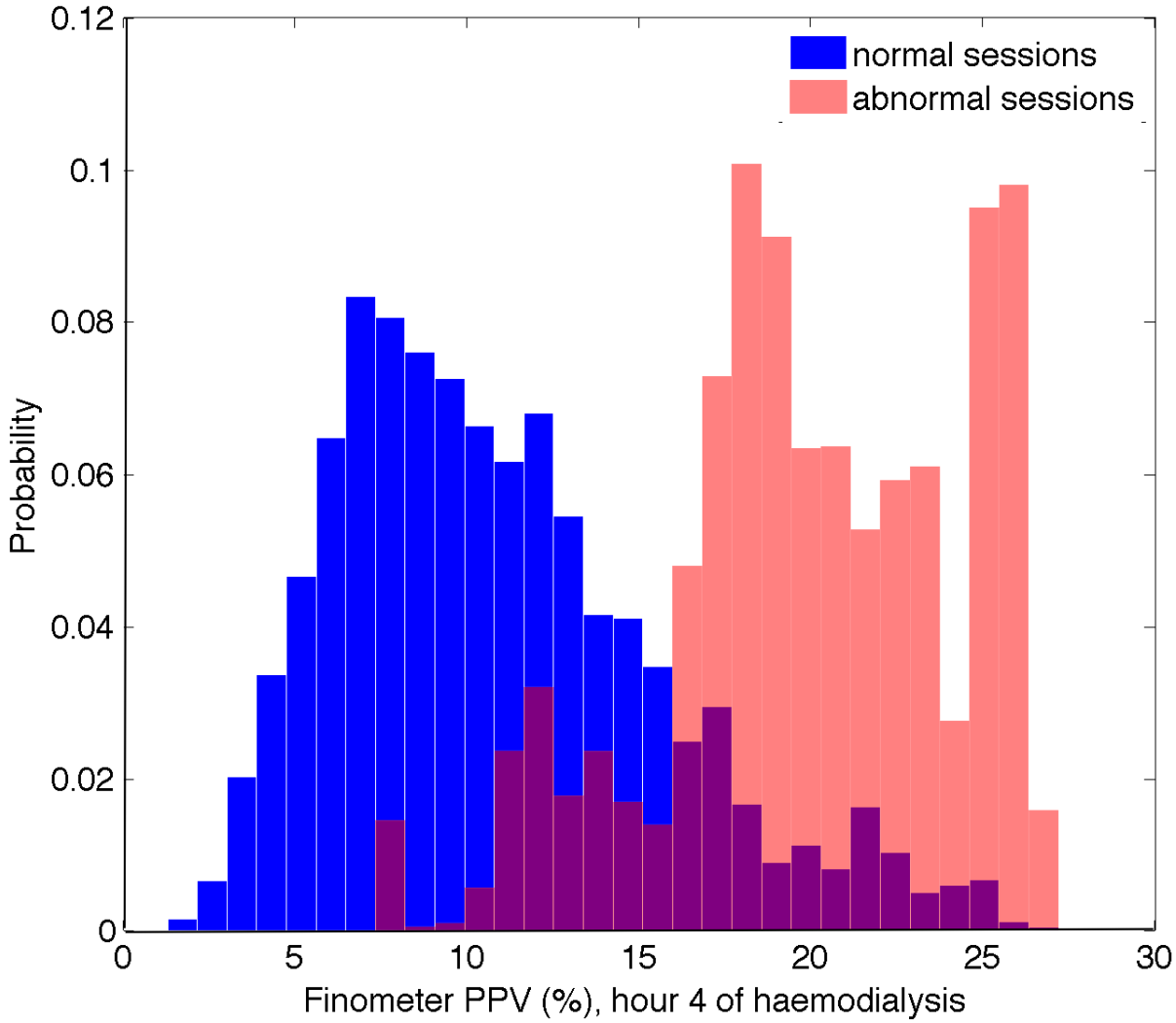

Figure 9.21: Comparison of PPV data from sessions with and without later development of severe hypotension

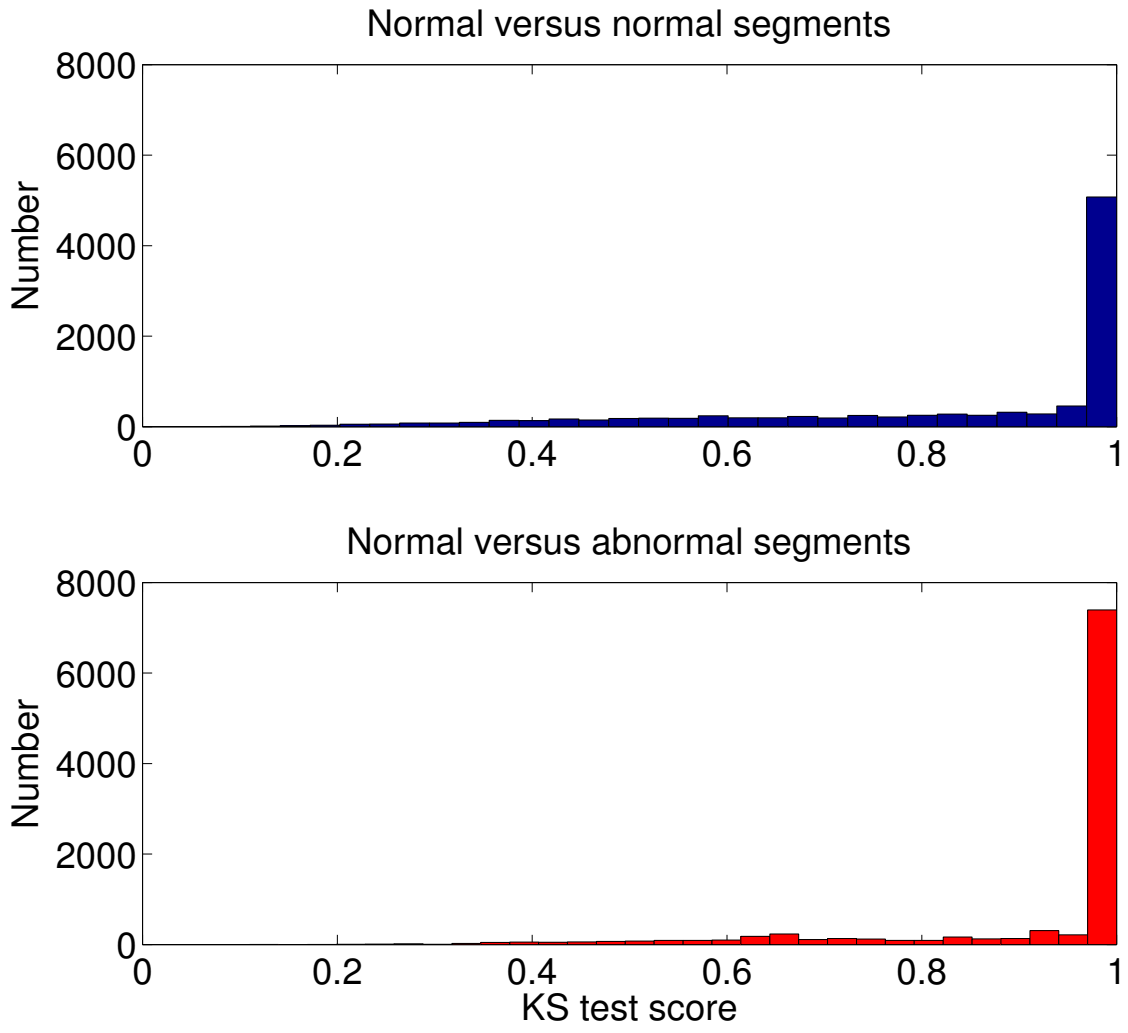

Figure 9.22: PPV during hour 1 in sessions with and without later development of cerebral ischaemia

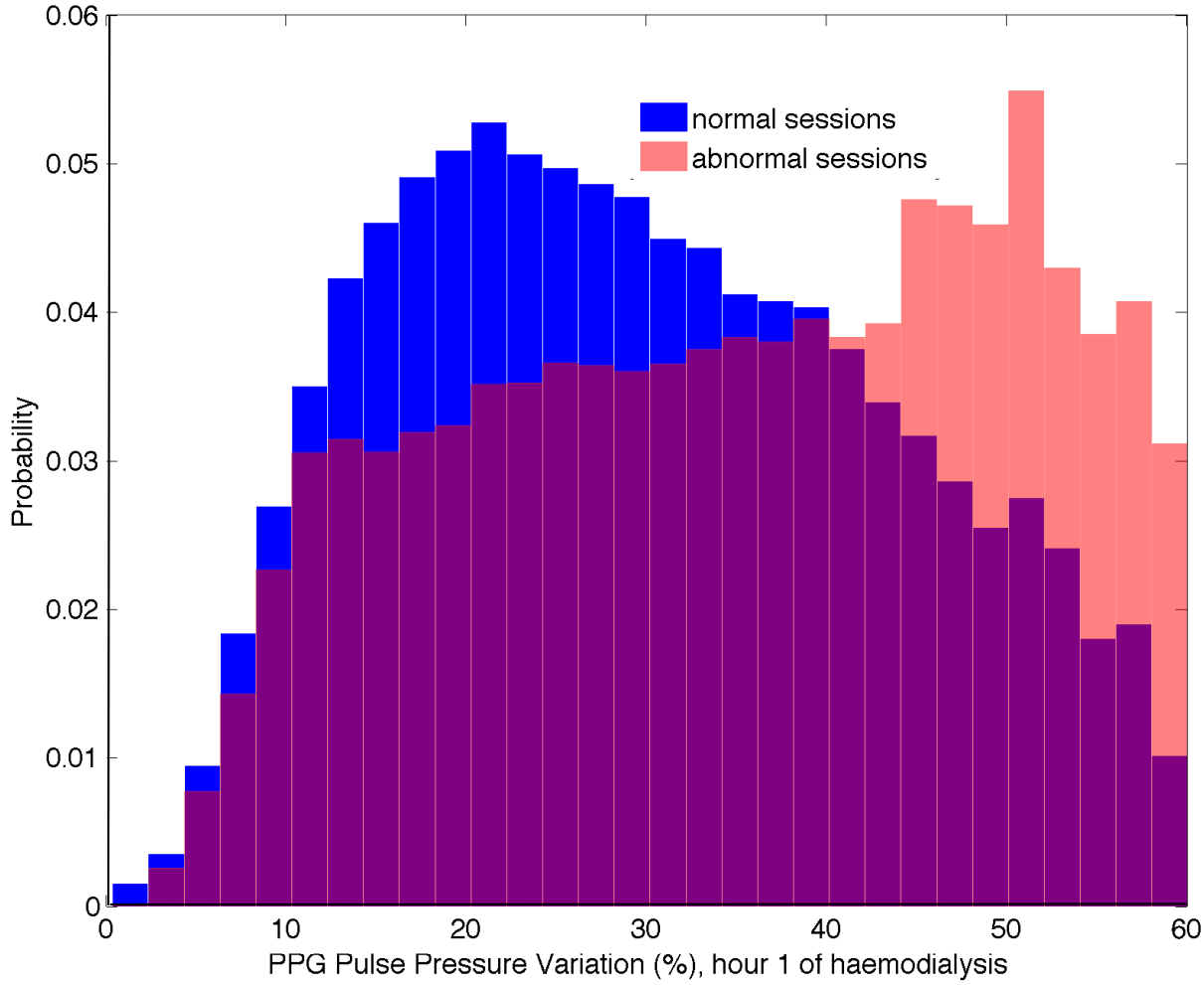

Figure 9.23: Comparison of PPV data from sessions with and without later development of cerebral ischaemia

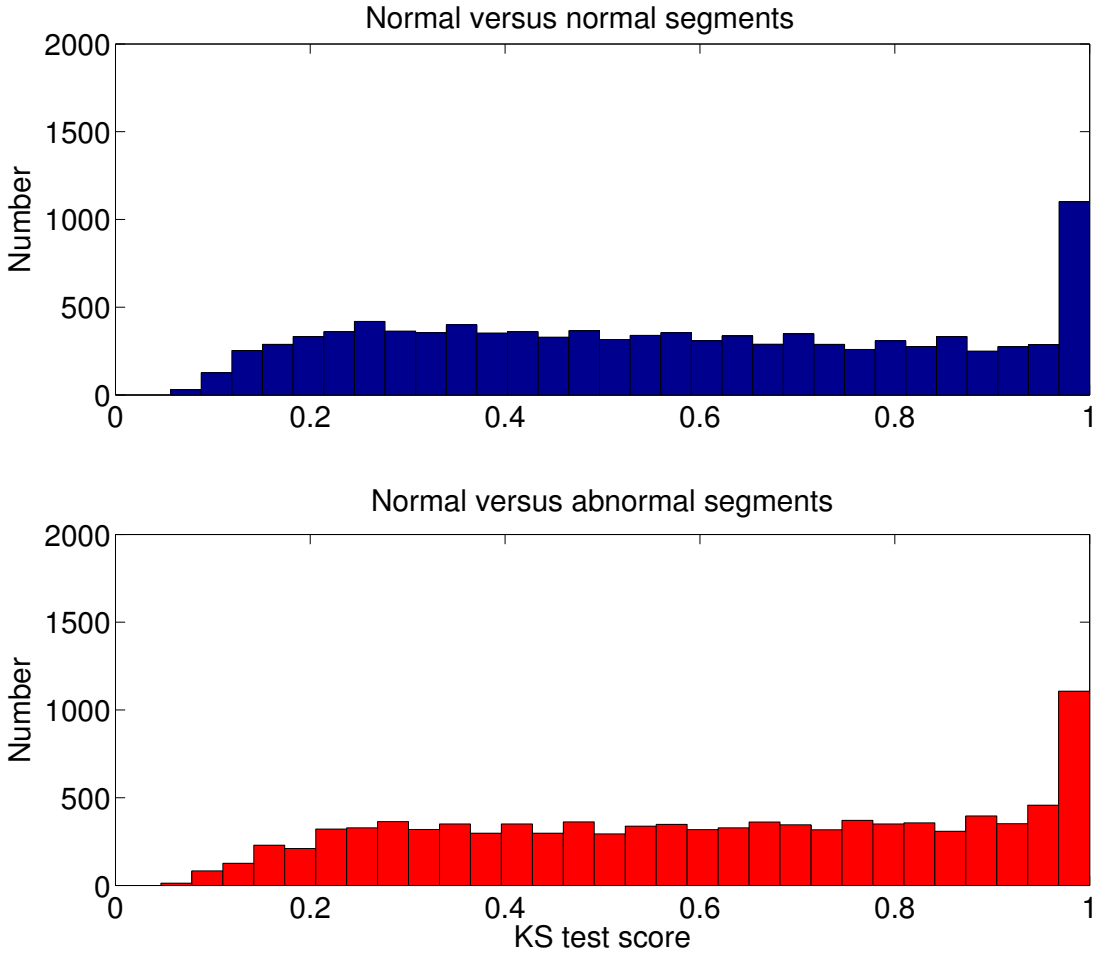

9.4 Discussion

Using univariate physiological variables on the population level, it was possible to see some separation between normal and abnormal sessions prior to an event, but the signal was weak. This is largely due to the huge range of both normal and abnormal data at the population level. On visual inspection, potential predictors included change in heart rate, absolute MAP, peripheral saturation variability, change in rSO2, and PPV. Some of these were expected due to the definition of an event (absolute MAP as a predictor for MAP <60mmHg, and change in rSO2 as a predictor for cerebral ischaemia), though it may not be unreasonable to use a variable to predict future values of itself.

The strength of each physiological data stream varied depending on the event being predicted. For KDOQI events (essentially a surrogate for severe symptoms), the most useful variables appeared to be change in heart rate, Finometer PPV and change in rSO2. Investigation of KDOQI events was limited by the small number meeting the stringent criteria. For MAP<60mmHg, change in heart rate, Finometer PPV and absolute MAP produced most separation. In contrast, for cerebral ischaemia, peripheral saturation variability, HRV and change in rSO2 appeared more promising.

Confirmation of these visual results with statistical tests of distance/difference in distribution proved problematic. Using the Wilcoxon rank sum test (or t test where appropriate) to compare pooled normal and abnormal data was overly sensitive for small, clinically insignificant differences, and severely confounded by patient clustering. Conversely, the comparison of KS test distributions was too blunt due to satiation of the KS test - the difference between normal segments of data on the population level was too great to allow separation of abnormal from normal segments. Nevertheless, using this KS test scores method, absolute MAP and PPV were significantly different in sessions with and without hypotension, and PPV was also significantly different in sessions with and without cerebral ischaemia.

The physiological variables identified as potential predictors have a precedent in the literature. Other authors have found that continuous MAP predicts later hypotension in the critically ill, and blood pressure has been used as the input in biofeedback dialysis [71, 76, 184, 185]. As regards PPV, periodic changes in peak-trough amplitude of arterial and PPG waveforms have been extensively investigated as a marker of fluid balance in the critical care setting [186, 187]. Breathing influences both periodic changes in beat frequency (i.e. the high frequency band of HRV) and periodic changes in beat amplitude. Am-

plitude changes are less dependent on autonomic function, so may be more informative in patients with autonomic impairment due to drugs or disease. This is because respiration influences PPG/Finometer waveform amplitude mechanically, due to changes in stroke volume with changes in intra-thoracic pressure, and may reflect intravascular fluid status [186, 187]. Respiratory-induced changes in the PPG waveform are less prominent in spontaneously breathing patients; nevertheless significant changes have been reported in non-ventilated individuals subject to negative lower body pressure or blood loss, as well as fluid removal during HD [188, 189].

9.5 Conclusions

Several univariate physiological variables show promise for identifying HD sessions which go on to develop severe hypotension and/or tissue ischaemia, but the signal at the population level is too weak to be clinically useful. Physiological variables worthy of further investigation at the personalised level include PPV, saturation variability, change in heart rate, MAP and trend in rSO2.

Chapter 10

Prediction of cerebral desaturation on haemodialysis using univariate variables at the personal level

10.1 Introduction

The previous chapter illustrated that, on the population level, univariate physiological variables showed some separation between sessions with and without adverse events. However, the signal was too weak to be clinically useful. This is largely due to the huge range of both normal and abnormal data at the population level. The key objective of this chapter is to establish whether univariate physiological variables, on the individual patient level, can distinguish normal dialysis sessions from those affected by cerebral ischaemia.

10.2 Methods

See the Methods chapter for full details of the trial and data collection. Selection and pre-processing of physiological variables was exactly as described in the previous chapter.

10.2.1 Visualisation and Statistical Analysis

Sessions were divided into normal and abnormal groups based on the occurrence of cerebral ischaemia, defined as an rSO2 drop of 15% or more of baseline value, sustained for at least 5 minutes. It was deemed, for modelling purposes, that at a minimum a patient must have 6 normal sessions and 1 abnormal session. At this investigative stage, the only patients considered were those with a full set of all possible physiological data streams of consistently high quality, i.e. only full study patients were included (see Methods chapter). Applying these stringent criteria, 15 individuals were selected for further analysis.

Each physiological variable within each patient was considered in turn, i.e. personalised univariate analysis. After pre-processing and application of SQIs as described previously, data streams from "normal sessions" in a given patient were used to construct envelopes representing "expected" values. These data streams were first downsampled to a frequency of 0.0187 Hz (i.e. one data point every minute). As "normal" physiology is likely to depend on the stage of HD, data from different sessions was aligned according to time into treatment, using the time of bleedout as the reference point. The distribution of each variable was assessed visually and with a probability-probability plot. Data was transformed as required to achieve a normal distribution. Following this, sliding 15 minute windows, starting at bleedout and updated every minute, were created, including data from all normal sessions. The mean and standard deviation of the pooled "normal session" data for each 15 minute window was calculated. The timestamp for each window was the centre of the window, i.e. the mean and standard deviation of the 15 surrounding minutes of data. After back transformation, the trajectory of the mean and 95% limits of the normal sessions was then plotted, creating an envelope of "expected" values according to time of treatment. Data after the first event in a session was discarded. If any intervention occurred in the sessions without cerebral ischaemia, typically a fluid bolus or use of minimal UF for asymptomatic hypotension, then data after the intervention was discarded.

For robustness, the normal envelope for a patient was reconstructed repeatedly, each time omitting one of the normal sessions. Each time the omitted normal session was plotted over the normal envelope, as a "test normal" session. This allowed an assessment of specificity, i.e. if unseen data from normal sessions could be correctly classified by the model. Data from each abnormal session was similarly processed and plotted over each possible normal envelope, in order to assess sensitivity, i.e. if unseen data from abnormal sessions could be correctly classified by the model. In order to count as an

"alert", data from the test session had to fall outside the particular envelope for 2 or more consecutive minutes. Confusion matrices were constructed using the total numbers of correctly classified test normal and test abnormal sessions, considering all combinations. The time lag between first warning and actual event in true positive sessions was calculated: only variables providing a median of at least 5 minutes warning were considered useful (to allow sufficient time for intervention in a future predictive model). In addition, to avoid short term noise, variables were not considered further if the total time spent in the abnormal zone before an event was less than 5 minutes median. The process was repeated using 99% normal limits to assess the trade off between potentially improved specificity and reduced sensitivity.

For this analysis, we envisaged a real-time system where every second, the mean value of data from the preceding minute was outputted. Unlike the sessions used to construct the normal envelope, the test sessions were therefore not downsampled to 0.0187 Hz, but to 1 Hz, and then subject to a moving average with one minute windows.

In addition to absolute values, the variance of selected physiological variables over 15 minute windows was also investigated: these variables were MAP, cardiac output, heart rate, respiratory rate, peripheral/access saturations, PPG amplitude and rSO2. PPV and saturation variability are already measures of variance, but very short term, over a minute or less. 15 minute variance of PPG amplitude and peripheral saturation provide longer term equivalents. The moving standard deviation of each normal session was calculated using 15 minute windows, and normalised according to the mean for the relevant window. The normalised moving standard deviations for normal sessions were aligned according to time into treatment, using time of bleedout as the reference point. The mean and 95% limits were calculated for 15 minute windows of pooled data, and plotted as the envelopes for "expected" values. In contrast to the models using absolute values, the timestamp was taken at the end of each window, i.e. representing the variance over the preceding minutes. This is because the models are ultimately designed to be used to predict abnormality in real-time sessions. When monitoring and processing a real-time session, a one minute average for absolute physiological values can easily be calculated; however, the variance of physiological variables by definition requires data from the preceding 15 minutes. The moving standard deviation of each abnormal session was calculated using 15 minute windows, and normalised according to the mean for the relevant window. This was then plotted against the envelope for the relevant window length. For some patients, there was often insufficient data for envelope construction at bleedout (i.e. there was not

always 15 minutes of data recorded before bleedout). As before, for robustness, the normal envelope was reconstructed repeatedly, each time omitting one of the normal sessions. Each time the omitted normal session was itself downsampled to 1 Hz and subject to a moving standard deviation calculation with 15 minute windows, before being plotted over the normal envelope. This allowed assessment of the ability of the various normal envelopes to distinguish sessions with and without cerebral ischaemia, using data not seen before by the model. Confusion matrices were constructed as before. The process was repeated using 99% normal limits to assess the trade off between potentially improved specificity and reduced sensitivity.

10.3 Results

Of the 15 patients selected for further analysis, 6 had only one abnormal session, 5 had 2 abnormal sessions, and the remainder 4 or more abnormal sessions. Where there is only one abnormal session, a sensitivity of 1 simply indicates that, for the variable in question, the data from the single abnormal session deviates from all possible constructions of the normal envelope. Therefore, to select variables that might have use in a subsequent multivariate, real-time model, for these individuals we chose the strict cut off of at least 90% sensitivity (i.e. the abnormal data fell within no more than one normal envelope), and at least 60% specificity. Variables meeting these criteria in patients with only one abnormal session are documented in tables 10.1 to 10.6, along with the median lag time between deviation from the expected trajectory and onset of cerebral ischaemia. As a visual example, figures 10.1 to 10.3 illustrate the trajectory of three potential predictive variables identified for patient DF12 against a selection of normal envelopes, and figures 10.4 to 10.5 show the trajectory of an excluded variable against the same envelopes.

Figure 10.1: Peripheral saturation variability in one abnormal and two normal abnormal sessions, plotted against two different normal envelopes in patient DF12. The "test" normal session is the one that has been excluded when constructing that particular normal envelope.

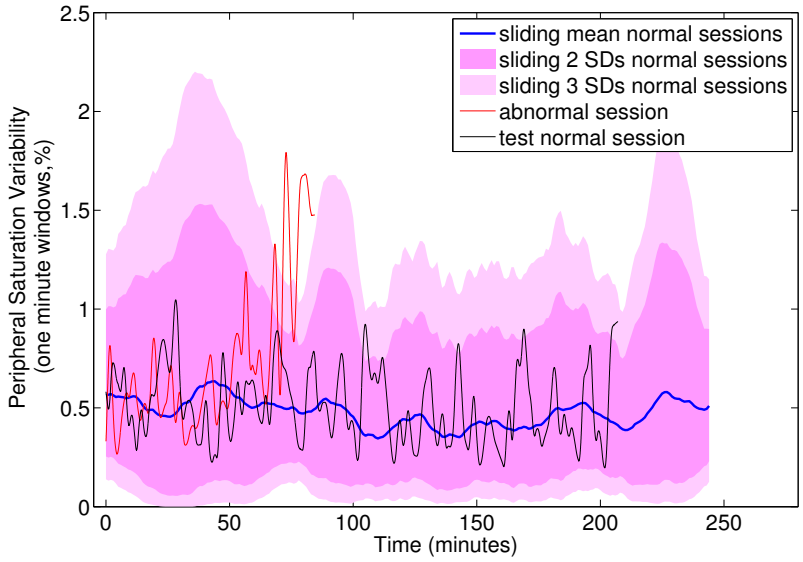

(a)

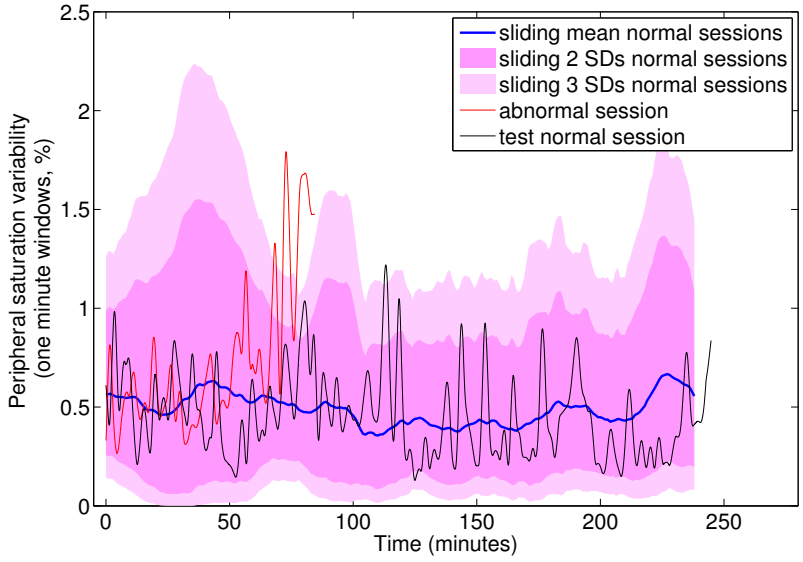

(b)

Figure 10.2: MAP in one abnormal and two normal abnormal sessions, plotted against two different normal envelopes in patient DF12. The "test" normal session is the one that has been excluded when constructing that particular normal envelope.

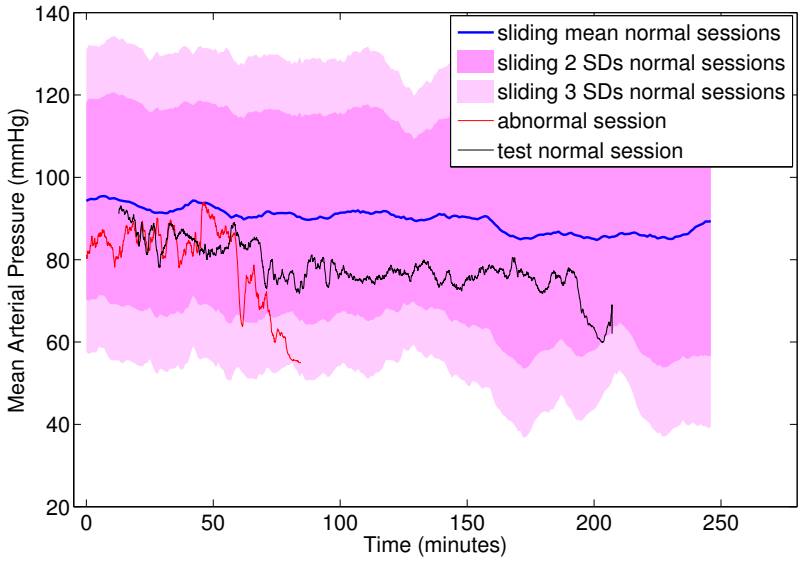

(a)

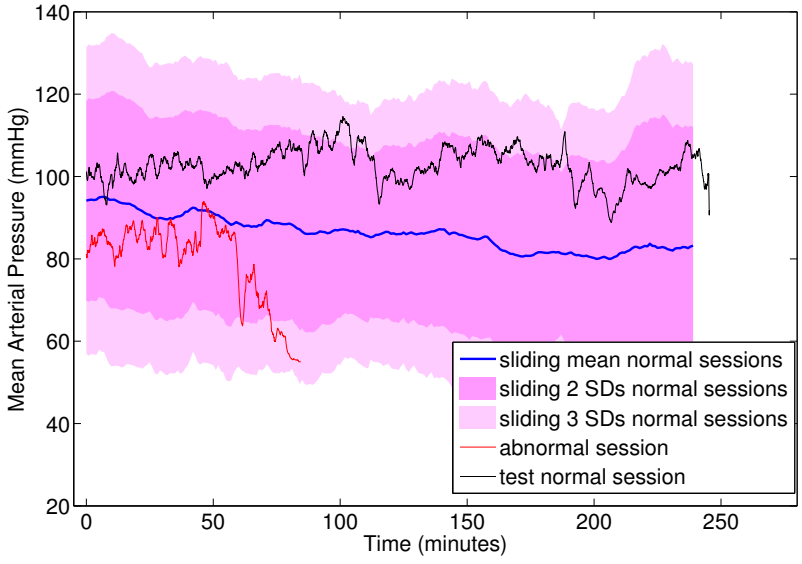

(b)

Figure 10.3: Heart rate in one abnormal and two normal abnormal sessions, plotted against two different normal envelopes in patient DF12. The "test" normal session is the one that has been excluded when constructing that particular normal envelope.

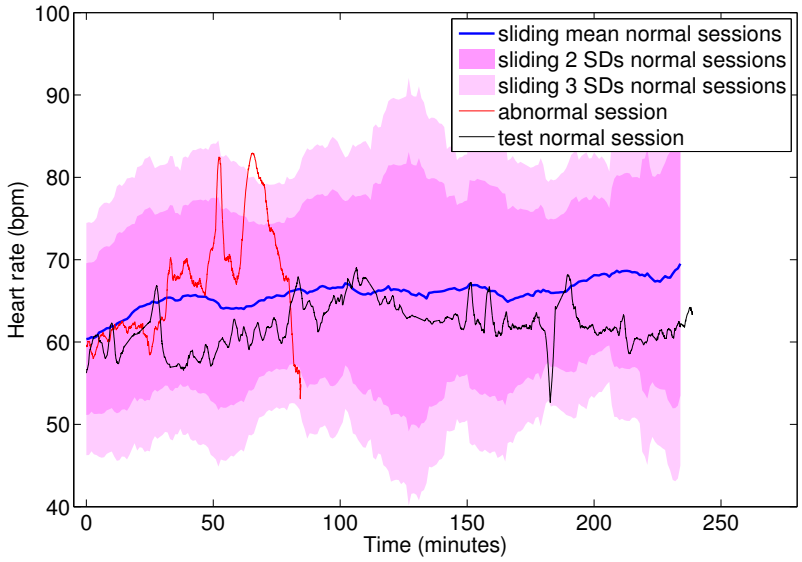

(a)

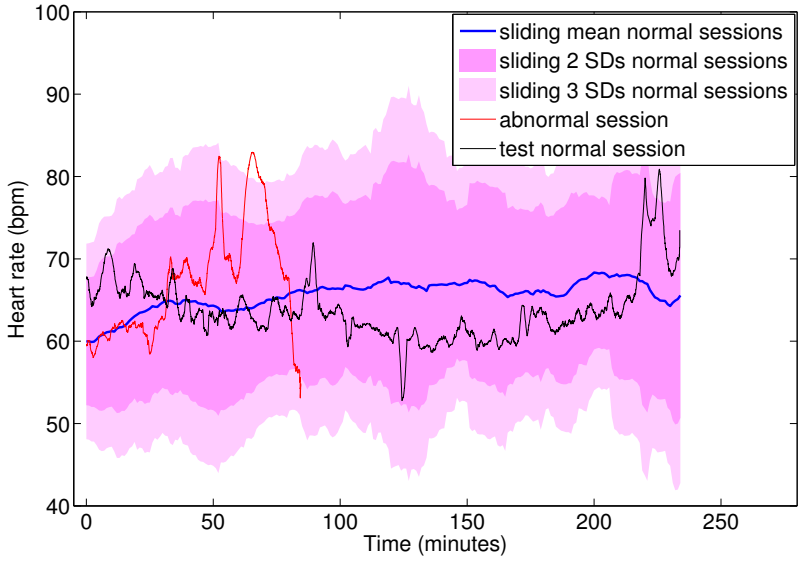

(b)

Figure 10.4: Peripheral saturations in one abnormal and two normal abnormal sessions, plotted against two different normal envelopes in patient DF12. The "test" normal session is the one that has been excluded when constructing that particular normal envelope. Peripheral saturations did not prove useful in distinguishing normal and abnormal sessions in this individual.

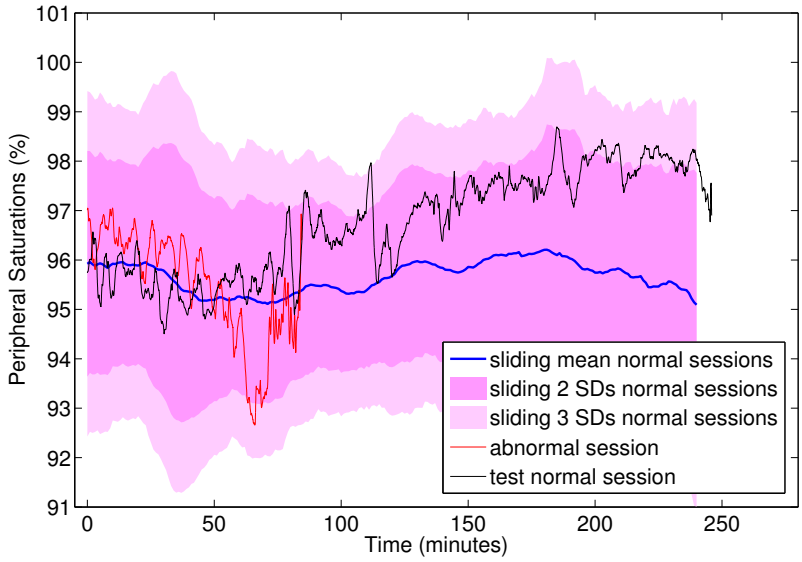

(a)

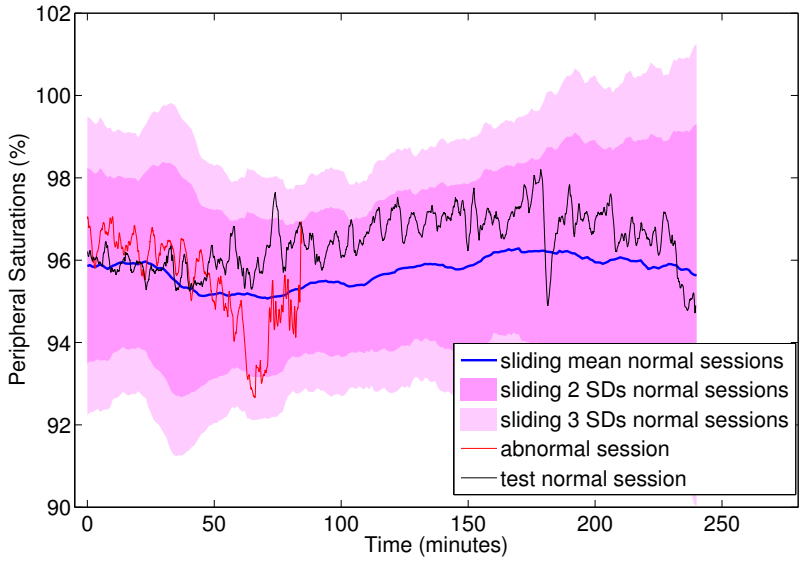

(b)

Figure 10.5: Respiratory rate in one abnormal and two normal abnormal sessions, plotted against two different normal envelopes in patient DF12. The "test" normal session is the one that has been excluded when constructing that particular normal envelope. Respiratory rate did not prove useful in distinguishing normal and abnormal sessions in this individual.

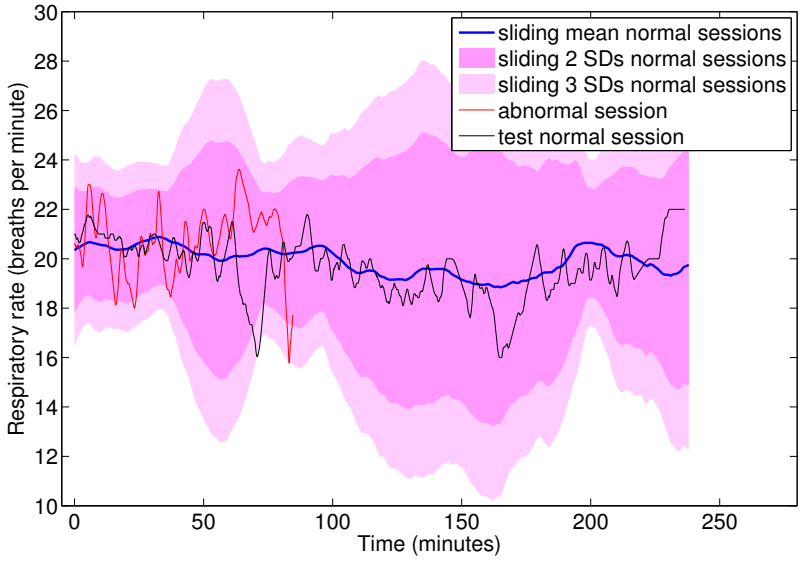

(a)

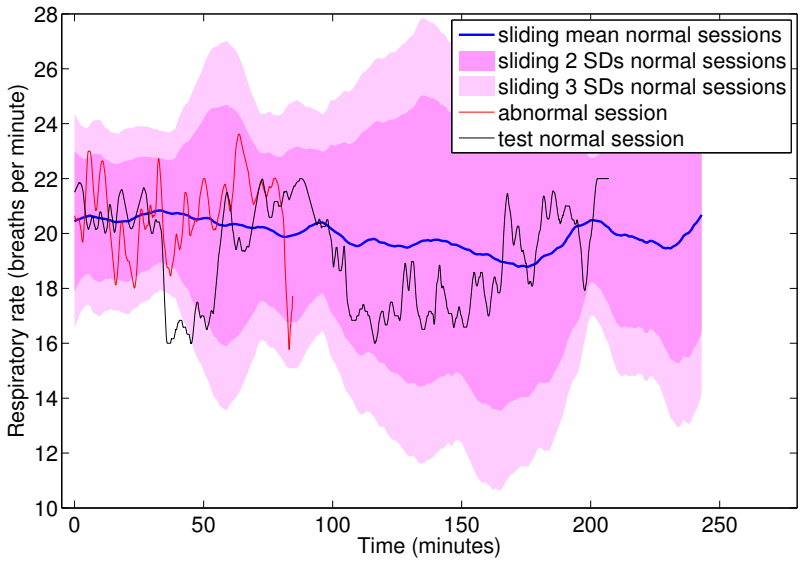

(b)

Table 10.1: Potential predictive variables for patient DF01, 34 year old male with focal segmental glomerulosclerosis (11 normal sessions and 1 abnormal session, event at 150 minutes)

Variable (limits used)	Sensitivity	Specificity	Warning given (minutes, median)
Cardiac Output (95%)	1.00	0.70	137.2
PPG amplitude (95%)	1.00	0.70	67.2
Change in heart rate (95%)	1.00	0.64	78.2
Heart rate variance (99%) (15 minute windows)	1.00	0.73	57.2
Peripheral saturations (95%)	1.00	0.64	125.2
Peripheral saturations variability (99%) (1 minute windows)	1.00	0.82	72.2
rSO2 saturations variance (99%) (15 minute windows)	1.00	0.75	146.2
Fistula saturations variance (99%) (15 minute windows)	1.00	0.78	103.2

Table 10.2: Potential predictive variables for patient DF12, 89 year old male with glomerulonephritis (11 normal sessions and 1 abnormal session, event at 84 minutes)

Variable (limits used)	Sensitivity	Specificity	Warning given (minutes, median)
MAP (95%)	1.00	0.72	31.5
MAP variance (99%) (15 minute windows)	1.00	0.82	17.5
Heart rate (99%)	1.00	0.80	21.5
Change in heart rate (99%)	1.00	0.78	31.5
Peripheral saturation variability (99%) (1 minute windows)	1.00	0.70	15.5
rSO2 variance (99%) (15 minute windows)	1.00	1.00	14.5

Table 10.3: Potential predictive variables for patient DF13, 73 year old male with cardiorenal failure/renovascular disease (11 normal sessions and 1 abnormal session, event at 76 minutes)

Variable (limits used)	Sensitivity	Specificity	Warning given (minutes, median)
MAP (99%)	1.00	0.82	19.0
MAP variance (99%) (15 minute windows)	1.00	0.82	29.1
Cardiac output (99%)	1.00	0.82	22.0
Cardiac output variance (99%) (15 minute windows)	1.00	0.73	32.1
PPG amplitude (99%)	1.00	0.90	36.0
rSO2 variance (99%) (15 minute windows)	1.00	0.70	38.1

Table 10.4: Potential predictive variables for patient DF37, 60 year old male with diabetic nephropathy (11 normal sessions and 1 abnormal session, event at 101 minutes)

Variable (limits used)	Sensitivity	Specificity	Warning given (minutes, median)
Fistula saturations variance (99%) (15 minute windows)	1.00	0.70	29.7
rSO2 variance (99%) (15 minute windows)	1.00	0.91	9.7
Peripheral saturations variability (99%) (1 minute windows)	1.00	0.80	69.7
Peripheral saturations variance (99%) (15 minute windows)	1.00	0.80	43.7

Table 10.5: Potential predictive variables for patient DF43, 26 year old male with reflux nephropathy (11 normal sessions and 1 abnormal session, event at 170 minutes)

Variable (limits used)	Sensitivity	Specificity	Warning given (minutes, median)
MAP (95%)	1.00	0.70	146.5
Heart rate (95%)	1.00	0.64	163.5
PPG amplitude variance (99%) (15 minute windows)	1.00	0.81	78.5
Peripheral saturations variability (99%) (1 minute windows)	1.00	0.91	61.5
Peripheral saturations variance (99%) (15 minute windows)	1.00	0.73	46.5
rSO2 variance (99%) (15 minute windows)	1.00	0.91	126.5

Table 10.6: Potential predictive variables for patient DF45, 35 year old with sickle cell nephropathy (11 normal sessions and 1 abnormal session, event at 199 minutes)

Variable (limits used)	Sensitivity	Specificity	Warning given (minutes, median)
Cardiac output (95%)	1.00	0.73	93.9
Cardiac output variance (99%) (15 minute windows)	1.00	1.00	101.9
Heart rate (99%)	1.00	0.67	88.9
rSO2 variance (99%) (15 minute windows)	1.00	0.65	13.9

In patients with multiple abnormal sessions, the sensitivity of a variable depended largely on the homogeneity of the events. However, even within the same patient, the abnormal sessions did not appear to be stereotypical. For example, some patients had sessions with fairly sudden cardiovascular collapse as well as sessions with an insidious onset of cerebral ischaemia, and these had very different patterns of physiological derangement. Therefore, when identifying variables of potential use in multivariate models in patients with multiple eventful sessions, the cut-off for sensitivity was lowered to over 50%, i.e. at least half of abnormal sessions falling outside all possible normal envelopes. As before, only variables which became abnormal at least 5 minutes before the event were considered, and variables were excluded if the total time spent in the abnormal zone before an event was less than 5 minutes median. Variables meeting these criteria in patients with multiple abnormal sessions are documented in tables 10.7 to 10.14, along with the median lag time between deviation from the expected trajectory and onset of cerebral ischaemia.

Table 10.7: Potential predictive variables for patient DF05, 53 year old male with polycystic kidney disease (11 normal sessions and 2 eventful sessions)

Variable (limits used)	Sensitivity	Specificity	Warning given (minutes, median)
MAP (95%)	1.00	0.64	103.8
MAP variance (99%) (15 minute windows)	0.55	0.82	48.3
Heart rate (95%)	0.55	0.60	146.3
Cardiac output (99%)	1.00	0.82	197.3
PPG amplitude variance (99%) (15 minute windows)	0.91	0.73	121.3
PPG PPV (95%) (1 minute windows)	0.55	0.91	45.3
Fistula saturations (99%)	0.55	0.78	85.7
Saturation variability (99%) (1 minute windows)	1.00	0.64	143.3

Table 10.8: Potential predictive variables for patient DF26, 78 year old male with renovascular disease (8 normal sessions and 2 eventful sessions)

Variable (limits used)	Sensitivity	Specificity	Warning given (minutes, median)
Central venous saturations (95%)	1.00	0.63	176.8
rSO2 variance (99%) (15 minute windows)	1.00	0.75	92.8

Table 10.9: Potential predictive variables for patient DF49, 39 year old male with IgA nephropathy (10 normal sessions and 2 eventful sessions)

Variable (limits used)	Sensitivity	Specificity	Warning given (minutes, median)
Cardiac output variance (99%) (15 minute windows)	0.55	0.60	59.3
rSO2 variance (99%) (15 minute windows)	1.00	0.70	68.5
Peripheral saturations (95%)	0.65	0.75	55.3
Respiratory rate (95%)	0.55	0.78	52.6

Table 10.10: Potential predictive variables for patient DF60, 63 year old male with IgA nephropathy (7 normal sessions and 2 eventful sessions)

Variable (limits used)	Sensitivity	Specificity	Warning given (minutes, median)
Peripheral saturations (95%)	1.00	0.80	186.5
Peripheral saturations variance (99%) (15 minute windows)	0.79	0.60	140.4
Peripheral saturations variability (99%) (1 minute windows)	1.00	0.60	186.0
Respiratory rate (99%)	1.00	0.60	186

Table 10.11: Potential predictive variables for patient DF30, 59 year old female with reflux nephropathy (6 normal sessions and 4 eventful sessions)

Variable (limits used)	Sensitivity	Specificity	Warning given (minutes, median)
MAP (95%)	0.58	0.67	134.6
MAP variance (99%) (15 minute windows)	0.54	0.67	77.6
Cardiac output (95%)	0.75	0.67	131.6
Peripheral saturation variability (99%) (1 minute windows)	0.75	0.75	164.8

Table 10.12: Potential predictive variables for patient DF18, 56 year old male with diabetic nephropathy (8 normal sessions and 4 eventful sessions)

Variable (limits used)	Sensitivity	Specificity	Warning given (minutes, median)
MAP variance (99%) (15 minute windows)	0.59	0.86	162.5
Heart rate (95%)	0.72	0.63	49.7
Change in heart rate (99%)	0.56	0.87	54.5
Peripheral saturations (95%)	0.81	0.63	45.5
Peripheral saturation variability (99%) (1 minute windows)	0.75	0.88	89.6

Table 10.13: Potential predictive variables for patient DF24, 72 year old female with diabetic nephropathy (7 normal sessions and 5 eventful sessions)

Variable (limits used)	Sensitivity	Specificity	Warning given (minutes, median)
Peripheral saturations (99%)	0.60	0.86	32.0
Respiratory rate (95%)	0.83	0.71	83.0

Table 10.14: Potential predictive variables for patient DF11, 59 year old female with diabetic nephropathy (6 normal sessions and 6 eventful sessions)

Variable (limits used)	Sensitivity	Specificity	Warning given (minutes, median)
Heart rate (99%)	0.53	0.67	44.9

No potentially predictive variables could be identified for one patient of the 15 studied. This was a gentleman with a history of ischaemic strokes who had multiple events often soon after bleedout: it may be that there was insufficient time for a pre-emptive warning. In addition, his baseline tissue oxygenation was low even for this population at 35%, meaning that a drop of 15% of baseline was only an absolute drop of 5%: this is approaching the limits of repeatability of the Covidien NIRS device, estimated at 3.4% by one study [190]).

It is noticeable that the warning times are unexpectedly long, with it not being infrequent for the first deviation from the normal envelope to be one or even two hours before the onset of cerebral ischaemia. Some events occurred fairly abruptly, with continuous abnormality from the point of first warning to the time of event, as in the abnormal session shown in figures 10.1 to 10.5. However, the more typical pattern was fluctuant rather than continuous abnormality, with repeated, often infrequent, excursions outside the normal envelope over a prolonged period before the actual event. An example is given in figure 10.6, which illustrates the trajectories of peripheral saturation variability and heart rate in an eventful session in patient DF18.

Figure 10.6: An example of a common pattern of physiological abnormality in eventful sessions. Intermittent, infrequent excursions beyond the 95% limits occur over a prolonged period before the final event of cerebral desaturation at 154 minutes into dialysis)

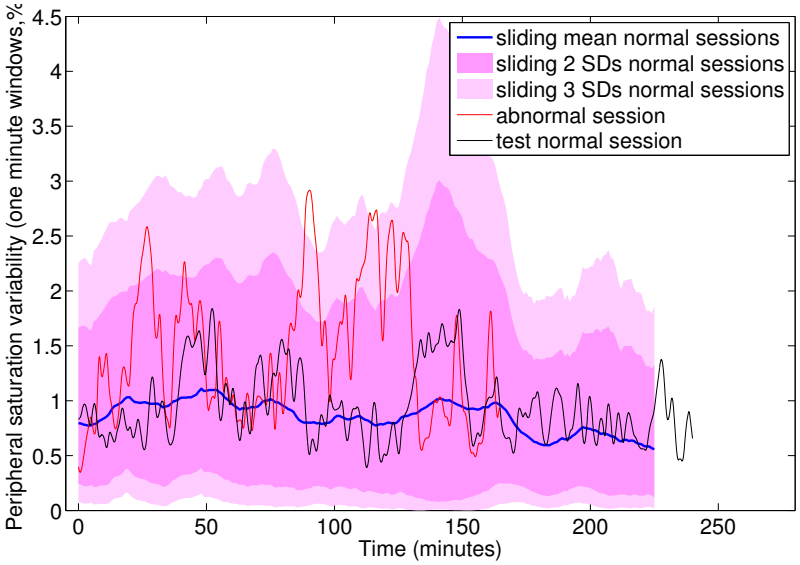

(a) Peripheral Saturation Variability

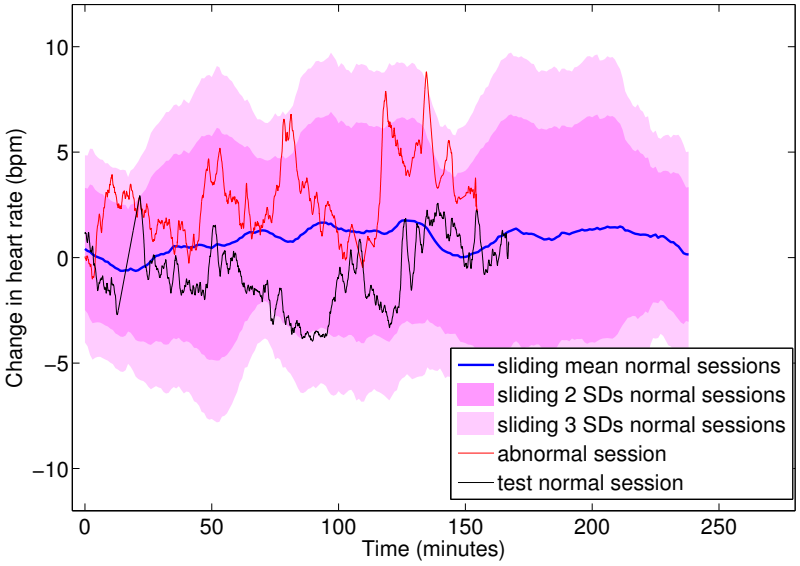

(b) Heart rate

10.4 Discussion (see in addition discussion of chapters 9 and 11)

It may be possible to anticipate well in advance the development of cerebral desaturation on HD, using deviations of univariate physiological data from the expected trajectory for a given patient. Whilst there is variation between patients, some physiological data streams are clearly more useful than others overall. For example, RBV and LFnu did not prove to have predictive value according to the specified criteria in any individual, whereas heart rate, MAP and measures of saturation variance (cerebral and/or peripheral) were found to provide early warning in multiple patients. Variables which offered similar information, e.g. cardiac output and PPG amplitude, were seen to cluster. Unsurprisingly, measures of saturation variance (access, peripheral and cerebral) also clustered, i.e. in patients where one measure of saturation variance was useful, other indices of saturation variance were also likely to be of predictive value. This was not true for absolute saturations, which were consistently less helpful. Classically defined peripheral saturation variability, over one minute windows, offered similar information to peripheral saturation variance over 15 minute windows, but as expected was capable of providing a warning approximately 10 minutes earlier. The long warning times exclude the possibility that the rSO2 variance measures are only picking up a terminal deterioration in the absolute variable.

It is apparent that the greater the proportion of abnormal to normal sessions, the greater the difficulty in identifying useful univariate predictors. This is likely to be due to the combination of overestimated performance when there was only one abnormal session for testing the model, and reduced certainty as to the location of the normal envelope with fewer normal sessions for training.

The main weakness of this analysis is that it is retrospective, and as such the models may be overfitted, although we attempted to mediate this by resampling and cross-validation. The models ultimately need to be tested on a new dataset, which would involve gathering more data on the same patients. It may be that considering the area outside the normal envelope, i.e. taking into account the magnitude as well as the duration of the excursion, may improve performance. We chose 2 consecutive minutes as the minimum length of abnormal data to generate an alert: it may be that lengthening this could have improved specificity, although it was apparent that in many eventful sessions, repeated short bursts of abnormal data was the predominant pattern. In addition, it may be overly blunt to define the sensitivity and specificity of predictive variables according to their performance in classifying entire sessions as normal or abnormal rather than, for example, 30 minute segments of data.

The univariate approach suffers from the caveat that physiological derangements clearly differ between abnormal sessions even within the same patient, e.g. change in heart rate and MAP may only characterise a subset of events, whereas others may instead feature increased saturation variance. Therefore, only looking at one of these variables would miss some abnormal sessions altogether. With a multivariate approach, sensitivity would be much improved, and potentially specificity too: this is the aim of the next chapter.

10.5 Conclusions

It may be possible to predict intra-dialytic cerebral desaturation using deviations of univariate physiological data from the expected trajectory for that given patient, but sensitivity is limited by the heterogeneity of abnormal events even within one individual. Multivariate analysis, i.e. data fusion, may be able to surmount this difficulty.

Chapter 11

Prediction of cerebral desaturation on haemodialysis using multivariate variables at the personal level

11.1 Introduction

The last chapter demonstrated that it may be possible to predict intra-dialytic cerebral desaturation using deviations of univariate physiological data from the expected trajectory for that given patient. However, sensitivity is limited by the heterogeneity of abnormal events even within one individual. Multivariate analysis, i.e. data fusion, may be able to surmount this difficulty. In addition, it offers the advantage that if one data stream becomes unavailable, as often happens in real-world clinical practice, a predictive model can still run. Specificity may also be improved: if one data stream becomes transiently abnormal, but the others remain within the expected range, an alert is less likely to be generated. The objective of this chapter was therefore to generate multivariate, personalised predictive models of intra-dialytic cerebral ischaemia, which might have use in providing a real-time early warning system.

11.2 Methods

Data pre-processing was performed as outlined in the last chapter. As before, sessions were divided into normal and abnormal groups based on the occurrence of cerebral ischaemia, defined as an rSO2 decrease

of 15% or more of baseline value, sustained for at least 5 minutes. The same 15 individuals studied in the last chapter were selected for this preliminary analysis.

For multivariate analysis, data fusion techniques were used to create multidimensional probabilistic models of normality. The Neuroscale algorithm, a radial basis function (RBF) neural network, was used to create a "multivariate normal envelope" and map it to two dimensional space for ease of visualisation [116]. The neuroscale method first represents input data (here the data from normal dialysis sessions) as a Gaussian mixture model with a specified number of "centres", determined by the Expectation-Maximisation algorithm. Each centre then becomes the centre for a Gaussian RBF. Essentially each input data point "activates" each centre according to distance from that centre. The final two dimensional output of the network is a linear combination of weighted outputs from the centres, the weights being determined to minimise the "stress" (Euclidean distance) between the multi-and two-dimensional representations of each data point. New data (i.e. from a new dialysis session) can then be fed into the Neuroscale algorithm, and plotted against the "normal" map . In this way, early deviations from the predefined zone of multidimensional normality for a given patient can be visualised. Further information, including details of the mathematical procedures, can be found in the original publication [116].

Four input data streams were chosen as a compromise between information and acceptability of required monitoring. Three different sets of four input variables were tested, guided by the results of the previous chapter. The first set comprised a mixture of haemodynamic and oxygenation variables which had proven particularly promising on univariate analysis: MAP, heart rate, peripheral saturation variability (one minute windows) and cerebral saturation variance (15 minute windows). The second set used four inputs that could be derived from the two probes that, according to informal feedback, had the greatest patient acceptability, namely the respiratory belt and the finger PPG. This set consisted of heart rate, respiratory rate, PPG pulse pressure variability and peripheral saturation variability (one minute windows). The final set used four inputs that could be derived from a single probe (PPG/sats monitor): peripheral saturation variability (one minute windows); PPG pulse pressure variability (PPV); heart rate; peripheral saturations.

All the data from the normal sessions, regardless of the time of dialysis, was pooled. We took this approach rather than assessing data in sliding 15 minute blocks as in the univariate analysis, partly due

to the computational intensity of a sliding windows neuroscale model, but also because the performance of the neural network depends on the number of input data points (the number of training vectors determines the robustness of the normal model), and the volume of data available for a 15 minute window was suboptimal for training. In addition, the multidimensional approach can indirectly control for the time of dialysis: rather than being normalised to time of dialysis directly, each variable is normalised to three other variables which vary with time of dialysis.

If any intervention occurred in the normal sessions used to train the network (i.e. those without cerebral ischaemia), typically a fluid bolus or use of minimal UF for asymptomatic hypotension, then data after the intervention was discarded.

Each data stream was normalised by subtracting the mean of the pooled data, then dividing by the standard deviation of the pooled data for that variable (i.e. zero mean, unit variance transformation). This step was taken so that all variables had approximately the same dynamic range. This data was then used to generate a neural network, or training network, as described above. The models continued to run if one of the four inputs was missing (in which case the value was set to the mean for that variable) but if two of the inputs were missing, no output was generated for that input vector. The structure of the network can be depicted as follows:

Figure 11.1: Structure of radial basis function network used in this analysis. The output from each output node is a linear combination of the weighted outputs from all the centres, plus a term for bias specific to each output node, as shown in equation 2.3. W=weight, L=output node, j=centre

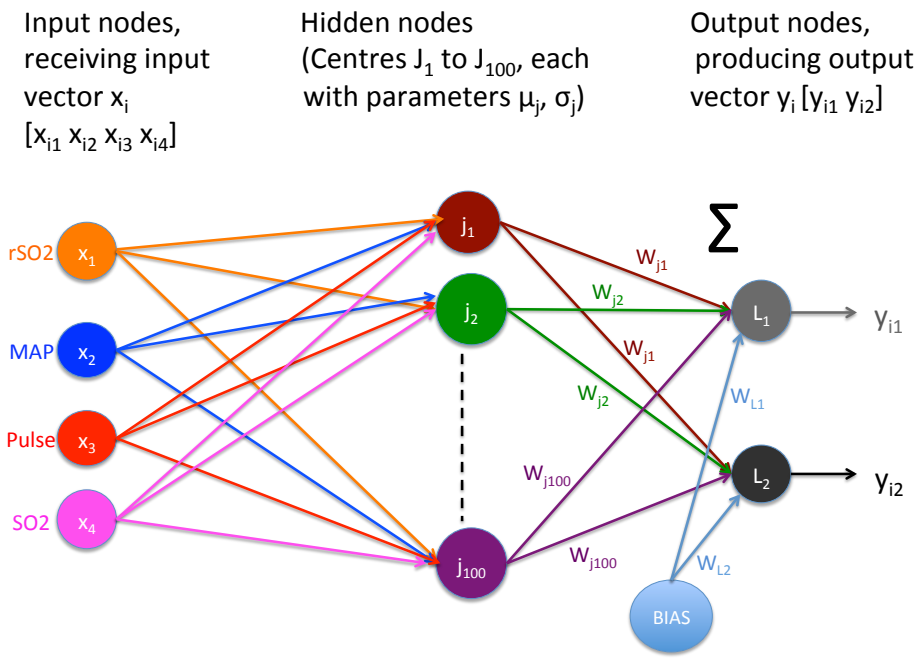

The inputs to the algorithm for each patient were four-dimensional vectors representing all the normalised data from all normal sessions. The number of vectors varied from patient to patient, but was typically 115,000 to 140,000 (one data point per second, 32-40 continuous hours of normal data for an average patient) . K means clustering was used to represent the input data vectors as 500 representative clusters, making the number of training vectors more manageable. The 10% of k means clusters which had been assigned the fewest data points were excluded. The remaining 450 vectors were then used to train a RBF network, with 100 kernels (centres) and a Gaussian activation function. The probability distribution function (pdf or $p(x)$) of the normal data was estimated using the Parzen windows kernel density estimator method as shown in the following equation:

$$p(\mathbf{x}|\mathbf{x}_i, \sigma^2) = \frac{1}{N(2\pi)^{D/2}\,\sigma^D} \sum_{i=1}^{N} e^{-\frac{||\mathbf{x}-\mathbf{x}_i||^2}{2\sigma^2}} \tag{11.2.1}$$

where D is the number of dimensions, x is the mean of the data, σ is the standard deviation of the

data (or bandwidth of the kernel), and x_i is the ith data point.

This is essentially the weighted sum of Gaussian kernels centred on the normal vectors, and represents the likelihood for all normal data.

The centres were determined by fitting a Gaussian mixture model with symmetrical covariances using the Expectation Maximisation algorithm. The mixture model was initialised using a small number of iterations of the K-means algorithm. The values of σ were determined by the squared maximum distance between centres. The RBF for each centre can be represented as follows:

$$\phi_j(\mathbf{x}_i) = e^{-\frac{||\mathbf{x}_i - \mu_j||^2}{2\sigma_j^2}} \tag{11.2.2}$$

where μ_j is the location of centre j, as determined by the Expectation Maximisation algorithm.

Propagation of the 450 input vectors through the RBF, with initial values for the output and bias weights chosen by random numbers from a standard normal distribution, results in a 450 by 2 matrix of output vectors (the activations matrix). The hidden to output weights were initialised using principal component analysis (PCA) applied to this matrix, ie the matrix was represented as two vectors, called shadow targets, the location in the visualisation map for that input vector. Once calculated, the pseudoinverse of the activations matrix was used to solve the weights for the target vectors using least squares. The iterative shadow targets algorithm, with a maximum of 100 iterations, was then used to refine the hidden to output weights. This procedure is described in detail by Nabney [191]. The final output of the RBF network is now a 2 dimensional vector, with the output from each output node (L1 and L2 in diagram 11.1), given by the following equation:

$$y_L(x_i) = \sum_{j=1}^{100} W_j \phi_j(x_i - \mu_j) + W_L \tag{11.2.3}$$

where y_L is the output from node L, W_j is the weight for centre j, ϕ is the RBF for centre j, and W_L is the bias for node L.

In this way, the pooled data from the normal sessions was then fed through the neural network, to generate a two-dimensional representation of the normal data. With enough data this approximates to

a circle centred on the origin, as shown in figure 11.2.

Figure 11.2: Two dimensional representation of pooled training data from patient DF49 (9 sessions), 129,600 data points

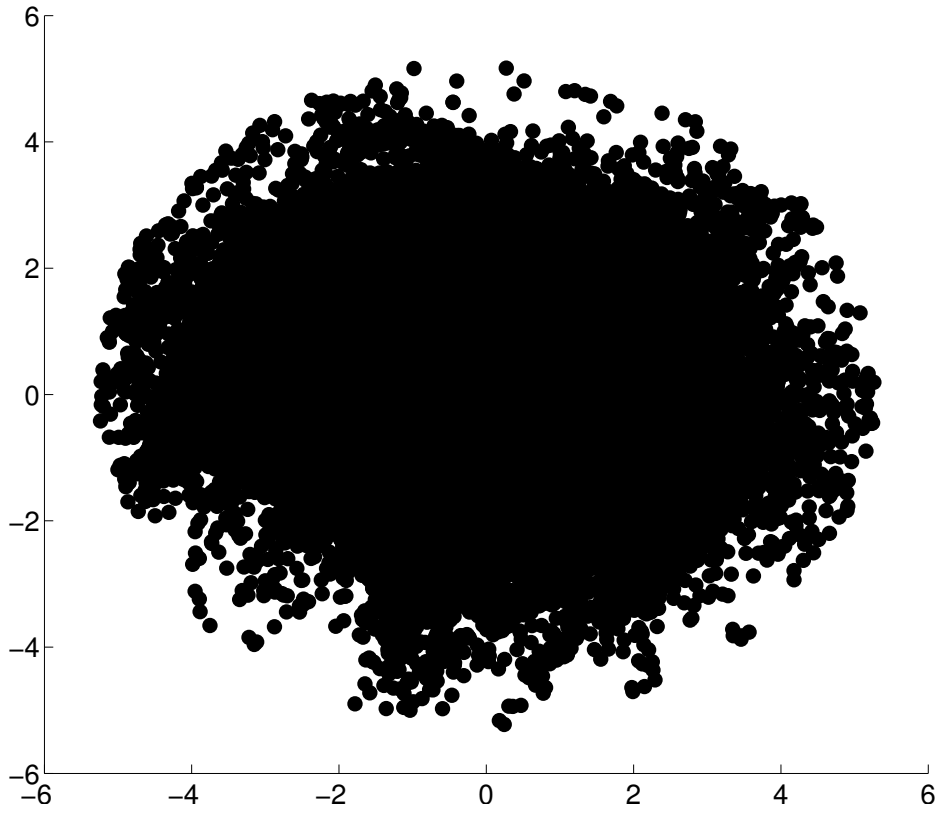

In order to define abnormality, we used a novelty detection algorithm which has proven its value in other medical and aerospace early warning systems [192, 193]. In order to quantify the departure from normality of a vector x, a novelty score z(x) is calculated as -log $p(x)$, where $p(x)$ is the unconditional probability density of x, or likelihood of x. This is calculated using equation 2.1 and priors from the normal model as follows:

$$p(x) = \sum_{j=1}^{100} p(j)p(x|j) \tag{11.2.4}$$

where $p(j)$ is the prior probability that the data x will be assigned to centre j, and $p(x|j)$ the proba-

bility of the data x conditioned on the normal model.

In accordance with previous literature, the threshold for an abnormal novelty score was set as the 99th centile of $z(x)$ for the pooled normal data [193].

11.3 Results

11.3.1 First set of input variables: rSO2 Variance, Pulse, MAP, Peripheral Saturation Variability

Visual inspection using the Neuroscale algorithm, confirmed quantitatively with novelty detection scores, revealed that the first set of variables performed very well in the majority of patients. Results from a selection of patients using the first set of variables are shown in figures 11.3 to 11.7. As can be seen throughout these examples, almost all substantial deviations from the normal model occurred in abnormal sessions. In addition, it can be seen that when the novelty score did reach the abnormality threshold in normal sessions, excursions were generally small in magnitude and duration compared to those occurring in abnormal sessions in the same patient, suggesting that the novelty detection threshold could be improved, e.g. by taking into account the length of time spent over the threshold, i.e. a persistence criteria.

Patients with multiple, heterogeneous abnormal sessions and fewer normal sessions, proved more difficult to model, with the difference in novelty scores between normal and abnormal sessions not always being clearcut, for example, DF18 (figure 11.8, see abnormal session 3 versus the unseen normal session). However it was clear that multivariate modelling was superior to univariate modelling in this individual, in whom no single physiological variable had been able to anticipate cerebral ischaemia.

Figure 11.3: The results of feeding an unseen normal session and an abnormal session through the training network for patient DF01, a 34 year old man with focal segmental glomerulosclerosis, first set of variables

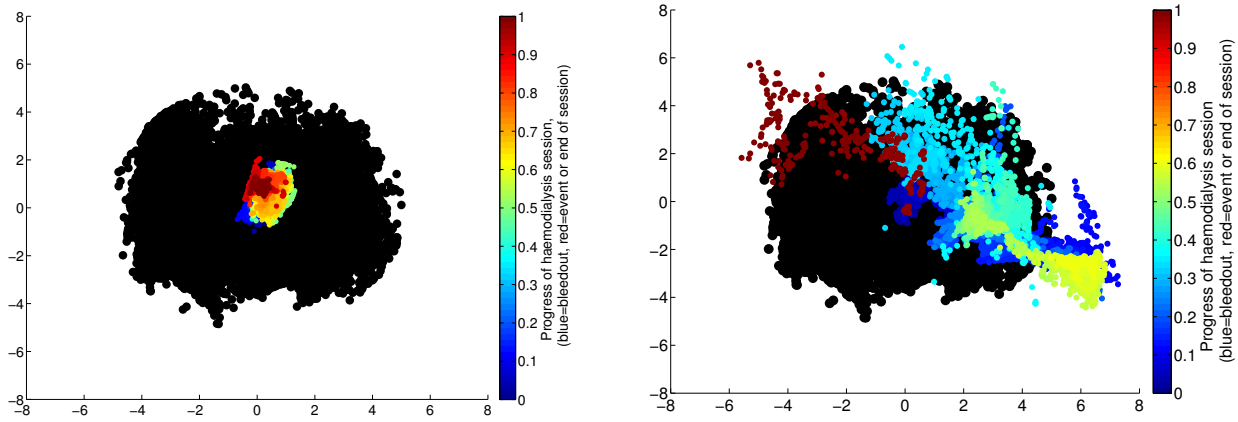

(a) Projection of unseen normal data (coloured) against training data (10 sessions, black)

(b) Projection of abnormal data (coloured) against training data (10 sessions, black)

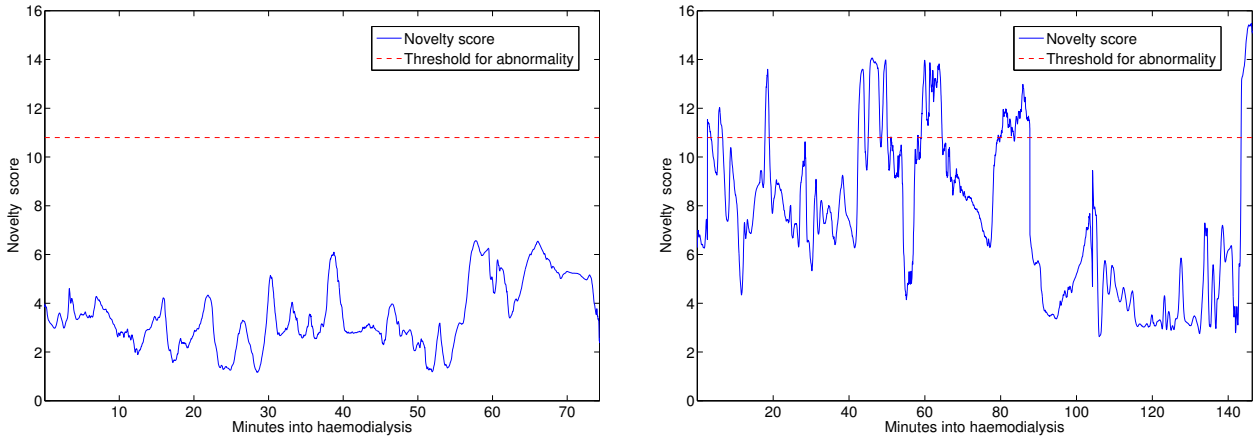

(c) Novelty score over time for unseen normal session

(d) Novelty score over time for abnormal session

Figure 11.4: The results of feeding an unseen normal session and an abnormal session through the training network for patient DF12, a 89 year old man with glomerulonephritis, first set of variables (note different scales)

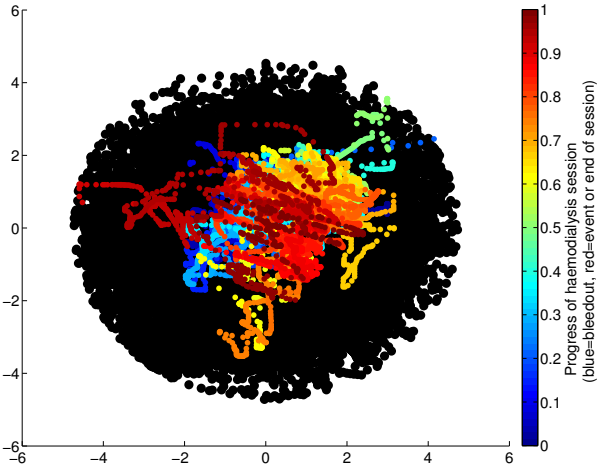

(a) Projection of unseen normal data (coloured) against training data (10 sessions, black)

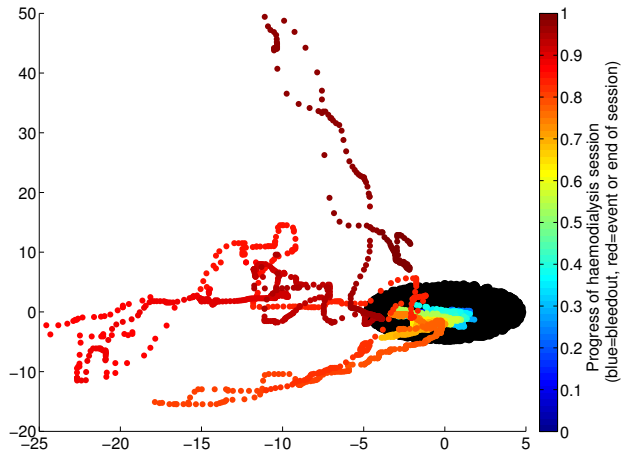

(b) Projection of abnormal data (coloured) against training data (10 sessions, black)

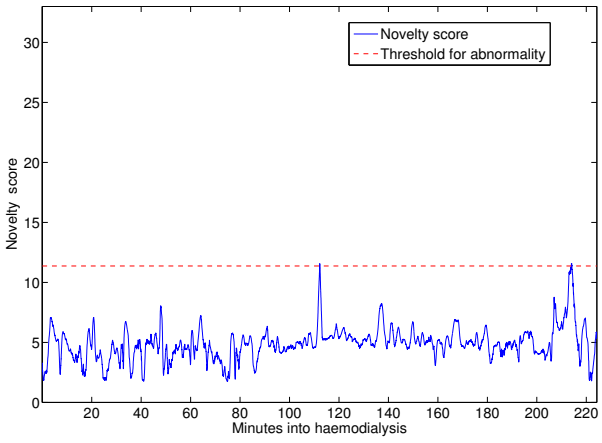

(c) Novelty score over time for unseen normal session

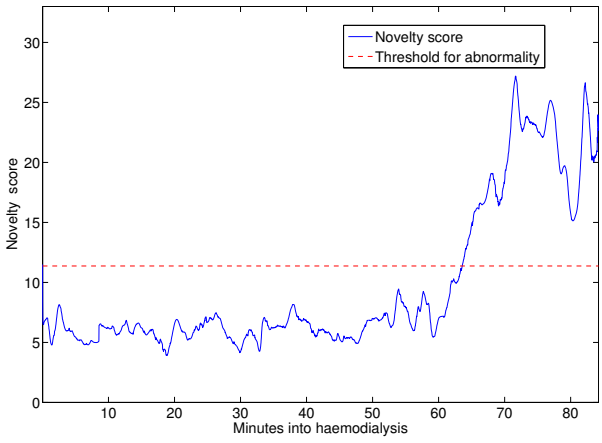

(d) Novelty score over time for abnormal session

Figure 11.5: The results of feeding an abnormal session and an unseen normal session through the training network for patient DF13, a 73 year old male with cardiorenal failure/renovascular disease, first set of variables

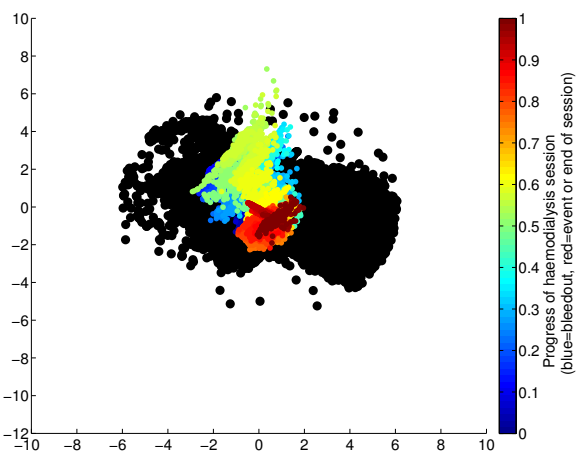

(a) Projection of unseen normal data (coloured) against training data (10 sessions, black)

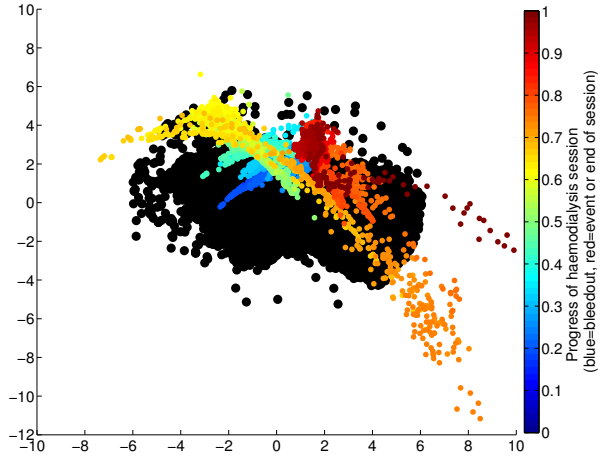

(b) Projection of abnormal data (coloured) against training data (10 sessions, black)

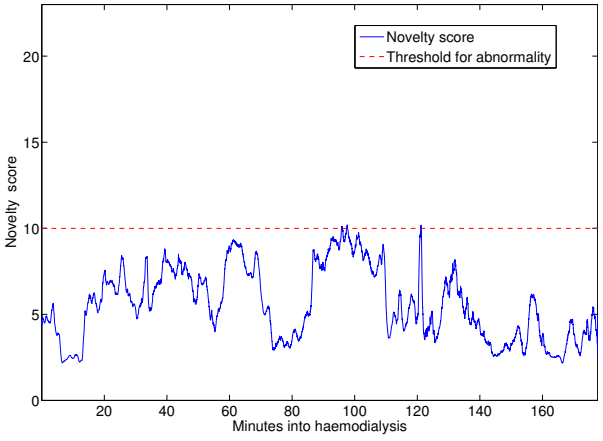

(c) Novelty score over time for unseen normal session

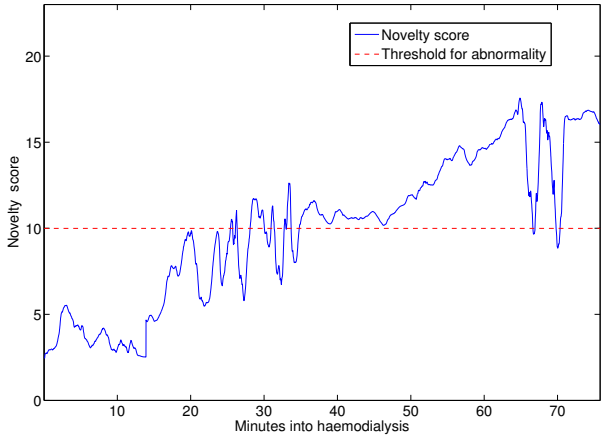

(d) Novelty score over time for abnormal session

Figure 11.6: The results of feeding an unseen normal session and an abnormal session through the training network for patient DF37, a 60 year old male with diabetic nephropathy, first set of variables (Neuroscale visualisations not shown for brevity)

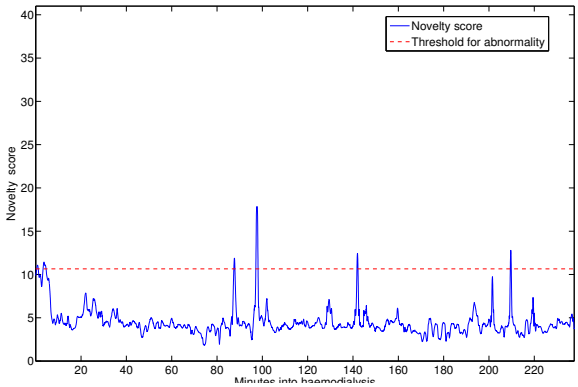

(a) Novelty score over time for unseen normal data

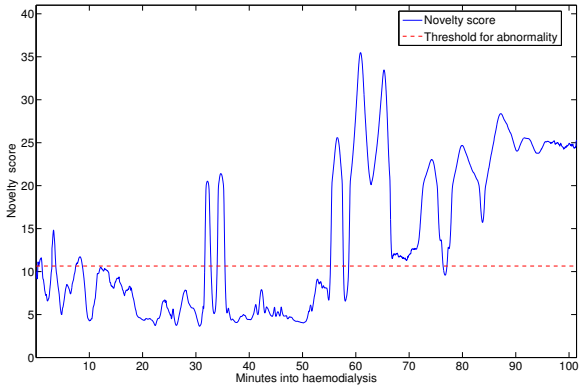

(b) Novelty score over time for first abnormal session

Figure 11.7: The results of feeding an unseen normal session and two abnormal sessions through the training network for patient DF49, a 39 year old male with IgA nephropathy, first set of variables (Neuroscale visualisations not shown for brevity)

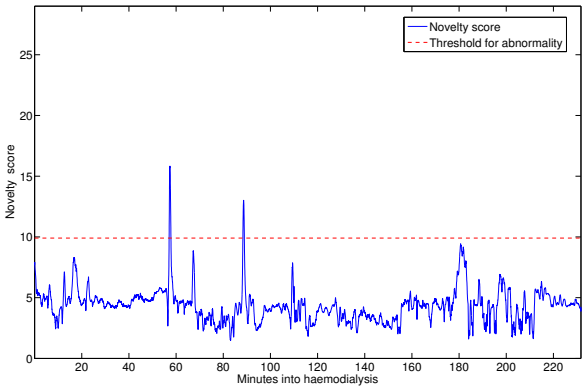

(a) Novelty score over time for unseen normal session

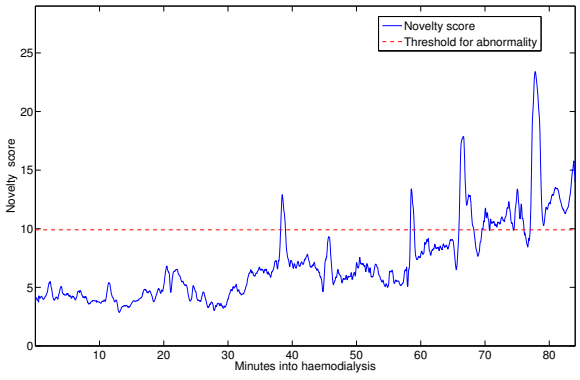

(b) Novelty score over time for first abnormal session

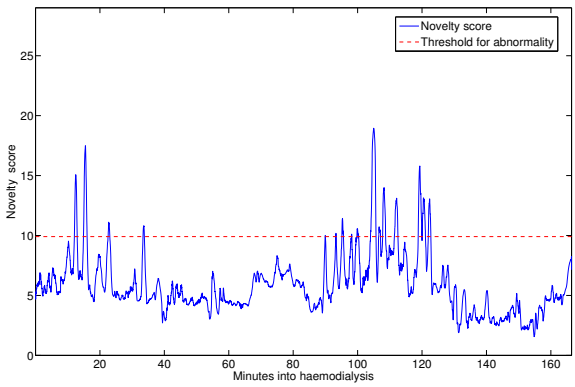

(c) Novelty score over time for second abnormal session

Figure 11.8: The results of feeding an unseen normal session and four abnormal sessions through the training network for patient DF18, a 54 year old male with diabetic nephropathy, first set of variables

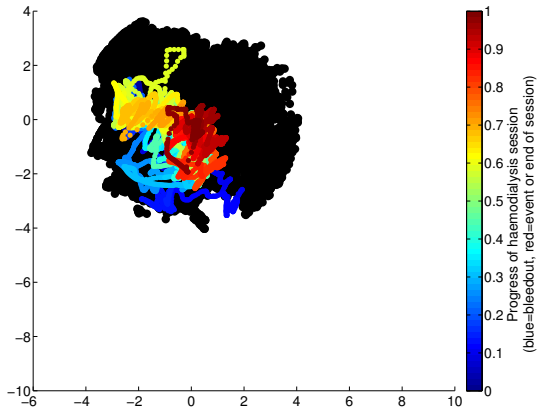

(a) Projection of unseen normal data (coloured) against training data (7 sessions, black)

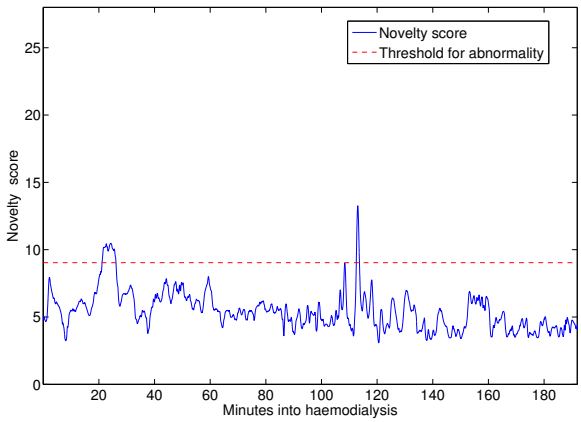

(b) Novelty score over time for unseen normal data

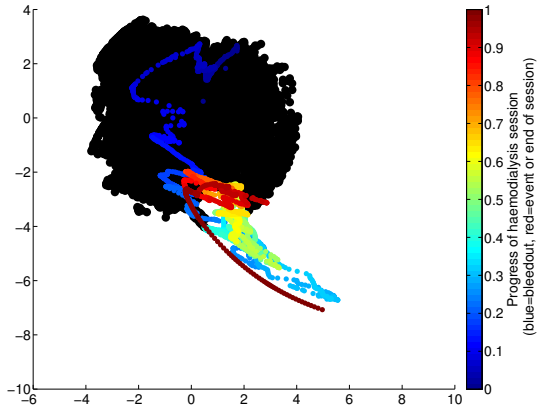

(c) Projection of first abnormal session (coloured) against training data (7 sessions, black)

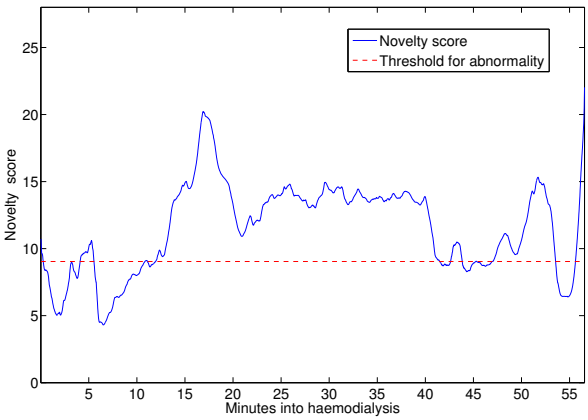

(d) Novelty score over time for first abnormal session

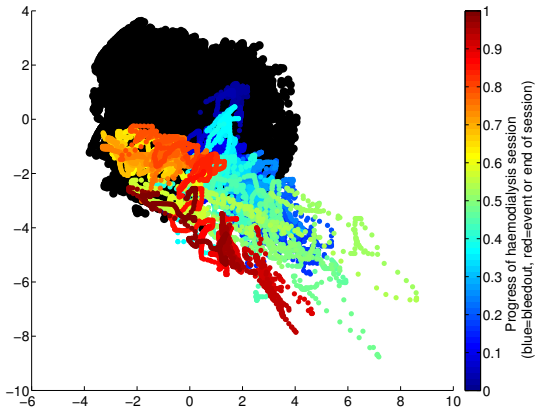

(e) Projection second abnormal session (coloured) against training data (7 sessions, black)

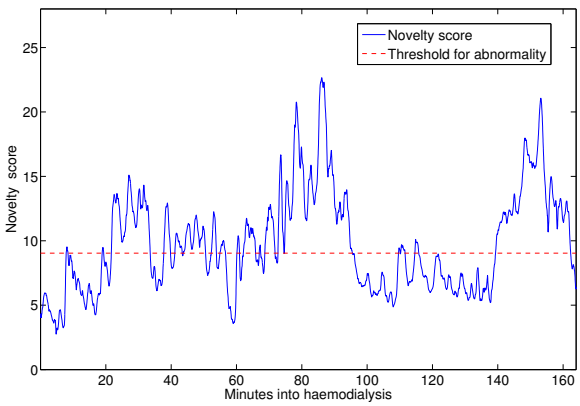

(f) Novelty score over time for second abnormal session

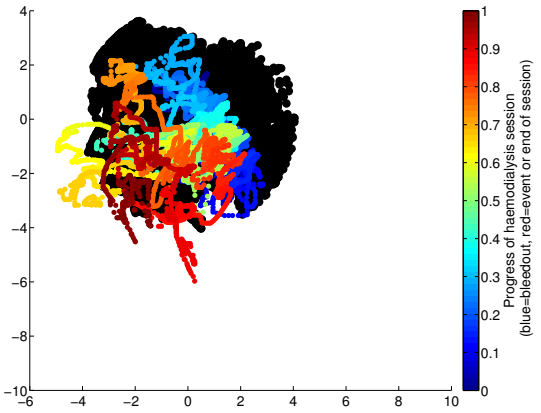

(g) Projection third abnormal session (coloured) against training data (7 sessions, black)

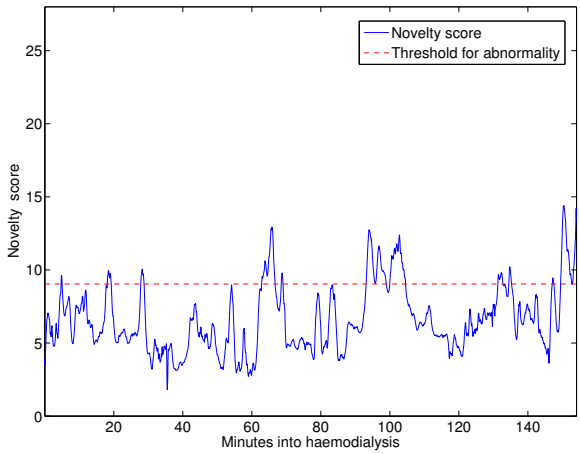

(h) Novelty score over time for third abnormal session

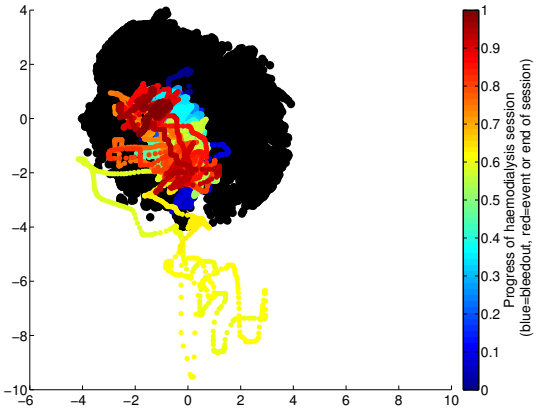

(i) Projection fourth abnormal session (coloured) against training data (7 sessions, black)

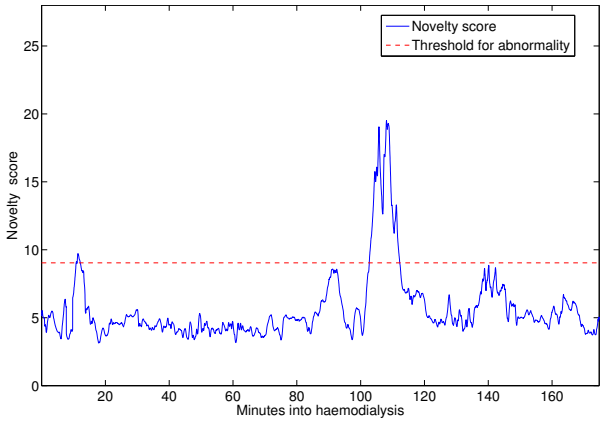

(j) Novelty score over time for fourth abnormal session

11.3.2 Second set of input variables: Respiratory Rate, Pulse, MAP, Peripheral Saturation Variability

Models based on the second set of variables, where rSO2 variance and MAP were replaced by respiratory rate and PPV (as defined in the Methods chapter), performed reasonably well but were less sensitive for abnormality in some individuals (compare figures 11.4 and 11.9 for an example for which the two sets of variables performed similarly, and figures 11.3 and 11.10 for an example for which the first set of variables was better able to identify abnormality). Univariate analysis in the last chapter demonstrated that rSO2 variance and MAP were amongst the most useful variables, so this was not unexpected: however, rSO2 and continuous MAP are not easy to measure in routine clinical practice. Results from a selection of patients using the second set of variables are shown in figures 11.9 to 11.14.

One example is notable for the extreme novelty score, and extreme deviation from the normal model (figure 11.12, first abnormal session). This was genuine data: on reviewing the time series of the four inputs and the clinical history, it was apparent that the patient had pulmonary oedema, with a respiratory rate approaching 30 breaths/min rather than his usual 16-20, and significant episodes of desaturation. This patient had two events marked by very different physiology, with the second abnormal session being much more subtle. The unseen normal session appears to deviate from the normal model on Neuroscale visualisation (although not to the same extent as the abnormal sessions). However, the use of novelty detection with four-dimensional data as inputs shows that the deviation in the normal session is in fact minimal.

Figure 11.9: The results of feeding an unseen normal session and an abnormal session through the training network for patient DF12, second set of variables (see figure 11.4 for comparison)

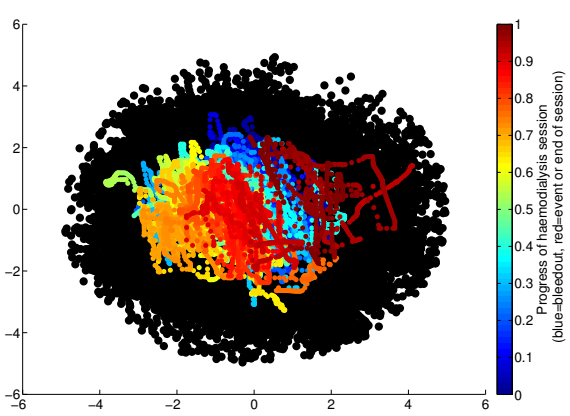

(a) Projection of unseen normal data (coloured) against training data (10 sessions, black)

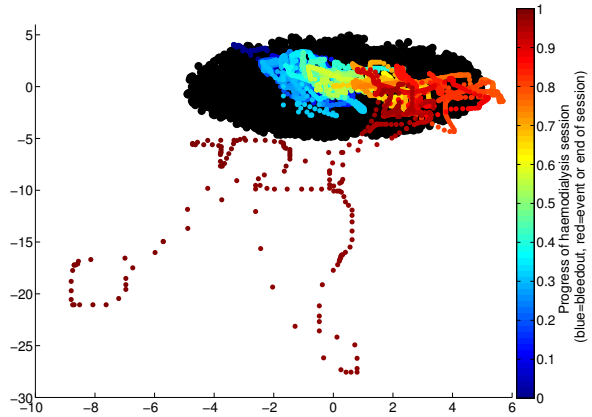

(b) Projection of abnormal data (coloured) against training data (10 sessions, black)

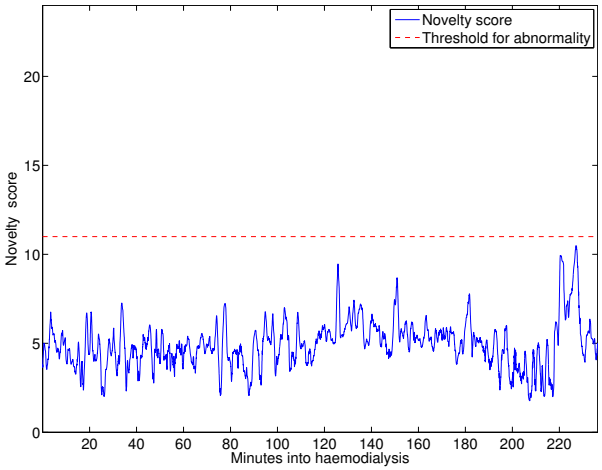

(c) Novelty score over time for unseen normal session

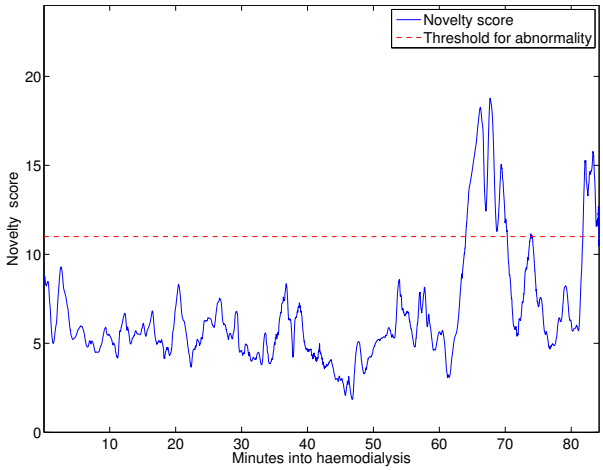

(d) Novelty score over time for abnormal session

Figure 11.10: The results of feeding an unseen normal session and an abnormal session through the training network for patient DF01, second set of variables (see figure 11.3 for comparison)

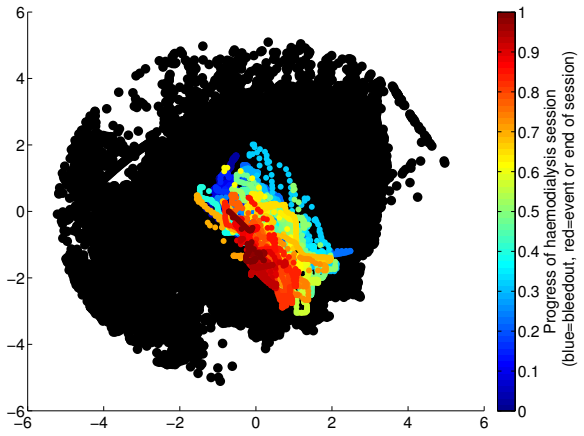

(a) Projection of unseen normal data (coloured) against training data (10 sessions, black)

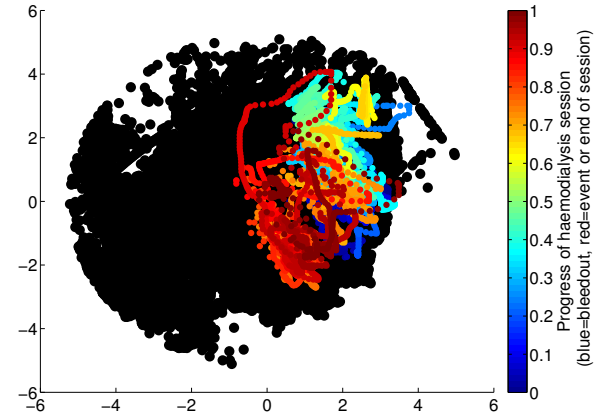

(b) Projection of abnormal data (coloured) against training data (10 sessions, black)

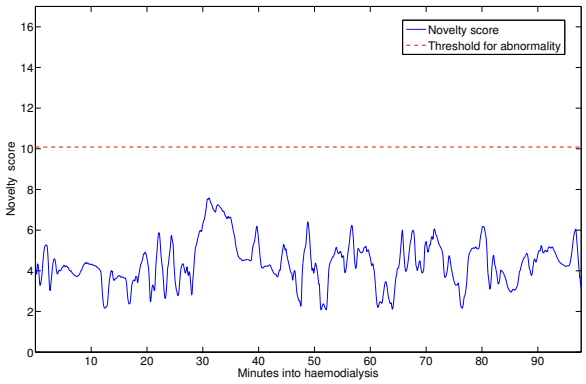

(c) Novelty score over time for unseen normal session

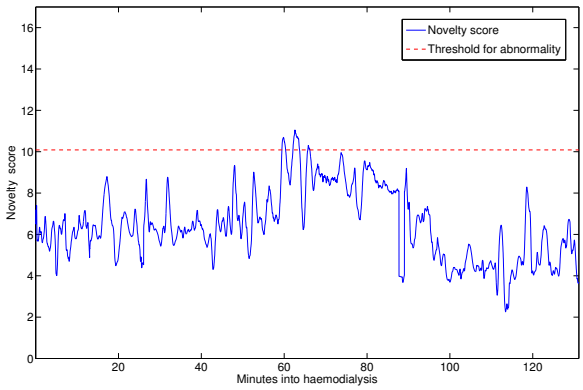

(d) Novelty score over time for abnormal session

Figure 11.11: The results of feeding an unseen normal session and an abnormal session through the training network for patient DF45, a 35 year old female with sickle cell disease, second set of variables

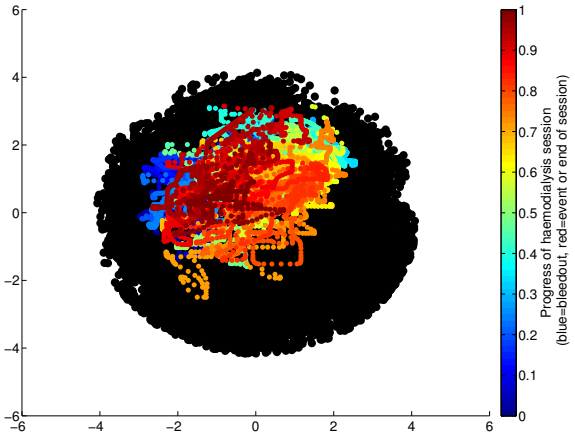

(a) Projection of unseen normal data (coloured) against training data (10 sessions, black)

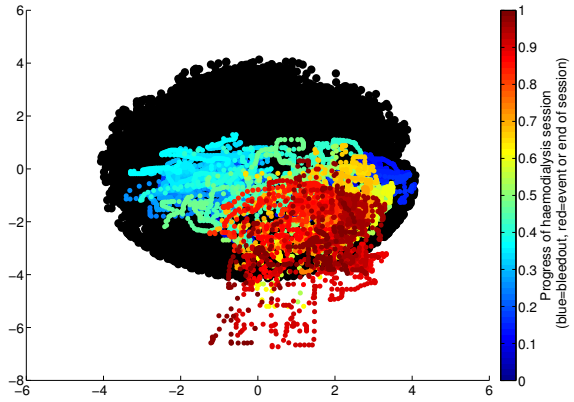

(b) Projection of abnormal data (coloured) against training data (10 sessions, black)

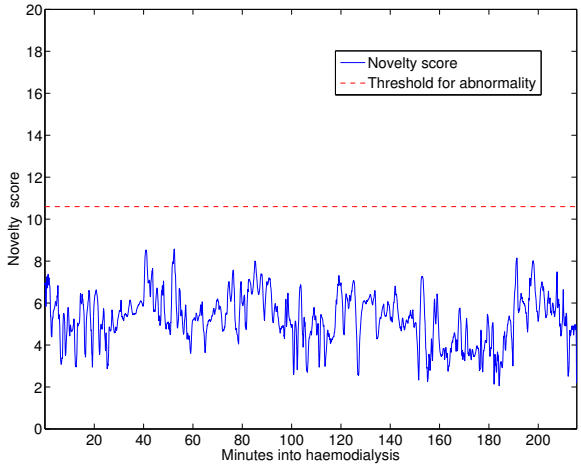

(c) Novelty score over time for unseen normal session

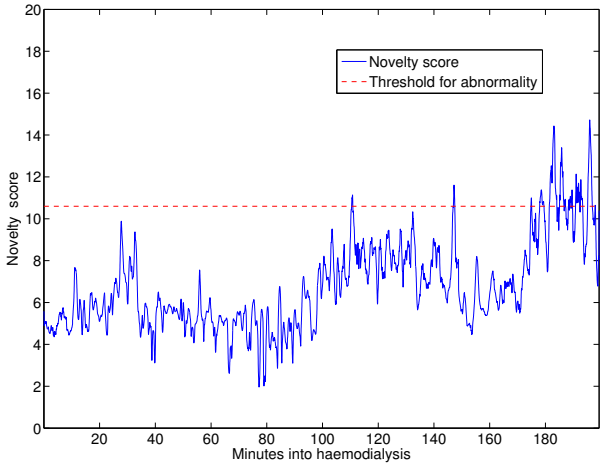

(d) Novelty score over time for abnormal session

Figure 11.12: The results of feeding two abnormal and an unseen normal session through the training network for patient DF60, a 63 year old male with IgA nephropathy, second set of variables. Note the change in scale for the first abnormal session.

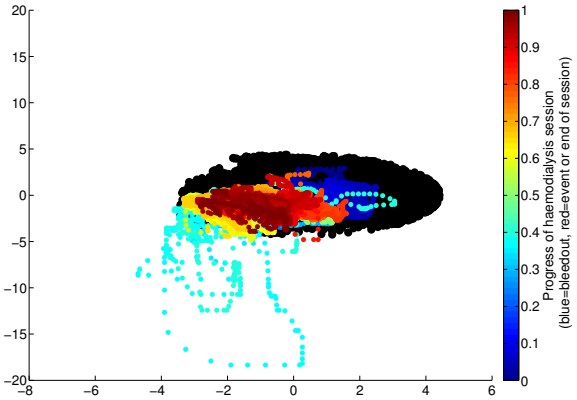

(a) Projection of unseen normal data (coloured) against training data (6 sessions, black)

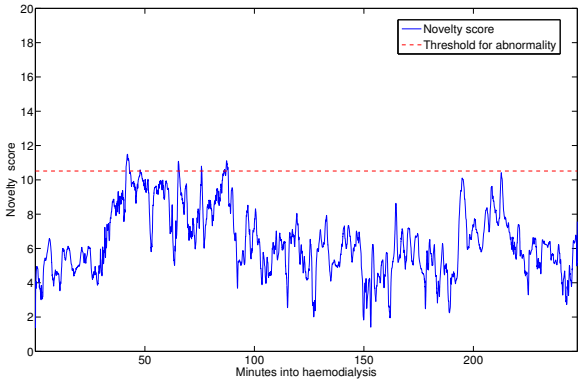

(b) Novelty score over time for unseen normal session

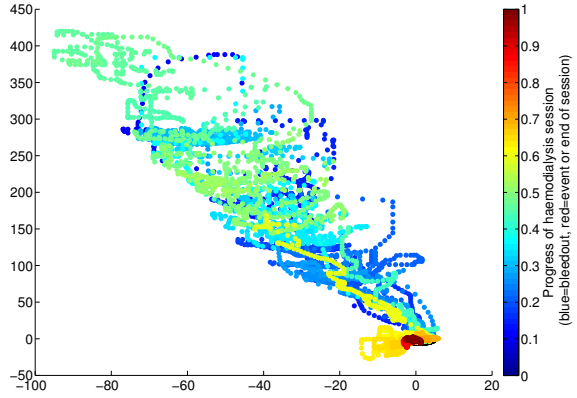

(c) Projection of first abnormal session (coloured) against training data (6 sessions, black)

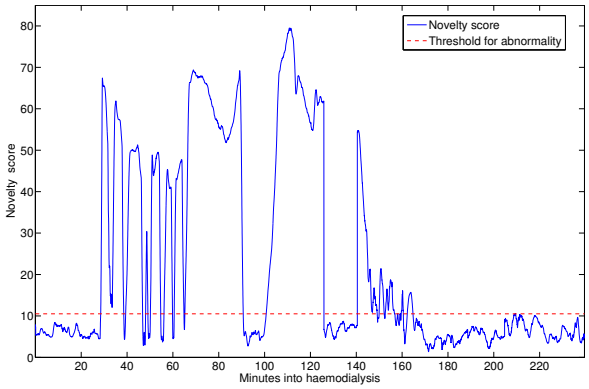

(d) Novelty score over time for first abnormal session

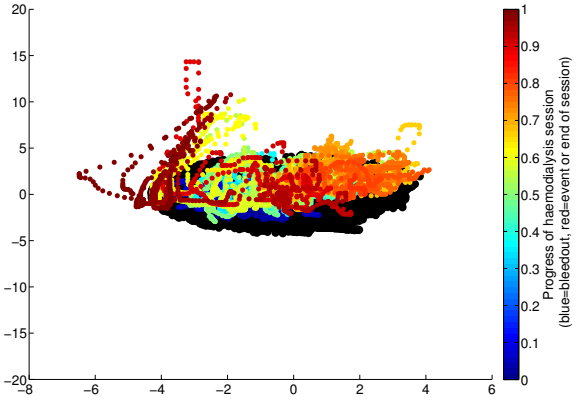

(e) Projection of second abnormal session (coloured) against training data (6 sessions, black)

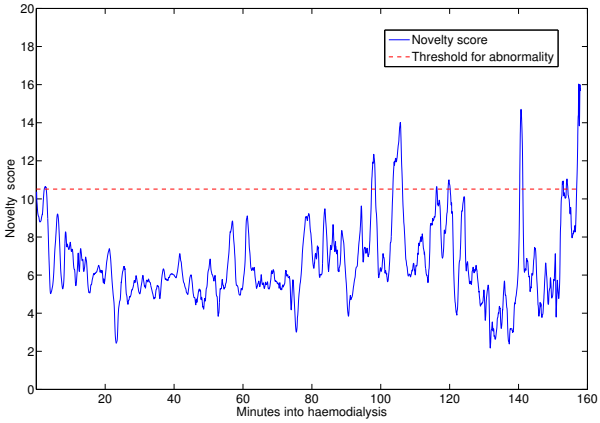

(f) Novelty score over time for second abnormal session

Figure 11.13: The results of feeding two abnormal sessions and an unseen normal session through the training network for patient DF05, a 53 year old male with polycystic kidney disease, second set of variables (Neuroscale visualisations not shown for brevity)

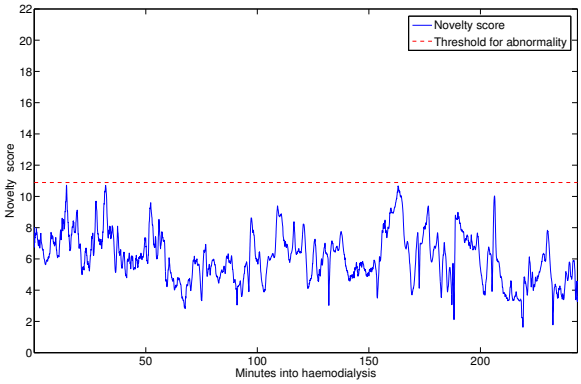

(a) Novelty score over time for unseen normal data

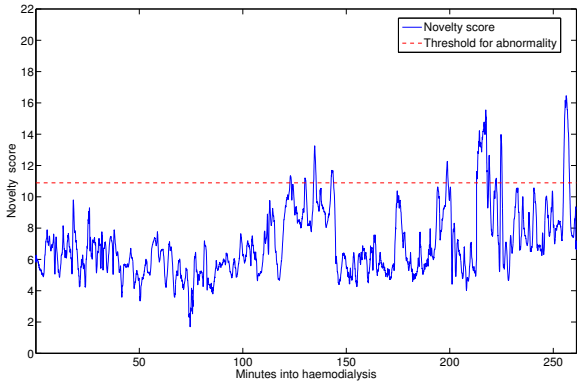

(b) Novelty score over time for first abnormal session

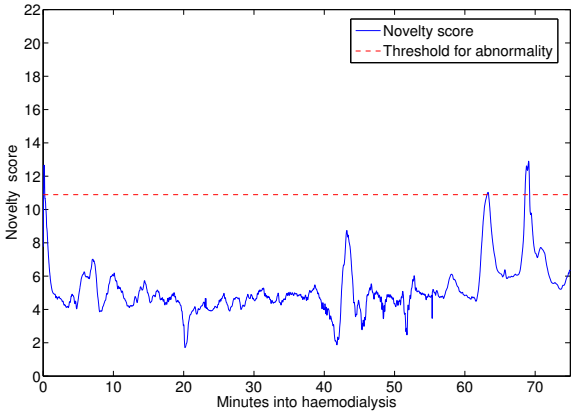

(c) Novelty score over time for second abnormal session

Figure 11.14: The results of feeding two abnormal sessions and an unseen normal session through the training network for patient DF43, a 26 year old male with reflux nephropathy, second set of variables (Neuroscale visualisations not shown for brevity)

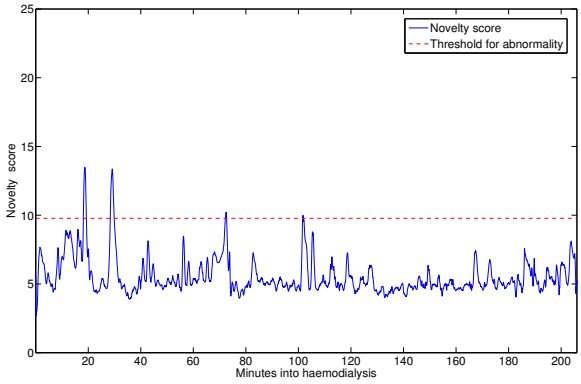

(a) Novelty score over time for unseen normal data

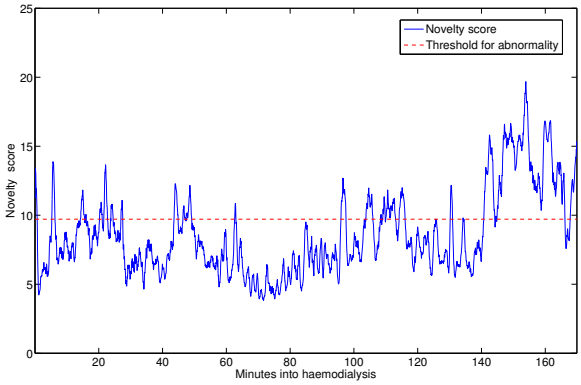

(b) Novelty score over time for first abnormal session

In all patients, the final set of variables (PPG heart rate, PPG PPV, peripheral saturations and peripheral saturation variability) had very poor specificity and are not further considered. It is probable that deriving all data streams from a single probe, though preferable for the patient, reduced the benefit of data fusion. Although these individuals had good-quality data and stringent SQIs were applied to the time series, it is still possible for artefact, e.g. from movement, to create transient abnormalities in all four data streams.

11.4 Discussion

In this preliminary analysis, data fusion techniques created promising personalised models capable of predicting tissue deoxygenation on HD, generally outperforming univariate predictive models on qualitative analysis. Formal quantitative analysis, with calculation of patient-level sensitivity and specificity, was not performed at this juncture as it was apparent that further work was first needed on setting the novelty threshold. For most patients, it was possible to empirically define an individualised threshold which would correctly classify all sessions in that patient, but this is not a principled or easily generalisable approach. However, the probabilistic method of threshold determination did not appear to perform as well in this application as in other settings [193], and borderline false positives were not uncommon. Using the thresholds presented here would both underestimate the usefulness of the models and limit clinical utility. A persistence criteria might substantially improve performance, i.e. taking into account the duration as well as the magnitude of abnormality. There are a number of methods of tackling the problem of novelty thresholds, which have been recently reviewed, but exceed the scope of this thesis [194].

It is always difficult to define a threshold on what is essentially a continuous spectrum of abnormality, and of course the definition of cerebral ischaemia is arbitrary. A session may show significant deterioration in tissue oxygenation but not reach a decrease of -15% in rSO2: therefore some normal sessions are going to be "more normal" than others. Information may be lost by not considering the magnitude and duration of threshold violation, i.e. the area above the novelty threshold. It is clear that patients with multiple, heterogeneous events require more training data in order to create accurate models. The multivariate models performed best in the patients with at least 5 normal sessions for every abnormal session. Such an individual would need to be monitored over a more prolonged period of time to generate a usable model.

The novelty threshold was often crossed a significant time before the actual ischaemic event. We considered threshold attainment at any time during a session in which cerebral ischaemia subsequently developed to be a true positive, as it is physiologically plausible that subtle deviation from the expected trajectory could occur some time before the actual event, and alterations in the dialysis prescription at this stage could well prevent later decompensation. Moreover, in keeping with the results from the previous chapter it was apparent that when abnormality did develop, it was often fluctuating rather than continuous.

Comparison with results from the previous chapter suggests that multivariate models would not outperform univariate models in all cases - e.g. the individual components of the third set of input variables proved useful in a number of patients on univariate analysis, but when combined in multivariate models performed poorly. Univariate models had the advantage that time of dialysis was taken into account by separating data into sliding 15 minute windows relative to bleedout. Consequent to the effect of fluid removal and warming, normal physiology for the first hour of dialysis is not the same as normal physiology for the final hour of dialysis. It would be possible to create similar sliding 15 minute windows using neuroscale techniques, but it would be computationally very intense, and possibly require more data than 7-9 normal sessions could provide. Therefore we considered all training data together regardless of stage of dialysis. This chapter represents a preliminary investigation using a simple topographical technique. More advanced data fusion procedures, e.g. multivariate time series analysis using Gaussian processes, are likely to better categorise normal and abnormal data, taking into account the stage of treatment [195].

Although HD is a stereotypical procedure, performed multiple times within the same individual, fluid balance may change from one session to the next, with substantial effects on expected physiology [8]. Creating a separate model for sessions following the "long break", where patients go without dialysis for 72 hours rather than the usual 48 hours, may improve sensitivity and specificity. Normalising for body weight would be another possibility. We had insufficient data to test these hypotheses.

Finally, it must be borne in mind that this is a retrospective study, and as such the models may be overfitted. The models ultimately need to be tested on a new dataset, which would involve gathering more data on the same patients. The practicality of monitoring must also be considered. rSO2 variance

was one of the most promising predictive variables for eventual cerebral ischaemia, generally becoming abnormal some time before the event (i.e. it did not simply reflect the terminal decline in cerebral tissue oxygenation). However, it is not something that is practical to measure routinely in a dialysis unit. A two-probe solution, plus information from the dialysis machine itself (which does not require additional monitoring to be attached to the patient) might be the optimal compromise.

11.5 Conclusion

Data fusion techniques have great promise for predicting cerebral ischaemia on HD on these preliminary models, and are able to detect abnormality in a timely fashion in many cases where univariate techniques fail. More advanced data fusion procedures, e.g. multivariate time series analysis using Gaussian processes, are likely to better categorise normal and abnormal data, taking into account the stage of treatment [195].

Chapter 12

Conclusions and Future Work

12.1 Primary Objectives

Our first primary objective was to model the dynamic relationship between blood pressure, real-time symptoms, and downstream organ ischaemia during HD. Despite their use in clinical practice, we found that blood pressure thresholds alone have a poor trade off between sensitivity and specificity for predicting downstream tissue ischaemia during HD. The duration and magnitude of excursions either below a δ MAP 40mmHg or absolute MAP of 60mmHg best predicted the total depth and duration of cerebral ischaemia for a given dialysis session. These indices likely represent the most extreme hypotension in the population, and are in keeping with the SBP 90mmHg threshold identified by the sole study to date linking intra-dialytic blood pressure to hard outcomes [4]. However, waiting until these thresholds were breached would result in over two thirds of ischaemic events being missed over the whole population.

We found that the performance of blood pressure thresholds could be improved by stratification for the presence or absence of cerebral autoregulation, and personalising thresholds according to the individual lower limit of autoregulation. Over a third of the HD patients sampled had absent autoregulation, and isolating these individuals resulted in a very respectable ROC curve for absolute MAP alone as a predictor of ischaemic events, with 70mmHg being the optimal threshold. For individuals with intact autoregulation, the optimal threshold was +10mmHg from the lower limit. If the presence of autoregulation and its limits could be established for each HD patient, these thresholds would be a substantial improvement to the population-based blood pressure targets currently used in clinical practice.

Ideally, next steps would include a controlled trial in a larger number of patients, assessing the benefit of autoregulation-guided blood pressure targets on short term outcomes such as patient symptoms and wellbeing, as well as longer term outcomes such as cognitive function. It was possible to model the lower limit of autoregulation with reasonable accuracy using baseline blood pressure and age, but unfortunately the absence of autoregulation could not be reliably predicted on the basis of demographic and clinical factors. Therefore, this approach would require patients to undergo monitoring with cerebral NIRS for a number of HD sessions, sufficient to construct their individual autoregulation curve and estimate their personal threshold for onset of ischaemia. Whilst a method of continuous blood pressure monitoring would be ideal, we have shown that it is possible to construct autoregulation curves with NIBP measurements at 15 minute intervals. To temper the cost and inconvenience in real-world practice, the technique could be limited to incident or vulnerable patients, so that only one NIRS machine would be needed for a renal unit. Targeting a higher risk population would have the additional benefit of improving the positive predictive value of autoregulation-guided blood pressure thresholds, which remained suboptimal, though surpassing the performance of population based blood pressure targets.

Our second primary objective was to predict the development of intra-dialytic cerebral ischaemia using probabilistic models based on one or more physiological data streams, chosen from a range of cardiovascular, respiratory and dialysis-related parameters. We confirmed previous unpublished work showing that personalised models were necessary because of the huge heterogeneity of both normal and abnormal physiology at the population level. We were able to demonstrate that the development of cerebral desaturation on HD could be anticipated from earlier deviations of univariate physiological data from the expected trajectory for a given patient. The most useful physiological data streams varied between patients, but frequently included peripheral saturation variance, rSO2 variance, heart rate and MAP. The sensitivity of univariate modelling was found to be limited by the heterogeneity of abnormal events even within one individual. Therefore the final iteration was a multivariate personalised approach, i.e. data fusion. In this preliminary analysis, data fusion techniques created promising personalised models capable of predicting tissue deoxygenation on HD. They did not consistently outperform univariate predictive models in all individuals, but the univariate models had the advantage that time into HD could be taken into account. Future efforts should focus on applying more sophisticated probabilistic modelling techniques, such as Gaussian processes, to the wealth of multivariate time series data gathered during this thesis, with prospective testing of the models on the same patients from which they were derived.

12.2 Secondary Objectives

A number of secondary objectives focused on the agreement between haemodynamic variables measured by the Finometer compared to usual clinical technology. There was a large error in Finometer-measured absolute cardiac output in this population, compared to the gold standard of ultrasound dilution. However there was a good correlation for trend in cardiac output, and post-calibration agreement was reasonable, albeit with limits that did not quite reach clinical standards. Patients with greater HD vintage had poorer agreement between Finometer and ultrasound dilution measurements. We also assessed the agreement between oscillometer and Finometer measured blood pressure, accepting neither was a gold standard method. Agreement was suboptimal but comparable to that reported for oscillometer and intra-arterial line measurements (for MAP, bias was -3.5mmHg and limits +/- 27mmHg). Diabetes vintage, obesity and PVD accounted for much of the patient-level variation in agreement.

We investigated the potential of non-invasive surrogate measures of continuous blood pressure using the Finometer data as reference. It was not possible to reliably estimate changes in systemic blood pressures from dynamic access pressures. The δarterial access pressure measured from brachial AVFs showed the greatest relationship with systemic blood pressure changes, but the correlation was weak. We found that the majority of patients had a significant negative correlation between PTT and Finometer-measured blood pressure, but the strength of the relationship was generally weak, and not only variable between individuals, but between sessions within the same patient. The relationship between PTT and blood pressure is altered by a number of factors that change dynamically during HD: it is possible that frequent recalibration will to be necessary to track blood pressure in this population. However, it should be borne in mind that the Finometer arterial waveform has not been validated against the intra-arterial waveform in HD patients, and thus it is possible that these results were at least partly due to errors arising from Finometer measurements. Further work in the search for a non-invasive, convenient, affordable surrogate for continuous blood pressure must use intra-arterial lines as the reference measurement, or at least run a comparison between intra-arterial and Finometer-measured blood pressure in a substantial body of HD patients.

The final objective was to assess the relationship between intra-dialytic physiology, particularly cere-

bral oxygenation, and deterioration in cognitive function tests. In keeping with other investigators, we identified significant abnormalities in executive cognitive function in this HD population [34, 47, 35]. The key, novel finding was that cumulative intra-dialytic exposure to cerebral ischaemia, arbitrarily defined as less than 15% of baseline value, corresponded to change in executive cognitive function. Cerebral desaturation far outperformed relative or absolute blood pressure thresholds in terms of predicting decline in cognition. Findings must now be confirmed in a larger cohort of patients. Ultimately a controlled trial pairing continuous cerebral tissue oxygenation monitoring with interventions such as cooling or biofeedback dialysis might help to establish if such interventions can improve intra-dialytic cerebral perfusion; following up with robust functional tests would then allow detection of any clinically significant cerebral protection. Supporting information would also arise from a trial, proposed above, into the benefit of autoregulation-guided blood pressure targets on long term cognitive function.

List of Figures

3.1 Counts for cerebral desaturation AUC ((%* minutes below threshold)$^{0.5}$) for sessions where ischaemia threshold was reached 43
3.2 Univariate relationship between relative MAP threshold and onset of cerebral desaturation 48
3.3 Univariate relationship between absolute MAP threshold and onset of cerebral desaturation 49
3.4 Sensitivity and specificity of change in MAP for predicting onset of cerebral ischaemia . . 52
3.5 Sensitivity and specificity of absolute MAP for predicting onset of cerebral ischaemia . . . 53
3.6 Best two part model for total cerebral ischaemia during a HD session 55
3.7 Patient specific intercepts for (a) the count and (b) the hurdle parts of the model, with 95% confidence intervals (log odds) 56

4.1 Curve fitting method of determining limits of cerebral autoregulation 66
4.2 MAP versus cerebral rSO2 in a patient with intact autoregulation, third degree polynomial fitted 69
4.3 MAP versus cerebral rSO2 in a patient with no autoregulation, linear model fitted 70
4.4 Histogram of probability densities for lower limit of cerebral autoregulation 71
4.5 Relationship between MAP and COX at the population level 72
4.6 Relationship between MAP and cerebral rSO2 at the population level 73
4.7 Example of a chronically hypertensive patient with loss of autoregulation at unusually high MAP 74
4.8 Relationship between baseline MAP and lower limit of autoregulation (with line of best fit, Pearson's correlation 0.73) 76
4.9 Predicted versus actual lower limits of autoregulation 77
4.10 Sensitivity and specificity of absolute MAP thresholds for onset of cerebral ischaemia in patients WITHOUT autoregulation 80

4.11 ROC curve: absolute MAP thresholds for predicting onset of cerebral ischaemia in patients WITHOUT autoregulation . . . 81
4.12 Sensitivity and specificity of MAP thresholds relative to lower autoregulation limit 82
4.13 Performance of MAP for predicting cerebral desaturation: personalised models 84

5.1 Bland-Altman plots for difference between oscillometer and Finometer MAP 95
5.2 Bland-Altman plots for difference between oscillometer and Finometer SBP 96
5.3 Bland-Altman plots for difference between oscillometer and Finometer DBP 97
5.4 Finometer versus oscillometer MAP, all patients 98
5.5 Patient-average means and standard deviations for difference between oscillometer and Finometer measurements 101
5.6 Bland Altmann plots for individual patients 102

6.1 Measurement differences between Finometer and ultrasound dilution cardiac output, expressed as percentage of absolute cardiac output 111
6.2 Measurement differences between Finometer and ultrasound dilution cardiac output, absolute values 112
6.3 Box plots of within-patient differences between Finometer and ultrasound dilution cardiac output measurements 113
6.4 Relative change in cardiac output between baseline and mid-dialysis 115
6.5 Measurement differences between calibrated Finometer and ultrasound dilution cardiac output, two hours after calibration (expressed as percentage of absolute cardiac output) . 116
6.6 Measurement differences between calibrated Finometer and ultrasound dilution cardiac output, two hours after calibration (absolute values) 117

7.1 PTT was defined as the time between the R wave (point A) and the mid-point of the PPG upstroke (point B) 123
7.2 Diagram of a basic HD circuit illustrating the sites of arterial and venous access pressure measurement [161] 125
7.3 Session-level correlations between PTT and Finometer MAP 128
7.4 Session-level correlations between PTT and Finometer SBP 129
7.5 MAP versus PTT for a haemodialysis session in a 53 year old man with polycystic kidneys, R= -0.69, p <0.001 130

7.6 MAP versus PTT for a haemodialysis session in a 30 year old man with hypertensive renal disease and fluid overload, R= -0.76, p <0.001 131
7.7 MAP versus PTT for a haemodialysis session in a 56 year old man with longstanding diabetes, R= -0.51, p <0.001 132
7.8 MAP versus PTT for a haemodialysis session in the same patient as figure 19, R= +0.20, p <0.002 133
7.9 Patient-specific intercepts for session-level correlation between PTT and MAP 134
7.10 Absolute MAP versus absolute PTT for all sessions in a 34 year old male patient 137
7.11 Relative MAP versus relative PTT for all sessions in a 34 year old male patient 138
7.12 Absolute SBP versus absolute PTT for all sessions in a 34 year old male patient 139
7.13 Relative SBP versus relative PTT for all sessions in a 34 year old male patient 140
7.14 Relationship between δarterial needle pressures and δMAP, all AVFs (regression terms for access pressures as covariate and MAP as dependent variable) 142
7.15 Relationship between δarterial needle pressures and δMAP, brachial AVFs only (regression terms for access pressures as covariate and MAP as dependent variable) 143
7.16 Measurement differences between δarterial needle pressures and δMAP, all AVFs 144
7.17 Measurement differences between δarterial needle pressures and δMAP, brachial AVFs . . 145
7.18 Session-level correlations between arterial access pressure and Finometer MAP, all AVFs . 148
7.19 Session-level correlations between arterial access pressure and oscillometer MAP, all AVFs 148
7.20 Variation in session-level correlations (x-axis) between patients (represented by numbers on y axis) 149
7.21 Standard deviation of differences between δarterial access pressure and δMAP (Finometer) for each patient 150
7.22 Mean difference between δarterial access pressure and δMAP (Finometer) for each patient 150
7.23 Box plots of within-patient differences between δarterial access pressure and δMAP (Finometer), brachial AVFs only 152
7.24 Plot of δarterial access pressure and δMAP for best example patient 153
7.25 Measurement differences between δarterial needle pressures and δMAP for best example patient 154

8.1 Histogram of baseline cerebral rSO2 163
8.2 Baseline 3MS scores against age for this population 164

8.3 Probability densities of follow up TTB scores against baseline TTB scores (the second peak results from the use of a cutoff when more than 5 minutes was required to complete the task) . . . 167
8.4 Follow up 3MS scores against age for this population . . . 168

9.1 Absolute MAP in normal and abnormal sessions . . . 182
9.2 Relative MAP in normal and abnormal sessions . . . 183
9.3 Heart rate in normal and abnormal sessions . . . 184
9.4 Change in heart rate in normal and abnormal sessions . . . 185
9.5 Normalised low frequency power in normal and abnormal sessions . . . 186
9.6 Cardiac output in normal and abnormal sessions . . . 187
9.7 Change in PPG amplitude in normal and abnormal sessions . . . 188
9.8 Relative blood volume in normal and abnormal sessions . . . 189
9.9 Finometer pulse pressure variation in normal and abnormal sessions . . . 190
9.10 Respiratory rate in normal and abnormal sessions . . . 191
9.11 Peripheral saturations in normal and abnormal sessions . . . 192
9.12 Fistula (arterialised) saturations in normal and abnormal sessions . . . 193
9.13 Central venous saturations in normal and abnormal sessions - patients with Tesio only . . . 194
9.14 Peripheral saturation variability in normal and abnormal sessions . . . 195
9.15 Change in cerebral oxygenation in normal and abnormal sessions . . . 196
9.16 RBV during hour 1 in sessions with and without later development of cerebral ischaemia . . . 199
9.17 Comparison of RBV data from sessions with and without later development of cerebral ischaemia . . . 200
9.18 MAP during hour 3 in sessions with and without later development of severe hypotension 201
9.19 Comparison of MAP data from sessions with and without later development of severe hypotension . . . 202
9.20 PPV during hour 4 in sessions with and without later development of severe hypotension 203
9.21 Comparison of PPV data from sessions with and without later development of severe hypotension . . . 204
9.22 PPV during hour 1 in sessions with and without later development of cerebral ischaemia . . . 205
9.23 Comparison of PPV data from sessions with and without later development of cerebral ischaemia . . . 206

10.1 Peripheral saturation variability in one abnormal and two normal abnormal sessions, plotted against two different normal envelopes in patient DF12. The "test" normal session is the one that has been excluded when constructing that particular normal envelope. 213
10.2 MAP in one abnormal and two normal abnormal sessions, plotted against two different normal envelopes in patient DF12. The "test" normal session is the one that has been excluded when constructing that particular normal envelope. 214
10.3 Heart rate in one abnormal and two normal abnormal sessions, plotted against two different normal envelopes in patient DF12. The "test" normal session is the one that has been excluded when constructing that particular normal envelope. 215
10.4 Peripheral saturations in one abnormal and two normal abnormal sessions, plotted against two different normal envelopes in patient DF12. The "test" normal session is the one that has been excluded when constructing that particular normal envelope. Peripheral saturations did not prove useful in distinguishing normal and abnormal sessions in this individual. 216
10.5 Respiratory rate in one abnormal and two normal abnormal sessions, plotted against two different normal envelopes in patient DF12. The "test" normal session is the one that has been excluded when constructing that particular normal envelope. Respiratory rate did not prove useful in distinguishing normal and abnormal sessions in this individual. 217
10.6 An example of a common pattern of physiological abnormality in eventful sessions. Intermittent, infrequent excursions beyond the 95% limits occur over a prolonged period before the final event of cerebral desaturation at 154 minutes into dialysis) 224

11.1 Structure of radial basis function network used in this analysis. The output from each output node is a linear combination of the weighted outputs from all the centres, plus a term for bias specific to each output node, as shown in equation 2.3. W=weight, L=output node, j=centre 230
11.2 Two dimensional representation of pooled training data from patient DF49 (9 sessions), 129,600 data points 232
11.3 The results of feeding an unseen normal session and an abnormal session through the training network for patient DF01, a 34 year old man with focal segmental glomerulosclerosis, first set of variables 234

11.4 The results of feeding an unseen normal session and an abnormal session through the training network for patient DF12, a 89 year old man with glomerulonephritis, first set of variables (note different scales) 235
11.5 The results of feeding an abnormal session and an unseen normal session through the training network for patient DF13, a 73 year old male with cardiorenal failure/renovascular disease, first set of variables 236
11.6 The results of feeding an unseen normal session and an abnormal session through the training network for patient DF37, a 60 year old male with diabetic nephropathy, first set of variables (Neuroscale visualisations not shown for brevity) 237
11.7 The results of feeding an unseen normal session and two abnormal sessions through the training network for patient DF49, a 39 year old male with IgA nephropathy, first set of variables (Neuroscale visualisations not shown for brevity) 237
11.8 The results of feeding an unseen normal session and four abnormal sessions through the training network for patient DF18, a 54 year old male with diabetic nephropathy, first set of variables 238
11.9 The results of feeding an unseen normal session and an abnormal session through the training network for patient DF12, second set of variables (see figure 11.4 for comparison) 241
11.10 The results of feeding an unseen normal session and an abnormal session through the training network for patient DF01, second set of variables (see figure 11.3 for comparison) 242
11.11 The results of feeding an unseen normal session and an abnormal session through the training network for patient DF45, a 35 year old female with sickle cell disease, second set of variables 243
11.12 The results of feeding two abnormal and an unseen normal session through the training network for patient DF60, a 63 year old male with IgA nephropathy, second set of variables. Note the change in scale for the first abnormal session. 244
11.13 The results of feeding two abnormal sessions and an unseen normal session through the training network for patient DF05, a 53 year old male with polycystic kidney disease, second set of variables (Neuroscale visualisations not shown for brevity) 245
11.14 The results of feeding two abnormal sessions and an unseen normal session through the training network for patient DF43, a 26 year old male with reflux nephropathy, second set of variables (Neuroscale visualisations not shown for brevity) 245

List of Tables

2.1 Demographics 37

3.1 Events associated with MAP change from baseline 46
3.2 Events associated with absolute MAP 47
3.3 Sensitivity and specificity of change in MAP for predicting cerebral desaturation 50
3.4 Sensitivity and specificity of absolute MAP for predicting cerebral desaturation 50
3.5 Sensitivity and specificity of change in MAP with symptoms for predicting cerebral desaturation 51
3.6 Sensitivity and specificity of absolute MAP with symptoms for predicting cerebral desaturation 51
3.7 Factors significantly associated with symptomatic HD 57

4.1 Association of cerebral ischaemia with absolute MAP thresholds in patients WITHOUT autoregulation 79
4.2 Association of cerebral ischaemia with MAP thresholds relative to lower autoregulation limit 79

5.1 Agreement between oscillometer and Finometer absolute blood pressure at population level, all patients 94
5.2 Agreement between oscillometer and Finometer absolute blood pressure at population level, excluding 9 patients where there were technical difficulties with measurement 94
5.3 Agreement between oscillometer and Finometer relative blood pressure at population level, all patients 99
5.4 Agreement between oscillometer and Finometer relative blood pressure at population level,excluding 9 patients where there were technical difficulties with measurement 99

7.1 Patient-specific linear regression terms for PTT=β MAP + constant (only patients with at least four sessions of data) . . . 136
7.2 Regression and correlation statistics, AVF sessions only . . . 146
7.3 Regression and correlation statistics, brachial AVF sessions only . . . 146
7.4 Regression and correlation statistics, Tesio sessions only . . . 146

8.1 Factors significantly associated with baseline 3MS score . . . 164
8.2 Factors significantly associated with baseline TTB score . . . 165
8.3 TTB scores for study population compared to reference values in red [176] . . . 165

10.1 Potential predictive variables for patient DF01, 34 year old male with focal segmental glomerulosclerosis (11 normal sessions and 1 abnormal session, event at 150 minutes) . . . 218
10.2 Potential predictive variables for patient DF12, 89 year old male with glomerulonephritis (11 normal sessions and 1 abnormal session, event at 84 minutes) . . . 218
10.3 Potential predictive variables for patient DF13, 73 year old male with cardiorenal failure/renovascular disease (11 normal sessions and 1 abnormal session, event at 76 minutes) . . . 219
10.4 Potential predictive variables for patient DF37, 60 year old male with diabetic nephropathy (11 normal sessions and 1 abnormal session, event at 101 minutes) . . . 219
10.5 Potential predictive variables for patient DF43, 26 year old male with reflux nephropathy (11 normal sessions and 1 abnormal session, event at 170 minutes) . . . 219
10.6 Potential predictive variables for patient DF45, 35 year old with sickle cell nephropathy (11 normal sessions and 1 abnormal session, event at 199 minutes) . . . 220
10.7 Potential predictive variables for patient DF05, 53 year old male with polycystic kidney disease (11 normal sessions and 2 eventful sessions) . . . 221
10.8 Potential predictive variables for patient DF26, 78 year old male with renovascular disease (8 normal sessions and 2 eventful sessions) . . . 221
10.9 Potential predictive variables for patient DF49, 39 year old male with IgA nephropathy (10 normal sessions and 2 eventful sessions) . . . 221
10.10 Potential predictive variables for patient DF60, 63 year old male with IgA nephropathy (7 normal sessions and 2 eventful sessions) . . . 222

10.11Potential predictive variables for patient DF30, 59 year old female with reflux nephropathy (6 normal sessions and 4 eventful sessions) 222
10.12Potential predictive variables for patient DF18, 56 year old male with diabetic nephropathy (8 normal sessions and 4 eventful sessions) 222
10.13Potential predictive variables for patient DF24, 72 year old female with diabetic nephropathy (7 normal sessions and 5 eventful sessions) 222
10.14Potential predictive variables for patient DF11, 59 year old female with diabetic nephropathy (6 normal sessions and 6 eventful sessions) 223

Bibliography

[1] Renal-Association. Sixteenth annual report. *UK Renal Registry*, 2013.

[2] J T Daugirdas. Pathophysiology of dialysis hypotension: an update. *Am J Kidney Dis*, 38:S11–7, 2001.

[3] Jeroen Kooman, Ali Basci, Francesco Pizzarelli, Bernard Canaud, Patrick Haage, Denis Fouque, Klaus Konner, Alejandro Martin-Malo, Luciano Pedrini, James Tattersall, Jan Tordoir, Marianne Vennegoor, Christoph Wanner, Piet ter Wee, and Raymond Vanholder. Ebpg guideline on haemodynamic instability. *Nephrol Dial Transplant*, 22 Suppl 2:22–44, 2007.

[4] Jennifer E Flythe, Hui Xue, Katherine E Lynch, Gary C Curhan, and Steven M Brunelli. Association of mortality risk with various definitions of intradialytic hypotension. *J Am Soc Nephrol*, 26:724–34, 2015.

[5] Tatsuya Shoji, Yoshiharu Tsubakihara, Masamitsu Fujii, and Enyu Imai. Hemodialysis-associated hypotension as an independent risk factor for two-year mortality in hemodialysis patients. *Kidney Int*, 66:1212–20, 2004.

[6] András Tislér, Katalin Akócsi, Béla Borbás, László Fazakas, Sándor Ferenczi, Sándor Görögh, Imre Kulcsár, Lajos Nagy, József Sámik, János Szegedi, Eszter Tóth, Gyula Wágner, and István Kiss. The effect of frequent or occasional dialysis-associated hypotension on survival of patients on maintenance haemodialysis. *Nephrol Dial Transplant*, 18:2601–5, 2003.

[7] Nicola Tessitore, Antonio Santoro, Giovanni Oliviero Panzetta, Volker Wizemann, Rafael Perez-Garcia, Jorge Martinez Ara, Bruno Perrone, William Mantovani, and Albino Poli. Acetate-free biofiltration reduces intradialytic hypotension: a european multicenter randomized controlled trial. *Blood Purif*, 34:354–63, 2012.

[8] Johanna Kuipers, Len A Usvyat, Jurjen K Oosterhuis, Judith J Dasselaar, Paul E de Jong, Ralf Westerhuis, Jeffrey J Sands, Yuedong Wang, Peter Kotanko, and Casper F M Franssen. Variability of predialytic, intradialytic, and postdialytic blood pressures in the course of a week: a study of dutch and us maintenance hemodialysis patients. *Am J Kidney Dis*, 62:779–88, 2013.

[9] N McMahon, L A Hogg, A R Corfield, and A D Exton. Comparison of non-invasive and invasive blood pressure in aeromedical care. *Anaesthesia*, 67:1343–7, 2012.

[10] Karim Lakhal, Christine Macq, Stephan Ehrmann, Thierry Boulain, and Xavier Capdevila. Non-invasive monitoring of blood pressure in the critically ill: reliability according to the cuff site (arm, thigh, or ankle). *Crit Care Med*, 40:1207–13, 2012.

[11] A Bur, M M Hirschl, H Herkner, E Oschatz, J Kofler, C Woisetschläger, and A N Laggner. Accuracy of oscillometric blood pressure measurement according to the relation between cuff size and upper-arm circumference in critically ill patients. *Crit Care Med*, 28:371–6, 2000.

[12] Sara Ribezzo, Eleonora Spina, Stefano Di Bartolomeo, and Gianfranco Sanson. Noninvasive techniques for blood pressure measurement are not a reliable alternative to direct measurement: a randomized crossover trial in icu. *ScientificWorldJournal*, 2014:353628, 2014.

[13] James O Burton, Helen J Jefferies, Nicholas M Selby, and Christopher W McIntyre. Hemodialysis-induced cardiac injury: determinants and associated outcomes. *Clin J Am Soc Nephrol*, 4:914–20, 2009.

[14] Helen J Jefferies, James O Burton, and Christopher W McIntyre. Individualised dialysate temperature improves intradialytic haemodynamics and abrogates haemodialysis-induced myocardial stunning, without compromising tolerability. *Blood Purif*, 32:63–8, 2011.

[15] Helen J Jefferies, Bhupinder Virk, Brigitte Schiller, John Moran, and Christopher W McIntyre. Frequent hemodialysis schedules are associated with reduced levels of dialysis-induced cardiac injury (myocardial stunning). *Clin J Am Soc Nephrol*, 6:1326–32, 2011.

[16] Nicholas M Selby and Christopher W McIntyre. A systematic review of the clinical effects of reducing dialysate fluid temperature. *Nephrol Dial Transplant*, 21:1883–98, 2006.

[17] K Miura, A R Dyer, P Greenland, M L Daviglus, M Hill, K Liu, D B Garside, J Stamler, and Chicago Heart Association. Pulse pressure compared with other blood pressure indexes in the

prediction of 25-year cardiovascular and all-cause mortality rates: The chicago heart association detection project in industry study. *Hypertension*, 38:232–7, 2001.

[18] Julie K K Vishram, Anders Borglykke, Anne H Andreasen, Jørgen Jeppesen, Hans Ibsen, Torben Jørgensen, Grazyna Broda, Luigi Palmieri, Simona Giampaoli, Chiara Donfrancesco, Frank Kee, Giuseppe Mancia, Giancarlo Cesana, Kari Kuulasmaa, Susana Sans, Michael H Olsen, and MORGAM Project. Impact of age on the importance of systolic and diastolic blood pressures for stroke risk: the monica, risk, genetics, archiving, and monograph (morgam) project. *Hypertension*, 60:1117–23, 2012.

[19] S M Jakob, E Ruokonen, O Vuolteenaho, E Lampainen, and J Takala. Splanchnic perfusion during hemodialysis: evidence for marginal tissue perfusion. *Crit Care Med*, 29:1393–8, 2001.

[20] Christopher W McIntyre, James O Burton, Nicholas M Selby, Lucia Leccisotti, Shvan Korsheed, Christopher S R Baker, and Paolo G Camici. Hemodialysis-induced cardiac dysfunction is associated with an acute reduction in global and segmental myocardial blood flow. *Clin J Am Soc Nephrol*, 3:19–26, 2008.

[21] Patrick Schober and Lothar A Schwarte. From system to organ to cell: oxygenation and perfusion measurement in anesthesia and critical care. *J Clin Monit Comput*, 26:255–65, 2012.

[22] Daniel De Backer, Katia Donadello, and Diego Orbegozo Cortes. Monitoring the microcirculation. *J Clin Monit Comput*, 26:361–6, 2012.

[23] Aurélie Thooft, Raphaël Favory, Diamantino Ribeiro Salgado, Fabio S Taccone, Katia Donadello, Daniel De Backer, Jacques Creteur, and Jean-Louis Vincent. Effects of changes in arterial pressure on organ perfusion during septic shock. *Crit Care*, 15:222, 2011.

[24] Marjut Varpula, Minna Tallgren, Katri Saukkonen, Liisa-Maria Voipio-Pulkki, and Ville Pettilä. Hemodynamic variables related to outcome in septic shock. *Intensive Care Med*, 31:1066–71, 2005.

[25] Shaman Jhanji, Sarah Stirling, Nakul Patel, Charles J Hinds, and Rupert M Pearse. The effect of increasing doses of norepinephrine on tissue oxygenation and microvascular flow in patients with septic shock. *Crit Care Med*, 37:1961–6, 2009.

[26] Arnaldo Dubin, Mario O Pozo, Christian A Casabella, Fernando Pálizas, Jr, Gastón Murias, Miriam C Moseinco, Vanina S Kanoore Edul, Fernando Pálizas, Elisa Estenssoro, and Can Ince.

Increasing arterial blood pressure with norepinephrine does not improve microcirculatory blood flow: a prospective study. *Crit Care*, 13:92, 2009.

[27] D Kremastinos, I Paraskevaidis, S Voudiklari, T Apostolou, Z Kyriakides, P Zirogiannis, and P Toutouzas. Painless myocardial ischemia in chronic hemodialysed patients: a real event? *Nephron*, 60:164–70, 1992.

[28] A S Narula, V Jha, H K Bali, V Sakhuja, and R P Sapru. Cardiac arrhythmias and silent myocardial ischemia during hemodialysis. *Ren Fail*, 22:355–68, 2000.

[29] N Singh, A Langer, M R Freeman, and M B Goldstein. Myocardial alterations during hemodialysis: insights from new noninvasive technology. *Am J Nephrol*, 14:173–81, 1994.

[30] Roger De Andrade, Tessa Kotze, Maia Lesosky, and Charles Swanepoel. Comparison of myocardial perfusion during hemodialysis and hemodiafiltration. *Nephron Clin Pract*, 126:151–8, 2014.

[31] Lindsay J Chesterton, Nicholas M Selby, James O Burton, and Chris W McIntyre. Cool dialysate reduces asymptomatic intradialytic hypotension and increases baroreflex variability. *Hemodial Int*, 13:189–96, 2009.

[32] Judith J Dasselaar, Riemer H J A Slart, Martine Knip, Jan Pruim, René A Tio, Christopher W McIntyre, Paul E de Jong, and Casper F M Franssen. Haemodialysis is associated with a pronounced fall in myocardial perfusion. *Nephrol Dial Transplant*, 24:604–10, 2009.

[33] Yelena Slinin, Misti L Paudel, Areef Ishani, Brent C Taylor, Kristine Yaffe, Anne M Murray, Howard A Fink, Eric S Orwoll, Steven R Cummings, Elizabeth Barrett-Connor, Simerjot Jassal, Kristine E Ensrud, and Osteoporotic Fractures in Men Study Group. Kidney function and cognitive performance and decline in older men. *J Am Geriatr Soc*, 56:2082–8, 2008.

[34] Manjula Kurella, Glenn M Chertow, Jennifer Luan, and Kristine Yaffe. Cognitive impairment in chronic kidney disease. *J Am Geriatr Soc*, 52:1863–9, 2004.

[35] Daniel E Weiner, Tammy M Scott, Lena M Giang, Brian T Agganis, Eric P Sorensen, Hocine Tighiouart, and Mark J Sarnak. Cardiovascular disease and cognitive function in maintenance hemodialysis patients. *Am J Kidney Dis*, 58:773–81, 2011.

[36] Daniel E Weiner and Stephen L Seliger. Cognitive and physical function in chronic kidney disease. *Curr Opin Nephrol Hypertens*, 23:291–7, 2014.

[37] Toshihide Naganuma, Yoshiaki Takemoto, Tetsuo Shoji, Hideaki Shima, Eiji Ishimura, Mikio Okamura, and Tatsuya Nakatani. Cerebral white matter hyperintensity predicts cardiovascular events in haemodialysis patients. *Nephrology (Carlton)*, 18:676–81, 2013.

[38] Dawn F Wolfgram, Lily Sunio, Elisabeth Vogt, Heather M Smith, Alexis Visotcky, Purushottam Laud, and Jeff Whittle. Haemodynamics during dialysis and cognitive performance. *Nephrology (Carlton)*, 19:771–6, 2014.

[39] Manjula Kurella Tamura, Brett Larive, Mark L Unruh, John B Stokes, Allen Nissenson, Ravindra L Mehta, Glenn M Chertow, and Frequent Hemodialysis Network Trial Group. Prevalence and correlates of cognitive impairment in hemodialysis patients: the frequent hemodialysis network trials. *Clin J Am Soc Nephrol*, 5:1429–38, 2010.

[40] Tsyh-Jyi Hsieh, Jer-Ming Chang, Hung-Yi Chuang, Chih-Hung Ko, Miao-Ling Hsieh, Gin-Chang Liu, and Jui-Sheng Hsu. End-stage renal disease: in vivo diffusion-tensor imaging of silent white matter damage. *Radiology*, 252:518–25, 2009.

[41] Ruijie Zhang, Kai Liu, Linfeng Yang, Tao Zhou, Shaowen Qian, Bo Li, Zhaohui Peng, Min Li, Shengpeng Sang, Qingjun Jiang, and Gang Sun. Reduced white matter integrity and cognitive deficits in maintenance hemodialysis esrd patients: a diffusion-tensor study. *Eur Radiol*, 25:661–8, 2015.

[42] M-C Chou, T-J Hsieh, Y-L Lin, Y-T Hsieh, W-Z Li, J-M Chang, C-H Ko, E-F Kao, T-S Jaw, and G-C Liu. Widespread white matter alterations in patients with end-stage renal disease: a voxelwise diffusion tensor imaging study. *AJNR Am J Neuroradiol*, 34:1945–51, 2013.

[43] Mohamed T Eldehni, Aghogho Odudu, and Christopher W McIntyre. Randomized clinical trial of dialysate cooling and effects on brain white matter. *J Am Soc Nephrol*, 26:957–65, 2015.

[44] Xiang Kong, Ji-qiu Wen, Rong-feng Qi, Song Luo, Jian-hui Zhong, Hui-juan Chen, Gong-jun Ji, Guang Ming Lu, and Long Jiang Zhang. Diffuse interstitial brain edema in patients with end-stage renal disease undergoing hemodialysis: a tract-based spatial statistics study. *Medicine (Baltimore)*, 93:313, 2014.

[45] Shuzo Kobayashi, Yasuhiro Mochida, Kunihiro Ishioka, Machiko Oka, Kyouko Maesato, Hidekazu Moriya, Sumi Hidaka, and Takayasu Ohtake. The effects of blood pressure and the renin-

angiotensin-aldosterone system on regional cerebral blood flow and cognitive impairment in dialysis patients. *Hypertens Res*, 37:636–41, 2014.

[46] Said S Dahbour, Ayman M Wahbeh, and Mohammad Z Hamdan. Mini mental status examination (mmse) in stable chronic renal failure patients on hemodialysis: The effects of hemodialysis on the mmse score. a prospective study. *Hemodial Int*, 13:80–5, 2009.

[47] Arema A Pereira, Daniel E Weiner, Tammy Scott, Priya Chandra, Robyn Bluestein, John Griffith, and Mark J Sarnak. Subcortical cognitive impairment in dialysis patients. *Hemodial Int*, 11:309–14, 2007.

[48] A Postiglione, F Faccenda, G Gallotta, P Rubba, and S Federico. Changes in middle cerebral artery blood velocity in uremic patients after hemodialysis. *Stroke*, 22:1508–11, 1991.

[49] R Hata, M Matsumoto, N Handa, H Terakawa, Y Sugitani, and T Kamada. Effects of hemodialysis on cerebral circulation evaluated by transcranial doppler ultrasonography. *Stroke*, 25:408–12, 1994.

[50] H Skinner, C Mackaness, N Bedforth, and R Mahajan. Cerebral haemodynamics in patients with chronic renal failure: effects of haemodialysis. *Br J Anaesth*, 94:203–5, 2005.

[51] Giuseppe Regolisti, Umberto Maggiore, Carola Cademartiri, Aderville Cabassi, Alberto Caiazza, Stefano Tedeschi, Elio Antonucci, and Enrico Fiaccadori. Cerebral blood flow decreases during intermittent hemodialysis in patients with acute kidney injury, but not in patients with end-stage renal disease. *Nephrol Dial Transplant*, 28:79–85, 2013.

[52] I Stefanidis, R Bach, P R Mertens, V Liakopoulos, G Liapi, H Mann, and B Heintz. Influence of hemodialysis on the mean blood flow velocity in the middle cerebral artery. *Clin Nephrol*, 64:129–37, 2005.

[53] George Metry, Margaret Spittle, Shahriar Rahmati, Cole Giller, Angela Giller, Allen Kaufman, Daniel Schneditz, Edward Manno, Zohar Brener, Irene Boniece, Federico Ronco, Claudio Ronco, and Nathan W Levin. Online monitoring of cerebral hemodynamics during hemodialysis. *Am J Kidney Dis*, 40:996–1004, 2002.

[54] Akke Bakker, Brianne Smith, Philip Ainslie, and Kurt Smith. Near-infrared spectroscopy. *http://www.intechopen.com/books/applied-aspects-of-ultrasonography-in-humans/near-infrared-spectroscopy*, (accessed May 2013).

[55] Kenneth Brady, Brijen Joshi, Christian Zweifel, Peter Smielewski, Marek Czosnyka, R Blaine Easley, and Charles W Hogue, Jr. Real-time continuous monitoring of cerebral blood flow autoregulation using near-infrared spectroscopy in patients undergoing cardiopulmonary bypass. *Stroke*, 41:1951–6, 2010.

[56] T Alderliesten, J B De Vis, P M A Lemmers, F van Bel, M J N L Benders, J Hendrikse, and E T Petersen. Simultaneous quantitative assessment of cerebral physiology using respiratory-calibrated mri and near-infrared spectroscopy in healthy adults. *Neuroimage*, 85:255–63, 2014.

[57] Taro Hoshino, Susumu Ookawara, Sawako Goto, Haruhisa Miyazawa, Kiyonori Ito, Yuichiro Ueda, Yoshio Kaku, Keiji Hirai, Aoi Nabata, Honami Mori, Izumi Yoshida, and Kaoru Tabei. Evaluation of cerebral oxygenation in patients undergoing long-term hemodialysis. *Nephron Clin Pract*, 126:57–61, 2014.

[58] Georgios Papadopoulos, Evangelia Dounousi, Athanasios Papathanasiou, Georgios Papathanakos, and Petros Tzimas. Cerebral oximetry values in dialyzed surgical patients: a comparison between hemodialysis and peritoneal dialysis. *Ren Fail*, 35:855–9, 2013.

[59] Kiyonori Ito, Susumu Ookawara, Yuichiro Ueda, Sawako Goto, Haruhisa Miyazawa, Hodaka Yamada, Taisuke Kitano, Mitsunobu Shindo, Yoshio Kaku, Keiji Hirai, Masashi Yoshida, Taro Hoshino, Aoi Nabata, Honami Mori, Izumi Yoshida, Masafumi Kakei, and Kaoru Tabei. Factors affecting cerebral oxygenation in hemodialysis patients: Cerebral oxygenation associates with ph, hemodialysis duration, serum albumin concentration, and diabetes mellitus. *PLoS One*, 10:e0117474, 2015.

[60] Daina Kashiwazaki, Satoshi Kuroda, Shunsuke Terasaka, and Yoshinobu Iwasaki. Detection of hemodynamic transient ischemic attack during hemodialysis with near-infrared monitoring in a patient with internal carotid artery occlusion. *Surg Neurol*, 68:292–4, 2007.

[61] A W Yu, Z M Nawab, W E Barnes, K N Lai, T S Ing, and J T Daugirdas. Splanchnic erythrocyte content decreases during hemodialysis: a new compensatory mechanism for hypovolemia. *Kidney Int*, 51:1986–90, 1997.

[62] Simone Gonçalves, Roberto Pecoits-Filho, Sônia Perreto, Silvio H Barberato, Andréa E M Stinghen, Emmanuel G A Lima, Roseana Fuerbringer, Sirlene M Sauthier, and Miguel C Riella. Associations

between renal function, volume status and endotoxaemia in chronic kidney disease patients. *Nephrol Dial Transplant*, 21:2788–94, 2006.

[63] Takeshi Hasegawa, Shigeru Nakai, Ikuto Masakane, Yuzo Watanabe, Kunitoshi Iseki, Yoshiharu Tsubakihara, and Tadao Akizawa. Dialysis fluid endotoxin level and mortality in maintenance hemodialysis: A nationwide cohort study. *Am J Kidney Dis*, 65:899–904, 2015.

[64] Christopher W McIntyre, Laura E A Harrison, M Tarek Eldehni, Helen J Jefferies, Cheuk-Chun Szeto, Stephen G John, Mhairi K Sigrist, James O Burton, Daljit Hothi, Shvan Korsheed, Paul J Owen, Ka-Bik Lai, and Philip K T Li. Circulating endotoxemia: a novel factor in systemic inflammation and cardiovascular disease in chronic kidney disease. *Clin J Am Soc Nephrol*, 6:133–41, 2011.

[65] A Uusaro, E Ruokonen, and J Takala. Estimation of splanchnic blood flow by the fick principle in man and problems in the use of indocyanine green. *Cardiovasc Res*, 30:106–12, 1995.

[66] L Diebel, R Kozol, R F Wilson, S Mahajan, D Abu-Hamdan, and D Thomas. Gastric intramucosal acidosis in patients with chronic kidney failure. *Surgery*, 113:520–6, 1993.

[67] Robert J Hinchliffe, Bernie Kirk, Dipankar Bhattacharjee, Simon Roe, William Jeffcoate, and Fran Game. The effect of haemodialysis on transcutaneous oxygen tension in patients with diabetes-a pilot study. *Nephrol Dial Transplant*, 21:1981–3, 2006.

[68] Leif Sörnmo, Frida Sandberg, Eduardo Gil, and Kristian Solem. Noninvasive techniques for prevention of intradialytic hypotension. *IEEE Rev Biomed Eng*, 5:45–59, 2012.

[69] Andrew Davenport. Using dialysis machine technology to reduce intradialytic hypotension. *Hemodial Int*, 15 Suppl 1:S37–42, 2011.

[70] Claudia Barth, Walter Boer, Daniela Garzoni, Thomas Kuenzi, Wolfgang Ries, Ralf Schaefer, Daniel Schneditz, Theoharis Tsobanelis, Frank van der Sande, Ralf Wojke, Holger Schilling, and Jutta Passlick-Deetjen. Characteristics of hypotension-prone haemodialysis patients: is there a critical relative blood volume? *Nephrol Dial Transplant*, 18:1353–60, 2003.

[71] Elena Mancini, Emanuele Mambelli, Mina Irpinia, Danila Gabrielli, Carmelo Cascone, Ferruccio Conte, Gina Meneghel, Fosco Cavatorta, Alessandro Antonelli, Giuseppe Villa, Antonio Dal Canton, Leonardo Cagnoli, Filippo Aucella, Fulvio Fiorini, Enzo Gaggiotti, Giorgio Triolo, Vitale

Nuzzo, and Antonio Santoro. Prevention of dialysis hypotension episodes using fuzzy logic control system. *Nephrol Dial Transplant*, 22:1420–7, 2007.

[72] E Mancini, L Corazza, DC Cannarile, ML Soverini, S Calvacanti, S Cavani, A Fiorenzi, and A Santoro. Short term variability of oxygen saturation during hemodialysis is a warning parameter for hypotension appearance. *Computers in Cardiology*, 35:881–883, 2008.

[73] Kristian Solem, Bo Olde, and Leif Sörnmo. Prediction of intradialytic hypotension using photoplethysmography. *IEEE Trans Biomed Eng*, 57:1611–9, 2010.

[74] Kristian Solem, Anders Nilsson, and Leif Sörnmo. An electrocardiogram-based method for early detection of abrupt changes in blood pressure during hemodialysis. *ASAIO J*, 52:282–90, 2006.

[75] Emanuele Mambelli, Elena Mancini, and Antonio Santoro. A continuous and non-invasive arterial pressure monitoring system in dialysis patients. *Nephron Clin Pract*, 107:170–6, 2007.

[76] Gihad E Nesrallah, Rita S Suri, Gordon Guyatt, Reem A Mustafa, Stephen D Walter, Robert M Lindsay, and Elie A Akl. Biofeedback dialysis for hypotension and hypervolemia: a systematic review and meta-analysis. *Nephrol Dial Transplant*, 28:182–91, 2013.

[77] Teddie Annette Tanguay, Louise Jensen, and Curt Johnston. Predicting episodes of hypotension by continuous blood volume monitoring among critically ill patients in acute renal failure on intermittent hemodialysis. *Dynamics*, 18:19–24, 2007.

[78] Nicholas M Selby, James O Burton, Lindsay J Chesterton, and Christopher W McIntyre. Dialysis-induced regional left ventricular dysfunction is ameliorated by cooling the dialysate. *Clin J Am Soc Nephrol*, 1:1216–25, 2006.

[79] Sanjeev Kumar, Maryam Khosravi, Annick Massart, Madhu Potluri, and Andrew Davenport. Haemodiafiltration results in similar changes in intracellular water and extracellular water compared to cooled haemodialysis. *Am J Nephrol*, 37:320–4, 2013.

[80] Thomas Oates, Jennifer Cross, and Andrew Davenport. Cost comparison of online haemodiafiltration with high-flux haemodialysis. *J Nephrol*, 25:192–7, 2012.

[81] Jennifer H Pinney, Thomas Oates, and Andrew Davenport. Haemodiafiltration does not reduce the frequency of intradialytic hypotensive episodes when compared to cooled high-flux haemodialysis. *Nephron Clin Pract*, 119:138–44, 2011.

[82] L Tarassenko, A Hann, and D Young. Integrated monitoring and analysis for early warning of patient deterioration. *Br J Anaesth*, 97:64–8, 2006.

[83] Marilyn Hravnak, Leslie Edwards, Amy Clontz, Cynthia Valenta, Michael A Devita, and Michael R Pinsky. Defining the incidence of cardiorespiratory instability in patients in step-down units using an electronic integrated monitoring system. *Arch Intern Med*, 168:1300–8, 2008.

[84] Marilyn Hravnak, Michael A Devita, Amy Clontz, Leslie Edwards, Cynthia Valenta, and Michael R Pinsky. Cardiorespiratory instability before and after implementing an integrated monitoring system. *Crit Care Med*, 39:65–72, 2011.

[85] Lysander W J Bogert and Johannes J van Lieshout. Non-invasive pulsatile arterial pressure and stroke volume changes from the human finger. *Exp Physiol*, 90:437–46, 2005.

[86] Ilja Guelen, Berend E Westerhof, Gertrude L Van Der Sar, Gert A Van Montfrans, Ferdinand Kiemeneij, Karel H Wesseling, and Willem Jan Bos. Finometer, finger pressure measurements with the possibility to reconstruct brachial pressure. *Blood Press Monit*, 8:27–30, 2003.

[87] Ilja Guelen, Berend E Westerhof, Gertrude L van der Sar, Gert A van Montfrans, Ferdinand Kiemeneij, Karel H Wesseling, and Willem Jan W Bos. Validation of brachial artery pressure reconstruction from finger arterial pressure. *J Hypertens*, 26:1321–7, 2008.

[88] B P Imholz, G J Langewouters, G A van Montfrans, G Parati, J van Goudoever, K H Wesseling, W Wieling, and G Mancia. Feasibility of ambulatory, continuous 24-hour finger arterial pressure recording. *Hypertension*, 21:65–73, 1993.

[89] B P Imholz, W Wieling, G A van Montfrans, and K H Wesseling. Fifteen years experience with finger arterial pressure monitoring: assessment of the technology. *Cardiovasc Res*, 38:605–16, 1998.

[90] A E Schutte, H W Huisman, J M van Rooyen, N T Malan, and R Schutte. Validation of the finometer device for measurement of blood pressure in black women. *J Hum Hypertens*, 18:79–84, 2004.

[91] R Maestri, G D Pinna, E Robbi, S Capomolla, and M T La Rovere. Noninvasive measurement of blood pressure variability: accuracy of the finometer monitor and comparison with the finapres device. *Physiol Meas*, 26:1125–36, 2005.

[92] Wouter J K Hehenkamp, Saskia Rang, Jeroen van Goudoever, Willem J W Bos, Hans Wolf, and Joris A M van der Post. Comparison of portapres with standard sphygmomanometry in pregnancy. *Hypertens Pregnancy*, 21:65–76, 2002.

[93] G A Rongen, W J Bos, J W Lenders, G A van Montfrans, H J van Lier, J van Goudoever, K H Wesseling, and T Thien. Comparison of intrabrachial and finger blood pressure in healthy elderly volunteers. *Am J Hypertens*, 8:237–48, 1995.

[94] KA Hakim. Continuous non-invasive bp monitoring; service evaluation during induction of anaesthesia and haemodialysis. PhD thesis, University of Nottingham, 2011.

[95] M G Barnas, W H Boer, and H A Koomans. Hemodynamic patterns and spectral analysis of heart rate variability during dialysis hypotension. *J Am Soc Nephrol*, 10:2577–84, 1999.

[96] Jaap J Remmen, Wim R M Aengevaeren, Freek W A Verheugt, Tjeerd van ver Werf, Hans E Luijten, Anja Bos, and René W M M Jansen. Finapres arterial pulse wave analysis with modelflow is not a reliable non-invasive method for assessment of cardiac output. *Clin Sci (Lond)*, 103:143–9, 2002.

[97] J R Jansen, J J Schreuder, J P Mulier, N T Smith, J J Settels, and K H Wesseling. A comparison of cardiac output derived from the arterial pressure wave against thermodilution in cardiac surgery patients. *Br J Anaesth*, 87:212–22, 2001.

[98] V V Kisloukhine and D A Dean. Validation of a novel ultrasound dilution method to measure cardiac output during hemodialysis. *ASAIO J*, 42:M906–7, 1996.

[99] James P Slater, Theresa Guarino, Jessica Stack, Kateki Vinod, Rami T Bustami, John M Brown, 3rd, Alejandro L Rodriguez, Christopher J Magovern, Thomas Zaubler, Kenneth Freundlich, and Grant V S Parr. Cerebral oxygen desaturation predicts cognitive decline and longer hospital stay after cardiac surgery. *Ann Thorac Surg*, 87:36–44; discussion 44–5, 2009.

[100] L Tang, R Kazan, R Taddei, C Zaouter, S Cyr, and T M Hemmerling. Reduced cerebral oxygen saturation during thoracic surgery predicts early postoperative cognitive dysfunction. *Br J Anaesth*, 108:623–9, 2012.

[101] Emilie de Tournay-Jetté, Gilles Dupuis, Louis Bherer, Alain Deschamps, Raymond Cartier, and André Denault. The relationship between cerebral oxygen saturation changes and postoperative

cognitive dysfunction in elderly patients after coronary artery bypass graft surgery. *J Cardiothorac Vasc Anesth*, 25:95–104, 2011.

[102] Koichi Suehiro and Ryu Okutai. Duration of cerebral desaturation time during single-lung ventilation correlates with mini mental state examination score. *J Anesth*, 25:345–9, 2011.

[103] John M Murkin, Sandra J Adams, Richard J Novick, Mackenzie Quantz, Daniel Bainbridge, Ivan Iglesias, Andrew Cleland, Betsy Schaefer, Beverly Irwin, and Stephanie Fox. Monitoring brain oxygen saturation during coronary bypass surgery: a randomized, prospective study. *Anesth Analg*, 104:51–8, 2007.

[104] R Kazan, D Bracco, and T M Hemmerling. Reduced cerebral oxygen saturation measured by absolute cerebral oximetry during thoracic surgery correlates with postoperative complications. *Br J Anaesth*, 103:811–6, 2009.

[105] Masahiro Ono, George J Arnaoutakis, Derek M Fine, Kenneth Brady, R Blaine Easley, Yueying Zheng, Charles Brown, Nevin M Katz, Morgan E Grams, and Charles W Hogue. Blood pressure excursions below the cerebral autoregulation threshold during cardiac surgery are associated with acute kidney injury. *Crit Care Med*, 41:464–71, 2013.

[106] Masahiro Ono, Kenneth Brady, R Blaine Easley, Charles Brown, Michael Kraut, Rebecca F Gottesman, and Charles W Hogue, Jr. Duration and magnitude of blood pressure below cerebral autoregulation threshold during cardiopulmonary bypass is associated with major morbidity and operative mortality. *J Thorac Cardiovasc Surg*, 147:483–9, 2014.

[107] M T Douds, E J Straub, A C Kent, C H Bistrick, and J J Sistino. A systematic review of cerebral oxygenation-monitoring devices in cardiac surgery. *Perfusion*, 29:545–52, 2014.

[108] Martin Smith. Shedding light on the adult brain: a review of the clinical applications of near-infrared spectroscopy. *Philos Trans A Math Phys Eng Sci*, 369:4452–69, 2011.

[109] Irmgard Hadolt and Gerhard Litscher. Noninvasive assessment of cerebral oxygenation during high altitude trekking in the nepal himalayas (2850-5600 m). *Neurol Res*, 25:183–8, 2003.

[110] Mark J Sarnak, Hocine Tighiouart, Tammy M Scott, Kristina V Lou, Eric P Sorensen, Lena M Giang, David A Drew, Kamran Shaffi, James A Strom, Ajay K Singh, and Daniel E Weiner.

Frequency of and risk factors for poor cognitive performance in hemodialysis patients. *Neurology*, 80:471–80, 2013.

[111] Luke Rodriguez, Hocine Tighiouart, Tammy Scott, Kristina Lou, Lena Giang, Eric Sorensen, Daniel E Weiner, and Mark J Sarnak. Association of sleep disturbances with cognitive impairment and depression in maintenance hemodialysis patients. *J Nephrol*, 26:101–10, 2013.

[112] Tom N Tombaugh. Test-retest reliable coefficients and 5-year change scores for the mmse and 3ms. *Arch Clin Neuropsychol*, 20:485–503, 2005.

[113] Piero Amodio, Helmut Wenin, Franco Del Piccolo, Daniela Mapelli, Sara Montagnese, Andrea Pellegrini, Carmine Musto, Angelo Gatta, and Carlo Umiltà. Variability of trail making test, symbol digit test and line trait test in normal people. a normative study taking into account age-dependent decline and sociobiological variables. *Aging Clin Exp Res*, 14:117–31, 2002.

[114] P S Hamilton and W J Tompkins. Quantitative investigation of qrs detection rules using the mit/bih arrhythmia database. *IEEE Trans Biomed Eng*, 33:1157–65, 1986.

[115] The national statistics socio-economic classification. *http://www.ons.gov.uk/ons/guide-method/classifications/current-standard-classifications/soc2010/soc2010-volume-3-ns-sec–rebased-on-soc2010–user-manual/index.html*, 2010 (accessed August 2013).

[116] M.E Tipping and D. Lowe. Neuroscale: Novel topographic feature extraction with radial basis function networks. *In M. Mozer, M.Jordan and T.Petsche (Eds.), Advances in Neural Information Processing Systems. Cambridge, Mass:MIT Press*, 9:543–549, 1997.

[117] Henning B Nielsen. Systematic review of near-infrared spectroscopy determined cerebral oxygenation during non-cardiac surgery. *Front Physiol*, 5:93, 2014.

[118] George Vretzakis, Stauroula Georgopoulou, Konstantinos Stamoulis, Georgia Stamatiou, Kosmas Tsakiridis, Paul Zarogoulidis, Nikolaos Katsikogianis, Ioanna Kougioumtzi, Nikolaos Machairiotis, Theodora Tsiouda, Andreas Mpakas, Thomas Beleveslis, Alexander Koletas, Stavros N Siminelakis, and Konstantinos Zarogoulidis. Cerebral oximetry in cardiac anesthesia. *J Thorac Dis*, 6 Suppl 1:S60–9, 2014.

[119] Masahiko Tozawa, Kunitoshi Iseki, Chiho Iseki, Saori Oshiro, Masanobu Yamazato, Yasushi Higashiuesato, Nozomi Tomiyama, Takeshi Tana, Yoshiharu Ikemiya, and Shuichi Takishita. Evidence

for elevated pulse pressure in patients on chronic hemodialysis: a case-control study. *Kidney Int*, 62:2195–201, 2002.

[120] Karl-Jürgen Bär, Stanislaw Brehm, Michael Karl Boettger, Silke Boettger, Gerd Wagner, and Heinrich Sauer. Pain perception in major depression depends on pain modality. *Pain*, 117:97–103, 2005.

[121] M K Boettger and K J Bär. Perception for ischemic pain shows similarities in adjustment disorder and major depression. *Eur J Pain*, 11:819–22, 2007.

[122] Nadine S Bekkouche, Andrew J Wawrzyniak, Kerry S Whittaker, Mark W Ketterer, and David S Krantz. Psychological and physiological predictors of angina during exercise-induced ischemia in patients with coronary artery disease. *Psychosom Med*, 75:413–21, 2013.

[123] Arnoud Arntz and Lily Claassens. The meaning of pain influences its experienced intensity. *Pain*, 109:20–5, 2004.

[124] Stefan Lautenbacher. Experimental approaches in the study of pain in the elderly. *Pain Med*, 13 Suppl 2:S44–50, 2012.

[125] O B Paulson, S Strandgaard, and L Edvinsson. Cerebral autoregulation. *Cerebrovasc Brain Metab Rev*, 2:161–92, 1990.

[126] J C Drummond. The lower limit of autoregulation: time to revise our thinking? *Anesthesiology*, 86:1431–3, 1997.

[127] J H Moyer and G Morris. Cerebral hemodynamics during controlled hypotension induced by the continuous infusion of ganglionic blocking agents (hexamethonium, pendiomide and arfonad). *J Clin Invest*, 33:1081–8, 1954.

[128] F A Finnerty, Jr, L Witkin, and J F Fazekas. Cerebral hemodynamics during cerebral ischemia induced by acute hypotension. *J Clin Invest*, 33:1227–32, 1954.

[129] S Strandgaard. Autoregulation of cerebral blood flow in hypertensive patients. the modifying influence of prolonged antihypertensive treatment on the tolerance to acute, drug-induced hypotension. *Circulation*, 53:720–7, 1976.

[130] K S Olsen, L B Svendsen, F S Larsen, and O B Paulson. Effect of labetalol on cerebral blood flow, oxygen metabolism and autoregulation in healthy humans. *Br J Anaesth*, 75:51–4, 1995.

[131] F S Larsen, K S Olsen, B A Hansen, O B Paulson, and G M Knudsen. Transcranial doppler is valid for determination of the lower limit of cerebral blood flow autoregulation. *Stroke*, 25:1985–8, 1994.

[132] K S Olsen, L B Svendsen, and F S Larsen. Validation of transcranial near-infrared spectroscopy for evaluation of cerebral blood flow autoregulation. *J Neurosurg Anesthesiol*, 8:280–5, 1996.

[133] J P Bourdarias. Coronary reserve: concept and physiological variations. *Eur Heart J*, 16 Suppl I:2–6, 1995.

[134] Marilyn Burke, Mallikarjuna R Pabbidi, Jerry Farley, and Richard J Roman. Molecular mechanisms of renal blood flow autoregulation. *Curr Vasc Pharmacol*, 12:845–58, 2014.

[135] M J Hernández, R W Brennan, and G S Bowman. Cerebral blood flow autoregulation in the rat. *Stroke*, 9:150–4, 1978.

[136] M Sato, G Pawlik, and W D Heiss. Comparative studies of regional cns blood flow autoregulation and responses to co2 in the cat. effects of altering arterial blood pressure and paco2 on rcbf of cerebrum, cerebellum, and spinal cord. *Stroke*, 15:91–7, 1984.

[137] U Dirnagl and W Pulsinelli. Autoregulation of cerebral blood flow in experimental focal brain ischemia. *J Cereb Blood Flow Metab*, 10:327–36, 1990.

[138] M Ono, B Joshi, K Brady, R B Easley, Y Zheng, C Brown, W Baumgartner, and C W Hogue. Risks for impaired cerebral autoregulation during cardiopulmonary bypass and postoperative stroke. *Br J Anaesth*, 109:391–8, 2012.

[139] Marek Czosnyka, Ken Brady, Matthias Reinhard, Piotr Smielewski, and Luzius A Steiner. Monitoring of cerebrovascular autoregulation: facts, myths, and missing links. *Neurocrit Care*, 10:373–86, 2009.

[140] Brijen Joshi, Masahiro Ono, Charles Brown, Kenneth Brady, R Blaine Easley, Gayane Yenokyan, Rebecca F Gottesman, and Charles W Hogue. Predicting the limits of cerebral autoregulation during cardiopulmonary bypass. *Anesth Analg*, 114:503–10, 2012.

[141] Christian Zweifel, Celeste Dias, Peter Smielewski, and Marek Czosnyka. Continuous time-domain monitoring of cerebral autoregulation in neurocritical care. *Med Eng Phys*, 36:638–45, 2014.

[142] G Waldemar, J F Schmidt, A R Andersen, S Vorstrup, H Ibsen, and O B Paulson. Angiotensin converting enzyme inhibition and cerebral blood flow autoregulation in normotensive and hypertensive man. *J Hypertens*, 7:229–35, 1989.

[143] E O'Brien, N Atkins, F Mee, and K O'Malley. Evaluation of blood pressure measuring devices. *Clin Exp Hypertens*, 15:1087–97, 1993.

[144] L M Prisant, B S Alpert, C B Robbins, A S Berson, M Hayes, M L Cohen, and S G Sheps. American national standard for nonautomated sphygmomanometers. summary report. *Am J Hypertens*, 8:210–3, 1995.

[145] Samuel A Mireles, Richard A Jaffe, David R Drover, and John G Brock-Utne. A poor correlation exists between oscillometric and radial arterial blood pressure as measured by the philips mp90 monitor. *J Clin Monit Comput*, 23:169–74, 2009.

[146] Mahboob Rahman, Valerie Griffin, Arun Kumar, Fauzia Manzoor, Jackson T Wright, Jr, and Michael C Smith. A comparison of standardized versus "usual" blood pressure measurements in hemodialysis patients. *Am J Kidney Dis*, 39:1226–30, 2002.

[147] Andreas Bur, Harald Herkner, Marianne Vlcek, Christian Woisetschläger, Ulla Derhaschnig, Georg Delle Karth, Anton N Laggner, and Michael M Hirschl. Factors influencing the accuracy of oscillometric blood pressure measurement in critically ill patients. *Crit Care Med*, 31:793–9, 2003.

[148] J M Bland and D G Altman. Measuring agreement in method comparison studies. *Stat Methods Med Res*, 8:135–60, 1999.

[149] N M van Popele, W J Bos, N A de Beer, D A van Der Kuip, A Hofman, D E Grobbee, and J C Witteman. Arterial stiffness as underlying mechanism of disagreement between an oscillometric blood pressure monitor and a sphygmomanometer. *Hypertension*, 36:484–8, 2000.

[150] Yequn Chen, Yi Zhu, Chang Chen, Xiaojun Chen, Hongxing Pan, Shaoqi Chen, and Xuerui Tan. Relationship between noninvasive and invasive blood pressure values in end-stage renal disease patients on dialysis. *Blood Press Monit*, 19:72–5, 2014.

[151] M Ursino and C Cristalli. A mathematical study of some biomechanical factors affecting the oscillometric blood pressure measurement. *IEEE Trans Biomed Eng*, 43:761–78, 1996.

[152] Carlo Alberto Lodi, Charles Estridge, and Carlo Ghidini. In vitro and in vivo evaluation of an oscillometric device for monitoring blood pressure in dialysis patients. *Nephrol Dial Transplant*, 22:2950–61, 2007.

[153] Joakim Cordtz and Soeren D Ladefoged. Pulse contour-derived cardiac output in hemodialysis patients. *Hemodial Int*, 14:78–83, 2010.

[154] L A Critchley and J A Critchley. A meta-analysis of studies using bias and precision statistics to compare cardiac output measurement techniques. *J Clin Monit Comput*, 15:85–91, 1999.

[155] J M Bland and D G Altman. Statistical methods for assessing agreement between two methods of clinical measurement. *Lancet*, 1:307–10, 1986.

[156] Manabu Shibasaki, Thad E Wilson, Morten Bundgaard-Nielsen, Thomas Seifert, Niels H Secher, and Craig G Crandall. Modelflow underestimates cardiac output in heat-stressed individuals. *Am J Physiol Regul Integr Comp Physiol*, 300:486–91, 2011.

[157] Ramakrishna Mukkamala, Jin-Oh Hahn, Omer T Inan, Lalit K Mestha, Chang-Sei Kim, Hakan Toreyin, and Survi Kyal. Toward ubiquitous blood pressure monitoring via pulse transit time: Theory and practice. *IEEE Trans Biomed Eng*, 62:1879–901, 2015.

[158] K Nakane, T Shinzato, and K Maeda. Continuous measurement of pressure in internal arteriovenous fistulae and prevention of symptomatic hypotension during hemodialysis. *ASAIO Trans*, 37:M232–4, 1991.

[159] T Agishi, I Kaneko, E Kumagai, and K Ota. Continuous blood pressure monitoring during hemodialysis. *Artif Organs*, 3:237–40, 1979.

[160] A Besarab, S Dorrell, M Moritz, H Michael, and K Sullivan. Determinants of measured dialysis venous pressure and its relationship to true intra-access venous pressure. *ASAIO Trans*, 37:270–1, 1991.

[161] NIDDK. Treatment methods for kidney failure: Haemodialysis. *www.niddk.nih.gov/health-information/health-topics/kidney-disease/hemodialysis*, (accessed June 2015).

[162] Mico Yee-Man Wong, Emma Pickwell-MacPherson, and Yuan-Ting Zhang. The acute effects of running on blood pressure estimation using pulse transit time in normotensive subjects. *Eur J Appl Physiol*, 107:169–75, 2009.

[163] J Lass, K Meigas, D Karai, R Kattai, J Kaik, and M Rossmann. Continuous blood pressure monitoring during exercise using pulse wave transit time measurement. *Conf Proc IEEE Eng Med Biol Soc*, 3:2239–42, 2004.

[164] R A Payne, C N Symeonides, D J Webb, and S R J Maxwell. Pulse transit time measured from the ecg: an unreliable marker of beat-to-beat blood pressure. *J Appl Physiol*, 100:136–41, 2006.

[165] M J Drinnan, J Allen, and A Murray. Relation between heart rate and pulse transit time during paced respiration. *Physiol Meas*, 22:425–32, 2001.

[166] Pierre Lantelme, Christine Mestre, Michel Lievre, Alain Gressard, and Hugues Milon. Heart rate: an important confounder of pulse wave velocity assessment. *Hypertension*, 39:1083–7, 2002.

[167] P Albaladejo, X Copie, P Boutouyrie, B Laloux, A D Déclère, H Smulyan, and A Bénétos. Heart rate, arterial stiffness, and wave reflections in paced patients. *Hypertension*, 38:949–52, 2001.

[168] A A Mangoni, L Mircoli, C Giannattasio, A U Ferrari, and G Mancia. Heart rate-dependence of arterial distensibility in vivo. *J Hypertens*, 14:897–901, 1996.

[169] Rajiv Dhamija, Shawn K Nash, Shawn V Nguyen, Kyle Slack, and Joseph Tadeo. Monitoring and surveillance of hemodialysis vascular access using stentec and physical exam. *Semin Dial*, 28:299–304, 2015.

[170] Koen Van Canneyt, Thierry Pourchez, Sunny Eloot, Caroline Guillame, Alexandre Bonnet, Patrick Segers, and Pascal Verdonck. Hemodynamic impact of anastomosis size and angle in side-to-end arteriovenous fistulae: a computer analysis. *J Vasc Access*, 11:52–8, 2010.

[171] A Besarab, T Lubkowski, A Vu, A Aslam, and S Frinak. Effects of systemic hemodynamics on flow within vascular accesses used for hemodialysis. *ASAIO J*, 47:501–6, 2001.

[172] A Besarab, S Frinak, R A Sherman, J Goldman, F Dumler, M V Devita, T Kapoian, F Al-Saghir, and T Lubkowski. Simplified measurement of intra-access pressure. *J Am Soc Nephrol*, 9:284–9, 1998.

[173] Stanley Frinak, Gerard Zasuwa, Thomas Dunfee, Anatole Besarab, and Jerry Yee. Dynamic venous access pressure ratio test for hemodialysis access monitoring. *Am J Kidney Dis*, 40:760–8, 2002.

[174] Stephen R Ash, Rajiv Dhamija, Mohamad Y Zaroura, and Dirk M Hentschel. The stentec gauge for measuring static intra-access pressure ratio (p(ia ratio)) of fistulas and grafts. *Semin Dial*, 25:474–81, 2012.

[175] M E O'Connell, H Tuokko, R E Graves, and H Kadlec. Correcting the 3ms for bias does not improve accuracy when screening for cognitive impairment or dementia. *J Clin Exp Neuropsychol*, 26:970–80, 2004.

[176] Tom N Tombaugh. Trail making test a and b: normative data stratified by age and education. *Arch Clin Neuropsychol*, 19:203–14, 2004.

[177] Tatyana G Jones, John A Schinka, Rodney D Vanderploeg, Brent J Small, Amy Borenstein Graves, and James A Mortimer. 3ms normative data for the elderly. *Arch Clin Neuropsychol*, 17:171–7, 2002.

[178] Johannes Hessler, Oliver Tucha, Hans Förstl, Edelgard Mösch, and Horst Bickel. Age-correction of test scores reduces the validity of mild cognitive impairment in predicting progression to dementia. *PLoS One*, 9:e106284, 2014.

[179] M Misra, J Stark, M Dujovny, R Widman, and J I Ausman. Transcranial cerebral oximetry in random normal subjects. *Neurol Res*, 20:137–41, 1998.

[180] Melissa K Andrew and Kenneth Rockwood. A five-point change in modified mini-mental state examination was clinically meaningful in community-dwelling elderly people. *J Clin Epidemiol*, 61:827–31, 2008.

[181] Manjula Kurella Tamura, Mark L Unruh, Allen R Nissenson, Brett Larive, Paul W Eggers, Jennifer Gassman, Ravindra L Mehta, Alan S Kliger, John B Stokes, and Frequent Hemodialysis Network (FHN) Trial Group. Effect of more frequent hemodialysis on cognitive function in the frequent hemodialysis network trials. *Am J Kidney Dis*, 61:228–37, 2013.

[182] Heart rate variability. standards of measurement, physiological interpretation, and clinical use. task force of the european society of cardiology and the north american society of pacing and electrophysiology. *Eur Heart J*, 17:354–81, 1996.

[183] I Feferman. Letter: Acute pulmonary edema and phlebotomy. *JACEP*, 5:211, 1976.

[184] P Langley, ST King, D Zheng, EJ Bowers, K Wang, J Allen, and A Murray. Predicting acute hypotensive episodes from mean arterial pressure. *Computers in Cardiology*, 36:553–556, 2009.

[185] X Chen, D Xu, G Zhang, and R Mukkamala. Forecasting acute hypotensive episodes in intensive care patients based on a peripheral arterial blood pressure waveform. *Computers in Cardiology*, 36(545-548), 2009.

[186] Reuven Pizov, Arieh Eden, Dmitri Bystritski, Elena Kalina, Ada Tamir, and Simon Gelman. Arterial and plethysmographic waveform analysis in anesthetized patients with hypovolemia. *Anesthesiology*, 113:83–91, 2010.

[187] Claudio Sandroni, Fabio Cavallaro, Cristina Marano, Chiara Falcone, Paolo De Santis, and Massimo Antonelli. Accuracy of plethysmographic indices as predictors of fluid responsiveness in mechanically ventilated adults: a systematic review and meta-analysis. *Intensive Care Med*, 38:1429–37, 2012.

[188] Aymen A Alian, Nicholas J Galante, Nina S Stachenfeld, David G Silverman, and Kirk H Shelley. Impact of central hypovolemia on photoplethysmographic waveform parameters in healthy volunteers part 2: frequency domain analysis. *J Clin Monit Comput*, 25:387–96, 2011.

[189] Nandakumar Selvaraj, Christopher G Scully, Kirk H Shelley, David G Silverman, and Ki H Chon. Early detection of spontaneous blood loss using amplitude modulation of photoplethysmogram. *Conf Proc IEEE Eng Med Biol Soc*, 2011:5499–502, 2011.

[190] Simon Hyttel-Sorensen, Trine Witzner Hessel, Amalia la Cour, and Gorm Greisen. A comparison between two nirs oximeters (invos, oxyprem) using measurement on the arm of adults and head of infants after caesarean section. *Biomed Opt Express*, 5:3671–83, 2014.

[191] Ian T Nabney. *Netlab: Algorithms for Pattern Recognition.* London, England: Springer-Verlag, 2004.

[192] Lionel Tarassenko, David A. Clifton, Peter R. Bannister, Steve King, and Dennis King. *Novelty Detection.* John Wiley & Sons, Ltd, 2009.

[193] Marco A. F. Pimentel, David A. Clifton, Lei Clifton, Peter J. Watkinson, and Lionel Tarassenko. Modelling physiological deterioration in post-operative patient vital-sign data. *Med Biol Eng Comput*, 51:869–877, 2013.

[194] Marco A.F. Pimentel, David A. Clifton, Lei Clifton, and Lionel Tarassenko. A review of novelty detection. *Signal Processing*, 99:215 – 249, 2014.

[195] Robert Dürichen, Marco A F Pimentel, Lei Clifton, Achim Schweikard, and David A Clifton. Multitask gaussian processes for multivariate physiological time-series analysis. *IEEE Trans Biomed Eng*, 62:314–22, 2015.